

**OFFICE OF CIVILIAN RADIOACTIVE WASTE MANAGEMENT
ANALYSIS/MODEL COVER SHEET**

1. OA: OA

Page: 1 of 126

Complete Only Applicable Items

2. Analysis Check all that apply

Type of Analysis	<input type="checkbox"/> Engineering <input type="checkbox"/> Performance Assessment <input checked="" type="checkbox"/> Scientific
Intended Use of Analysis	<input type="checkbox"/> Input to Calculation <input checked="" type="checkbox"/> Input to another Analysis or Model <input checked="" type="checkbox"/> Input to Technical Document
Describe use:	
Provides chemistry of water entering drifts for other AMRs and the UZ and NFE PMRs.	

3. Model Check all that apply

Type of Model	<input checked="" type="checkbox"/> Conceptual Model <input type="checkbox"/> Abstraction Model <input type="checkbox"/> Mathematical Model <input type="checkbox"/> System Model <input checked="" type="checkbox"/> Process Model
Intended Use of Model	<input type="checkbox"/> Input to Calculation <input checked="" type="checkbox"/> Input to another Model or Analysis <input checked="" type="checkbox"/> Input to Technical Document
Describe use:	
Provides THC models for abstraction and use by PA, and for use in analysis of Drift Scale Test, and for supporting the UZ and NFE PMRs.	

4. Title:
Drift-Scale Coupled Processes (DST and THC Seepage) Models

5. Document Identifier (including Rev. No. and Change No., if applicable):
MDL-NBS-HS-000001 REV00

6. Total Attachments: 8	7. Attachment Numbers - No. of Pages in Each: I-24, II-2, III-2, IV-3, V-4, VI-3, VII-3, VIII-69
----------------------------	---

	Printed Name	Signature	Date
8. Originator	Eric Sonnenthal	<i>Eric Sonnenthal</i>	3/13/00
	Nicolas Spycher	<i>Nicolas Spycher</i>	3/13/00
9. Checker	P. Persoff	<i>Peter Persoff</i>	3/13/00
10. Lead/Supervisor	G.S. Bodvarsson	<i>Bob Bodvarsson</i>	3/13/00
11. Responsible Manager	G.S. Bodvarsson	<i>Bob Bodvarsson</i>	3/13/00

12. Remarks:

Editorial correction to page 4, Table of Contents. JET 4/3/00
Editorial correction to Attachment I - N/A added to 'change' box throughout. JET 4/3/00
Editorial correction to Attachment VIII - pagination throughout JET 4/3/00
obliterations in Attachment VIII do not affect technical content. JET 4/3/00

**OFFICE OF CIVILIAN RADIOACTIVE WASTE MANAGEMENT
ANALYSIS/MODEL REVISION RECORD**

Complete Only Applicable Items

1. Page: 2 of 126

2. Analysis or Model Title:

Drift-Scale Coupled Processes (DST and THC Seepage) Models

3. Document Identifier (including Rev. No. and Change No., if applicable):

MDL-NBS-HS-000001 REV00

4. Revision/Change No.

5. Description of Revision/Change

00

Initial Issue

CONTENTS

	Page
ACRONYMS	11
1. PURPOSE	13
2. QUALITY ASSURANCE	15
3. COMPUTER SOFTWARE AND MODEL USAGE	17
4. INPUTS	19
4.1 DATA AND PARAMETERS	19
4.1.1 Hydrological and Thermal Properties	19
4.1.2 Mineralogical Data	19
4.1.3 Water and Gas Chemistry	21
4.1.4 Thermodynamic Database	22
4.1.5 Kinetic Data	22
4.1.6 Transport Parameters	25
4.1.7 Design Data	26
4.2 CRITERIA	29
4.3 CODES AND STANDARDS	29
5. ASSUMPTIONS	31
6. ANALYSIS/MODEL	35
6.1 THE DRIFT SCALE THC CONCEPTUAL MODEL	35
6.1.1 Dual-Permeability Model for THC Processes	35
6.1.2 Initial Water Chemistry	36
6.1.3 Numerical Model for Coupled THC Processes	37
6.1.4 Kinetic Rate Laws	38
6.1.5 Fracture and Matrix Mineral Reactive Surface Areas	40
6.1.6 Effects of Mineral Precipitation/Dissolution on Hydrologic Properties	42
6.1.7 Geochemical Systems	43
6.2 THE DRIFT SCALE TEST THC MODEL	45
6.2.1 Background Information	45
6.2.2 Drift Scale Test 2-D Numerical Grid	46
6.2.3 Heater Power	47
6.2.4 Hydrological and Thermal Boundary and Initial Conditions	47
6.2.5 Geochemical Boundary and Initial Conditions	47
6.2.6 Measured Geochemical Data Used for Comparison to Simulation Results	48
6.2.7 Validation of DST THC Model by Comparison of Simulation Results to Measured Data	45
6.3 THC SEEPAGE MODEL	75
6.3.1 Numerical Mesh	75
6.3.2 Boundary Conditions	79
6.3.3 Modeling Procedure	80

CONTENTS (Continued)

	Page
6.3.4 Model Runs	81
6.3.5 Simulation Results	82
7. CONCLUSIONS	113
8. INPUTS AND REFERENCES	117
8.1 DOCUMENTS CITED	117
8.2 CODES, STANDARDS, REGULATIONS, AND PROCEDURES	121
8.3 SOURCE DATA, LISTED BY DATA TRACKING NUMBER	122 121 <i>peH</i>
8.4 OUTPUT DATA, LISTED BY DATA TRACKING NUMBER	123 <i>3/3/00</i>
9. ATTACHMENTS	125
ATTACHMENT I - DOCUMENT INPUT REFERENCE SHEET	
ATTACHMENT II - MINERAL INITIAL VOLUME FRACTIONS	
ATTACHMENT III - MINERAL REACTIVE SURFACE AREAS	
ATTACHMENT IV - THERMODYNAMIC DATABASE	
ATTACHMENT V - WASTE PACKAGE AVERAGE HEAT TRANSFER	
ATTACHMENT VI - EFFECTIVE THERMAL CONDUCTIVITY FOR IN-DRIFT OPEN SPACES	
ATTACHMENT VII - LIST OF MODEL INPUT AND OUTPUT FILES	
ATTACHMENT VIII - SOFTWARE ROUTINES	

FIGURES

	Page
1. Sketch (Not to Scale) Corresponding to In-Drift Data for Drift-Scale Models for TSPA-SR (Rev 01)	28
2. Conceptual Model (Schematic) for Reaction-Transport Processes In Dual Permeability Media	36
3. Close-Up of Numerical Mesh Used for Drift Scale Test THC Model Simulations.....	46
4. Liquid Saturation (Colors) and Temperature (Contour Lines) around the DST (Case 2) at 12 Months, and at 20 Months	49
5. CO ₂ Concentration in Gas Phase (Case 2) Around the DST at 6 Months and at 12 Months	52
6. CO ₂ Concentration in Gas Phase around the DST (Case 2) at 15 Months and at 20 Months	54
7. CO ₂ Concentration in Gas Phase (Case 1) around the DST at 12 Months and at 20 Months	56
8. Measured Concentrations of CO ₂ in Gas Phase around the DST at 12 Months and at 15 Months	58
9. Close-Up of DST Grid, Showing Nodes Used to Extract Model Data for Comparison to Concentrations Measured in Gas Samples.....	59
10. Comparison of Modeled CO ₂ Concentrations (Case 2) in Fractures and Matrix over Time to Measured Concentrations in Boreholes.....	61
11. (a) Modeled air mass fraction in gas phase at center of borehole interval 78-3 (fracture) over time. (b) Ratio of modeled CO ₂ concentration to air mass fraction at same location as 11a over time (Case 2), with comparison to measured CO ₂ concentrations over time	63
12. Modeled CO ₂ Concentrations in Heater Drift Air over Time, Compared to Measured Concentrations. Also shown are concentrations measured in air from the Observation Drift.....	64
13. Distribution of pH and Temperature at 12 Months and at 20 Months. Results are for the simplified geochemical system (Case 2)	67
14. Distribution of pH at 12 Months and at 20 Months. Results are for the full geochemical system (Case 1).....	69

FIGURES (Continued)

	Page
15. Chloride Concentration (log mg/l) and Temperature at 12 Months and at 20 Months (Case 2).....	71
16. Distribution of Calcite Precipitation (+) or Dissolution (-) as a Change in the Volume of the Total Medium (% x 10) at 20 Months. Results are for the simplified geochemical system (Case 2) and the full geochemical system (Case 1).....	73
17. Change in Fracture Porosity after 20 Months (Case 2). Negative values indicate a net porosity reduction due to mineral precipitation and positive values reflect a net porosity increase owing to mineral dissolution	74
18. THC Seepage Model Mesh with Hydrogeologic Units Shown in the Vicinity of the Drift: Topopah Spring Tuff Upper Lithophysal (tsw33), Middle Non-Lithophysal (tsw34), and Lower Lithophysal (tsw35) Units	76
19. Discretization of the Repository Drift in the THC Seepage Model.....	78
20. TH Simulation. Time profiles of modeled temperatures and liquid saturations in fractures and matrix at three drift wall locations	83
21. TH Simulation. Contour plot of modeled temperatures and liquid saturations in the matrix at 600 years (near maximum extent of dryout)	84
22. TH Simulation. Time profiles of modeled air mass fractions in the gas phase in fractures and matrix at three drift wall locations	85
23. Time Profiles of Modeled Temperatures in Fractures at Three Drift Wall Locations for Different Climate Scenarios (THC - Case 1).....	87
24. Time Profiles of Modeled Liquid Saturations in Fractures at Three Drift Wall Locations for Different Climate Scenarios (THC - Case 1)	88
25. Time Profiles of Modeled Liquid Saturations in the Matrix at Three Drift Wall Locations for Different Climate Scenarios (THC - Case 1)	89
26. Contour Plot of Modeled Temperatures and Liquid Saturations in the Matrix at 600 years (Near Maximum Dryout) for Three Climate Scenarios: (a) Lower Bound, (b) Mean, and (c) Upper Bound (THC - Case 1).....	90
27. Time Profiles of Modeled Air Mass Fractions in the Gas Phase in Fractures (Essentially Identical in the Matrix) at Three Drift Wall Locations for Different Climate Scenarios. (THC - Case 1)	91

FIGURES (Continued)

	Page
28. Time Profiles of Modeled CO ₂ Concentrations in the Gas Phase in Fractures at Three Drift Wall Locations for Different Climate Scenarios (Case 1).....	93
29. Time Profiles of Modeled CO ₂ Concentrations in the Gas Phase in Fractures at Three Drift Wall Locations for Different Climate Scenarios (Case 2).....	94
30. Time Profiles of the Modeled pH of Fracture Water at Three Drift Wall Locations for Different Climate Scenarios (Case 1).....	96
31. Time Profiles of the Modeled pH of Fracture Water at Three Drift Wall Locations for Different Climate Scenarios (Case 2).....	97
32. Time Profiles of Modeled Total Aqueous Carbonate Concentrations (as HCO ₃ ⁻) in Fracture Water at Three Drift Wall Locations for Different Climate Scenarios (Case 1).....	98
33. Time Profiles of Modeled Total Aqueous Carbonate Concentrations (as HCO ₃ ⁻) in Fracture Water at Three Drift Wall Locations for Different Climate Scenarios (Case 2).....	99
34. Time Profiles of Modeled Total Aqueous Calcium Concentrations in Fracture Water at Three Drift Wall Locations for Different Climate Scenarios (Case 1).....	101
35. Time Profiles of Modeled Total Aqueous Calcium Concentrations in Fracture Water at Three Drift Wall Locations for Different Climate Scenarios (Case 2).....	102
36. Time Profiles of Modeled Total Aqueous Sodium Concentrations in Fracture Water at Three Drift Wall Locations for Different Climate Scenarios (Case 1).....	103
37. Time Profiles of Modeled Total Aqueous Sodium Concentrations in Fracture Water at Three Drift Wall Locations for Different Climate Scenarios (Case 2).....	104
38. Time Profiles of Modeled Total Aqueous Chloride Concentrations in Fracture Water at Three Drift Wall Locations for Different Climate Scenarios (Case 1).....	106
39. Time Profiles of Modeled Total Aqueous Chloride Concentrations in Fracture Water at Three Drift Wall Locations for Different Climate Scenarios (Case 2).....	107
40. Time Profiles of Modeled Total Aqueous Fluoride Concentrations in Fracture Water at Three Drift Wall Locations for Different Climate Scenarios (Case 1).....	109

FIGURES (Continued)

	Page
41. Contour Plot of Modeled Total Fracture Porosity Change at 10,000 years for Three Climate Scenarios: (a) Lower Bound, (b) Mean, and (c) Upper Bound. Red areas indicate maximum decrease in porosity due to mineral precipitation (Case 1)	110
42. Contour Plot of Calculated Total Fracture Porosity Change at 10,000 years for Three Climate Scenarios: (a) Lower Bound, (b) Mean, and (c) Upper Bound. Red areas indicate maximum decrease in porosity due to mineral precipitation (Case 2)	111

TABLES

	Page
1. Computer Software and Routines	17
2. Data Tracking Numbers for Sources of Data Input to the DST THC Model and THC Seepage Model.....	20
3. Initial Water Composition and CO ₂ Partial Pressure in Fractures, Matrix, and Recharge Waters.	21
4. Kinetic Rate Law Data For Mineral-Water Dissolution and Precipitation	23
5. Drift Design Parameters.....	27
6. Scientific Notebooks.....	35
7. Case-1 Mineral Assemblage, Aqueous and Gaseous Species	44
8. Case-2 (Simplified) Mineral Assemblage, Aqueous and Gaseous Species.....	45
9. Measured Concentrations in TSw Pore Water from Alcove 5 and Chemistry of Water Taken from Hydrology Boreholes	66
10. Vertical Mesh Dimensions and Geologic Contacts in the THC Seepage Model.....	77
11. THC Seepage Model Boundary Conditions	79
12. THC Seepage Model Infiltration Rates and Corresponding Rock Properties Sets.....	80
13. THC Seepage Model Runs	81

INTENTIONALLY LEFT BLANK

ACRONYMS

2D, 2-D	two-dimensional, two dimensions
3D, 3-D	three-dimensional, three dimensions
ACC	Accession Number
AMR	Analysis/Model Report
AP	Administrative Procedure
aq	aqueous
CHn	Calico Hills nonwelded
CRWMS	Civilian Radioactive Waste Management
DIRS	Document Input Reference Sheet
DST	Drift Scale Test
DTN	Data Tracking Number
EDA	Enhanced Design Alternatives
ESF	Exploratory Studies Facility
LBNL	Lawrence Berkeley National Laboratory
M&O	Management and Operating Contractor
NFE	Near-Field Environment
OCRWM	Office of Civilian Radioactive Waste Management
PA	Performance Assessment
PMR	Process Model Report
PTn	Paintbrush Tuff nonwelded
Q	Qualified
QA	Quality Assurance
QARD	Quality Assurance Requirements and Description
QIP	Quality Implementing Procedure
SHT	Single Heater Test
SN	Scientific Notebook
SR	Site Recommendation
STN	Software Tracking Number
TBD	To Be Determined
TBV	To Be Verified
TCw	Tiva Canyon welded unit
TH	Thermal-Hydrological
THC	Thermal-Hydrological-Chemical
TSw	Topopah Spring welded unit

ACRONYMS (Continued)

U.S. United States

UZ Unsaturated Zone

YMP Yucca Mountain Site Characterization Project

1. PURPOSE

The purpose of this Analysis/Model Report (AMR) is to document the Near Field Environment (NFE) and Unsaturated Zone (UZ) models used to evaluate the potential effects of coupled thermal-hydrologic-chemical (THC) processes on unsaturated zone flow and transport. This is in accordance with *AMR Development Plan for U0110 Drift-Scale Coupled Processes (Drift Scale Test and THC Seepage) Models* (CRWMS M&O 1999a). These models include the Drift Scale Test (DST) THC Model and the THC Seepage Model. These models provide the framework to evaluate THC coupled processes at the drift scale, predict flow and transport behavior for specified thermal loading conditions, and predict the chemistry of waters and gases entering potential waste-emplacement drifts. This AMR provides input for the following:

- Performance Assessment (PA)
- AMR documenting the abstraction of drift-scale coupled processes models
- UZ Flow and Transport Process Model Report (PMR)
- NFE PMR

The DST THC Model, constructed for the DST, is used to investigate THC processes during the DST. Measured data from the DST are used to evaluate the conceptual and numerical models. The iterative approach of evaluating, refining, and comparing the DST numerical model against measured data is performed throughout the DST study. The THC Seepage Model provides an analysis of the effects of THC processes in the near field host rock around the potential emplacement drifts on the seepage water chemistry and gas-phase composition. This includes a complete description of the pertinent mineral-water processes in the host rock and their effect on the NFE. The model is used to evaluate the effects of mineral dissolution and precipitation, the effects of CO₂ exsolution and transport in the region surrounding the drift, the potential for forming calcite, silica or other mineral assemblage “precipitation caps,” and the resulting changes to porosity, permeability, and seepage.

Caveats and Limitations

The THC Seepage model was developed with data for a specific hydrogeologic unit, the Topopah Spring Middle Nonlithophysal, in which part of the potential repository would be sited. Although many aspects of the model are applicable to other host rock units of the potential repository, differences in the mineralogy, geochemistry, and thermohydrological properties must be considered before the results are directly applied elsewhere in the potential repository. One limitation of the model is that it is a continuum model with limited initial heterogeneity, and therefore is meant to represent the overall changes in space and time. Thus it cannot be applied with certainty at a specific location.

The model must be recognized as an idealization of the real world that represents specific physical processes occurring in the real world. Input data summarized in Section 4 characterize the physical properties of the rock but are not intended to include every detail. In particular, we note that the initial thermohydrologic properties of the rock vary vertically according to the stratigraphy, but are treated as laterally uniform over the entire layer. The infiltration of water is also laterally uniform over the entire model area. As a result of these simplifications, the model

results describe overall changes in space and time within the model domain, but cannot be considered as predictions of future conditions at any specific location.

2. QUALITY ASSURANCE

This AMR was developed in accordance with AP-3.10Q, *Analyses and Models*. Other applicable Department of Energy (DOE) Office of Civilian Radioactive Waste Management (OCRWM) Administrative Procedures (APs) and YMP-LBNL Quality Implementing Procedures (QIPs) are identified in the *AMR Development Plan for U0110 Drift-Scale Coupled Processes (DST and THC Seepage) Models* (CRWMS M&O 1999a).

The activities documented in this Analysis/Model Report (AMR) were evaluated with other related activities in accordance with QAP-2-0, *Conduct of Activities*, and were determined to be subject to the requirements of the U.S. DOE Office of Civilian Radioactive Waste Management (OCRWM) *Quality Assurance Requirements and Description* (QARD) (DOE 1998). This evaluation is documented in *Activity Evaluation of M&O Site Investigations* CRWMS 1999b, c; and Wemheuer 1999 (*Activity Evaluation for Work Package WP 1401213UM1*).

INTENTIONALLY LEFT BLANK

3. COMPUTER SOFTWARE AND MODEL USAGE

The software and routines used in this study are listed in Table 1. These are appropriate for the intended application, were used only within the range of validation, and are under software configuration management in accordance with AP-SI.1Q, *Software Management*. The qualification status of these software and routines is given in the DIRS in Attachment I.

Table 1. Computer Software and Routines

Software Name	Version	Software Tracking Number (STN)	Computer Platform
TOUGHREACT	2.2	10154-2.2-00	SUN and DEC w/ Unix OS
SOLVEQ/ CHILLER	1.0	10057-1.0-00	SUN w/ Unix OS PC w/ DOS
SUPCRT92	1.0	10058-1.0-00	SUN w/ Unix OS PC w/ Windows MAC w/ MAC OS
TOUGH2	1.4	10061-1.4-00	SUN and DEC w/ Unix OS
AMESH	1.0	10045-1.0-00	SUN w/ Unix OS
Routines:		Accession Number (ACC):	
2kgridv1a.for	1.0	MOL.19991201.0555	SUN w/ Unix OS
mk_grav2.f	1.0	MOL.19991201.0556	SUN w/ Unix OS
sav1d_dst2d.f	1.0	MOL.19991201.0557	SUN w/ Unix OS
mrgdrift.f	1.0	see Attachment VIII	SUN w/Unix OS

NOTE: The source code for the software routines are provided in Attachment VIII. The supporting documentation is included under the ACC number listed above.

TOUGHREACT (TOUGHREACT V2.2, STN: 10154-2.2-00, Version 2.2) is the primary code used in the DST THC and THC Seepage models. The codes SOLVEQ/CHILLER (SOLVEQ/CHILLER V1.0, STN: 10057-1.0-00, Version 1.0) were utilized to perform supporting computations for the models. SUPCRT92 (SUPCRT92 V1.0, STN: 10058-1.0-00, Version 1.0) generates thermodynamic databases for use by SOLVEQ/CHILLER V1.0 and TOUGHREACT V2.2. The code TOUGH2 (TOUGH2 V1.4, STN: 10061-1.4-00, Version 1.4) was used to generate boundary conditions. The code AMESH (AMESH V1.0, STN: 10045-1.0-00, Version 1.0) was used to generate grids for the two models.

All software programs listed in Table 1, except TOUGHREACT V2.2, were reverified as part of the YMP Configuration Management Software revalidation effort. TOUGHREACT V2.2 is being qualified under AP-SI.1Q, Rev 2, ICN 1. After checking, errors in the calculation of capillary pressure changes due to THC processes and gas species diffusion coefficients were discovered. These are not expected to change the conclusions of this AMR, because they are not dominant effects in the system. They will be evaluated in an Impact Review. EQ3/6 V7.2b is cited in this AMR as a source of thermodynamic data, but was not used as software.

Standard spreadsheet and visual display graphics programs were also used but are not subject to software quality assurance requirements per Section 2.0 of AP-SI.1Q, Rev 2, ICN 1.

This AMR documents the DST THC and THC Seepage Model. The input and output files for the model runs presented in this AMR are listed in Attachment VII. This AMR also utilizes properties from the Calibrated Properties Model and boundary conditions from the UZ Flow and Transport Model. These models are documented in separate AMRs.

4. INPUTS

4.1 DATA AND PARAMETERS

4.1.1 Hydrological and Thermal Properties

The modeling analyses presented in this report utilized data from the lower, basecase and upper bound calibrated hydrological property sets for the present day climate (see DTNs in Table 2). The Q-status of all inputs is shown in the Document Input Reference Sheet (DIRS). Thermal parameters were obtained from the mean calibrated property set, and are identical for all property sets. These data are included in the DTNs in Table 2 for the calibrated property sets. The data sets include calibrated properties such as fracture and matrix permeabilities and van Genuchten parameters as well as uncalibrated properties such as porosity, heat capacity, and thermal conductivity. DTNs for infiltration rates and model boundary water temperatures are also included in Table 2. Specific hydrological and thermal parameters for the in-drift components of the THC Seepage Model are given in Section 4.1.7.2.

4.1.2 Mineralogical Data

This section describes mineralogical data that are specific to the geologic units encountered in Borehole SD-9 (the borehole closest to the Drift Scale Thermal Test) and in host rocks of Alcove 5 where this test is located. These data were used in the Drift Scale Test THC Model and the THC Seepage Model (therefore the depth at which heat is directly input into these models contains mineralogical data that are representative of the Topopah Spring Middle Nonlithophysal (Tptpmn) repository host unit). They are input as volume fractions of a given mineral per total solid volume, and as reactive surface areas (units of cm^2/g mineral or m^2/m^3 of total medium, including pore space). The two forms of the reactive surface area are used to describe minerals in the matrix of the rock (cm^2/g mineral) or those on the surface of fractures (m^2/m^3). These data are given in Attachments II (volume fractions) and III (reactive surface areas) for minerals initially present in the model hydrological units. The DTNs for data from which these properties were derived are given in Table 2, and include Borehole SD-9 mass percent minerals as determined by X-ray diffraction (3-D Mineralogical Model: LA9908JC831321.001). The calculation of the mineral volume fractions and reactive surface areas require significant additional information, such as mineral stoichiometries, mass densities, grain size and fracture-matrix surface area. The fracture-matrix surface area is part of the mean calibrated hydrological property set and is listed by DTN in Table 2. The calculation of the reactive surface areas and other mineral properties are described in scientific notebook YMP-LBNL-YWT-ELS-1 (pp. 37-42).

Table 2. Data Tracking Numbers for Sources of Data Input to the DST THC Model and THC Seepage Model

DTNs	Description
Hydrological and Thermal Rock Properties:	
LB990861233129.001	Calibrated property set [†] – Basecase
LB990861233129.002	Calibrated property set [†] – Upper bound
LB990861233129.003	Calibrated property set [†] – Lower bound
LB997141233129.001	Fracture porosity
LB991091233129.001	Infiltration rate – Basecase
LL000114004242.090	Infiltration rates - Average Infiltration Rate (mean, lower bound, and upper bound for present day, monsoon, and glacial transition climates) from the TH drift-scale models.
Mineralogic Data	
LASL831151AQ98.001	Mineralogic characterization of the ESF SHT Block
LA9912SL831151.001 LA9912SL831151.002	DST and SHT fracture mineralogy data
LA9908JC831321.001	Model input and output files for Mineralogic Model "MM3.0" Version 3.0.
Water and Gas Chemistry Data	
LB991215123142.001	CO ₂ gas analyses (1st, 2nd, 3rd and 7th Qtr.)
LB990630123142.003	4th, 5th, and 6th Qtr. DST CO ₂ data
LB000121123142.003	DST CO ₂ data (Aug. '99 - Nov. '99)
LL990702804244.100	Analyses of porewaters from the ESF (HD-PERM-1 and HD-PERM-2 samples) Chemistry of water from DST hydrology boreholes (Nov. '98 & Jan. '99)
Repository Drift Data	
SN9907T0872799.001	Heat load data and repository footprint
SN9908T0872799.004	Hydrologic and thermal properties of drift design elements
SN9907T0872799.002	Effective thermal conductivity
PA-SSR-99218.Ta (Design Criterion)	Drift spacing
THC Seepage Model Grid Data	
LB990501233129.004	Borehole SD-9 geology in UZ model grid UZ99_2_3D.mesh
LB990701233129.002	Top and bottom boundary temperatures, pressure, and boundary elevations

NOTES: Thermodynamic data for minerals, aqueous, and gaseous species are found in Attachment IV. Kinetic data for mineral-water reactions are found in Table 4.

[†] Data taken from the calibrated property sets include calibrated and uncalibrated hydrological and thermal properties.

4.1.3 Water and Gas Chemistry

The pore water composition chosen for the input to the simulations is summarized in Table 3. These data are the average of two samples obtained from the Topopah Spring Tuff middle nonlithophysal geologic unit (Ttpmn) in Alcove 5 near the DST (Table 3). These are the only relatively complete pore water analyses for samples collected from a potential repository unit near the potential repository footprint. For model simulations, the initial water composition was set to be the same in fractures and matrix, and the same throughout the model domain. This water composition was also used for infiltrating water, as discussed in Section 6.1.2.

The initial CO₂ partial pressure in fractures and matrix (Table 3) was calculated as the partial pressure of CO₂ in chemical equilibrium with the initial water at 25°C, assuming ideal gas behavior (i.e. partial pressure is equal to fugacity). The 25°C temperature is close to the initial temperature at the location of the drift.

Table 3. Initial Water Composition and CO₂ Partial Pressure in Fractures, Matrix, and Recharge Waters.⁽¹⁾

Parameter/Species	Units	Concentration
pH (at 25°C)	pH Units	8.32
Na ⁺	mg/l	61.3
SiO ₂ (aq)	mg/l	70.5
Ca ²⁺	mg/l	101
K ⁺	mg/l	8.0
Mg ²⁺	mg/l	17
Al ³⁺	mg/l	9.92x10 ⁻⁷ (2)
Fe ³⁺	mg/l	6.46x10 ⁻⁸ (3)
HCO ₃ ⁻ (4)	mg/l	200
Cl ⁻	mg/l	117
SO ₄ ²⁻	mg/l	116
F ⁻	mg/l	0.86
CO ₂ (gas) (5)	Pa	85.2

DTN: LB991200DSTTHC.001 (this Table), LL990702804244.100 for water composition (CRWMS M&O 1999e)

NOTES: (1) Average of Ttpmn Porewater Analyses ESF-HD-PERM-1 (30.1'-30.5') and ESF-HD-PERM-2 (34.8'-35.1').
 (2) Calculated by equilibrating with Ca-smectite at 25°C (using SOLVEQ 1.0).
 (3) Calculated by equilibrating with hematite at 25°C (using SOLVEQ 1.0).
 (4) Total aqueous carbonate as HCO₃⁻, calculated from charge balance computed by speciation at 25°C (using SOLVEQ 1.0).
 (5) Calculated at equilibrium with the solution at 25°C (using SOLVEQ 1.0).

The initial CO₂ partial pressure in the drift was set to be consistent with a CO₂ concentration of 400 parts per million by volume (ppmv) in the drift, which is within the range of measured concentrations in the ESF (DTN: LB990630123142.003). This concentration was also used for the top model boundary concentration in the gas phase. The infiltrating water injected into the grid block below the top boundary block is equilibrated with a CO₂ concentration that is elevated relative to the drift.

There are very few complete pore-water analyses from other units of the Topopah Spring Tuff, and none from the lower lithophysal unit (Tptpl). Data from the lower non-lithophysal unit (Tptpln) (DTN: GS950608312272.001) suggest pore waters from this unit may exhibit a slightly more sodium-carbonate character (and less calcium-chloride type) than the water composition shown in Table 3. However, the general water chemistry trends resulting from THC processes simulated in this study are not expected to vary significantly with the range of possible initial water composition. In addition, the model uncertainty with respect to initial water composition is likely to be insignificant relative to uncertainties in reaction rates, hydrologic parameters, and the variability of pore water compositions within a particular geologic unit.

4.1.4 Thermodynamic Database

Dissociation constants ($\log(K)$ values) for aqueous species, minerals, and CO₂ gas as a function of temperature were taken from various sources (Attachment IV). Most values are from the EQ3/6 V7.2b database (data0.com.R2, dated aug.2.1995, STN: LLNL:UCRL-MA-110662), which were themselves primarily derived using SUPCRT92 (Johnson et al. 1992). Other $\log(K)$ values were computed as indicated in Attachment IV and further documented in YMP Scientific Notebooks YMP-LBNL-YWT-NS-1 p. 72-77, 115, and 137, YMP-LBNL-YWT-NS-1.1 p. 96, and 104-117, and YMP-LBNL-YWT-JA-1A p. 39-41 and 48-50).

Other data included in the thermodynamic database include molecular weights, molar volumes, and parameters used for the calculation of activity coefficients for aqueous species. The latter consist of the ionic charge and the parameters a_0 used in the Debye-Hückel equation (e.g. Drever 1997, p. 28). These data were for the most part taken from the EQ3/6 v7.2b database, with exceptions as noted in Attachment IV. The molecular diameter of CO₂ (Lasaga 1998, p. 322) is also included in the database for calculation of the CO₂ diffusion coefficient.

4.1.5 Kinetic Data

Kinetic data refer to the reaction rate constants (k_0), activation energies (E_a), and related data required to describe the rates of dissolution and precipitation of minerals at different temperatures and fluid chemistries. These data are taken directly from or are recalculated from published scientific literature. These data and their sources are listed in Table 4.

Table 4. Kinetic Rate Law Data For Mineral-Water Dissolution and Precipitation

Mineral†	k_0 (mol m ⁻² s ⁻¹)	E_a (kJ/mol) ⁽¹⁾	m ⁽²⁾	n ⁽²⁾	Comment ⁽³⁾	Reference
α-Cristobalite	3.1623x10 ⁻¹³	69.08	1	1		Renders et al. (1995) Log k = -0.707-2598/T(K) from Rimstidt and Barnes (1980) p. 1683
	see reference	0.0	1	1		
Quartz	1.2589x10 ⁻¹⁴	87.5	1	1	no precip.	Tester et al. (1994)
Tridymite	3.1623x10 ⁻¹³	69.08	1	1	no precip.	Set to α-Cristobalite
Amor. Silica	7.9433x10 ⁻¹³	62.8	1	1		Rimstidt and Barnes (1980) p. 1683 Carroll et al. (1998) p. 1379
	1.0x10 ⁻¹⁰	0.0	4.4	1		
Calcite	1.6x10 ⁻⁹	41.87	1	1		Rate constant k modified after Svensson and Dreybrodt (1992) p. 129; average E_a from Inskeep and Bloom (1985), p. 2178
Microcline	1.0x10 ⁻¹²	57.78	1	1		Blum and Stillings (1995)
Albite-Low	1.0x10 ⁻¹²	67.83	1	1		Blum and Stillings (1995)
Anorthite	2.5x10 ⁻¹⁹	67.83	1	1	no precip.	Set to albite, then modified for equivalent Q/K
Smectite-Ca	1.0x10 ⁻¹⁴	58.62	1	1		Set to illite
Smectite-Na	1.0x10 ⁻¹⁴	58.62	1	1		Set to illite
Smectite-Mg	1.0x10 ⁻¹⁴	58.62	1	1		Set to illite
Smectite-K	1.0x10 ⁻¹⁴	58.62	1	1		Set to illite
Illite	1.0x10 ⁻¹⁴	58.62	1	1		Assumed equal to muscovite (Knauss and Wolery 1989)
Kaolinite	1.0x10 ⁻¹³	62.8	1	1		Nagy (1995)
Sepiolite	1.0x10 ⁻¹⁴	58.62	1	1		Set to illite
Stellerite	1.99x10 ⁻¹²	62.8	1	1		Set to heulandite
Heulandite	1.99x10 ⁻¹²	62.8	1	1		Ragnarsdottir (1993) p. 2439, 2447

DTN: LB991200DSTTHC.A01

NOTE: k_0 Rate Constant E_a Activation Energy

† First line refers to dissolution rate, second line to precipitation rate if different (unless otherwise stated in "Comment" column). "Vphyre" refers to the basal vitrophyre of the TSw unit. This composition of glass was used for all glass-bearing units, including the non-welded PTn glassy tuffs.

(1) Some values differ slightly from sources because of number of significant figures retained in unit conversions.

(2) Exponents m and n in Equation 6.

(3) "no precip" means precipitation of this mineral is not allowed.

Table 4. Kinetic Rate Law Data For Mineral-Water Dissolution and Precipitation (Cont.)

Mineral†	k_0 (mol m ⁻² s ⁻¹)	E_a (kJ/mol) ⁽¹⁾	m ⁽²⁾	n ⁽²⁾	Comment ⁽³⁾	Reference
Mordenite	1.99x10 ⁻¹²	62.8	1	1		Set to heulandite
Clinoptilolite	1.99x10 ⁻¹²	62.8	1	1		Set to heulandite
Glass (vphyr)	7.7233x10 ⁻¹⁵	91	1	1	no precip.	Recalculated k_0 based on diffusion-limited model of Mazer et al. (1992) pp. 573, 574
Gypsum	equilibrium	-	-	-		Not needed
Hematite	7.9433x10 ⁻¹³	62.8	1	1		Set to dissolution rate of amorphous silica
Goethite	equilibrium	-	-	-		Not needed
Fluorite	1.2224x10 ⁻⁷	0	1	2		Calculated k_0 from linear growth rate of Knowles-Van Cappellan et al. (1997) p. 1873

DTN: LB991200DSTTHC.A01

NOTE: k_0 Rate Constant E_a Activation Energy

† First line refers to dissolution rate, second line to precipitation rate if different (unless otherwise stated in "Comment" column). "Vphyr" refers to the basal vitrophyre of the TSw unit. This composition of glass was used for all glass-bearing units, including the non-welded PTn glassy tuffs.

(1) Some values differ slightly from sources because of number of significant figures retained in unit conversions.

(2) Exponents m and n in Equation 6.

(3) "no precip" means precipitation of this mineral is not allowed.

The quantities listed in Table 4 are defined and used in Equations 6 and 7 in Section 6.1.4. Most of the sources cited in Table 4 require pH to calculate k_0 ; in those cases a near-neutral pH (~7.0) was assumed as stated in Section 5. For minerals where no kinetic data were found in the literature, rate constants were assumed to be equal to those of minerals with similar crystal structure or mineral group (Klein and Hurlbut 1993). The value of k_0 assigned for calcite, $1.6 \times 10^{-9} \text{ mol m}^{-2} \text{ s}^{-1}$ is 1000 times smaller than the value reported in Svensson and Dreybrodt (1992); this adjustment was made so that model time steps would not need to be reduced to impractically small values (days or less). Even when divided by 1000, the calcite rate constant is large and reflects near-equilibrium precipitation/dissolution. Therefore, increasing the original value is not expected to significantly change the simulation results.

Reaction rate laws can take numerous forms of which a few different types are used for the model analysis. The form of these rate laws and their significance are described in Section 6.1.

4.1.6 Transport Parameters

Transport parameters considered in the model are diffusion coefficients for aqueous and gaseous species and tortuosities of the fracture, matrix, and engineered system components. Diffusion coefficients for aqueous species are considered to be identical and equal to the tracer diffusion coefficient of a single aqueous species (Cl) at infinite dilution. The aqueous diffusion coefficient of Cl at infinite dilution is $2.03 \times 10^{-9} \text{ m}^2/\text{s}$ at 25°C (Lasaga 1998, Table 4.1, p. 315), which in the model input was rounded to $2.0 \times 10^{-9} \text{ m}^2/\text{s}$. In the gas phase, CO_2 is the only transported reactive species (other than H_2O vapor). For an ideal gas, the tracer diffusion coefficient of a gaseous species can be expressed as a function of temperature and pressure in the following form (Lasaga 1998, p. 322):

$$D = \frac{RT}{3\sqrt{2}\pi P N_A d_m^2} \sqrt{\frac{8RT}{\pi M}} \quad (\text{Eq. 1})$$

where

D = diffusion coefficient (m^2/s)

R = gas constant ($8.31451 \text{ m}^2 \text{ kg s}^{-2} \text{ mol}^{-1} \text{ K}^{-1}$)

$T(K)$ = temperature in Kelvin units

P = pressure ($\text{kg m}^{-1} \text{ s}^{-2}$)

N_A = Avogadro's number ($6.0221367 \times 10^{23} \text{ mol}^{-1}$)

d_m = molecular diameter (m)

M = molecular weight (kg/mol)

For CO₂, the following values were used:

$$d_m = 2.5 \times 10^{-10} \text{ m (Lasaga, 1998, p. 322)}$$

$$M = .04401 \text{ kg/mol (calculated from atomic weights, Klein and Hurlbut 1993, p. 172)}$$

Tortuosities were set to 0.7 for fractures (DTN: LB990861233129.001) based on models of in-situ testing. This value corresponds to the highest tortuosity given by de Marsily (1986, p. 233), with the rationale that fracture tortuosity should be high compared to matrix tortuosity (i.e. less tortuous path in fractures than in the matrix). Fracture tortuosities were further modified for fracture-fracture connections by multiplication of the tortuosity by the fracture porosity of the bulk rock to obtain the correct value for the fracture to fracture interconnection area (only for calculation of diffusive fluxes; the entire grid block connection area is used for calculating advective fluxes, because the bulk fracture permeability of the entire grid block is entered into the model). Matrix tortuosities are unknown, and therefore a value of 0.2 was estimated from values reported by de Marsily (1986, p. 233).

4.1.7 Design Data

4.1.7.1 Drift Scale Test

The development of the two-dimensional numerical mesh for the Drift Scale Test is documented in notebook YMP-LBNL-YWT-SM-1 (pp. 291–308). These data include the drift layout (e.g., drift diameter, concrete invert, bulkhead and insulation) and the location of wing heaters. Other data include the drift and wing heater power output (YMP-LBNL-YWT-SM-1, pp. 309–313). Some modifications to the properties of the insulation are given in scientific notebook YMP-LBNL-YWT-ELS-1 (p. 35).

4.1.7.2 Design of Potential Waste-Emplacement Drifts

Two time periods are considered in the drift design and related data input into the model:

- A 50-year pre-closure period during which 70 percent of the heat released by the waste packages is removed by ventilation.
- A post-closure period immediately following the initial 50-year pre-closure period and extending to 100,000 years (the total simulation time), during which a drip shield and backfill are above the waste packages and no heat is removed by ventilation.

Accordingly, some of the drift-specific model input data are not the same for the pre-closure and post-closure time periods. These design data are for the TSPA-SR, Rev.0, Base Case.

The model drift geometry and thermophysical properties of design elements (waste package, backfill) are shown in Table 5 and Figure 1. These data are referenced in Table 2. These design data are for the TSPA-SR, Rev.0, Base Case. The discretization of the drift is consistent with the dimensions shown in Figure 1, within the limits imposed by the resolution of the model mesh.

Table 5. Drift Design Parameters

Model Input	Value
Drift diameter	5.5 meters
Waste package outer diameter	1.67 meters
Location of waste package center above bottom of drift	1.945 meters
Location of waste package center below the springline	0.805 meters
Angle of Repose	26°
Minimum depth of backfill cover (this occurs at an angle equivalent to the angle of repose measured off the vertical drawn from the waste package centerline)	1.495 meters
Drip shield thickness	0.02 meters
Air gap between waste package surface and the inside of drip shield	0.396 meters
Location of backfill spoil peak (this is the location where the top of the backfill intersects the vertical drawn from the drift centerline) above the drift springline	2.25 meters
Backfill/drift wall intersection point	1.0 meter above the springline at the drift wall intersection
Air gap above invert and below waste package surface	0.504 meters
Inside radius of drip shield	1.231 meters
Top of invert as measured from bottom of drift	0.606 meters
Waste package thermal conductivity	14.42 W/m-K
Waste package density	8189.2 kg/m ³
Waste package specific heat	488.86 J/kg-K
Invert intrinsic permeability	6.152x10 ⁻¹⁰ m ²
Invert porosity	0.545
Invert grain density	2530 kg/m ³
Invert residual liquid saturation	0.092
Invert alpha (van Genuchten)	1.2232x10 ⁻³ Pa ⁻¹
Invert n (van Genuchten)	2.7
Invert specific heat	948 J/kg-K
Invert thermal conductivity	0.66 W/m-K
Backfill intrinsic permeability	1.43x10 ⁻¹¹ m ²
Backfill porosity	0.41
Backfill grain density	2700 kg/m ³
Backfill residual liquid saturation	0.024
Backfill alpha (van Genuchten)	2.7523x10 ⁻⁴ Pa ⁻¹
Backfill n (van Genuchten)	2.0
Backfill specific heat	795.492 J/kg-K
Backfill thermal conductivity	0.33 W/m-K

DTN: SN9908T0872799.004

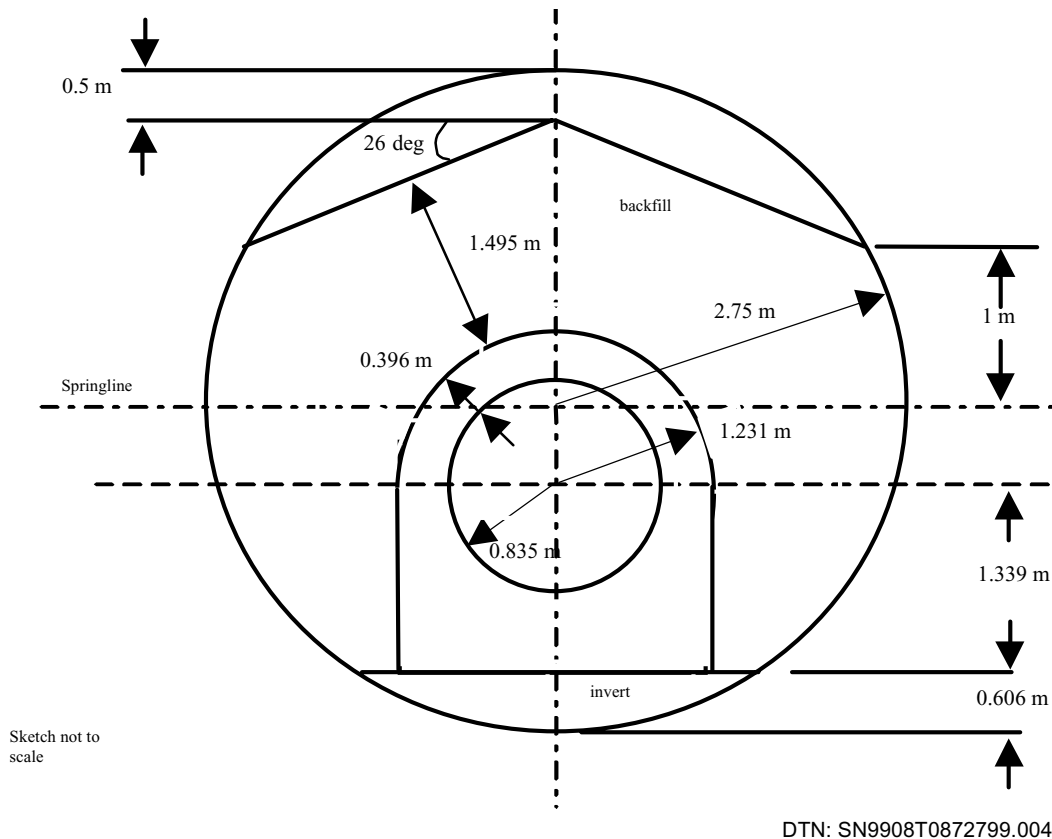


Figure 1. Sketch (Not to Scale) Corresponding to In-Drift Data for Drift-Scale Models for TSPA-SR (Rev 01)

To account for the 50-year pre-closure period without backfill, backfill (as shown on Figure 1) was included in the model only for simulation times greater than 50 years. The drip shield itself was not modeled, but its thickness and thermal conductivity were considered in the width and thermal properties, respectively, of the open zone between the waste package and backfill during the post-closure period.

The heat load from the waste package was obtained from DTN: SN9907T0872799.001. The averaged heat transfer from the waste package, as a function of time, is shown in Attachment V. The initial heat transfer from the waste package is $1.54 \text{ KW/m}_{(\text{drift})}$ and decays with time to 0.187 KW/m at 50 years, and less than $.003 \text{ KW/m}$ after 1000 years. For the simulated first 50 years only 30 percent of this heat is input into the model to account for 70 percent heat removal by ventilation during the pre-closure period.

Heat transfer from the waste package to the drift wall is implemented in the model by using time-varying “effective” thermal conductivities (for open spaces within the drift) that were calculated to account for radiative and convective heat-transport components. These time-varying data were input into the model as coefficients (values between 0 and 1) for each open zone within the drift. Each zone was also assigned a constant maximum thermal conductivity ($K_{th_{\text{max}}}$), which was then

multiplied by the corresponding time-varying coefficients to obtain effective conductivities as a function of time (Attachment VI). The sources of these data are listed in Table 2.

The effective thermal conductivities and corresponding open zones of the drift during preclosure are not the same as during post-closure. Only one open space between the waste package and the drift wall is considered for the pre-closure period (no backfill or dripshield, $K_{th_{max}} = 10.44$ W/m K). For post-closure, two zones are considered: (1) the open space between the waste package and the dripshield (Inner Zone, dripshield included, $K_{th_{max}} = 3.426$ W/m K), and (2) the open space between the backfill and the drift wall (Outer Zone, $K_{th_{max}} = 9.068$ W/m K) (Figure 1). Accordingly, model runs were started with the pre-closure thermal conductivity data, then stopped after 50 years and restarted with the corresponding post-closure data.

The implementation of the drift design into the model is further documented in Scientific Notebook YMP-LBNL-DSM-NS-1, p. 11-14.

4.2 CRITERIA

This AMR complies with the DOE interim guidance (Dyer 1999). Subparts of the interim guidance that apply to this analysis or modeling activity are those pertaining to the characterization of the Yucca Mountain site (Subpart B, Section 15), the compilation of information regarding geochemistry and mineral stability of the site in support of the License Application (Subpart B, Section 21(c)(1)(ii)), and the definition of geochemical parameters and conceptual models used in performance assessment (Subpart E, Section 114(a)).

4.3 CODES AND STANDARDS

No specific formally established standards have been identified as applying to this analysis and modeling activity.

INTENTIONALLY LEFT BLANK

5. ASSUMPTIONS

There are many assumptions that generally underlie numerical modeling of heat and fluid flow in unsaturated porous fractured media. In addition to these assumptions there are numerous assumptions underlying the calculation of mineral-water reactions, the transport of aqueous and gaseous species, and the conceptual models that are used to describe the chemical and physical systems.

The model assumptions are categorized according to the section into which they apply and are as follows:

A. General THC Process Model Assumptions (used in Sections 6.1, 6.2, and 6.3)

1. It is assumed that the rock can be described by the dual permeability model that considers separate, but interacting fracture and matrix continua. The fracture continuum is considered as separate but interacting with the matrix continuum, in terms of the flow of heat, water, and vapor through advection and conduction. Aqueous and gaseous species are transported via advection and molecular diffusion between fractures and matrix. Each continuum has its own well-defined initial physical and chemical properties. It is assumed that the dual-permeability approach, with appropriate material and fracture properties and an appropriate discretization of time and space, is an accurate approximation of the real world. The dual-permeability approach for modeling physical processes in fractured-porous media is discussed in detail in other AMRs. This approach is validated by the comparison of measured geochemical data to results of simulations presented in this AMR (Section 6.2.7). No further justification is necessary.
2. It is assumed that the thermal conductivity and heat capacity of the precipitated mineral assemblage are the same as the host rock. The mass of mineral precipitated is much smaller than the mass of mineral originally in place. Also, because nearly all of the minerals treated in the model are naturally occurring at Yucca Mountain, this assumption is reasonable and does not need to be validated.
3. It is assumed that the infiltrating water and that in the fractures have the same chemical composition as the matrix pore water that was collected from Alcove 5, near the Drift Scale Test location, as given in Table 3. This analysis is the average of two samples taken near the DST location; therefore it may be taken as typical. A more detailed discussion of this assumption is given in Section 6.1.2. No further justification is required for this assumption.
4. It is assumed that the physical properties of the gas phase are unaffected by changes in the partial pressure of CO₂ resulting from heating, calcite reactions, and gas-phase transport. This assumption is justified by the results of the model runs (Figures 28 and 29), which show that the volume fraction of CO₂ is generally less than 5% and always less than 10%. Although the molecular weight of CO₂ is greater than that of air (approximately 44 versus 29), the density is only increased proportionally to the volume fraction of CO₂ and the ratio of the molecular weights. This would result in a density

increase of about 5% for a gas with a volume fraction of CO₂ of 10%. These conditions make the effect of evolved CO₂ on the physical properties of the gas phase negligibly small, and justify the use of this assumption without further justification.

5. Diffusion coefficients of all aqueous species are assumed to be the same. This is justified because the tracer diffusion coefficients of aqueous species differ by at most about one order of magnitude, with many differing by less than a factor of 2 (Lasaga 1998, p. 315). This assumption does not need to be confirmed, for the above reason.
6. The dissolution rate of silica-rich glass has been found to follow a dependence of H₂O diffusion through a reaction-product layer (Mazer et al. 1992). Because the volcanic glass in the rocks at Yucca Mountain is approximately 10 million years old, and has undergone varying degrees of alteration, a constant thickness product layer on the glass surface was assumed for recalculation of the dissolution rate constant at 25°C. It is assumed that the uniform layer is 10 μm thick. The layer cannot be thicker than a typical grain diameter (100 μm). However if it is too thin, a typical grain would be completely dissolved in less than 10 million years. A thickness of 10 μm results in a grain dissolution thickness of about 30 μm, thus satisfying both the above requirements. Details of the calculations are given in scientific notebook YMP-LBNL-YWT-ELS-1, p. 43. No further justification or confirmation is necessary.

B. Specific Drift Scale Test THC Model Assumptions (used in Section 6.2)

1. Heat transfer from the electrical heaters in the drift to the wall of the drift is approximated by applying heat directly to the drift wall, instead of calculating radiative heat effects. Because THC processes in the rock outside the drift are our main objective, it is only necessary to capture the effective heat flux into the wall of the drift. This assumption does not need to be confirmed as it is solely used as an alternative method for specifying the heat flux into the rock mass.
2. The concrete invert is considered non-reactive and does not affect the chemistry of waters and gases outside the drift. Because the system is in a heating phase, the concrete is drying out over the time-scale investigated and thus there is no seepage water to interact with it.

C. Specific THC Seepage Model Assumptions (used in Section 6.3)

1. For the THC Seepage Model simulations, the drift wall is considered as a no-flux boundary for fluid and chemical species. There are a few major reasons for making this assumption. First, our objective is to calculate the water and gas compositions that reach the drift wall, and not THC processes in the drift itself; in-drift THC processes are being considered in AMRs that are being prepared in support of the Engineered Barrier Systems PMR. Because the consideration of a permeable drift wall would necessitate having transport of aqueous and gaseous species through very small volume elements, the computational effort is increased dramatically. In either case, processes in the rock outside the drift govern compositions of aqueous liquids and gases entering the drift and

therefore this assumption is valid. Second, for a homogeneous fracture system with constant surface infiltration, the wall would act as a capillary barrier, and thus the liquid fluxes very close to the drift wall are adequately described by the model as chosen, except where there is backfill. Advective fluxes of gas at the wall may differ with a closed boundary, because convection across the boundary would not occur locally. The net gas flux toward the drift wall should be good approximation of the total gas flux into or out of the drift, assuming that the drift responds mainly to pressure changes in the mountain. No further justification is required for this assumption.

2. The backfill and invert are assumed to be non-reactive. Because only THC processes outside the drift are considered, this assumption does not need to be confirmed.

INTENTIONALLY LEFT BLANK

6. ANALYSIS/MODEL

The conceptual model, the DST THC model, and the THC seepage model and results are presented in this section. Section 6.1 describes the conceptual model for THC processes. Section 6.2 describes the DST THC model and provides validation of the conceptual model by comparison to measured water and gas chemical data. The THC seepage model is presented in Section 6.3, giving predictions of coupled THC processes for 100,000 years under boundary conditions that are varied to represent the effects of potential climatic change.

The model development, data, and results are documented in the scientific notebooks listed in Table 6 below.

Table 6. Scientific Notebooks

LBNL Scientific Notebook ID	YMP M&O Scientific Notebook ID	Page numbers	Accession number
YMP-LBNL-YWT-ELS-1	SN-LBNL-SCI-109-V1	35-70	MOL.19991109.0319
YMP-LBNL-YWT-NS-1	SN-LBNL-SCI-112-V1	72-77, 115, 137	MOL.19991124.0388
YMP-LBNL-YWT-NS-1.1	SN-LBNL-SCI-112-V1	96, 104-117	MOL.19991109.0320
YMP-LBNL-YWT-JA-1A	SN-LBNL-SCI-005-V1	39-41, 48-50	MOL.19991123.0065
YMP-LBNL-DSM-ELS-1	SN-LBNL-SCI-142-V1	3-20	MOL.19991123.0063
YMP-LBNL-DSM-NS-1	SN-LBNL-SCI-141-V1	1-30	MOL.19991123.0064
YMP-LBNL-YWT-SM-1	SN-LBNL-SCI-100-V1	291-313, 321-324	MOL.19991207.0138

6.1 THE DRIFT SCALE THC CONCEPTUAL MODEL

This section describes the THC process model underlying the numerical simulations of THC processes in the DST and for the THC Seepage model. There are many considerations regarding the development of a conceptual model that describes processes involving liquid and vapor flow, heat transport and thermal effects due to boiling and condensation, transport of aqueous and gaseous species, mineralogical characteristics and changes, and aqueous and gaseous chemistry. A conceptual model of reaction-transport processes in the fractured welded tuffs of the potential repository host rock must also account for the different rates of transport in very permeable fractures, compared to the much less permeable rock matrix. The following subsections describe the conceptual models for the various physical and chemical processes.

6.1.1 Dual Permeability Model for THC Processes

Transport rates greater than the rate of equilibration via diffusion necessarily leads to disequilibrium between waters in fractures and matrix. This can lead to differences in the stable mineral assemblage and to differences in reaction rates. Because the system is unsaturated, and undergoes boiling, the transport of gaseous species is an important consideration. The model must also capture the differences between initial mineralogy in fractures and matrix and their evolution. To handle these separate yet interacting processes in fractures and matrix, we have adopted the dual permeability method. In this method, each grid block is separated into a matrix and fracture

continuum, each of which is characterized by its own pressure, temperature, liquid saturation, water and gas chemistry, and mineralogy. Figure 2 illustrates the dual permeability conceptual model used for THC processes in the DST THC Model and the THC Seepage Model.

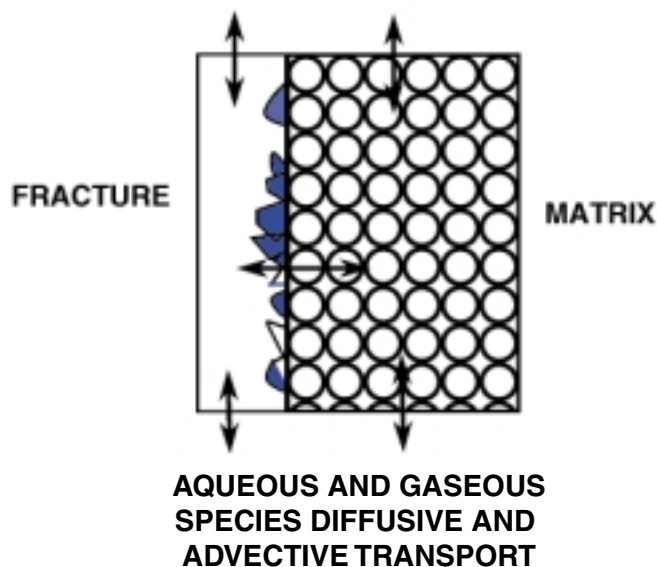


Figure 2. Conceptual Model (Schematic) for Reaction-Transport Processes In Dual-Permeability Media

6.1.2 Initial Water Chemistry

The infiltrating water chemistry could be chosen from either the pore water chemistry in the UZ at or above the potential repository horizon, or from a more dilute composition found in the perched water or saturated zone. The perched waters are much more dilute than UZ pore waters and isotopic compositions ($^{36}\text{Cl}/\text{Cl}$, $^{18}\text{O}/^{16}\text{O}$, D/H, ^{14}C) and Cl concentrations suggest that they have a large proportion of late Pleistocene/early Holocene water (Levy et al. 1997, p. 906; Sonnenthal and Bodvarsson 1999, p. 107–108).

However, for drift-scale THC processes in the TSw Unit, the water entering the top of the unit comes from the base of the PTn and is not necessarily the same composition as water entering the TCw near the land surface. A conceptual model that explains the aqueous chemistry and background $^{36}\text{Cl}/\text{Cl}$ isotopic ratios in the Exploratory Studies Facility holds that percolating water must pass mostly through the PTn matrix (because of its high permeability and low fracture density) before reverting to dominantly fracture flow in the TSw. As discussed in Levy et al. (1997, p. 907–908) this seems to be true for all areas except near large structural discontinuities in the PTn (i.e., faults). Hence, percolating water in the TSw, ultimately had come predominantly through the PTn matrix. Analyses of PTn pore waters (and some at the top of the TSw) and many Cl analyses of TSw pore waters are consistent with this interpretation (Sonnenthal and Bodvarsson 1999, p. 140-141). Therefore, as stated in Section 4.1.3, the infiltrating water and the water in the fractures are set to the same chemical composition as the matrix pore water collected from Alcove 5, and listed in Table 3.

6.1.3 Numerical Model for Coupled THC Processes

The geochemical module incorporated in TOUGHREACT V2.2 solves simultaneously a set of chemical mass-action, kinetic rate expressions for mineral dissolution/precipitation, and mass-balance equations. This provides the extent of reaction and mass transfer between a set of given aqueous species, minerals, and gases at each grid block of the flow model (Xu and Pruess 1998; Xu et al. 1999). Equations for heat, liquid and gas flow, aqueous and gaseous species transport, chemical reactions, and permeability/porosity changes are solved sequentially (e.g., Steefel and Lasaga 1994, p. 550).

The setup of mass-action and mass-balance equations in TOUGHREACT V2.2 is similar to the formulation implemented in Reed (1982, pp. 514–516). Additional provisions are made for mineral dissolution and precipitation under kinetic constraints and a volume-dependent formulation for gas equilibrium, as described below. The chemical system is described in terms of primary aqueous species (the independent variables). Minerals, gases, and secondary aqueous species are defined in terms of reactions involving only the primary species. It has been shown that if the diffusivities of all aqueous species are equal, as assumed in Section 5, only the transport of primary species (in terms of total dissolved concentrations) needs to be considered to solve the entire reactive flow/transport problem (Steefel and Lasaga 1994, p. 546).

The system of nonlinear equations, describing chemical mass-balance, mass-action, and kinetic rate expressions is solved by a Newton-Raphson iterative procedure. Activity coefficients of aqueous species are computed by an extended Debye-Huckel equation (e.g. Drever 1997, p. 28, eq. 2-12). Activity coefficients of neutral species are currently assumed equal to one, and the activity of water is computed using a method described in Garrels and Christ (1965, pp. 64–66).

Equilibration with mineral phases is computed by adding a mass-action equation, for each saturated mineral, into the system of nonlinear equations as follows:

$$\log(K_i) = \log(Q_i) \quad (\text{Eq. 2})$$

where K_i denotes the equilibrium constant and Q_i the product of the ion activities in the reaction that expresses mineral i in terms of the primary aqueous species. A term representing the amount of primary aqueous species consumed or produced by equilibration of minerals is added to the mass-balance equation for each primary species involved in mineral reactions, and is solved simultaneously with the concentrations of all primary species.

Gas species, such as CO_2 , are treated as ideal mixtures of gases in equilibrium with the aqueous solution. A mass-action equation is added to the system of simultaneous equations for each saturated gas present, except for H_2O vapor and air which are handled separately through the flow module in TOUGHREACT V2.2. The gas mass-action equation takes the form:

$$\log(K_i) = \log(Q_i) - \log(P_i) \quad (\text{Eq. 3})$$

where P_i is the partial pressure of gaseous species i . P_i is first calculated from the advective-diffusive gas transport equation in TOUGHREACT V2.2. Then P_i is replaced with the ideal gas law,

$$P_i = \frac{n_i RT}{V_g} \quad (\text{Eq. 4})$$

where n_i denotes the number of moles of gas species i , R is the gas constant, T is absolute temperature, and V_g is the gas total volume. By expressing V_g in terms of the gas saturation S_g , the porosity of the medium ϕ , and the volume of each grid block in the flow model V_{block} , Equation 4 is rewritten as:

$$P_i = \frac{n_i RT}{V_{block} \phi S_g} \quad (\text{Eq. 5})$$

The gas saturation is computed in the flow module of TOUGHREACT V2.2 (H₂O and air). The amount of trace gas species (n_i/V_{block}) is then obtained by substitution of Equation 5 into 3 and solving together with the concentrations of all primary species.

The partial pressures of gas species are not fed back to the multiphase flow module of TOUGHREACT V2.2 for solving the water and gas flow equations. Therefore, this method should only be applied to gases with partial pressures significantly lower than the total gas pressure. There is no absolute cutoff for which this approximation breaks down, and therefore it is validated by comparison to DST measured CO₂ concentrations. For cases where the partial pressures of a trace gas become closer to the total pressure, chemical equilibrium with the aqueous phase is computed correctly but the gas pressure will be underestimated in the mass-balance equation solved for gas flow. Because CO₂ concentrations encountered in the Drift Scale Test and model simulations are generally less than a few percent, and rarely over 10%, this model for the gas species is a reasonable approximation for this particular system (see Section 5).

6.1.4 Kinetic Rate Laws

Rates of mineral dissolution and precipitation close to equilibrium can be described via a relationship of the rate to the saturation index (Q/K), as follows (Steeffel and Lasaga 1994, p. 540):

$$\text{Rate}(\text{mol} / \text{s}) = \text{sgn} \left[\log \left(\frac{Q}{K} \right) \right] k A_m \prod_i a_i^p \left[\left(\frac{Q}{K} \right)^m - 1 \right]^n \quad (\text{Eq. 6})$$

where a_i is the activity of each inhibiting or catalyzing species, and p is an empirically determined exponent. The rate constant (k) is given as (Steeffel and Lasaga 1994, p. 541):

$$k = k_0 \exp \left[\frac{-E_a}{R} \left(\frac{1}{T} - \frac{1}{298.15} \right) \right] \quad (\text{Eq. 7})$$

Following Steefel and Lasaga (1994, p. 568), we set $p=0$ for each species so that the product $\prod_i a_i^p = 1$, and has been eliminated from Equation 6. The ratio of the species activity product (Q) and the equilibrium constant (K) describes the extent to which a mineral is in disequilibrium with a given solution composition. For Q/K equal to one, the mineral is at equilibrium and thus the net rate of reaction becomes zero. For Q/K greater than one, the mineral is oversaturated and thus the rate becomes positive. The expression “ $\text{sgn} [\log(Q/K)]$ ” ensures that the correct sign is enforced when the exponents m and n are not equal to one. The variable A_m is the reactive surface area expressed in units of m^2 mineral/kg water. The temperature dependence of reaction rates is given by the activation energy (E_a) in units of kJ/mol. T is the temperature in Kelvin units.

Carroll et al. (1998, p. 1379) noted that the calculated rates of amorphous silica precipitation, based on Rimstidt and Barnes (1980, p. 1683) are about three orders of magnitude lower than those observed in geothermal systems. Carroll et al. (1998, p. 1379) presented experimental data on amorphous silica precipitation for more complex geothermal fluids at higher degrees of supersaturation, and also for a near-saturation simple fluid chemistry. Under far from equilibrium conditions, the rate law for amorphous silica precipitation has been expressed as (Carroll et al. 1998, p. 1382):

$$\text{Rate}(\text{mol} / \text{s}) = k_0 A_m \left(\frac{Q}{K} \right)^m \quad (\text{Eq. 8})$$

This rate does not tend to zero as Q/K goes to one, and therefore, a modification was made to this law so that it tends to zero as Q/K approaches one (described in scientific notebook YMP-LBNL-YWT-ELS-1, p. 45).

The dissolution rate of silica-rich glass has been found to follow a dependence of H_2O diffusion through a reaction product layer (Mazer et al. 1992). Given that the volcanic glass in the rocks at Yucca Mountain is at least 10 million years old, and has undergone varying degrees of alteration, there should be significant development of a reaction product layer. A constant thickness product layer on the glass surface was assumed (Assumption A6 in Section 5) for recalculation of the rate constant at 25 °C. This thickness was taken to be 10 microns. Details of the calculation are given in scientific notebook YMP-LBNL-YWT-ELS-1 (p. 43).

The rate constant for dissolution and precipitation of fluorite was recalculated from the linear growth rate of grains (Knowles-van Cappellan et al. 1997, p. 1873) by taking the grain to have a cubic morphology. Details of the calculation are given in scientific notebook YMP-LBNL-YWT-ELS-1 (p. 44).

Kinetic data for minerals that were used in the simulation of drift-scale THC processes were given in Table 4, with comments regarding their sources and derivations.

Over a finite time step (Δt), the change in the concentration of each primary species j due to mineral precipitation or dissolution under kinetic constraints is computed from the sum of the rates, r_i , of all j -containing minerals i as follows:

$$\Delta C_j = -\sum r_i v_{i,j} \Delta t \quad (\text{Eq. 9})$$

where v_{ij} is the stoichiometric coefficient of component j in mineral i . These concentration changes are incorporated into the mass-balance equation of each primary species involved in mineral reactions, using Equations 6 through 8, and solved simultaneously with the concentrations of all primary species.

6.1.5 Fracture and Matrix Mineral Reactive Surface Areas

6.1.5.1 Fracture Mineral Reactive Surface Areas

In the dual-permeability method, the porosity of the fracture medium can be taken as 1.0; however, for modeling of mineral dissolution and precipitation, there would be no rock to dissolve. Because the dissolution rates of many minerals are quite small at temperatures below 100°C, only a small volume of rock adjoining the open space of the fracture need be considered as the starting rock fraction. The porosity of the fracture medium was set to 0.99, thus making available 1% of the total fracture volume for reaction, but producing a minimal effect on flow and transport in the fracture continuum.

Reactive surface areas of minerals on fracture walls were calculated from the fracture-matrix interface area/volume ratio, the fracture porosity, and the derived mineral volume fractions. The fracture-matrix interface areas and fracture porosities for each unit were taken from the calibrated properties set (DTN: LB990861233129.001). These areas were based on the fracture densities, fracture porosities, and mean fracture diameter. The wall of the fracture is treated as a surface covered by mineral grains having the form of uniform hemispheres. The geometric surface area of the fracture wall can be approximated by:

$$A_r = \frac{\pi A_{f-m}}{2\phi_{f-m}} \quad (\text{Eq. 10})$$

where A_r is the reactive surface area (m^2/m^3 fracture medium), A_{f-m} is the fracture matrix interface area/volume ratio (m^2 fracture/ m^3 fracture + matrix volume), and ϕ_{f-m} is the fracture porosity of the rock. This is the surface area that is given as an input to the model simulations as an approximation of the reactive surface area.

The reactive surface area of each mineral (in units of m^2 mineral /kg water) that is used in Equations 6 and 8 is then given by:

$$A_m \text{ (m}^2\text{/ kg water)} = \frac{A_r f_m}{\rho_w \phi_f} \quad (\text{Eq. 11})$$

where f_m is the volume fraction of the mineral in the mineral assemblage, ρ_w is the density of water (taken as a constant 1000 kg/m³) and ϕ_f is the porosity of the fracture medium, as opposed to the fracture porosity of the rock. This is the surface area/water mass ratio for a mineral in a liquid-saturated system.

To provide the correct rock/water ratio in an unsaturated system, the form of this surface area can be written as:

$$A_m \text{ (m}^2\text{/ kg water)} = \frac{A_r f_m}{\rho_w \phi_f S_w} \quad (\text{Eq. 12})$$

where S_w is the water saturation. However, as S_w goes to zero the reactive surface area would tend to infinity. Clearly, at a very low liquid saturation the surface area of the rock contacted by water likely is much smaller than the total area. Two methods have been implemented to address this phenomenon.

The first method considers that the surface area contacted by water diminishes proportionately to the saturation. This yields the saturated surface area given by Equation 11.

The second method employs the active-fracture-model concept (Liu et al. 1998, pp. 2636–2638) with a modification for the consideration of water-rock reactions taking place below the residual saturation. The form of the active fracture parameter for reaction is then given by the following set of equations:

$$S_{ar} = (S_w - S_m)/(1 - S_m) \quad (\text{Eq. 13})$$

$$a_{fmr} = S_{ar}^{(1+\gamma)} \quad (\text{Eq. 14})$$

where S_m is the minimum liquid saturation for which water-rock reactions are considered and S_{ar} is the effective saturation for reaction. The active fracture model parameter, γ , is obtained from the calibrated hydrological property set (DTN: LB990861233129.001). The factor that reduces the surface area contacted by the water phase is given by a_{fmr} . In all simulations S_m is set to the very small saturation of 1×10^{-4} , to ensure that reactions take place until there is virtually no water left (e.g., during dryout via ventilation or heating). Finally, the reactive surface area, using this modified form of the active fracture model, is given by:

$$A_m (\text{m}^2/\text{kg water}) = \frac{A_r a_{fmr} f_m}{\rho_w \phi_f S_w} \quad (\text{Eq. 15})$$

The surface area calculated in this way is applicable only to reactions taking place in the fracture medium.

6.1.5.2 Matrix Mineral Reactive Surface Areas

Mineral surface areas in the rock matrix were calculated using the geometric area of a cubic array of truncated spheres that make up the framework of the rock (Scientific Notebook YMP-LBNL-YWT-ELS-1, pp. 37–39, Sonnenthal and Orotoleva 1994, p. 405-406). Clay minerals are considered as coatings of plate-like grains. The mineral surface areas of framework grains (truncated spheres) in contact with the open pore space are calculated using an initial grain diameter, followed by successive truncation of the grains in the vertical direction until the porosity of this system is close to the measured porosity of the rock. In the welded tuff, crystals are often tightly intergrown with little or no pore space within the aggregate. Thus, a check is made so that the resultant mean pore throat size and spacing yields a permeability (calculated from a modified Hagen-Poiseuille relation—Ehrlich et al. 1991, p. 1582, Eq. 11) that is relatively close to the measured saturated permeability.

The grains forming the framework of this rock are considered to be the primary high-temperature phases of the tuff (i.e., quartz, cristobalite, tridymite, and feldspars). The abundance of secondary phases (i.e., those that formed as alteration products or low temperature coatings on the primary assemblage), such as clay minerals, are used to reduce the free surface area of the framework grains. The surface areas of the secondary phases are calculated assuming a tabular morphology.

The full details of the geometric calculations are given in scientific notebook YMP-LBNL-DSM-ELS-1 (pp. 37–39).

6.1.6 Effects of Mineral Precipitation/Dissolution on Hydrologic Properties

6.1.6.1 Porosity Changes

Changes in porosity and permeability from mineral dissolution and precipitation have the potential for modification of the percolation fluxes and seepage fluxes at the drift wall. In this analysis, porosity changes in matrix and fractures are directly tied to the volume changes due to mineral precipitation and dissolution. Since the molar volumes of minerals created by hydrolysis reactions (i.e., anhydrous phases, such as feldspars, reacting with aqueous fluids to form hydrous minerals such as zeolites or clays) are often larger than that of the primary reactant minerals, dissolution-precipitation reactions can often lead to porosity reductions. These changes are taken into account in this analysis. The porosity of the medium (fracture or matrix) is given by:

$$\phi = 1 - \sum_{m=1}^{nm} fr_m - fr_u \quad (\text{Eq. 16})$$

where, nm is the number of minerals, fr_m is the volume fraction of mineral m in the rock (including porosity) and fr_u is the volume fraction of unreactive rock. As the fr_m of each mineral changes, the porosity is recalculated at each time step. The porosity is not allowed to go below zero at any time.

6.1.6.2 Fracture Permeability Changes

Fracture permeability changes are approximated using the porosity change and an assumption of plane parallel fractures of uniform aperture (cubic law—Steefel and Lasaga 1994, p. 556). The modified permeability, k , is then given by:

$$k = k_i \left(\frac{\phi}{\phi_i} \right)^3 \quad (\text{Eq. 17})$$

where k_i and ϕ_i are the initial permeability and porosity, respectively.

6.1.6.3 Matrix Permeability Changes

Matrix permeability changes are calculated from changes in porosity using ratios of permeabilities calculated from the Carmen-Kozeny relation (Bear 1972, p. 166, eq. (5.10.18), symbolically replacing n by ϕ), and ignoring changes in grain size, tortuosity and specific surface area as follows:

$$k = k_i \frac{(1-\phi_i)^2}{(1-\phi)^2} \left(\frac{\phi}{\phi_i} \right)^3 \quad (\text{Eq. 18})$$

6.1.6.4 Effects of Permeability and Porosity Changes on Capillary Pressures

Changing permeability and porosity also implies changes in the unsaturated flow properties of the rock. This effect is treated by modifying the calculated capillary pressure (P_c) using the Leverett scaling relation (Slider 1976, p. 280) to obtain a scaled P_c' as follows:

$$P_c' = P_c \sqrt{\frac{k_i \phi}{k \phi_i}} \quad (\text{Eq. 19})$$

6.1.7 Geochemical Systems

Two sets of chemical components and mineral assemblages were used for the simulations for the Drift Scale Test and the THC Seepage Model. The systems are denoted Case 1 and Case 2 and are presented in Tables 7 and 8, respectively. Case 1 (“full” set) includes the major solid phases (minerals and glass) encountered in geologic units at Yucca Mountain, together with a range of possible reaction product minerals, CO_2 gas, and the aqueous species necessary to include these solid phases and the pore-water composition into the THC model. Case 2 (“simplified” set) is a

subset of Case 1 excluding aluminum silicate minerals, which form or dissolve much less easily than minerals such as calcite or gypsum, and for which thermodynamic and kinetic data are not as well established as for the other minerals. As discussed later (Sections 6.2.7.2 and 6.3.5.2), Case-2 THC simulations appear to predict more realistic pH and gas-phase CO₂ concentration trends than Case-1 simulations, because the latter may be overpredicting the reaction rates of aluminum silicate minerals, indirectly affecting these parameters. Therefore, even though Case 1 represents the near-field environment more completely than Case 2, the latter may yield more accurate THC model results than Case 1.

Table 7. Case-1 Mineral Assemblage, Aqueous and Gaseous Species

Species	Minerals
Aqueous:	
H ₂ O	Calcite
H ⁺	Tridymite
Na ⁺	α-Cristobalite
K ⁺	Quartz
Ca ⁺²	Amorphous Silica
Mg ⁺²	Hematite
SiO ₂	Fluorite
AlO ₂ ⁻	Gypsum
HFeO ₂	Goethite
HCO ₃ ⁻	Albite
Cl ⁻	Microcline
SO ₄ ⁻²	Anorthite
F ⁻	Ca-Smectite
	Mg-Smectite
Gas:	Na-Smectite
CO ₂	K-Smectite
	Illite
	Kaolinite
	Sepiolite
	Stellerite
	Heulandite
	Mordenite
	Clinoptilolite
	Glass

Table 8. Case-2 (Simplified) Mineral Assemblage, Aqueous and Gaseous Species

Species	Minerals
Aqueous:	
H ₂ O	Calcite
H ⁺	Tridymite
Na ⁺	α-Cristobalite
Ca ⁺²	Quartz
SiO ₂	Amorphous Silica
HCO ₃ ⁻	Glass
Cl ⁻	Gypsum
SO ₄ ⁻²	
Gas:	
CO ₂	

6.2 THE DRIFT SCALE TEST THC MODEL

The DST is the second underground thermal test that is being carried out in the ESF at Yucca Mountain, Nevada. The purpose of the test is to evaluate the coupled thermal, hydrological, chemical and mechanical processes that take place in unsaturated fractured tuff over a range of temperatures from approximately 25°C to 200°C. The DST THC Model provides an important validation test for the extension of the THC conceptual model to the THC Seepage Model. It should be noted that the geochemical model input parameters have not been calibrated to the data collected from the DST. Modifications to a few rate law parameters have been made because of some of the simplifications made in the mineralogy (endmembers instead of solid solutions) and because of the general effects of inhibition of precipitation or dissolution (e.g., quartz and calcite). However, these input data were not tailored to match any field data, but were modified to correct for processes that are not considered in the model. More important than matching any particular data, the goal is a better understanding of coupled processes so that the models can be applied to long-term predictions of near-field THC processes.

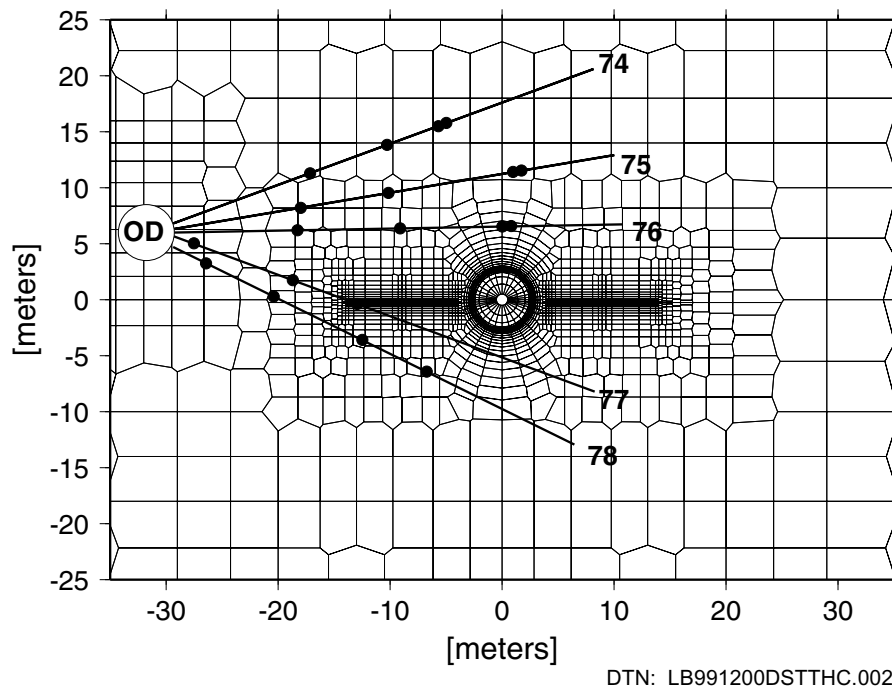
6.2.1 Background Information

The DST heaters were turned on on December 3, 1997 with a planned four-year period of heating, followed by four years of cooling. Our objectives were to make predictions of the coupled thermal, hydrological, and chemical (THC) processes, followed by model refinement and comparison to measured data. It was expected that some water (formed by condensation of steam in fractures) would be collected. Throughout 1998 and 1999, samples of water and gas were collected from boreholes, allowing for comparison of analytical data on water and gas chemistry to DST THC model results.

6.2.2 Drift Scale Test 2-D Numerical Grid

Because THC simulations are computationally intensive, and the model area is fairly large, 2-D simulations (rather than 3-D) were conducted, so that the number of model grid blocks, and thus computation time, could be kept to workable dimensions without losing too much resolution.

The development of the two-dimensional dual-permeability numerical grid for the DST is described in scientific notebook YMP-LBNL-YWT-SM-1 (pp. 291-308). It consists of 4,485 grid blocks, including fracture and matrix. It represents a vertical cross-section through the drift at a distance approximately 30 meters from the bulkhead (Figure 3). Between the grid elements within the drift interior and one representing the heater test alcove are elements designed to act as the bulkhead and the insulating material. Within the drift, heat is applied directly to the drift wall as an approximation to explicitly representing the electric heaters and calculating the heat transfer across the air mass inside the drift. The test includes a plane of linear wing heaters on each side of the drift that are given small grid elements in the model. Small grid elements are employed adjacent to the wing heaters and drift wall to capture the strong gradients in temperature and liquid saturation in these regions. For the simulations, some mesh elements in the drift interior were removed, and near the drift base were replaced by nodes representing the concrete invert.



NOTE: OD=Observation Drift. Locations of hydrology boreholes and sensor locations are shown for a vertical plane approximately 30 m inward from the bulkhead.

Figure 3. Close-Up of Numerical Mesh Used for Drift Scale Test THC Model Simulations.

6.2.3 Heater Power

The most recent calibrated heater power measurements are used in the model and are described in scientific notebook YMP-LBNL-YWT-SM-1 (pp. 309–313). The wing heaters are split into inner and outer zones with the outer zone producing a greater power output in order to approximate the presence of an adjacent parallel drift. The DST THC Model employs a 9-month period of preheat ventilation at ambient temperature corresponding approximately to the time that was required to set up the test. The heating schedule imposed on the model is then set in accordance with an interim plan for the test: 21 months of heating at full power (bringing the model simulation to early September 1999), followed by 10% power reduction for each of the next four months, then continuous heating at 60% of full power until 4 years after initiation of heating, and finally 4 more years of cooling. The 10% power reduction after September 1999 has not been implemented, and therefore only model data up to September 1999 will reflect closely the temperature history of the test. For the purpose of validating the THC conceptual model only results prior to this time for which chemical data on water and gases were collected will be discussed in this AMR.

6.2.4 Hydrological and Thermal Boundary and Initial Conditions

The top boundary is approximately 99 m above the drift center, with the bottom boundary at approximately 157 m below the center. The top and bottom boundaries were set to constant temperature, pressure, and liquid saturation, based on steady-state values obtained from simulations of a 1-D column extending from the land surface to the water table (see scientific notebook YMP-LBNL-YWT-SM-1, pp. 291–308). These values were obtained using the calibrated drift scale hydrologic parameter set for the present climate (mean infiltration) at an infiltration rate of approximately 1.05 mm/year (DTN: LB991091233129.001). The side boundaries of the domain are located outside of the test influence area (81.5 m away from the drift center on each side) and can therefore be considered as no-flux boundaries. The air pressure and temperature in the observation drift are set to constant values, and therefore do not reflect temporal fluctuations in barometric pressure or tunnel air temperatures. The Heater Drift wall is open to advection and conduction of heat and mass, and vapor diffusion.

6.2.5 Geochemical Boundary and Initial Conditions

Geochemical data used in the simulations are given in Tables 2 through 4 in Section 4 and Appendices II through IV. The top and bottom boundaries were set so that no mineral reactions take place, but they were open to aqueous and gaseous species transport. Their volumes were set to extremely large values so that they act essentially as constant concentration boundaries. All aqueous and gaseous species concentrations in the rock were set initially to a uniform value (given in Section 4). The heater drift, alcove, and observation drift CO₂ concentrations were set to approximately that of the atmosphere. The alcove and observation drift CO₂ concentrations were kept essentially constant, but the heater drift was allowed to exchange CO₂ between the rock and the observation drift. The side boundaries were treated as no-flux to advection and diffusion. Simulations were run using the initial geochemical model cases (full – Case 1 and simplified – Case 2).

6.2.6 Measured Geochemical Data Used for Comparison to Simulation Results

Two main sources of data are used in this report for comparison to simulation results. Aqueous species concentrations and pH were available for water samples collected from hydrology boreholes (DTN: LL9907028804244.100). Gas-phase CO₂ concentrations and stable isotopic ratios ($\delta^{13}\text{C}$, $\delta^{18}\text{O}$, δD , and ^{14}C) were measured from gases pumped from hydrology boreholes (DTNs listed in Table 2). For the gas phase compositions, direct comparisons of model results will be made only to CO₂ concentrations; however, isotopic data also has provided important insight into THC processes.

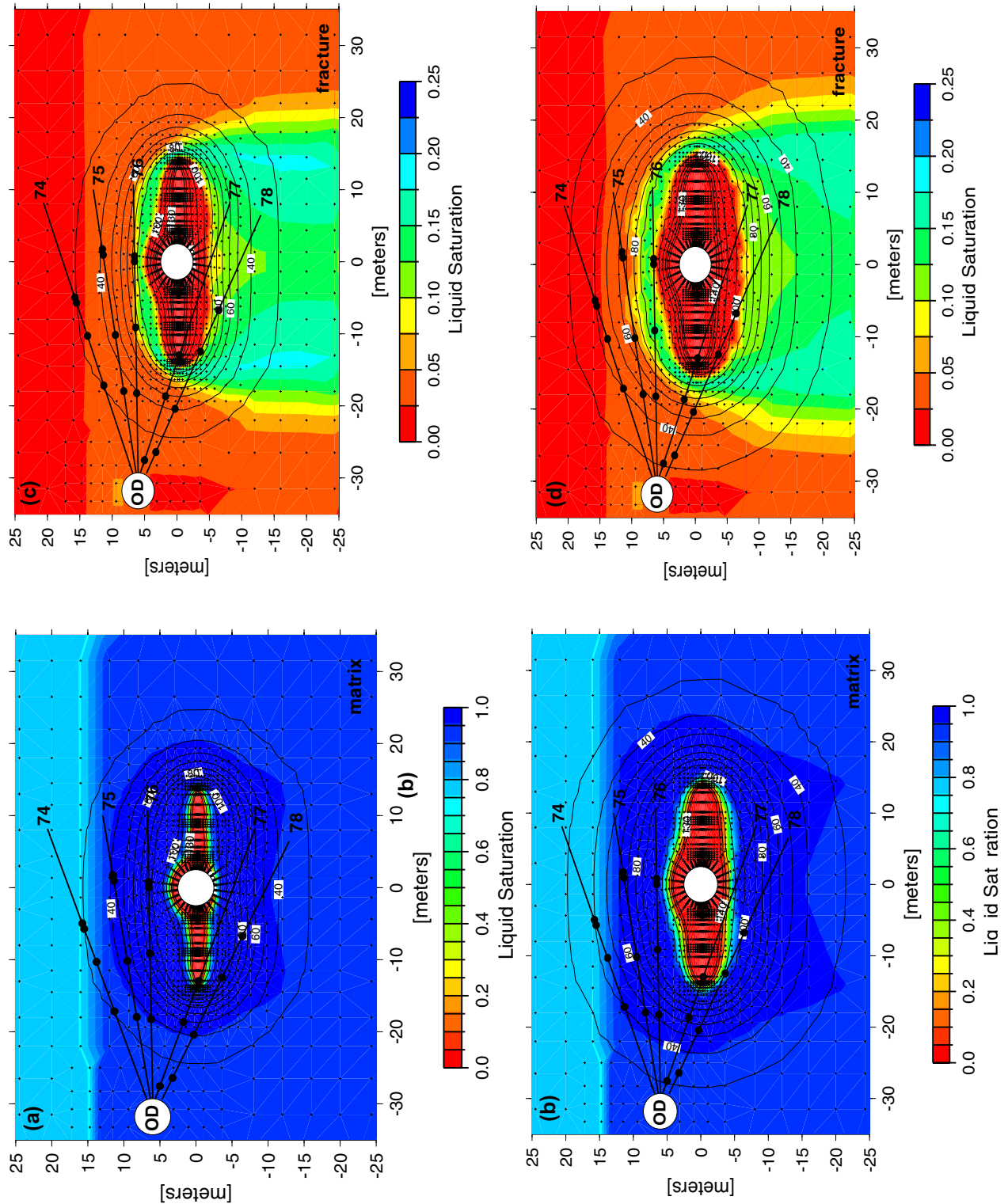
6.2.7 Validation of DST THC Model by Comparison of Simulation Results to Measured Data

6.2.7.1 Thermal and Hydrological Evolution

The main driving force for changes in the hydrological and chemical behavior of the system is, of course, the strong thermal load applied to the system. The resulting changes in temperature, liquid saturation, and gas phase composition lead to changes in the chemistry of water, gas, and minerals. Key aspects of the thermohydrological behavior of the DST that drive the chemical evolution of the system are treated in this section; however, a detailed analysis of the thermohydrology of the DST will be presented in another AMR.

The modeled distributions of temperature and liquid saturation are shown in Figures 4a-d, corresponding to twelve and twenty months during the heating phase of the DST. The zone of dryout increases over time, and a wider contour interval in temperature between the 90°C and 100°C isotherms indicates the presence of an isothermal boiling/condensation zone, especially above the wing heaters. A large drainage zone is apparent in the fractures below the heaters, and in the matrix as well, after 20 months. The buildup of water above the heaters is fairly localized, but moves up into the region of the upper hydrology boreholes after 20 months of heating.

Temperatures predicted by the two-dimensional model tend to be somewhat higher than for a three-dimensional model or the real system because there is no heat loss in the third dimension. Therefore, this model is most applicable to areas near the center of the test – away from both the bulkhead and the opposite end of the Heater Drift.



DTN: LB991200DSTTHC.002

Figure 4. Liquid Saturation (Colors) and Temperature (Contour Lines) around the DST (Case 2) at 12 Months (Matrix – 4a, Fracture – 4b), and at 20 Months (Matrix – 4c, Fracture – 4d).

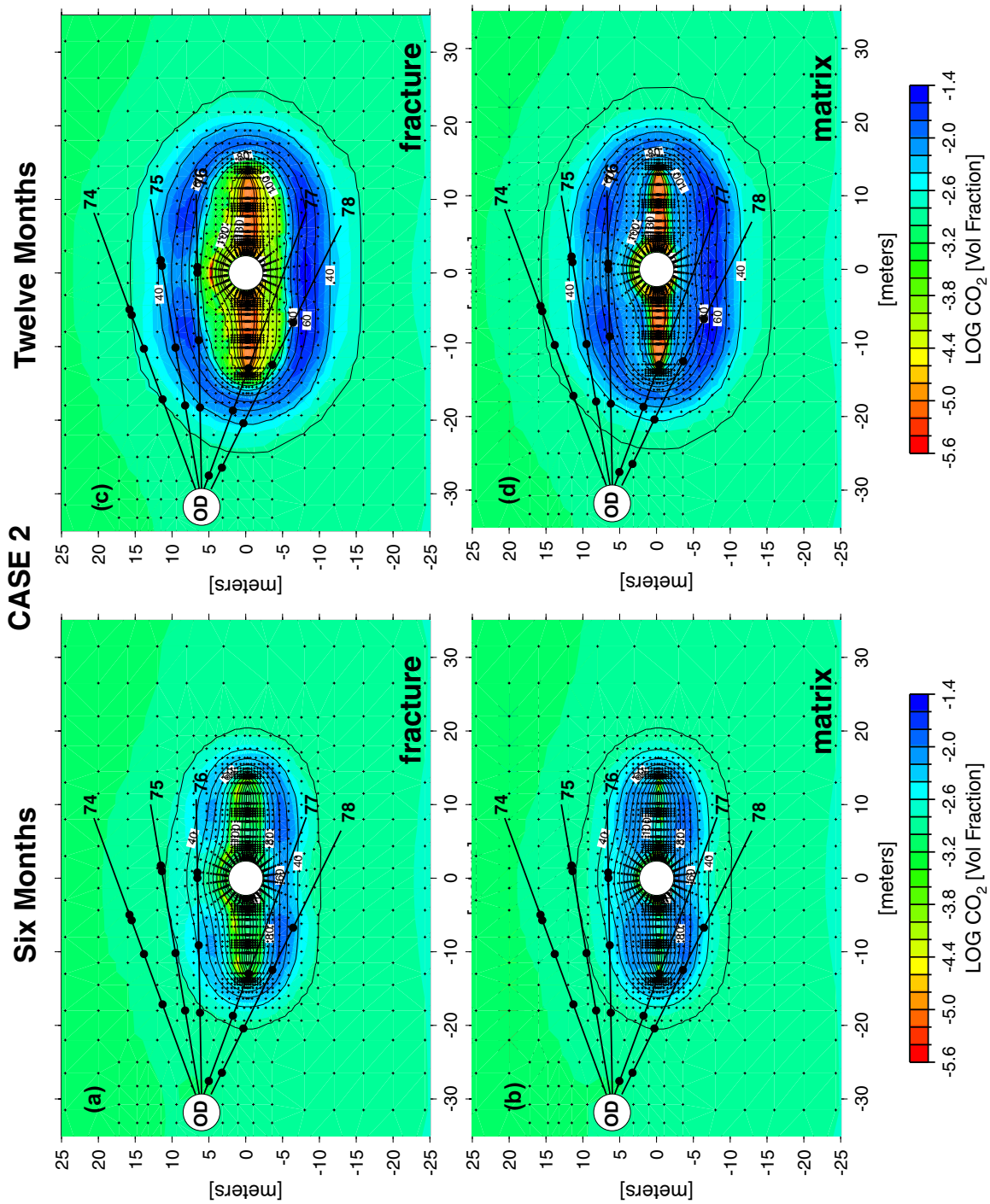
6.2.7.2 Gas Phase CO₂ Evolution

The concentration of CO₂ in the gas phase can change markedly owing to changes in temperature, aqueous phase chemical changes and mineral-water reactions, and through advective and diffusive transport. Because CO₂ partial pressure has a strong effect on water pH, it is important to validate the CO₂ behavior in our simulations. Numerous measurements of CO₂ concentrations in gases from the Drift Scale Test have been made as a function of space and time, so that a more detailed comparison of the model results to these data can be made than to measured water chemistry. Model results are presented for the two geochemical systems described in Tables 7 and 8 (Case 1 and Case 2).

In this section we present CO₂ concentrations measured in gas samples taken from boreholes during the DST, and compare them to simulation results using the DST THC Model (Section 6.2.7.2). Sampling locations are not identical to the mesh node coordinates, and are from borehole intervals that are several meters long and may encompass a wide range of temperatures as a result of their orientation relative to the heaters. The actual heater operation was also not exactly as planned. In addition, the model predicts both fracture and matrix CO₂ concentrations, whereas the measured data may consist of some mixture of gas derived from fractures and that from the matrix, especially if the matrix pore water was actively undergoing boiling. Another complication arises from the fact that the gas samples have had much of the water vapor removed whereas the model results are based on a “humid” gas. The criteria for model validation are therefore as follows:

1. Where a sampling interval lies between 2 nodes, the measured values fall between the simulated values (fracture and matrix).
2. The trend of CO₂ concentrations over time in the sampling interval are clearly followed, and are clearly distinct from trends in other sampling intervals.
3. Deviations between measured and simulated values are consistent with known major discrepancies between actual and simulated heater operation or extensive water loss by condensation from gas samples prior to measurement.

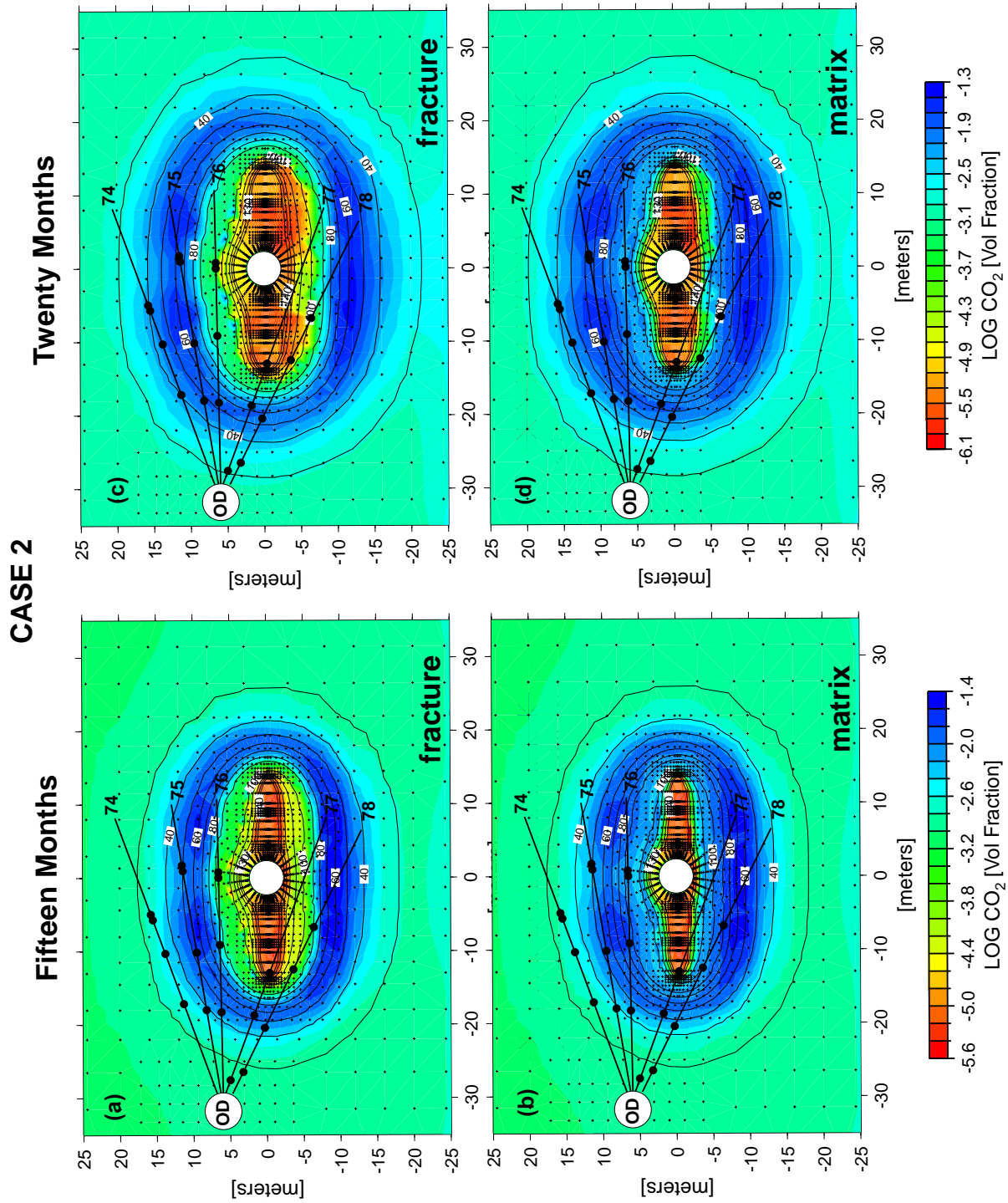
Modeled distributions of CO₂ concentrations (log volume fractions) and temperature in fractures and matrix are shown after six and twelve months of heating (which are also times for which CO₂ measurements are available) in Figure 5 for the reduced chemical system (Case 2). At both times, and in both fractures and matrix, there is a halo of increased CO₂ concentrations, centered approximately at the 60°C isotherm. Over the six-month period the halo increases in extent and magnitude considerably. Maximum CO₂ concentrations are located above and below the wing heaters and below the Heater Drift. Between approximately the 90°C and 100°C isotherms there is a region where fracture CO₂ concentrations have decreased to approximately 1000 ppmv, but matrix concentrations are still elevated. This area encompasses an isothermal boiling region, as evidenced from the wider spacing of the 90-100°C isotherms compared to adjacent lower and higher temperature contours. More rapid boiling in the matrix leads to higher partial pressures of CO₂ relative to the dry or nearly dry fractures. Within the dryout zone close to the drift and wing heaters, CO₂ concentrations decrease markedly in both fractures and matrix.



DTN: LB991200DSTTHC.002

Figure 5. CO₂ Concentration (log volume fraction) in Gas Phase (Case 2) around the DST at 6 Months (Fracture - 5a, Matrix - 5b) and at 12 Months (Fracture - 5c, Matrix - 5d). Results are for the reduced geochemical system (Case 2). Temperature contours are overlain.

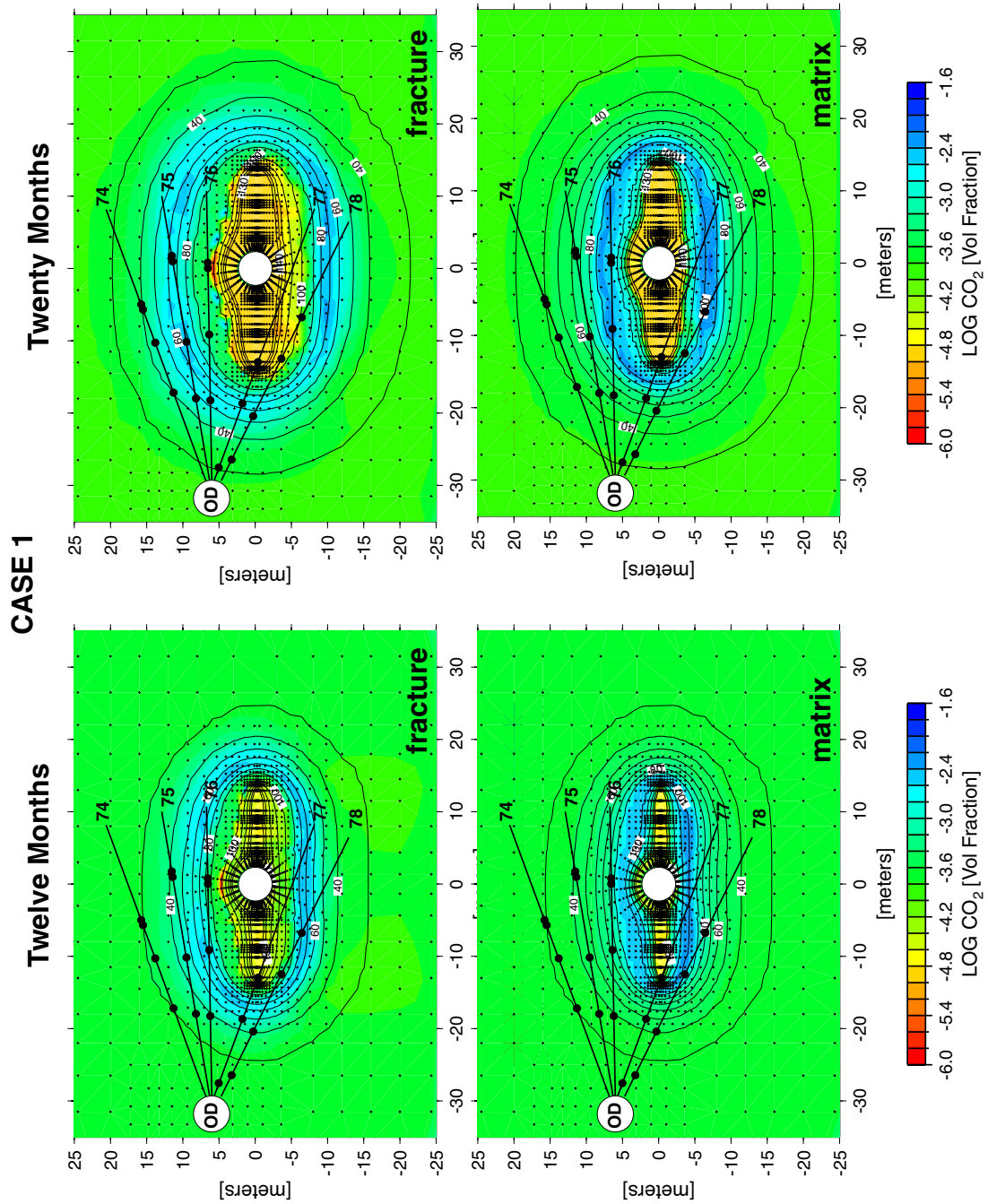
Figure 6 shows modeled CO₂ concentrations at 15 and 20 months from the same simulation. The patterns remain similar, and continue to grow outward from the heat source, with the area of the maximum concentrations decreasing slightly at 20 months relative to that at 12 months. This is a result of a widening of the zone of high concentrations as it moves away from the heat source, with the peak concentrations diminishing slightly as the isotherms widen. The highest concentration regions are situated above and below the wing heaters and over time pass progressively through the radial hydrology boreholes. Once the region around the borehole has dried out there is a sharp decrease to low CO₂ concentrations in the gas phase.



DTN: LB991200DSTTHC.002

Figure 6. CO₂ Concentration (log volume fraction) in Gas Phase around the DST (Case 2) at 15 Months (Fracture - 6a, Matrix - 6b) and at 20 Months (Fracture - 6c, Matrix - 6d). Results are for the reduced geochemical system (Case 2). Temperature contours are overlain.

For comparison, CO₂ concentrations for a simulation using the full geochemical system (Case 1) are shown in Figure 7. The pattern of concentrations is similar to the previous results; however, the maximum concentrations are significantly lower. Changes in gas chemistry are also taking place in the ambient temperature region.



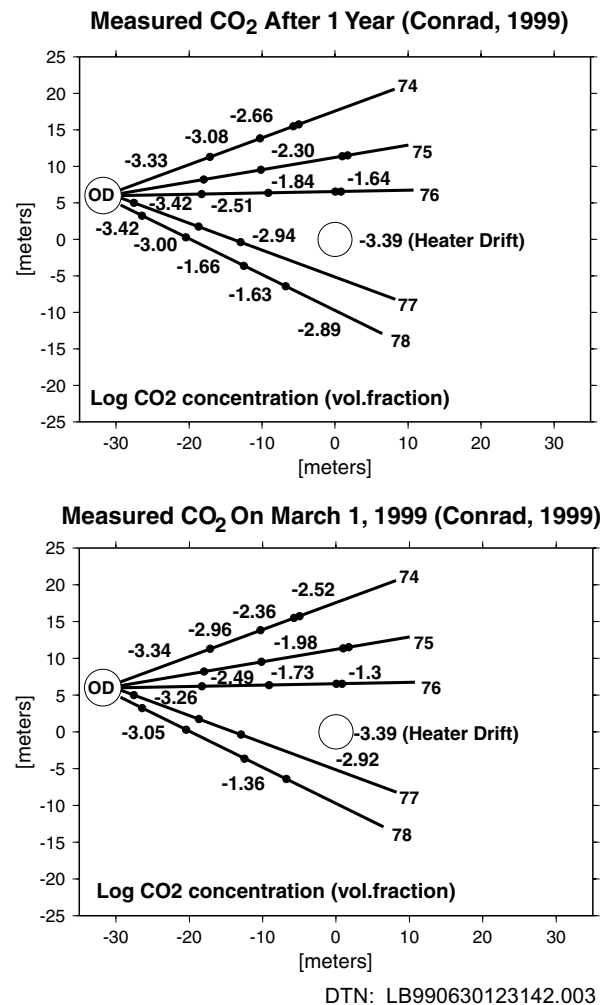
DTN: LB991200DSTTHC.002

Figure 7. CO₂ Concentration (log volume fraction) in Gas Phase (Case 1) around the DST at 12 Months (Fracture – 7a, Matrix – 7b) and at 20 Months (Fracture – 7c, Matrix – 7d). Results are for the full geochemical system (Case 1). Temperature contours are overlain.

The reason for the difference in the calculated CO₂ concentrations in this more complex geochemical system (compared to Case 2) is a result of dissolution and precipitation of various Ca-bearing minerals, such as stellerite, heulandite, calcite, anorthite, and Ca-smectite. Feldspar and calcite dissolve to form zeolites. This drives the pH up, which in turn decreases the CO₂ partial pressures through aqueous species reactions involving carbonate species (CO₂ is more soluble at elevated pH). Large differences in the relative rates of mineral-water reactions shift this equilibrium, even through the absolute rates are exceedingly small. The other controlling factor is the flux of aqueous species through percolation and of CO₂ through gas phase diffusion, relative to the rates of mineral reactions. Because the model starting conditions use measured water and gas compositions that reflect a set of conditions (infiltration, mixing, climate changes) that are unknown, it would be very difficult to reproduce a steady-state condition that matches the original data. The percolation flux has little effect over a few years, so that for comparison of the model results, we are left with the relative rates of reaction as the reason for the difference between Case 1 and Case 2 CO₂ concentrations.

Shifts in the ambient system CO₂ concentrations over a relatively short time (away from the areas of thermal effects) indicates that either the relative mineral-water reaction rates are somehow dissimilar to the real system, or that calculated starting water bicarbonate concentration (via charge balance) was off, or the measured pH was altered through the sample collection procedure. Because the starting water was supersaturated in calcite, the latter scenario is certainly a real possibility. In addition, the uncertainties in thermodynamic data for the aluminosilicates (e.g. zeolites and clays), the unknown reaction rates for many of the minerals, and the assumption of endmember mineral thermodynamic models instead of solid-solution models must play a role in the evaluation of the results. Therefore, comparison to measured data must play an important role in the evaluation of the results.

The distributions of measured CO₂ concentrations (DTNs listed in Table 2) after one year of heating and after fifteen months are shown in Figure 8. In general the locations of high concentrations are similar to the modeled concentrations with very high values above and below the wing heaters, with slightly elevated values in Borehole 74 well above the wing heaters. Comparison of the fifteen month to the one-year data, shows that in nearly all of the boreholes the CO₂ concentrations are higher. The range of measured values compares closely with the span of modeled concentrations.



NOTE: Concentrations refer to intervals between pairs of points.

Figure 8. Measured Concentrations of CO₂ (log volume fraction) in Gas Phase around the DST at 12 Months and at 15 Months.

To evaluate how the model predicts the time evolution of CO₂ concentration, which is dependent on numerous thermal, hydrological, transport, and geochemical processes, measured CO₂ concentrations from intervals that were repeatedly sampled from February 1998 to August 1999 (DTNs in Table 2) are compared to model results at the same times. The locations of these nodes relative to the borehole intervals from which the gas samples were taken are illustrated in Figure 9. Because the measured concentrations come from borehole intervals that are several meters long and not from a specific location, model data are chosen from the grid block that is closest to the center of the interval. If there is no grid block that is centered on the borehole, a node closest to the center is chosen on the outer (cooler) side of the borehole. Nodes on the cooler side are more comparable to the measured data because the 2-D model, having no heat loss in the rock perpendicular to the drift, gives temperatures that are somewhat higher than the measured

temperatures at a given time. Therefore, it is more appropriate to pick a node on the cooler rather than the hotter side. Some additional nodes around the intervals are included in some of the plots, so that the gradations in the CO₂ concentrations around or over the interval can be analyzed.

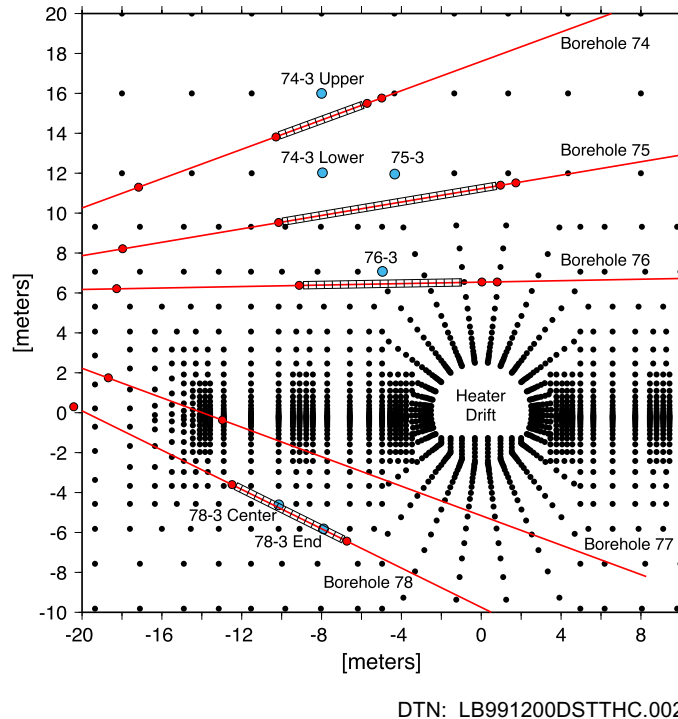


Figure 9. Close-Up of DST Grid, Showing Nodes Used to Extract Model Data for Comparison to Concentrations Measured in Gas Samples. Borehole intervals from which gas samples were taken are shown in the hatched regions.

Figures 10a-d show the time evolution of CO₂ concentrations in Borehole intervals 74-3, 75-3, 76-3, and 78-3. Measured CO₂ concentrations in interval 74-3 were observed to be only slightly elevated (1434 ppmv) over the ambient rock gas CO₂ concentration when the first sample was collected six months after the start of the test. Temperatures at the borehole sensor were still at the ambient value of 23.7°C. Concentrations rose gradually until about one year after the test at which time they rose somewhat more rapidly, to approximately 7000 ppmv at 18 months. The next sample, collected at just over 20 months into the test, had a composition close to the previous sample. The closest grid node to the center of Borehole interval 74-3 lies just about 1.5 meters above the borehole. The calculated concentrations follow a similar early history as the measured concentrations until about 12 months where the measured concentrations rise faster and to greater concentrations than the observed data. However, where the measured concentrations level out at 20 months, the modeled values are still rising and are close to the final value. For comparison, concentrations from a grid node about 2 meters below the interval also rise slowly over the first 10 to 12 months of the test and then increase more dramatically to much higher concentrations. These two nodes bracket the measured concentrations quite well. It is clear that there are very

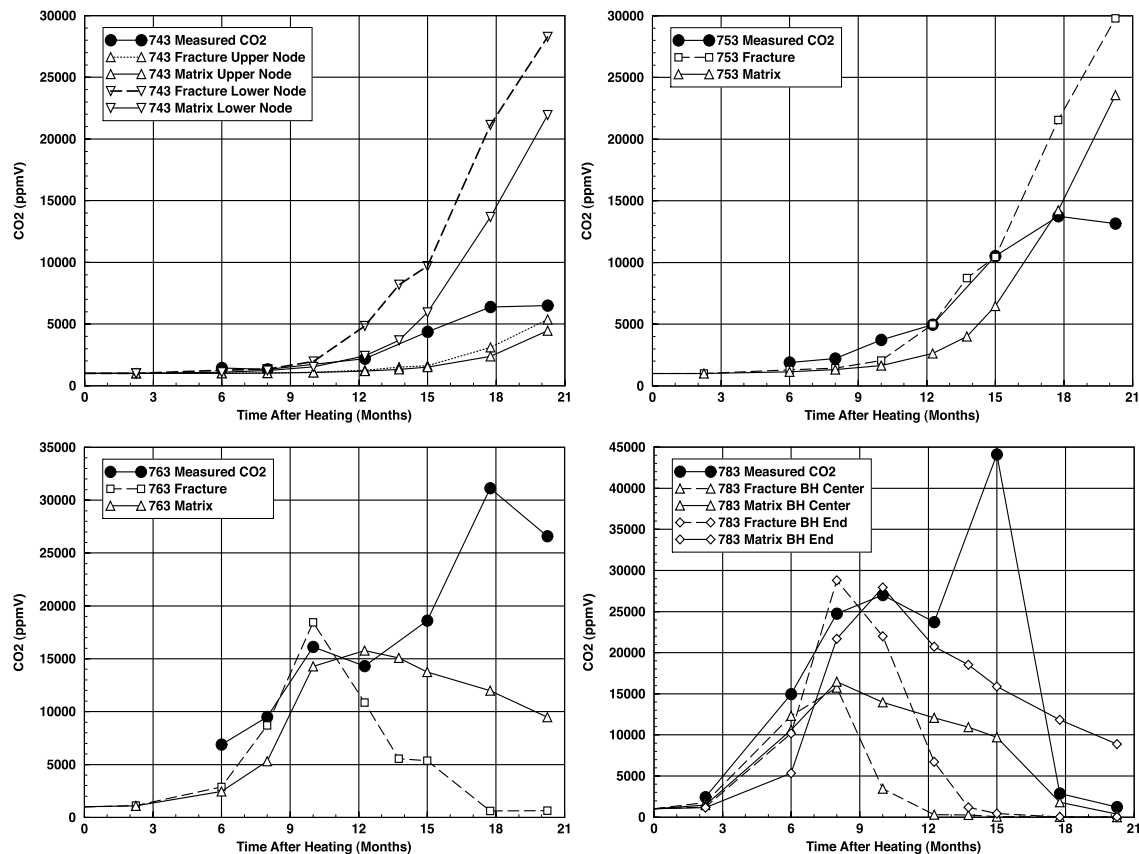
strong gradients in CO₂ concentrations over distances of only a few meters so that it would be expected that the collected gases would reflect some averaging over a region. Differences in fracture and matrix CO₂ concentrations increase as one nears the heat source and thus the sampling could be affected by this as the matrix liquid saturations decrease and more of the collected gas comes from the matrix compared to the open fractures.

In Figure 10b, the measured concentrations in Borehole interval 75-3, which is closer to the Heater Drift, are also at slightly elevated values after 6 months and rise smoothly but faster than in 74-3, until about 18 months where again the concentrations reach a plateau. The modeled concentrations match very closely the measured values until 20 months where measured concentrations stop rising.

The lack of a continuous rise in CO₂ concentrations measured in Borehole intervals 74-3 and 75-3 at 20 months does not seem to follow either the model results or the large increases in CO₂ concentrations that occurred in the other intervals as temperature rose in those regions. A 6-day period of heater power loss took place in July 1999, approximately a month previous to the time the last gas samples were collected. This may explain the low concentrations in these intervals at 20 months. Future sampling should indicate a return to increasing CO₂ concentrations.

CO₂ concentrations in Borehole interval 76-3 show a much more rapid rise to about 16,000 ppmv after only 10 months of heating. The concentrations appear to reach a plateau, but then continue to rise strongly until 20 months where they drop off somewhat. Modeled concentrations also rise rapidly to a peak in the fractures at 10 months, at which time they drop off sharply, whereas the modeled concentrations in the matrix continue to rise slowly and then drop off very gradually until 20 months. The samples collected at 18 and 20 months have considerably higher concentrations than the model predictions, even though the early samples compare closely to the calculated data.

A similar behavior can be seen in Borehole interval 78-3 (Figure 10d) where there is an even more rapid rise in measured CO₂ concentrations to about 25,000 ppmv after only 8 months, with nearly constant values to 12 months. This is followed by a large increase to 45,000 ppmv at 15 months, and then dropping off to much lower values at 18 and 20 months. Modeled data taken at the center of the interval and at the end of the interval (deeper part) follow the very steep rise to over 10,000 ppmv after 6 months of heating. From 8 to 12 months the model data from the end of the interval matches closely the measured levels (matrix only at 12 months). Except for the sharp peak at 15 months the model data also reproduces quite closely the low values at 18 and 20 months.



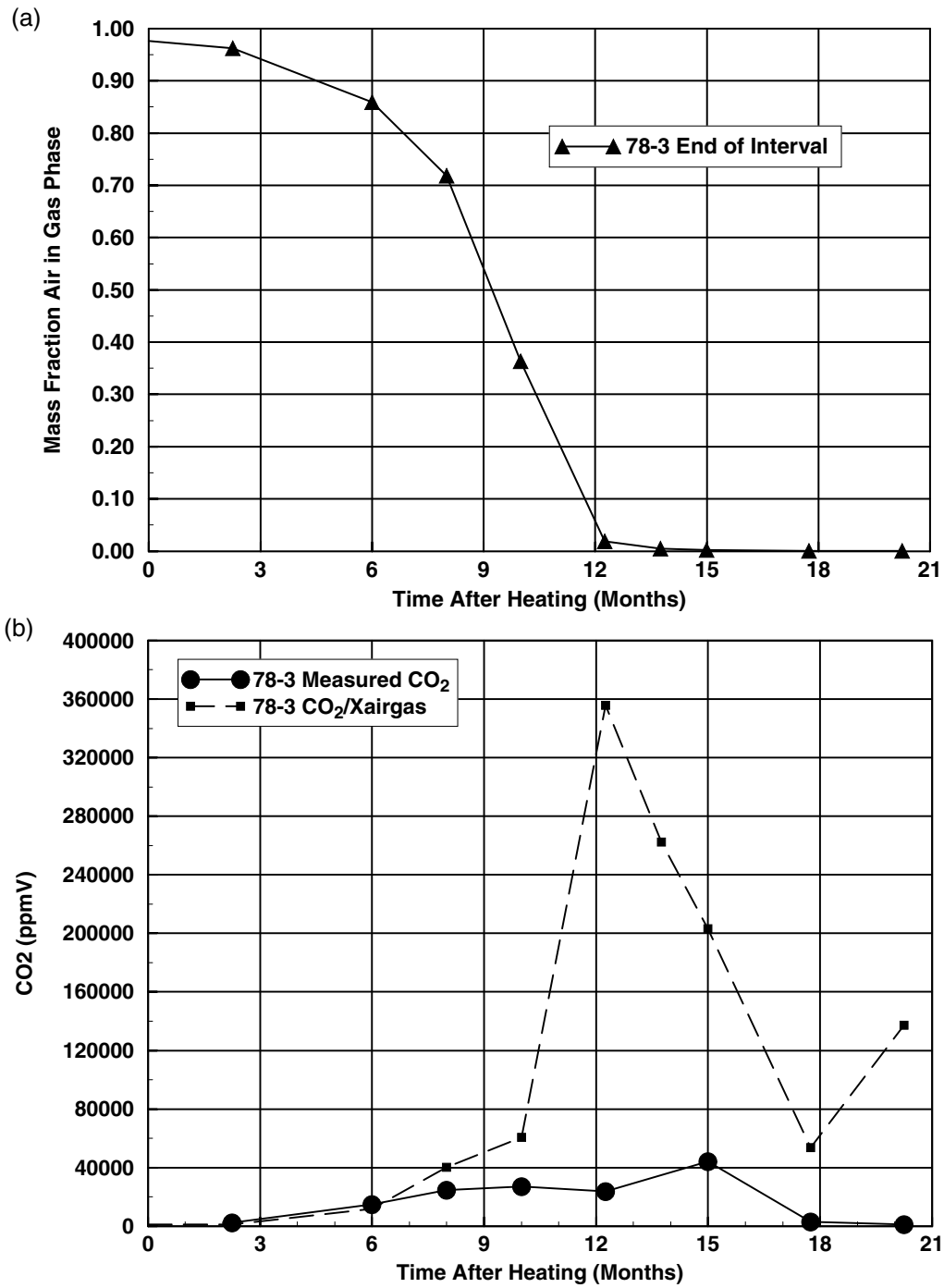
DTN: LB991200DSTTHC.002 (modeled)
 DTN: Table 2 (measured)

Figure 10. Comparison of Modeled CO₂ Concentrations (Case 2) in Fractures and Matrix over Time to Measured Concentrations in Boreholes. (a) Borehole interval 74-3 at nodes above and below. (b) Borehole interval 75-3. (c) Borehole interval 76-3. (d) Borehole interval 78-3 at nodes near center and end.

Here we examine the discrepancy between measured and modeled CO₂ concentrations in 76-3 and 78-3. The strong observed CO₂ concentration increase in 76-3 and 78-3 to values significantly higher than the predicted concentrations, after an apparent earlier maximum, occurs at different times in the two intervals, and therefore is not simply explained by some change in the heater power output. Comparison of the measured CO₂ concentrations to the model results at close to boiling temperatures could be significantly affected by the amount of water vapor in the gas phase when the sample was collected. Because the air mass fraction in the gas phase drops considerably due to the production of steam, and the samples are “dried” by condensing much of the water out at a low temperature (~ 4°C) the measured concentrations reflect the CO₂ in the air after water has been condensed out. The model results include the water vapor component and

therefore may be very different from the measured value once the air mass fraction drops to a low value and the CO₂/air ratio increases through the condensation of the water vapor.

Although no samples were collected that could be used to measure directly the water content of the gas, the model results can be used to assess the change in air mass fraction as the temperature in a borehole interval increases. Figure 11a shows the variation in air mass fraction in the gas phase over time in the center part of Borehole interval 78-3. The drop off to near zero air mass fraction at 12 months indicates that the system trends to relatively pure steam and that samples collected after this time could not be compared directly to model results without some correction for the effect of condensing out the water vapor during the sampling. A rough way to evaluate this effect qualitatively from the model results is to calculate the ratio of the CO₂ concentration in the gas phase to the air mass fraction. When the air mass fraction drops to very low values, the CO₂ concentration in the “dry” gas can be very different from that in the water-rich gas. Comparing the trend of the CO₂ to mass fraction air ratio to the measured CO₂ values in Borehole interval 78-3 shows clearly that the CO₂ in the dry gas will spike to a level much greater than the initial CO₂ peak in the air-rich gas, and at a later time. After this initial spike, the system loses much more CO₂, compared to air, and the ratio drops off sharply again. While this shows qualitatively the effect of comparing CO₂ concentrations in dry and wet gas samples, a quantitative assessment of the difference in CO₂ concentrations between the samples is more difficult because in the condensation of water during the gas sampling there will be some drive to equilibrium that would lower the CO₂ concentrations in the gas relative to what the ratio plotted in Figure 11b would predict.



DTN: LB991200DSTTHC.002 (modeled)
 DTN: Table 2 (measured)

Figure 11. (a) Modeled air mass fraction in gas phase at center of borehole interval 78-3 (fracture) over time. (b) Ratio of modeled CO₂ concentration to air mass fraction at same location as 11a over time (Case 2), with comparison to measured CO₂ concentrations over time.

The last topic on gas phase CO₂ is the composition of the Heater Drift gas compared to the model results. Because the bulkhead separating the Heater Drift from the Observation Drift is not completely sealed, the model considers some exchange of air between them. This was done originally to correct for heat loss, but it can also be used to assess the balance between the changes in CO₂ concentrations in the rock gas and those in the drift, which is open to advection and diffusion through the bulkhead. The trend of CO₂ concentration in the Heater Drift is shown in Figure 12 for a period 9 months before heating was initiated to about 20 months into the test. Three samples of Heater Drift air are shown as well as samples taken from the Observation Drift, the latter having essentially the composition of tunnel air. All of the samples and the model results stay at essentially 400 ppmv with fluctuations in the alcove greater than in the Heater Drift. Because the CO₂ concentrations in the rock around the test varies over a few orders of magnitude, the model captures the necessary exchange of CO₂ between the Heater Drift and the outside air (which is set to a constant value during the simulation).

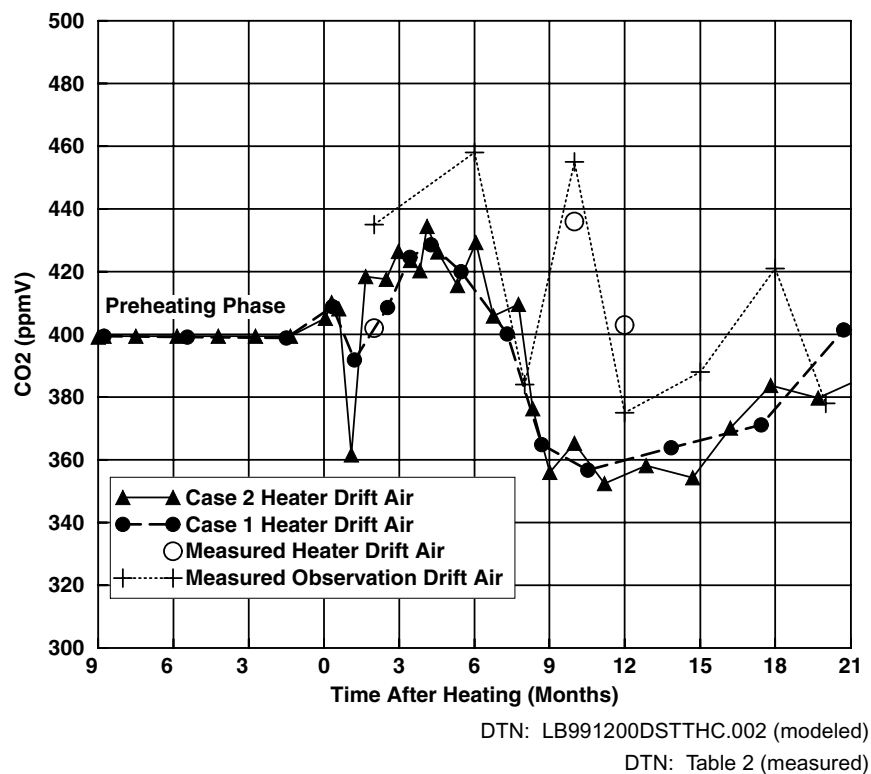


Figure 12. Modeled CO₂ Concentrations in Heater Drift Air over Time, Compared to Measured Concentrations. Also shown are concentrations measured in air from the Observation Drift.

6.2.7.3 Aqueous Species Evolution

6.2.7.3.1 Chemistry of Waters Sampled During the Drift Scale Test

The chemical compositions of four waters collected from hydrology boreholes 60 and 186 on November 12, 1998 and January 26, 1999 (DTN: LL990702804244.100) are shown in Table 9. The measured pore water composition (Table 3) is repeated here for direct comparison. The water samples collected during the test were obtained from zones that were hotter than the temperatures given for the samples, because water temperatures were measured after collection and they had cooled substantially. Both intervals are located in the zone below the wing heaters. Borehole interval 186-3 is lower and probably cooler than 60-3. Borehole 60 is located approximately in the same location as borehole 77, and borehole 186 corresponds to about the position of borehole 78.

Waters that were collected from the hydrology boreholes at elevated temperatures are generally more dilute (lower Cl and SO₄) and lower in pH than the initial pore water. Aqueous silica concentrations are similar to or much higher than in the pore water, indicating that these waters are not simple mixtures of pore water and pure condensate water. Some clear trends in water chemistry of the condensate waters in both intervals over time are increases in pH and SiO₂ (aq) concentration, and a drop in Ca. A similar trend for pH and SiO₂ (aq) exists between the boreholes, where the hotter interval (60-3) has a higher pH and SiO₂ (aq) concentration than the 186-3 interval at each time. The concentration of HCO₃ is also lower in 60-3 relative to 186-3 as expected from the higher temperature of 60-3. Other relationships are less obvious.

Some of the processes that could explain the water chemistry of samples collected in the hydrology boreholes include: mixing of pure condensate water with fracture pore waters, equilibration of condensate waters with matrix pore waters via molecular diffusion, reaction of condensate waters with fracture-lining minerals, and mineral precipitation due to reaction, boiling, temperature changes, or pH changes. The higher silica concentration in the waters collected in January compared to those collected in November, relative to chloride and the initial pore water silica concentration, is consistent with dissolution of a silicate phase, rather than increased concentration by boiling. However, concentrations of K, Mg, and Na are higher than what would be expected by dilution of original pore water (as evidenced by the low chloride concentrations). Therefore, the silicate phases that dissolved must have been some combination of cristobalite, opal, feldspar, clays or zeolites, rather than just a SiO₂-phase. The drop in Ca over time is consistent with calcite precipitation, which would be expected as the condensate waters were heated further and underwent CO₂ degassing, resulting in an increase in pH.

Table 9. Measured Concentrations in TSw Pore Water from Alcove 5 and Chemistry of Water Taken from Hydrology Boreholes

Parameter	Units	Pore Water ⁽¹⁾	60-3 ⁽²⁾ (11/12/98)	60-3 ⁽²⁾ (1/26/99)	186-3 ⁽²⁾ (11/12/98)	186-3 ⁽²⁾ (1/26/99)
Temperature	C	25	26.5-49.6	51.7	34.3-34.8	Unknown
pH		8.32	6.92	7.4	6.83	7.2
Na ⁺	mg/l	61.3	20.3	19.1	17	25.9
SiO ₂ (aq)	mg/l	70.5	115.5	139	58.2	105.5
Ca ²⁺	mg/l	101	13.9	5.9	20.2	2.92
K ⁺	mg/l	8.0	7.8	4.1	3.9	5.9
Mg ²⁺	mg/l	17	3	1.2	5.7	6.3
Al ³⁺	mg/l	9.92x10 ⁻⁷ (3)	n.d. (< 0.06)	n.d. (< 0.06)	n.d. (< 0.06)	n.d. (< 0.06)
HCO ₃ ⁻ (4)	mg/l	200	n.a.	41	n.a.	116
Cl ⁻	mg/l	117	20	10	19	23.3
SO ₄ ²⁻	mg/l	116	30.8	13.5	26.2	21

NOTES: (1) Average of porewater analyses ESF-HD-PERM-1 (30.1'-30.5') and ESF-HD-PERM-2 (34.8'-35.1'). DTN: LL990702804244.100.

(2) DTN: LL990702804244.100.

(3) Calculated by equilibrating with Ca-smectite at 25°C.

(4) Total aqueous carbonate as HCO₃⁻, calculated from charge balance.

n.a.=not analyzed, n.d.=not detected

6.2.7.3.2 Aqueous Species Simulation Results

The model simulates numerous aqueous species and only a limited discussion will be presented here. Data for all of the species are included in the output files (submitted under DTN: LB991200DSTTHC.002). The modeled variation in pH during the DST is shown in Figure 13 for the Case 2 simplified geochemical system. The most obvious effect on pH is a reduction to values predominantly around 6.5 in the condensate region, corresponding directly to the increases in CO₂ concentrations shown in Figure 6. As for the CO₂ concentrations, the low pH zone increases in size and moves outward with time. Within the dryout zone, the pH of the last residual water is also plotted, which reaches a maximum of nearly 9.5. However, the liquid saturation associated with these values is usually well below the residual liquid saturation. The modeled pH of condensate waters in fractures compares favorably with those collected from the hydrology boreholes (Table 9). As in the measured data collected at two times before the borehole intervals dried out, the model results show the effect of increasing pH with time and with increasing temperature in areas greater than 60°C. Therefore, in a given zone, the pH in the fractures first starts to drop because of steam condensation; then once the temperatures increase, so that the rate of evaporation and mineral-water reactions (and loss of CO₂) are greater than the rate of addition of water (and CO₂) via condensation, then the pH rises.

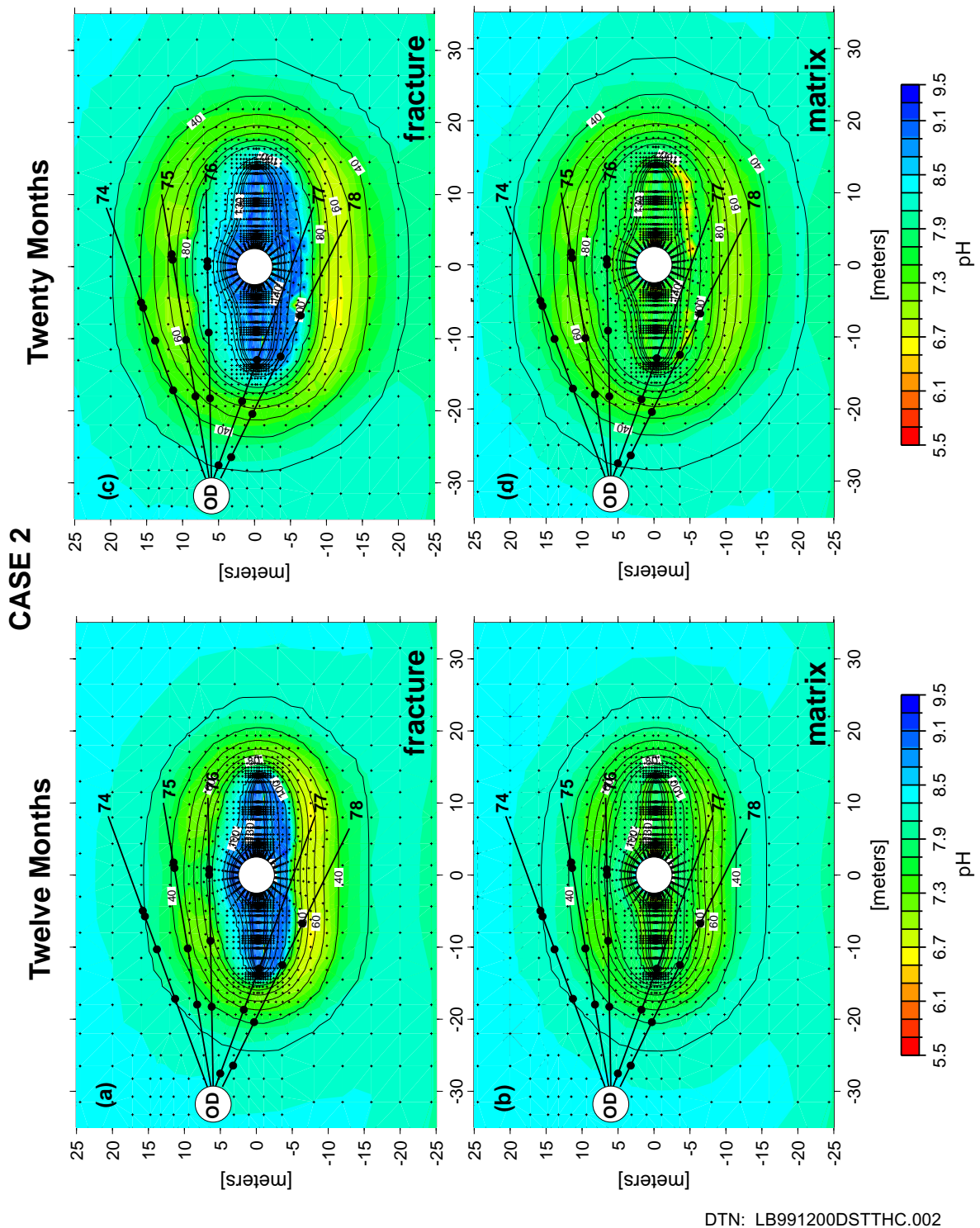
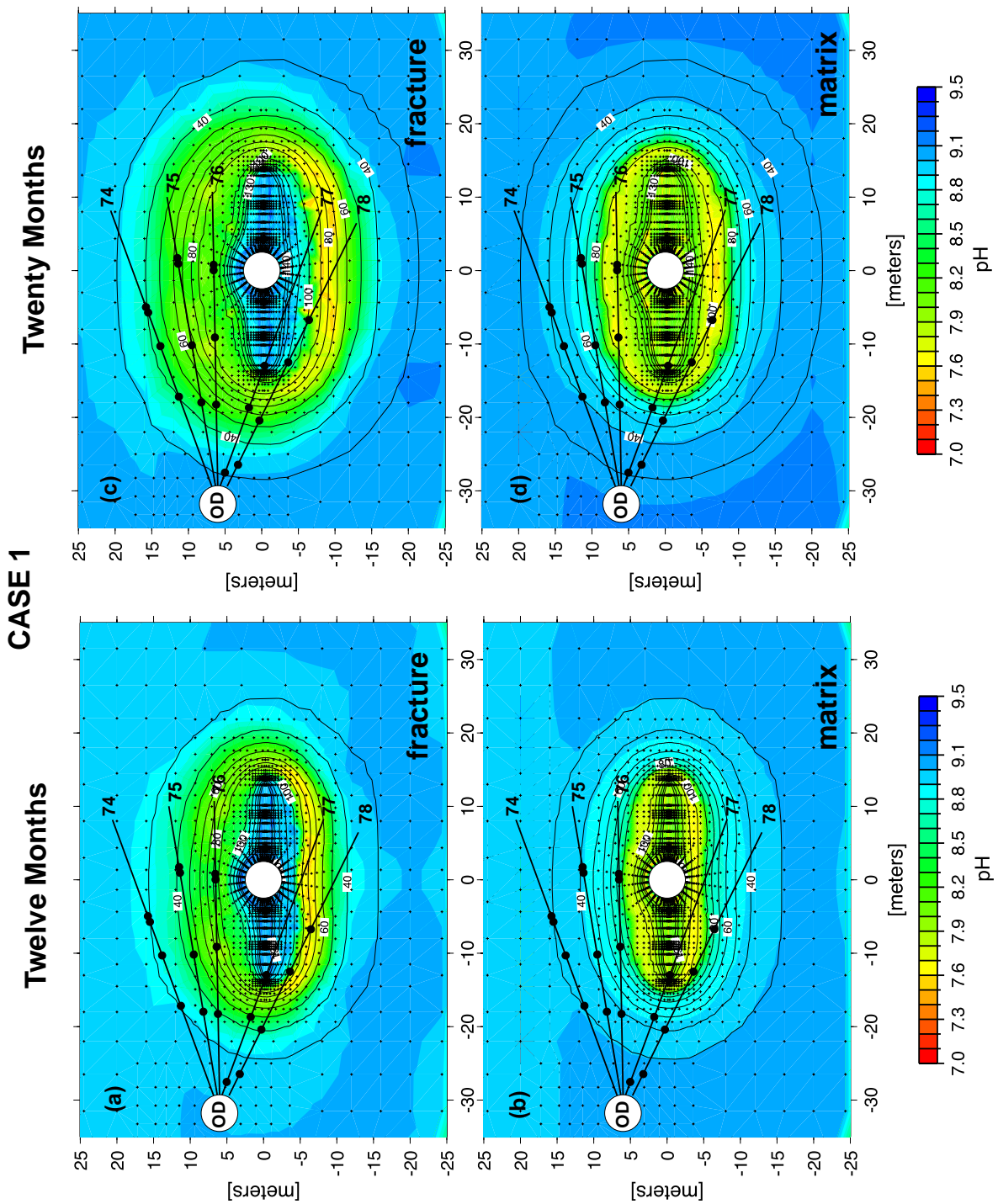


Figure 13. Distribution of pH and Temperature at 12 Months (Fracture – 13a, Matrix – 13b) and at 20 Months (Fracture – 13c, Matrix – 13d). Results are for the simplified geochemical system (Case 2).

The distribution of pH in fractures and matrix over time for the full geochemical system (Case 1) are plotted in Figure 14. The general trends are similar; however, the pH is shifted up to one unit higher in the condensate regions. However, the maximum pH in the water remaining just prior to dryout is at about the same value as in the Case 1 simulations (below 9.5). Because the fractures dry out before the matrix, and the CO₂ concentrations are higher in the matrix, the pH in the matrix pore water remains lower than in the fractures.

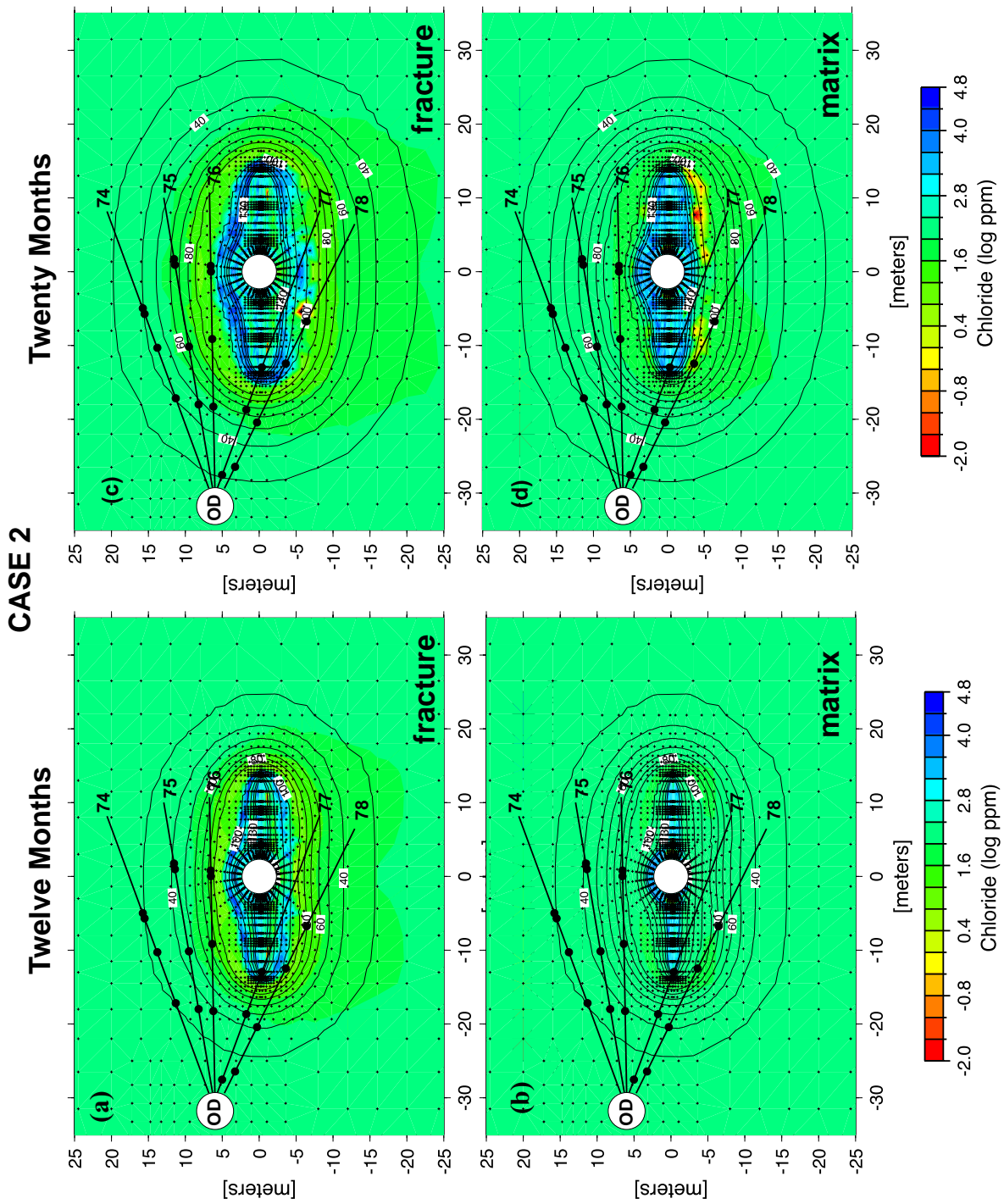
Validation criteria for the simulation of water chemistry are more difficult to establish because of the great variation possible in many species. For pH an order-of-magnitude change in the H⁺ concentration results in a single pH unit shift. Modeled pH values of fracture waters in the drainage zones of around 6.5 to 7.5 in Case 1 simulations are within a pH unit of measured waters in boreholes. This is much less difference than the possible changes which could trend to acidic (pH < 5) or basic values (pH > 9), and which would have stronger implications for PA. It is just as important to capture the trends in the values because they reflect the dynamic coupled process effects. For these changes, the direction is the validation criterion, and this has been met by the model results for the small amount of data examined.



DTN: LB991200DSTTHC.002

Figure 14. Distribution of pH at 12 Months (Fracture – 14a, Matrix – 14b) and at 20 Months (Fracture – 14c, Matrix – 14d). Results are for the full geochemical system. Temperature contours are overlain. (Case 1)

The effects of dilution through condensation of pure water vapor, of increases in concentration due to boiling, and the effects of fracture-matrix interaction can be assessed by the variation in a conservative species such as Cl. The variations in Cl concentration are plotted in Figure 15, at times of 12 and 20 months, and show marked decreases in the condensation zone. An interesting difference between the 12 and 20-month results is due to the slow imbibition of dilute condensate water into the matrix. At 12 months, there is a relatively large region of dilution of Cl in fractures due to condensation, and drainage well below the wing heaters and Heater Drift. In the matrix; however, there is little change, except in the dryout zone where the residual waters reached high concentrations at very low liquid saturations. At 20 months, the matrix is starting to show signs of decreased Cl concentration due to imbibition of fracture waters in the drainage zone, and significant dilution effects in the surrounding condensation zone.



DTN: LB991200DSTTHC.002

Figure 15. Chloride Concentration (log mg/l) and Temperature at 12 Months (Fracture – 15a, Matrix – 15b) and at 20 Months (Fracture – 15c, Matrix – 15d) (Case 2).

6.2.7.4 Mineralogical Changes

Over the course of the DST, there are marked changes in the water and gas chemistry that are strongly influenced by mineral-water reactions. The total amount of minerals precipitated or dissolved, though, is exceedingly small compared to the available fracture or matrix porosity. In terms of its effect on the chemistry of the system and its abundance in the precipitated mineral assemblage, calcite is the most important mineral over the short duration of the test.

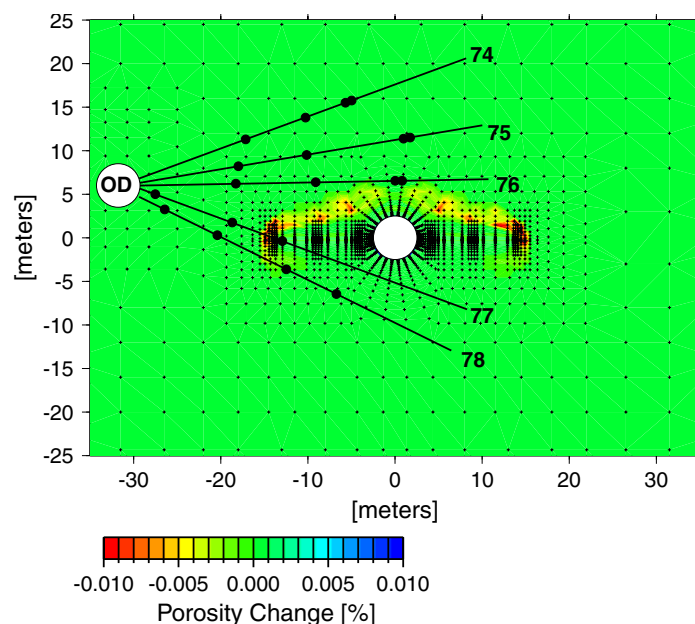
Predicted changes in calcite volume percent after 20 months of heating for both geochemical systems in fractures and matrix are shown in Figure 16. The reduced geochemical system shows a well-defined region of precipitation in the fractures above and to the margins of the Heater Drift and wing heaters. Some dissolution is occurring below the wing heaters; however, it is smaller in magnitude than the precipitation and does not show up on the plots. Within the matrix there is a fairly uniform region of calcite precipitation in the dryout zone. Precipitation in the matrix is driven mainly by increasing temperature, whereas in the fractures there is continuous boiling of condensate waters that are draining back to the heat source from cooler regions above. These waters pick up Ca through interaction with calcite and from mixing of ambient fracture pore water. The continuous process of condensate formation and drainage leads to a well-defined zone of calcite precipitation in the fractures. The results are consistent with the decrease in Ca seen in the condensate waters over time (Table 9).

The full geochemical system (Case 1) shows a similar maximum amount of calcite precipitation, although the band of calcite above the drift is much narrower and more poorly defined. The matrix shows a much broader region of fairly uniform calcite precipitation extending down temperature to about the 80°C isotherm. As in the Case 2 simulation, calcite is precipitating due to increasing temperature because of its reverse solubility. No dissolution of calcite takes place in the simulations using the full geochemical system. One obvious difference between the two systems is that in Case 1 calcite is predicted to precipitate in fractures in a zone extending well below the Heater Drift.

Predicted distributions of other minerals are not shown here due to the very small abundances of these phases. After this short period of time amorphous silica has only formed in the regions of dryout and in much smaller abundance than calcite.

6.2.7.5 Porosity and Permeability Changes

The predicted change in fracture porosity for the Case 2 mineral assemblage after 20 months of heating is shown in Figure 17. Although the simulations were carried out with a feedback between mineral dissolution/precipitation and porosity, permeability, and capillary pressure changes, the effect on the latter parameters and on fluid flow was negligible. Total changes in either fracture or matrix porosity were less than 0.1%. The greatest change takes the form of a few meter wide zone of decreased porosity a few meters above the Heater Drift and wing heaters. Much of this change is due to calcite precipitation. Likewise, permeability and capillary pressures were virtually unaffected. Even though the changes are very small, it is likely that the system would show localized precipitation and therefore greater heterogeneity than the model predictions.



DTN: LB991200DSTTHC.002

Figure 17. Change in Fracture Porosity after 20 Months (Case 2). Negative values indicate a net porosity reduction due to mineral precipitation and positive values reflect a net porosity increase owing to mineral dissolution.

6.3 THC SEEPAGE MODEL

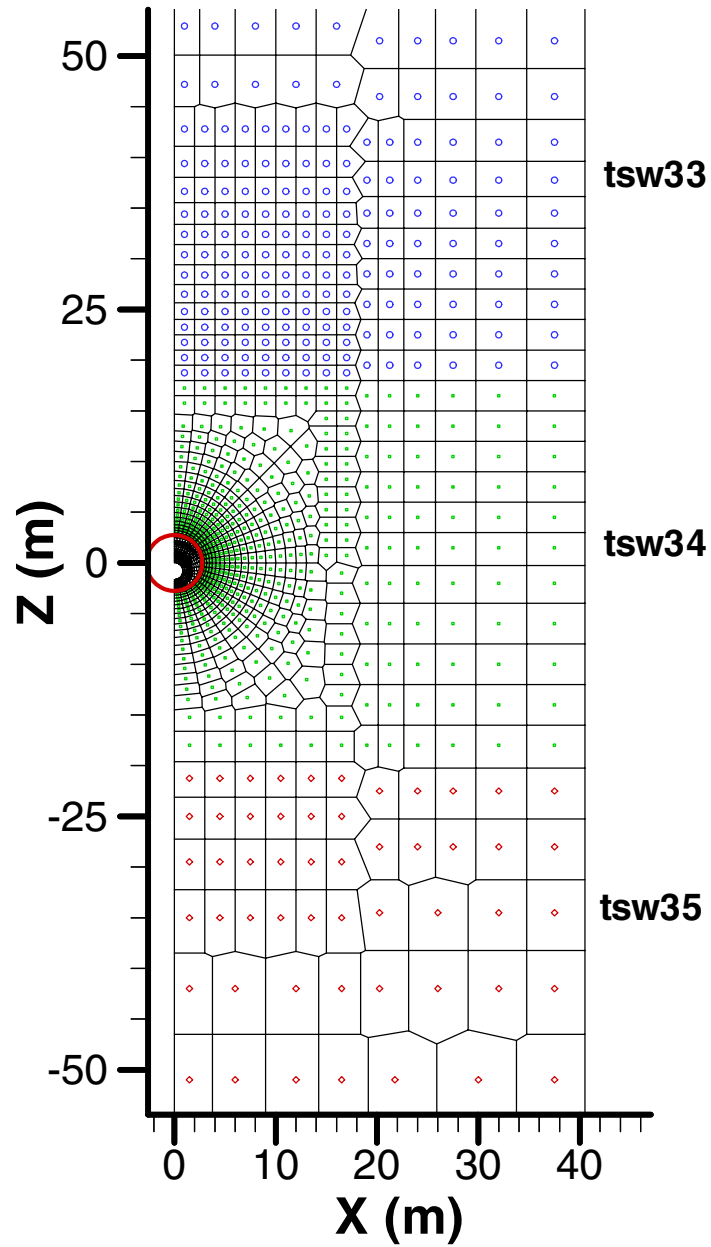
The purpose of the DST Model described in Section 6.2 was to compare simulation results against actual measurements during the first 21 months of the DST. The THC Seepage model then applies the same methods of simulating coupled THC processes to predict, at a drift scale, the performance of the potential repository during 100,000 years.

The general setup of this numerical model is described below. Simulations were performed in two dimensions along a laterally continuous, vertical geologic section with stratigraphy similar to that in borehole SD-9 (at Nevada State Plane coordinates E171234, N234074). The simulations consider a drift located in the Topopah Spring Tuff middle non-lithophysal geologic unit (Ttpmn unit, corresponding to model layer name tsw34, DTN: LB990501233129.004). Only part of the potential repository is planned to be located in the Ttpmn, and therefore the model may not be representative of the entire potential repository. However, most hydrogeologic data available for the potential repository are from the Ttpmn unit, including data from the Single Heater Test (SHT), DST, and many other data collected in the ESF.

6.3.1 Numerical Mesh

Simulations were performed on a vertical 2-D mesh, using a drift spacing of 81 m (center to center, Design Criterion PA-SSR-99218.Ta) and a drift radius of 2.75 m (DTN: SN9908T0872799.004). With rock properties laterally homogeneous between drifts (see Section 1.4.3), this setup can be viewed as a series of symmetrical, identical half-drift models with vertical no-flow boundaries between them. Therefore, 2-D simulations (rather than 3-D) were conducted. Accordingly, the numerical mesh was reduced to a half-drift model with a width of 40.5 m, corresponding to the midpoint between drifts (Figure 18). Geologic data from borehole SD-9, as implemented in UZ model grid UZ99_2_3D.mesh (DTN: LB990501233129.004), were used as a basis to map geologic contacts into the 2-D mesh, and the mesh coordinate system was set with reference to the center of the drift (Table 10). The gridblock size was kept fine enough to provide enough resolution at key model locations such as at the vicinity of drift and geologic contacts, but as coarse as possible to provide the computing efficiency needed for reasonable simulation times. The area extending approximately 50 meters above the drift is more finely gridded than other areas to capture THC effects potentially affecting seepage into the drift. Outside the drift, the smallest grid spacing was specified at the drift wall (20 cm), and increasing outward. Because of its minor relevance to this modeling effort, the geology below the tsw38 model layer was simplified compared to the original SD-9 data, which allowed for coarser gridding in this area. The mesh has a total of 2510 gridblocks, including those representing matrix, fracture, and in-drift design elements.

THC SEEPAGE MODEL MESH (top at +221m, bottom at -335m)



DTN: LB991200DSTTHC.002

NOTE: Grid detail around (0, 0) is shown in Figure 19.

Figure 18. THC Seepage Model Mesh with Hydrogeologic Units Shown in the Vicinity of the Drift: Topopah Spring Tuff Upper Lithophysal (tsw33 - circles), Middle Non-Lithophysal (tsw34 - dots), and Lower Lithophysal (tsw35 - diamonds) Units.

Table 10. Vertical Mesh Dimensions and Geologic Contacts in the THC Seepage Model

Model Layer	SD-9 Top of Layer Elevation (masl)	Mesh Top of Layer Z Coordinate (m)
Top	1286.00	220.7
tcw13	1285.44	220.1
ptn21	1279.57	214.2
ptn22	1275.00	209.7
ptn23	1269.09	203.7
ptn24	1264.51	199.2
ptn25	1255.45	190.1
ptn26	1233.79	168.4
tsw31	1221.01	155.7
tsw32	1219.01	153.7
tsw33	1165.71	100.4
tsw34	1080.37	18.0*
Drift center	1065.34	0.0
tsw35	1045.14	-20.2
tsw36	942.62	-122.7
tsw37	906.92	-158.4
tsw38	889.08	-176.3
ch2	868.38	-197.0
Bottom	730.00	-335.3

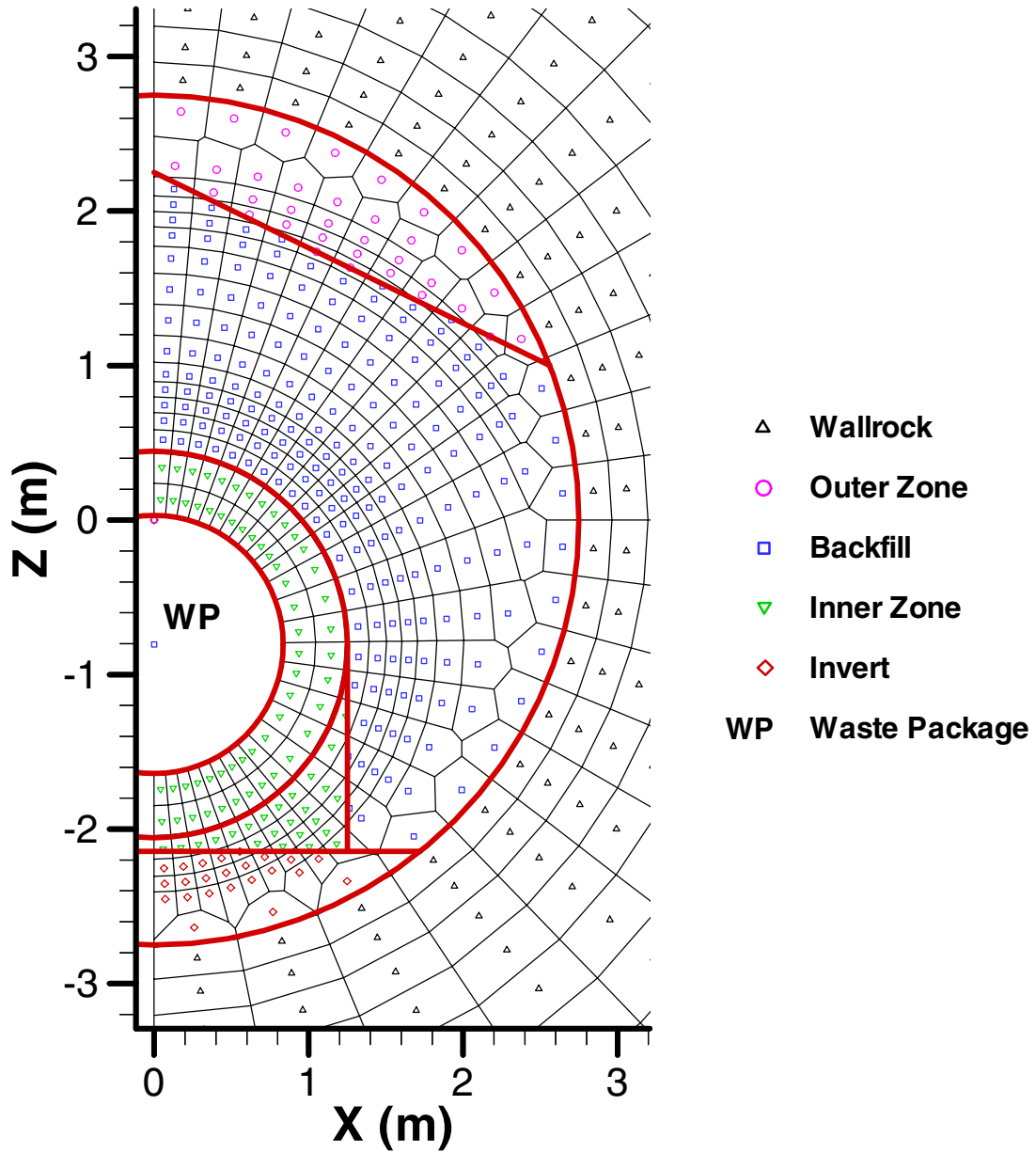
DTN: LB990501233129.004

NOTE: * Contact raised, compared to SD-9 data, to provide for better lateral continuity between the fine mesh above the drift and coarser mesh laterally away from the drift (See Figure 18)

The drift was discretized to include the design elements and dimensions shown on Figure 1 (338 gridblocks total). The gridblock size inside the drift was chosen small enough to provide a realistic drift model (Figure 19, compare to Figure 1). As mentioned earlier (Section 4.1.7.2), two drift configurations are considered in the THC Seepage Model:

- Pre-closure configuration: waste package, invert, and one open space between the waste package and the drift wall during the first 50 years (pre-closure)
- Post-closure configuration: waste package, invert, dripshield, backfill, and two open zones: the Inner Zone, between the waste package and the dripshield; and the Outer Zone, between the backfill and drift wall.

The discretization of the drift (Figure 19) was kept the same for the two configurations. As such, the pre-closure period was simulated by assigning identical open-space properties to gridblocks representing the Inner Zone, backfill, and Outer Zone.



DTN: LB991200DSTTHC.002

Figure 19. Discretization of the Repository Drift in the THC Seepage Model

6.3.2 Boundary Conditions

The following boundary conditions were imposed on the THC Seepage Model (Table 11):

- Top boundary: stepwise changing infiltration rate (Table 12), temperature, pressure, and gas saturation (representing open atmosphere); constant CO₂ partial pressure and composition of infiltrating water
- Bottom boundary: constant temperature, pressure, and liquid saturation (representing the water table). Constant water composition and CO₂ partial pressure at equilibrium
- Side boundaries: no heat, fluid, and chemical fluxes
- Waste package: variable heat load with time, including effect of 70% heat removal by ventilation for first 50 years (pre-closure).

Three different infiltration regimes were modeled simulating a range of future climate conditions (Table 12). These were developed to support TSPA-SR.

Table 11. THC Seepage Model Boundary Conditions

Boundary	Boundary Condition	Reference
Top	T = 17.68°C S _g = 0.99 P = 86339 Pa Time-varying infiltration rate Constant composition of infiltration and P _{CO₂}	Table 2 Table 2 Table 2 Table 12 Section 4.1.3
Bottom	T = 31.68°C S _L = 0.99999 P = 92000 Pa Constant water composition and P _{CO₂}	Table 2 Table 2 Table 2 Section 4.1.3
Sides	No flux for water, gas, heat, and chemical species	Not Applicable
Drift Wall	No-flux for water, gas and chemical species; conduction only for heat	Not Applicable
Waste Package	Heat load (radioactive decay and effect of 70% heat removal by ventilation for first 50 years)	Attachment V and Table 1

NOTES: T=Temperature
S_g=Gas saturation
S_L=Liquid saturation
P=Pressure

Table 12. THC Seepage Model Infiltration Rates and Corresponding Rock Properties Sets

Case	Infiltration Rate (mm/yr)	Time Period (years)	Calibrated Properties Set	Reference
Ambient Mean Infiltration at SD-9 (no thermal load)	1.05	0 to 100,000	Present Day Mean	Table 2
Mean Infiltration	6 16 25	0 to 600 (present day) 600 to 2000 (monsoon) 2000 to 100,000 (glacial transition)	Present Day Mean	Table 2
Upper Bound Infiltration	15 26 47	0 to 600 600 to 2000 2000 to 100,000	Present Day Upper Bound	Table 2
Lower Bound Infiltration	0.6 6 3	0 to 600 600 to 2000 2000 to 100,000	Present Day Lower Bound	Table 2

6.3.3 Modeling Procedure

Different calibrated rock-properties sets were used to run the various infiltration cases (Table 12). For each infiltration case, the model was first run without reactive transport, heat load, and drift (i.e., with rock at the location of the drift) until steady state thermal and hydrologic conditions were achieved. A steady-state was considered to have been met under the following conditions:

1. Liquid saturations, temperatures, and pressures remained constant within the model over a time span of at least 100,000 years, or
2. The total liquid and gas inflow at the top of the model matched the total liquid and gas outflow at the base of the model within a maximum of 0.01 percent.

THC simulations were run with the drift in place and heat transfer from the waste package, using the steady state temperatures, pressures, and liquid saturations as starting conditions. Open spaces within the drift were set to zero liquid saturation. “Ambient” reactive transport simulations with the drift in place but without heating (i.e. no heat release from the waste package) were also performed for comparison of chemical trends to simulations under thermal loading.

As discussed in Section 4.1.7.2, THC simulations were run for an initial period of 50 years using the pre-closure drift configuration and thermal properties. The simulations were then restarted using the post-closure drift configuration and properties from 50 years to a total simulation time of 100,000 years. At times corresponding to changes in infiltration rates (at 600 and 2000 years, Table 12), the simulations were stopped and then restarted with the new infiltration rate (thus resulting in a stepwise change in infiltration).

Sensitivity analyses were performed to determine a suitable maximum time step length for THC simulations. Maximum time steps of 6 months (pre-closure only), 1, 10, and 100 years were investigated. Maximum time-step lengths of 6 months for pre-closure simulations, 10 years for simulation times between 50 and 20,000 years, and 50 years for simulation times between 20,000 and 100,000 years provided a reasonable compromise between computing efficiency and accuracy.

6.3.4 Model Runs

The THC Seepage Model was run using the same two sets of chemical components and mineral assemblages as those used for the Drift Scale Test Simulations: Case 1 (Table 7), and Case 2 (Table 8). The latter is a subset of Case 1 without aluminum silicate minerals, fluorite, or iron minerals.

A total of nine simulations were completed, as summarized in Table 13. For each Case 1 and Case 2, THC simulations with thermal loading were carried out using three variable infiltration rates involving future climate changes. In addition, simulations under ambient conditions, without heating, were performed for Case 1 and Case 2 using a constant infiltration rate (about 1.05 mm/year). The latter represents the base-case present-day infiltration rate at the location of Borehole SD-9, which was used to define the geology of the model. These ambient simulations were run to assess the extent to which the Case-1 and Case-2 geochemical systems approached a geochemical steady state. These runs also provide a baseline to which the results of thermal loading simulations can be compared.

Table 13. THC Seepage Model Runs

Infiltration-Property Set (Table 12)	Geochemical System (Tables 7 and 8)	Simulation Type	Run ID (used in DTN: LB991200DSTTHC.002)
Mean Infiltration	None	TH	th6_16_25_3
Ambient Mean (no thermal load)	Case 1	THC	thc1mm_amb2
	Case 2	THC	thc1mm_amb1
Mean Infiltration	Case 1	THC	thc6_16_25_3
	Case 2	THC	thc6_16_25_4
Upper Bound Infiltration	Case 1	THC	thc15_26_47u_3
	Case 2	THC	thc15_26_47_4
Lower Bound Infiltration	Case 1	THC	thc0.6_6_3l_3
	Case 2	THC	thc0.6_6_3_4

6.3.5 Simulation Results

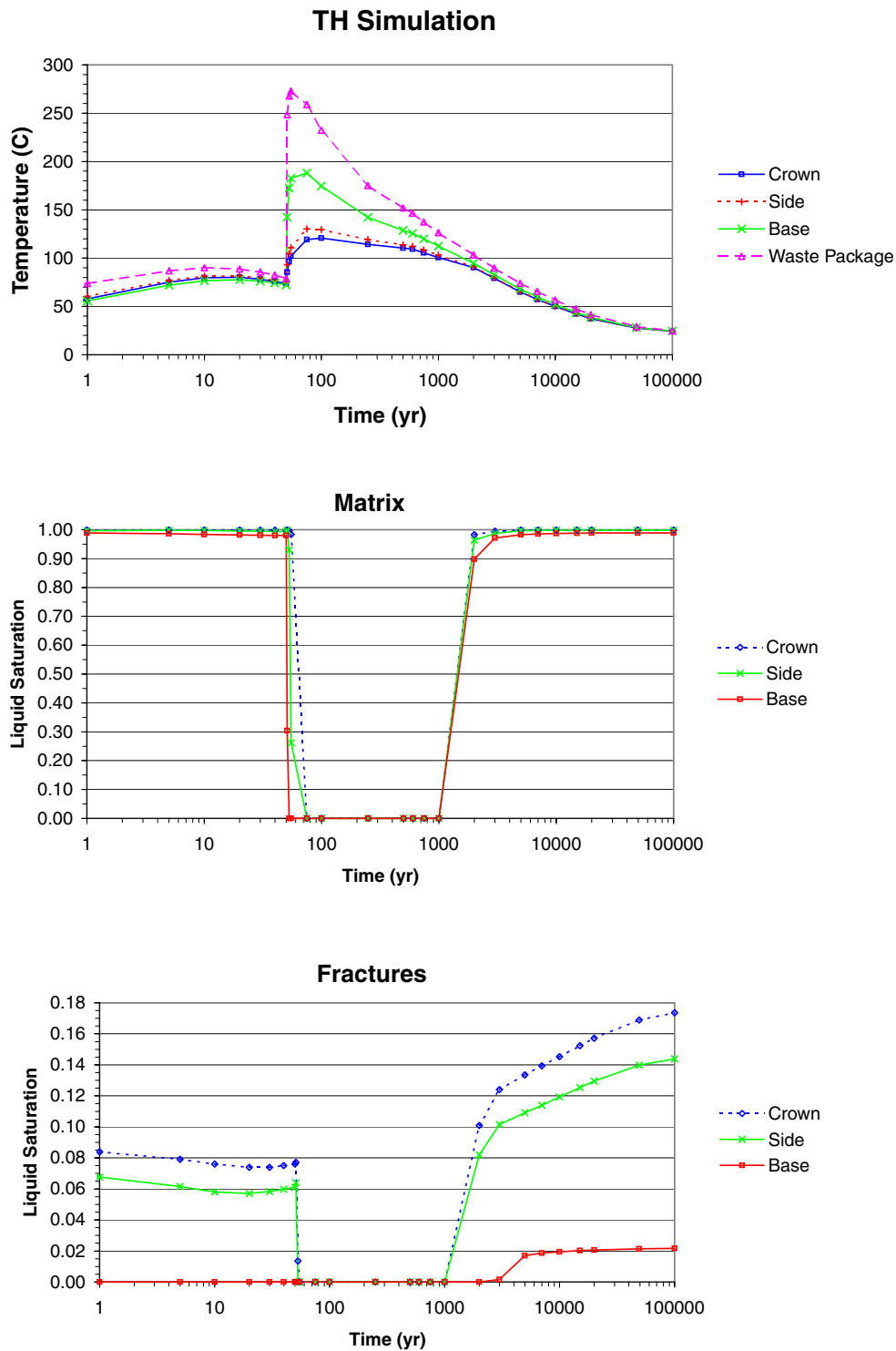
Model results are presented below in Figures 20 through 42, and focus on areas in the vicinity of the drift. Other areas are not discussed because they are not directly relevant to the primary objectives of this work. Much of the data (temperatures, liquid saturations, water compositions, CO₂ concentrations, and liquid/gas fluxes) are examined as a function of time at three locations around the modeled drift. These are the crown, the side (approximately 20 cm above the springline) and the base (model nodes F257, F 92, and F272, respectively), at points located 10 cm to the outside (i.e., in the rock) of the drift wall. These data are tabulated and submitted under DTN: LB991200DSTTHC.002 and further discussed below.

6.3.5.1 Thermohydrology Simulation Results

For comparison to the THC simulations, the THC Seepage Model was run with thermal loading and without reactive transport (i.e., considering only thermal and hydrological effects). This simulation was run using the mean infiltration rates and corresponding rock property set (Table 12) and serves as a basis for interpreting the effects of water-gas-rock chemical interaction on the thermal and hydrological behavior of the system. Calculated temperatures, liquid saturation, and air mass fractions around the drift are shown in Figures 20 through 22.

Post-closure temperatures quickly climb above the boiling point (near 97°C at Yucca Mountain), and are higher at the base of the drift where the waste package is closest to the drift wall (Figure 20). The return to ambient temperatures after heating takes 50,000 to 100,000 years. The highest modeled temperature in the waste package (near 270°C) is attained shortly after closure at a time of 55 years.

Around the drift, the matrix is predicted to rewet after 1,000 to 2,000 years (Figure 20). Rewetting of fractures occurs within the same time frame, except at the drift base where fractures do not rewet until approximately 3,000 years (Figure 20). A contour plot of temperatures and matrix saturations in the vicinity of the drift at a simulated time of 600 years (near maximum dryout) shows the dryout zone (represented by zero matrix saturations) extending approximately 10 meters above the drift, 17 meters to the side of it, and 22 meters below it (Figure 21). Air mass fractions at the drift wall (Figure 22) drop to near-zero values during dryout (i.e., the gas phase is almost entirely water vapor), and are essentially identical in matrix and fractures.



DTN: LB991200DSTTHC.002

Figure 20. TH Simulation. Time profiles of modeled temperatures and liquid saturations in fractures and matrix at three drift wall locations.

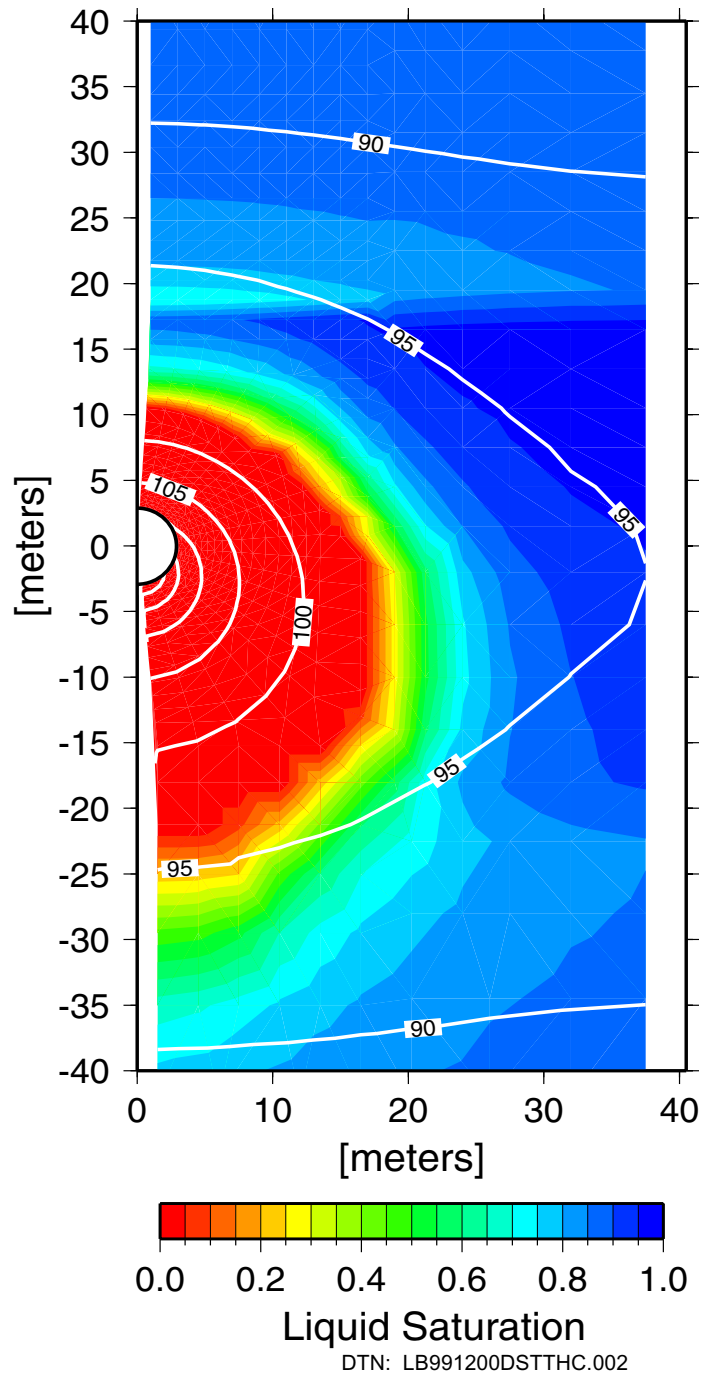
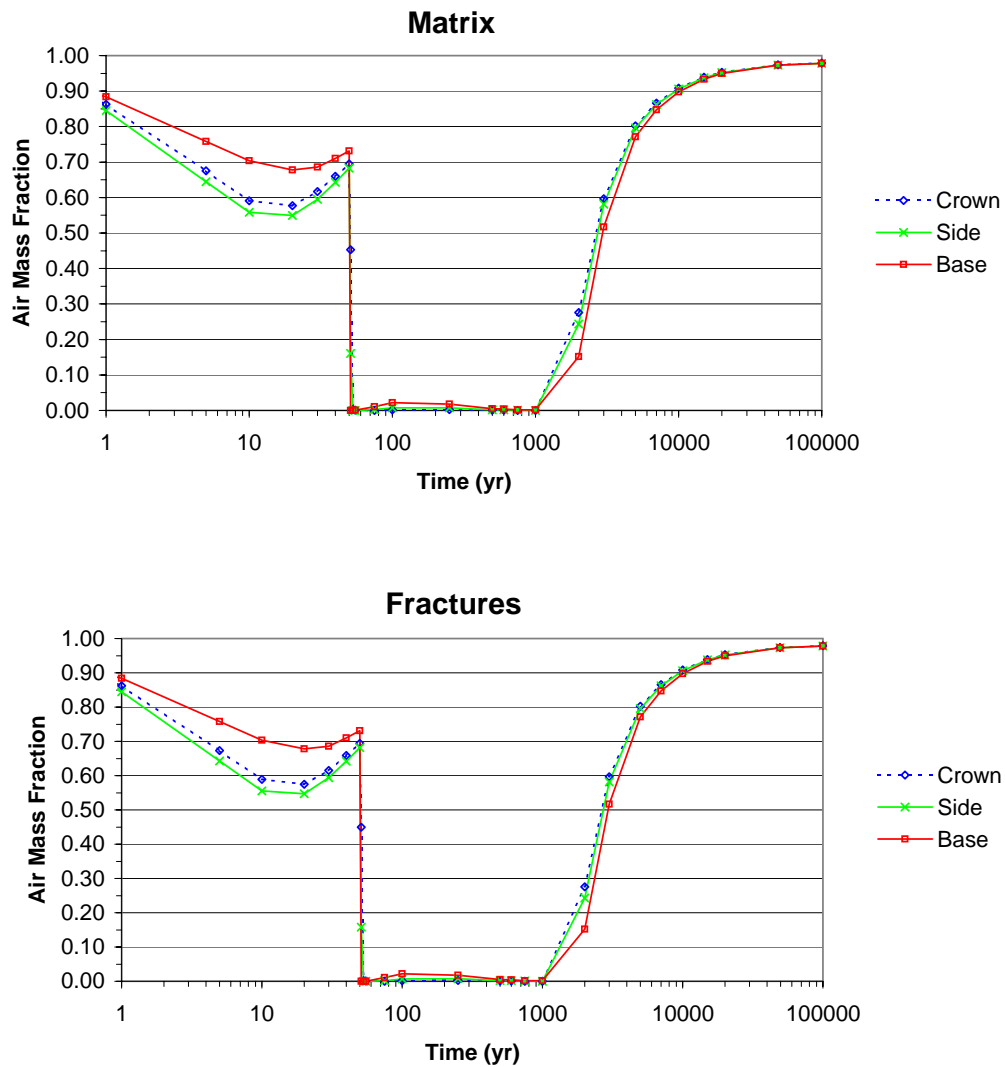


Figure 21. TH Simulation. Contour plot of modeled temperatures and liquid saturations in the matrix at 600 years (near maximum extent of dryout).



DTN: LB991200DSTTHC.002

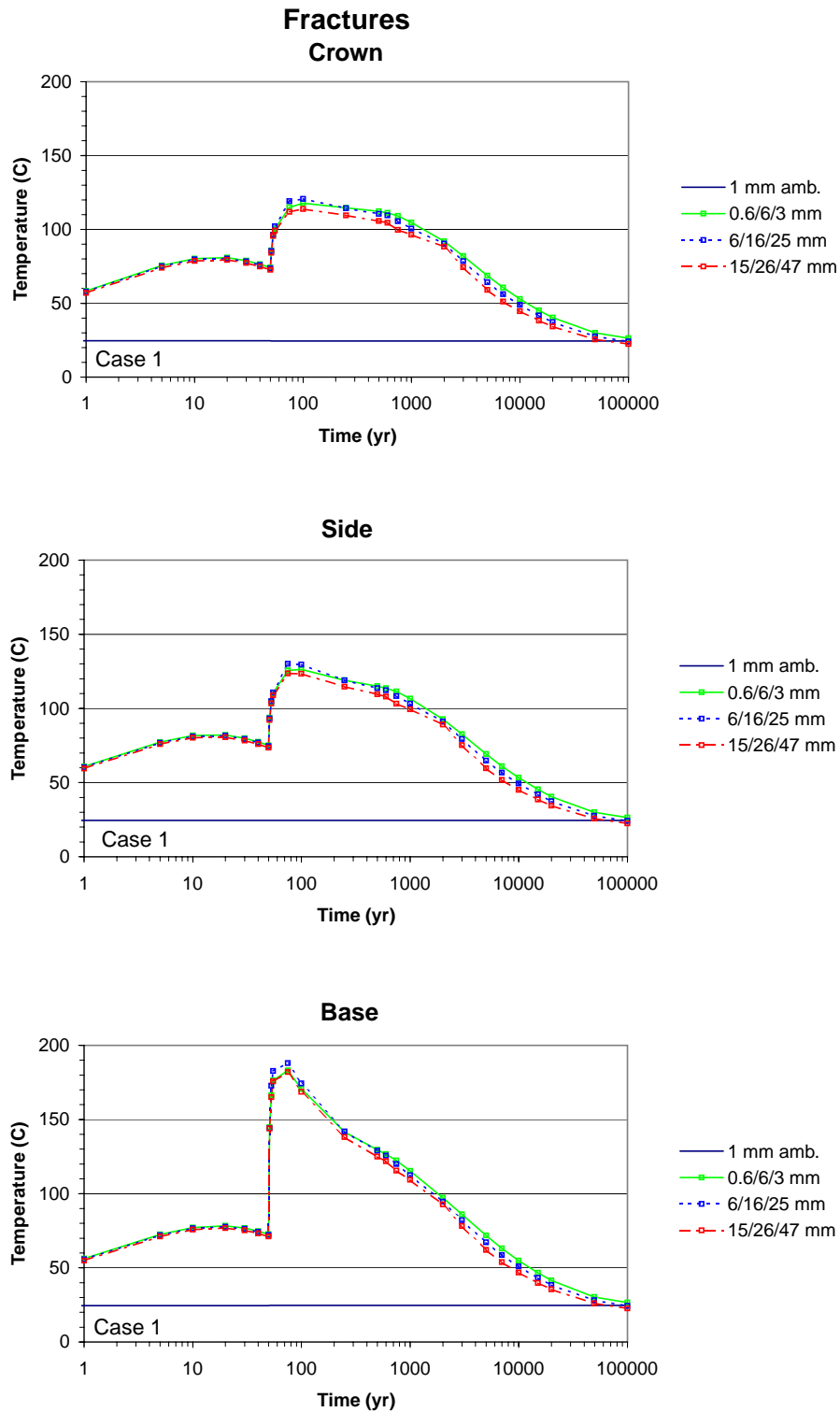
Figure 22. TH Simulation. Time profiles of modeled air mass fractions in the gas phase in fractures and matrix at three drift wall locations.

6.3.5.2 THC Simulation Results

Calculated temperatures, liquid saturations, and air mass fractions in fractures around the drift are shown in Figures 23 through 27. These thermohydrologic data are essentially identical for Case 1 and Case 2; therefore, results are presented only for Case 1. The data are shown for all four infiltration cases shown in Table 12. Temperatures, liquid saturation, and air mass fractions calculated for the mean infiltration case (6/16/25 mm/year) are directly comparable to those obtained from the TH simulation (Figures 20 through 22) because the latter was carried out using the same infiltration rates. The results of the TH and THC simulations are essentially identical. As discussed later, the thermal and hydrologic behavior of the system is not significantly affected by

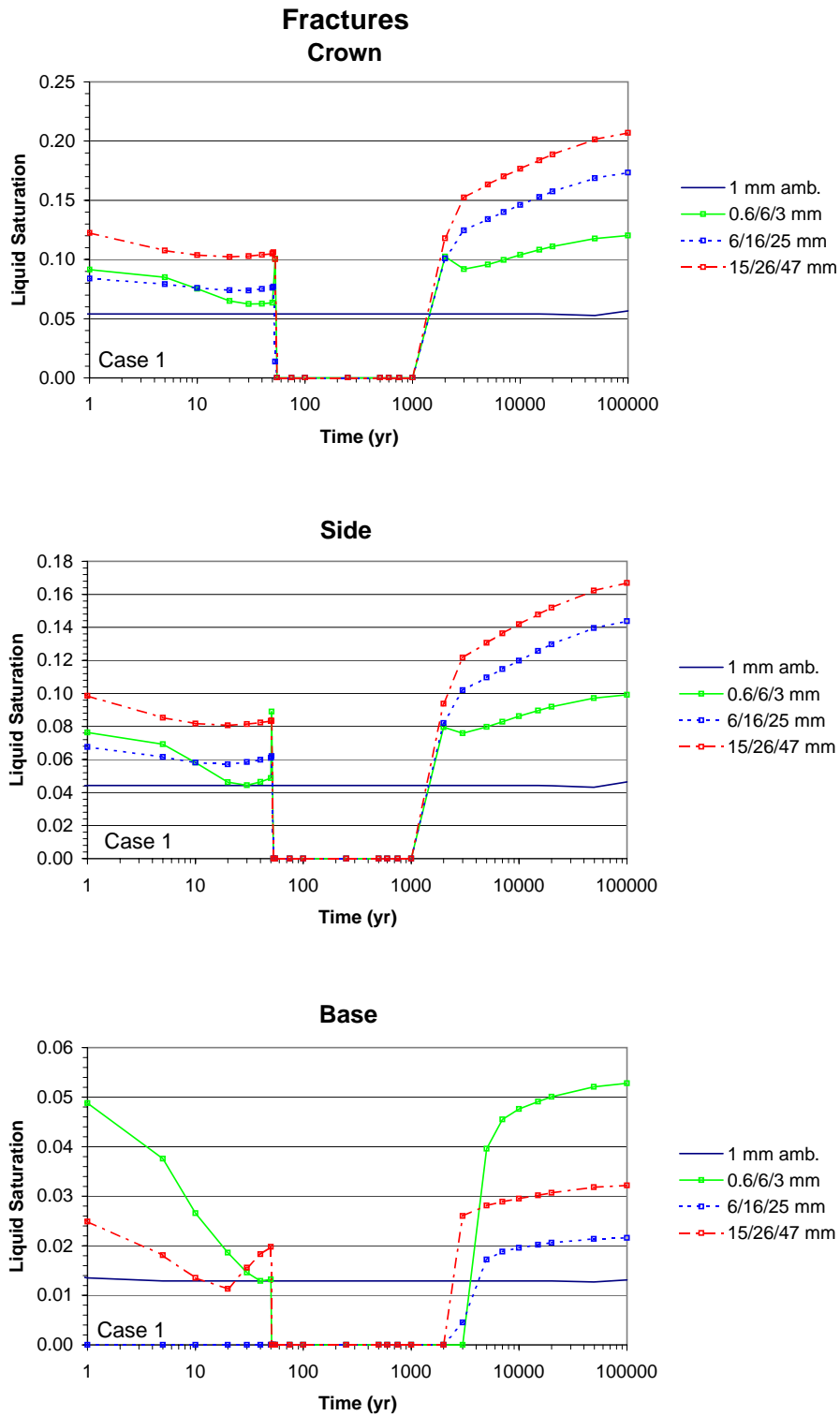
water-gas-rock chemical interactions and, therefore, temperatures, liquid saturations, and air mass fractions calculated with THC (Case 1 and Case 2) and TH simulations are nearly the same.

The temperature-time profiles for the different infiltration cases (Figure 23) remain within approximately 15°C of each other. The plots also show that the return to ambient temperatures takes about 100,000 years for all infiltration cases. At the drift crown, rewetting of fractures is predicted to occur around the same time period (1,000 to 2,000 years) for all infiltration cases (Figure 24). Matrix rewetting at the drift crown occurs around the same time period as fractures, except for the high infiltration case where the matrix rewets approximately 200 years earlier (Figure 25). The size of the dryout zone (represented by zero matrix saturations) decreases at the highest infiltration rate (Figure 26c), to approximately 6, 12, and 16 meters above, to the side and below the drift, respectively. The smaller dryout zone in the lowest infiltration case (Figure 26a) compared to the mean infiltration case is apparently the result of the differing property sets, rather than the infiltration rate. Air mass fractions (Figure 27) are little affected by the different infiltration rates.



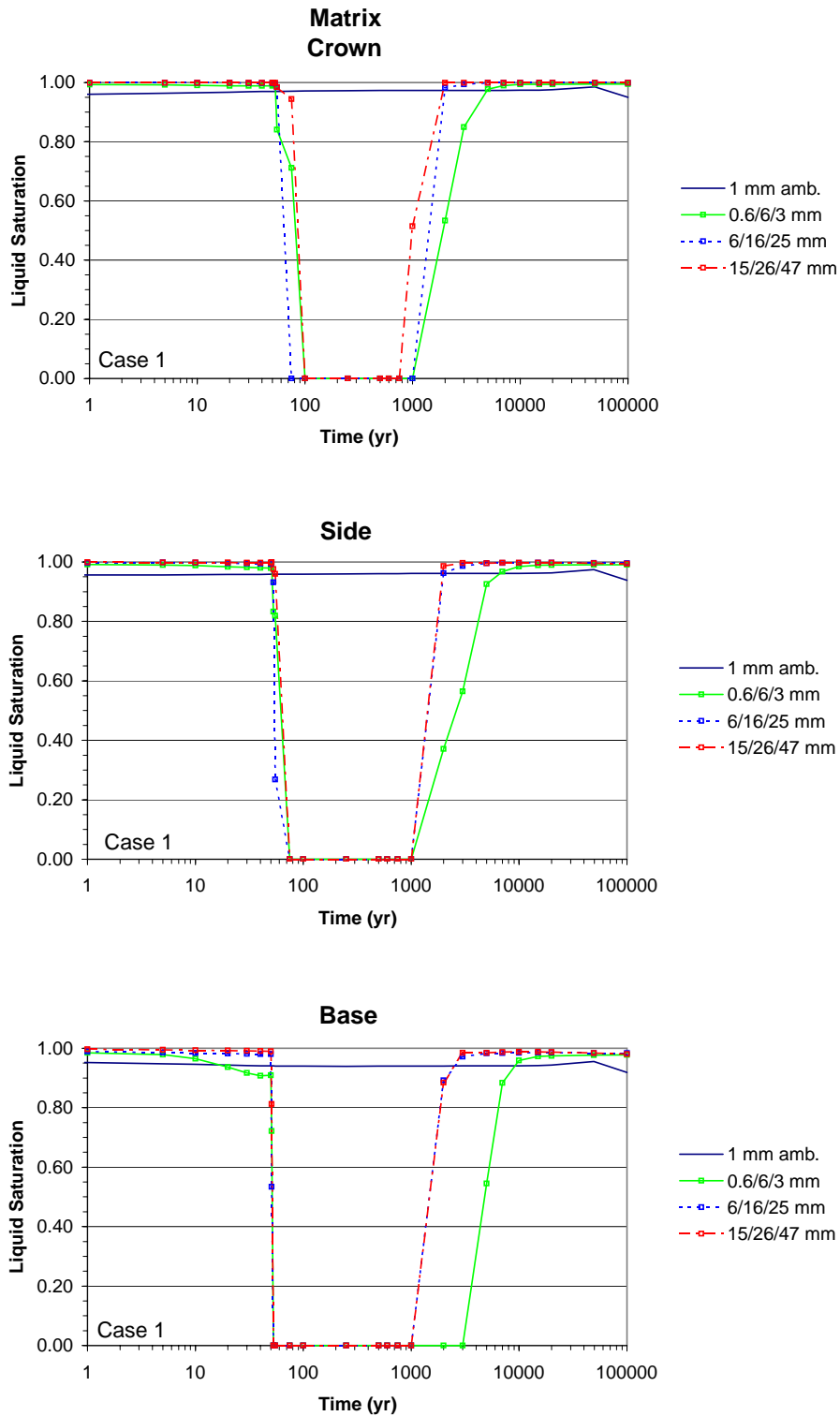
DTN: LB991200DSTTHC.002

Figure 23. Time Profiles of Modeled Temperatures in Fractures at Three Drift Wall Locations for Different Climate Scenarios (THC - Case 1).



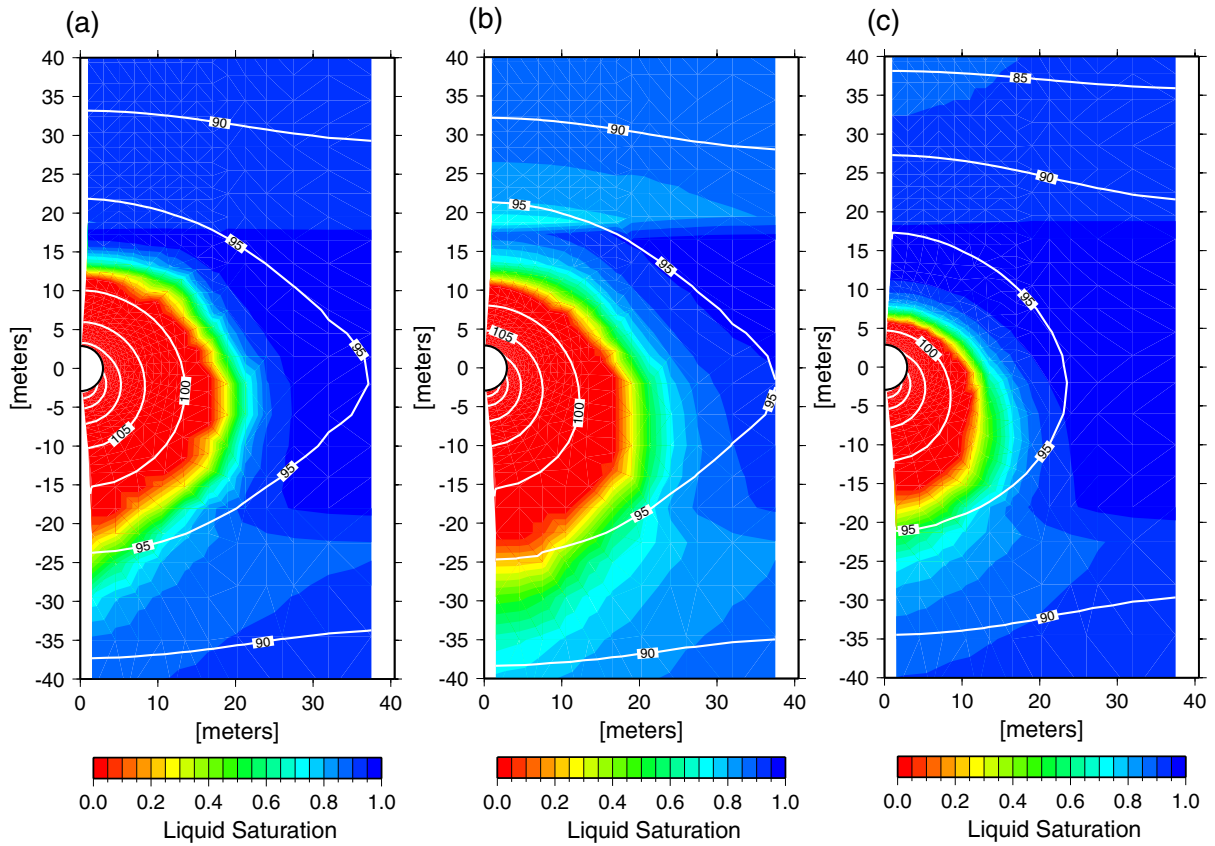
DTN: LB991200DSTTHC.002

Figure 24. Time Profiles of Modeled Liquid Saturations in Fractures at Three Drift Wall Locations for Different Climate Scenarios (THC - Case 1).



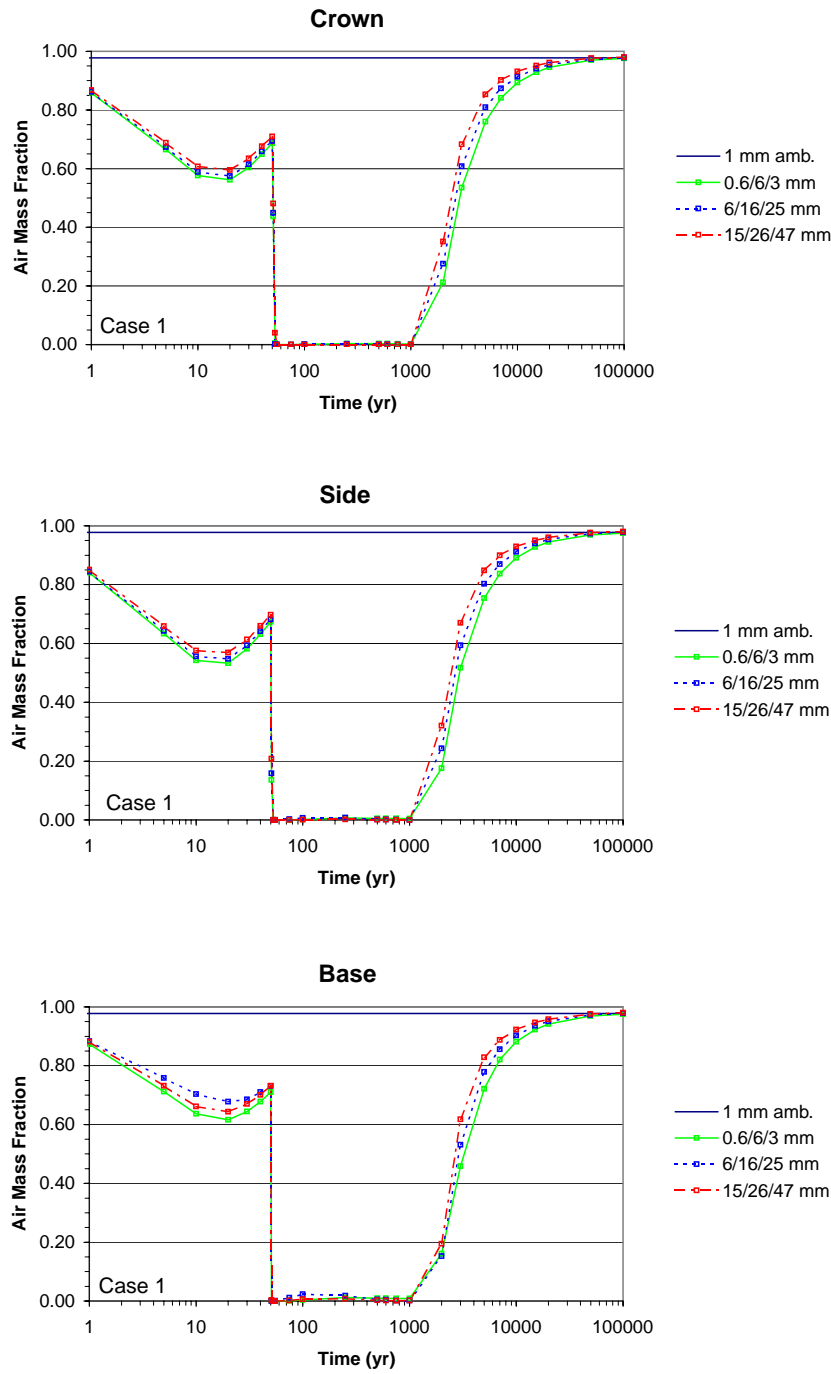
DTN: LB991200DSTTHC.002

Figure 25. Time Profiles of Modeled Liquid Saturations in the Matrix at Three Drift Wall Locations for Different Climate Scenarios (THC - Case 1).



DTN: LB991200DSTTHC.002

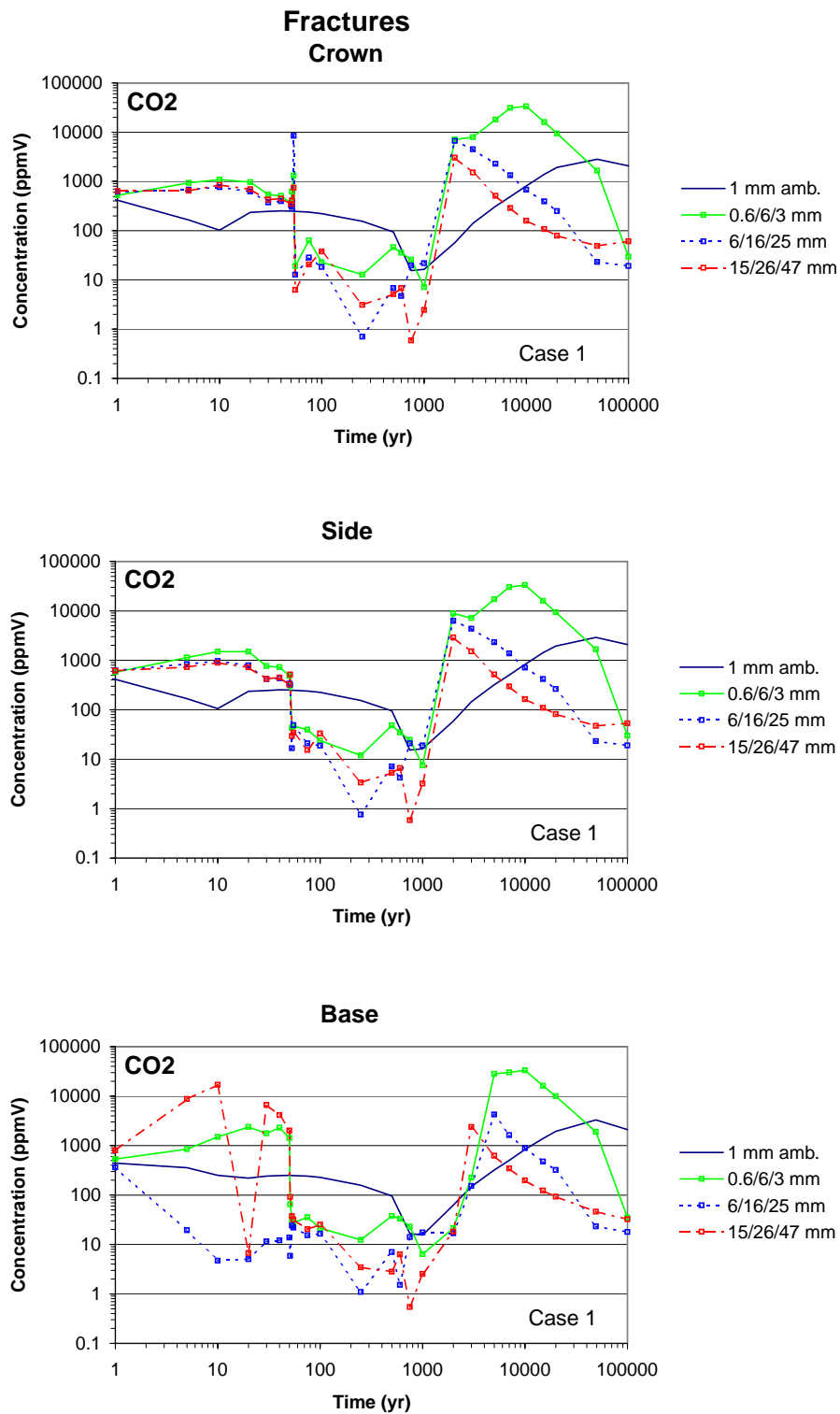
Figure 26. Contour Plot of Modeled Temperatures and Liquid Saturations in the Matrix at 600 years (Near Maximum Dryout) for Three Climate Scenarios: (a) Low, (b) Mean, and (c) High (THC - Case 1).



DTN: LB991200DSTTHC.002

Figure 27. Time Profiles of Modeled Air Mass Fractions in the Gas Phase in Fractures (Essentially Identical in the Matrix) at Three Drift Wall Locations for Different Climate Scenarios. (THC - Case 1).

Predicted CO₂ concentrations in the gas phase in fractures at equilibrium with the fracture pore water around the drift are shown in Figures 28 and 29 for the complete (Case 1) and reduced (Case 2) mineral assemblages, respectively. CO₂ concentrations in fractures drop significantly during dryout and increase again during rewetting. In Case 1, the most significant CO₂ concentration increase after rewetting (to approximately 33,000 ppmv) occurs in the low-infiltration case. In contrast, with Case 2, the largest CO₂ concentration after rewetting (near 12,000 ppmv) occurs for the high infiltration case.



DTN: LB991200DSTTHC.002

Figure 28. Time Profiles of Modeled CO₂ Concentrations in the Gas Phase in Fractures at Three Drift Wall Locations for Different Climate Scenarios (Case 1).

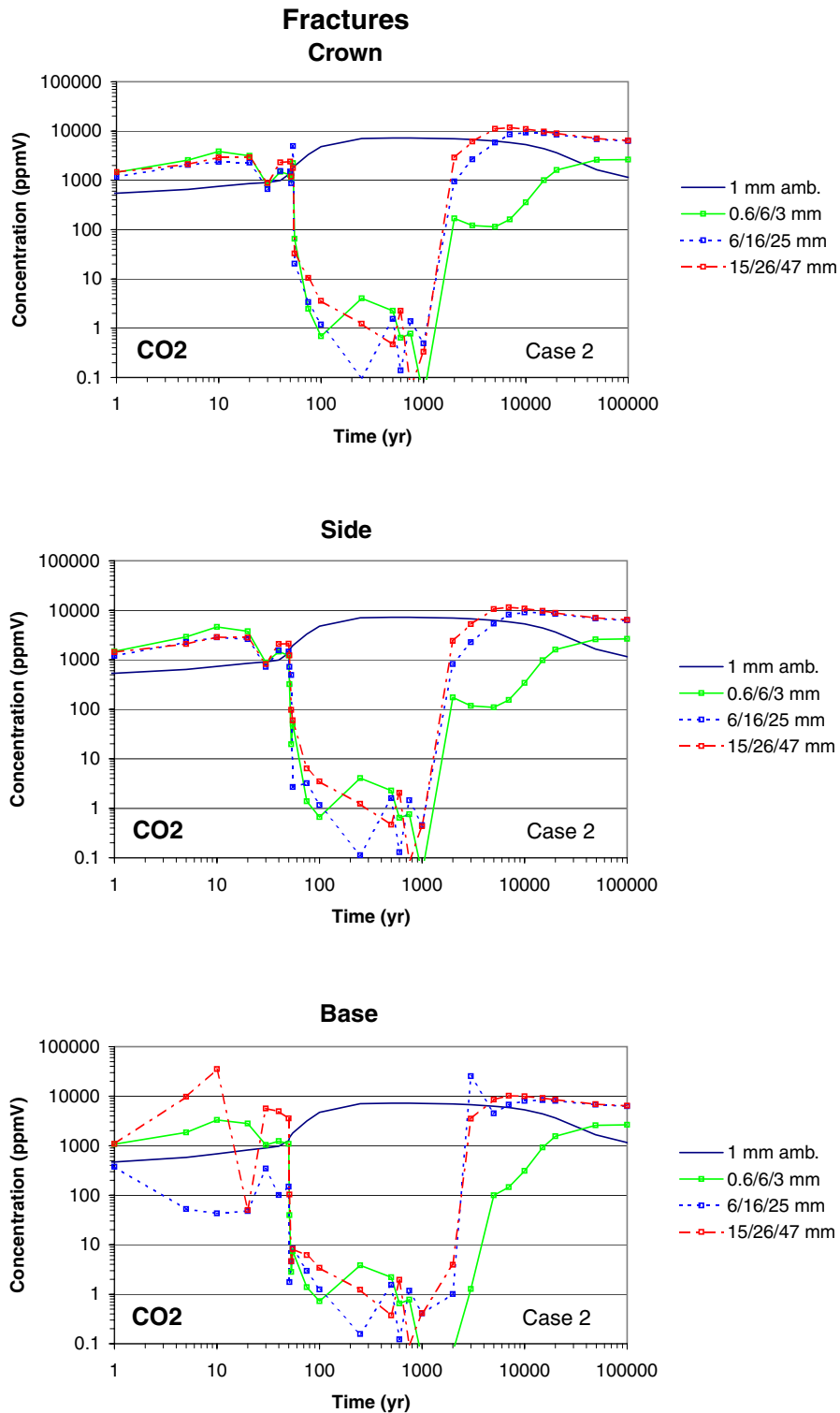
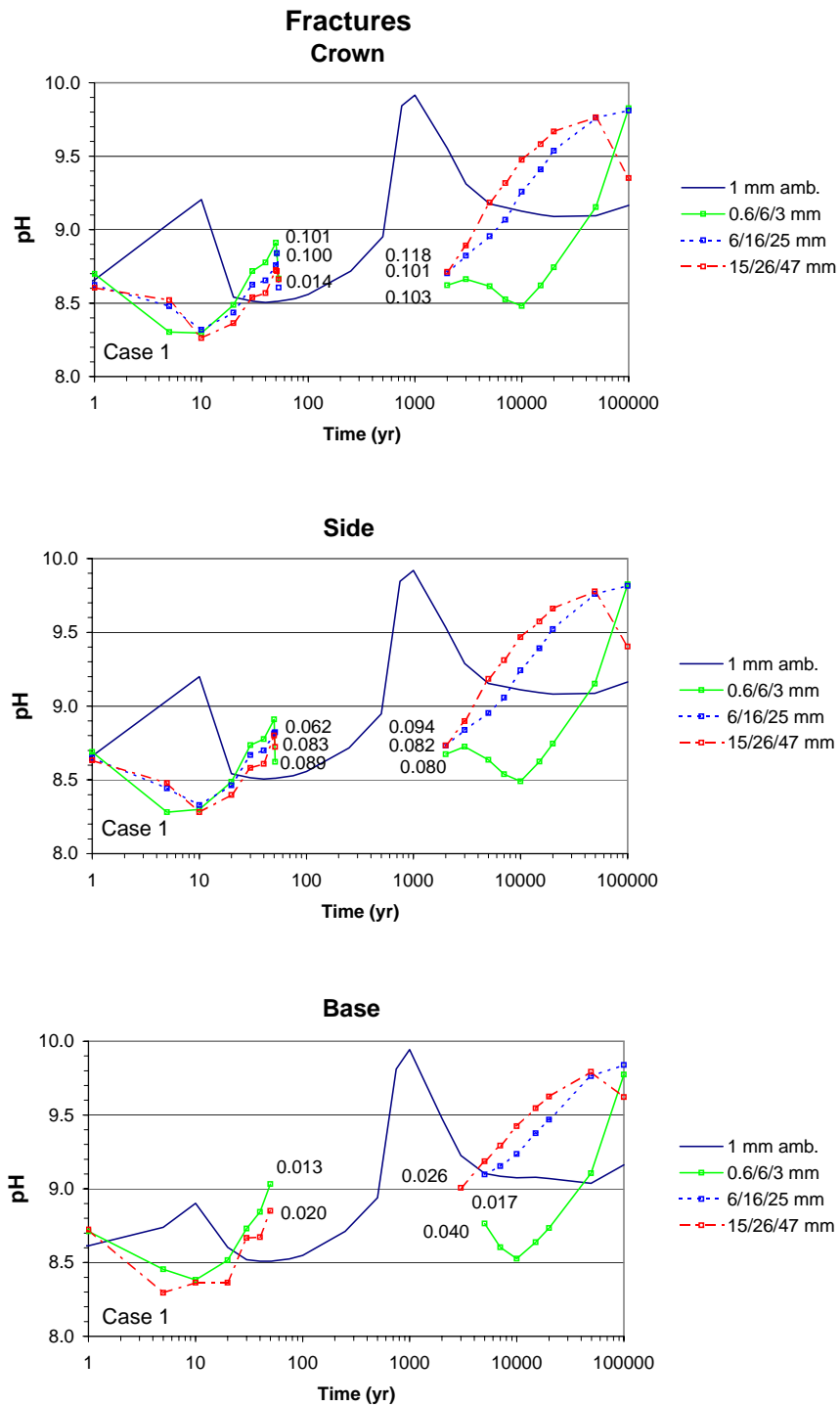


Figure 29. Time Profiles of Modeled CO₂ Concentrations in the Gas Phase in Fractures at Three Drift Wall Locations for Different Climate Scenarios (Case 2).

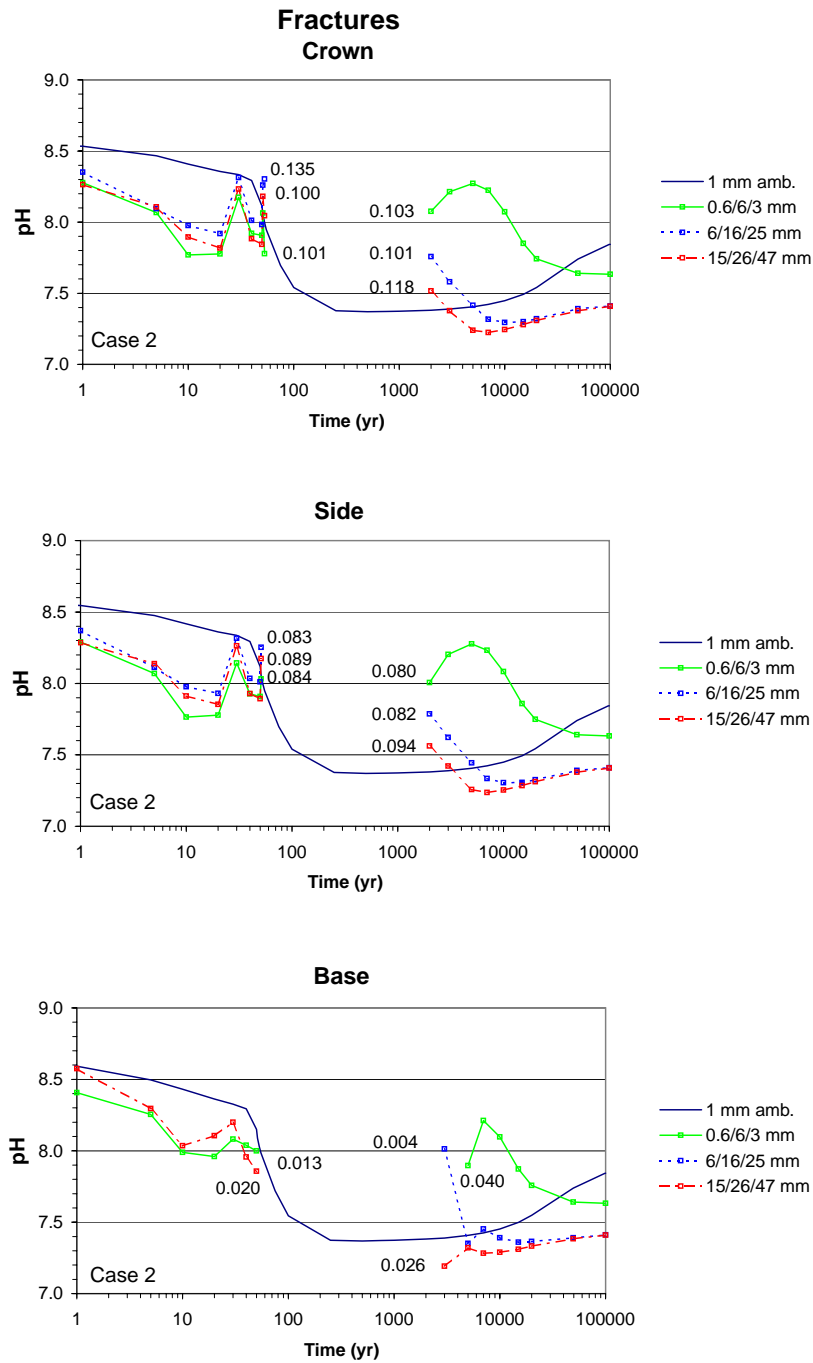
Predicted pH and total aqueous carbonate concentrations (as HCO_3^-) in fracture pore water are shown in Figures 30 through 33. The calculated pH is generally higher for Case 1 (approximate range 8.5 to 10) than for Case 2 (approximate range 7 to 8.5). Total aqueous carbonate concentrations are larger in Case 1 (maximum, after rewetting, near 10,000 mg/l for the low infiltration case) than in Case 2 (near ambient values of 200 mg/l after rewetting). Note that the mean infiltration case (6/16/25 mm) dries out before one year, therefore no results are shown until rewetting.

The large pH and carbonate concentration variations for the 1mm/yr ambient run in Case 1 (Figures 30 and 32) reflect an initially “unsteady” hydrochemical system. Obtaining an initial steady-state chemical system that is similar to the measured data for a few points is difficult because it depends on reaction rates as well as infiltration rates and rock properties. The difficulty increases with the number of reactive minerals included in the system, and with the uncertainty in reaction rates. This is the reason why calculated ambient concentration trends are less variable in Case 2 than in Case 1.



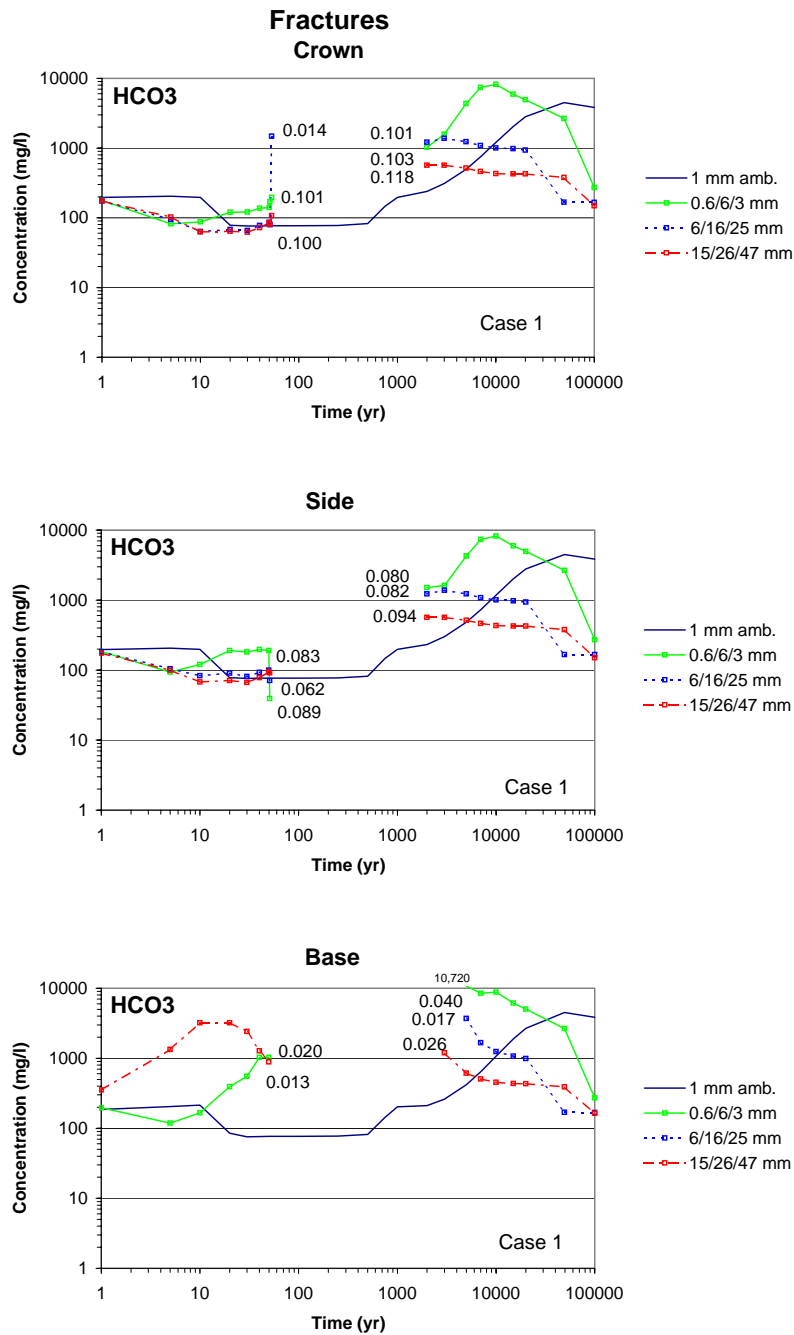
DTN: LB991200DSTTHC.002

Figure 30. Time Profiles of the Modeled pH of Fracture Water at Three Drift Wall Locations for Different Climate Scenarios (Case 1). The dryout period is left blank. The last output liquid saturation before dryout, and the first output liquid saturation during rewetting are noted on each curve.



DTN: LB991200DSTTHC.002

Figure 31. Time Profiles of the Modeled pH of Fracture Water at Three Drift Wall Locations for Different Climate Scenarios (Case 2). The dryout period is left blank. Numbers by each curve indicate the last output liquid saturation before dryout and the first output liquid saturation during rewetting.



DTN: LB991200DSTTHC.002

Figure 32. Time Profiles of Modeled Total Aqueous Carbonate Concentrations (as HCO₃⁻) in Fracture Water at Three Drift Wall Locations for Different Climate Scenarios (Case 1). The dryout period is left blank. Numbers by each curve indicate the last output liquid saturation before dryout and the first output liquid saturation during rewetting.

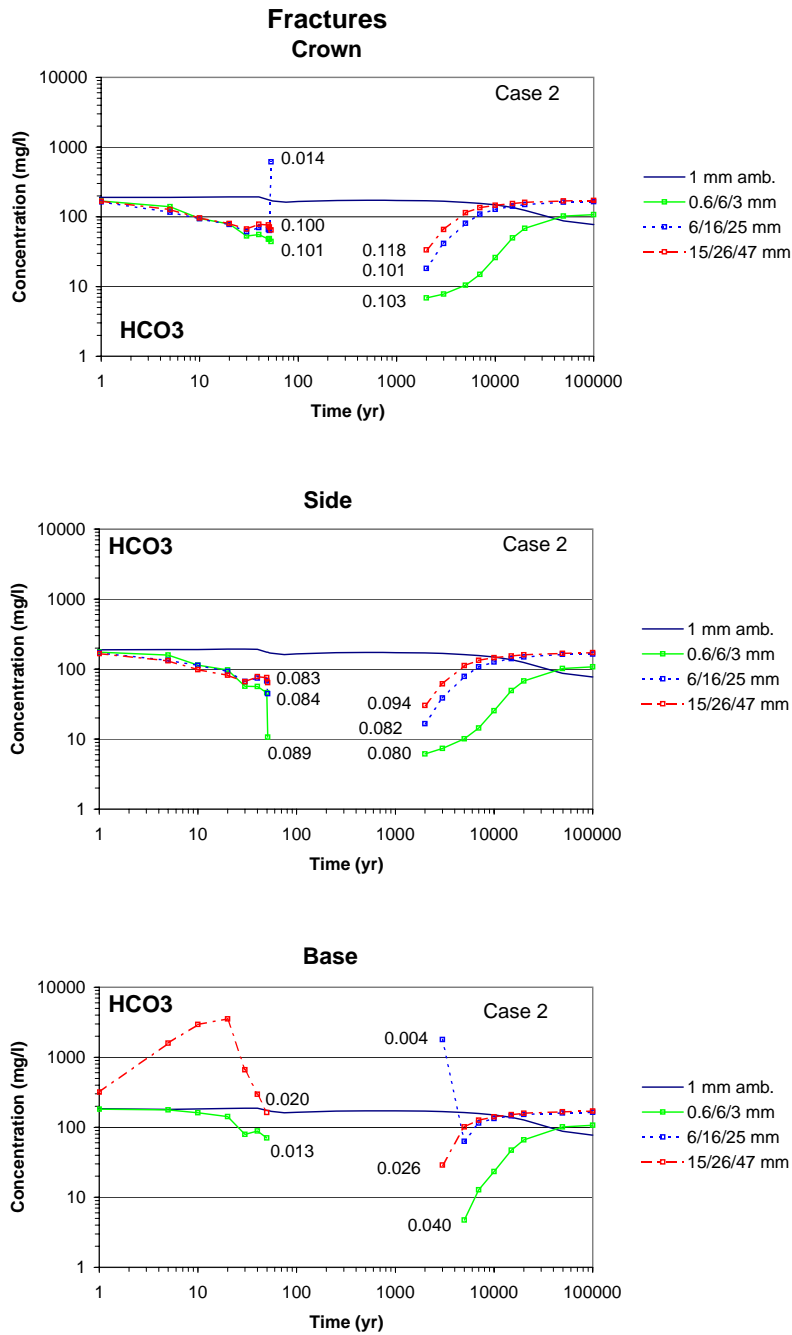


Figure 33. Time Profiles of Modeled Total Aqueous Carbonate Concentrations (as HCO_3^-) in Fracture Water at Three Drift Wall Locations for Different Climate Scenarios (Case 2). The dryout period is left blank. Numbers by each curve indicate the last output liquid saturation before dryout and the first output liquid saturation during rewetting.

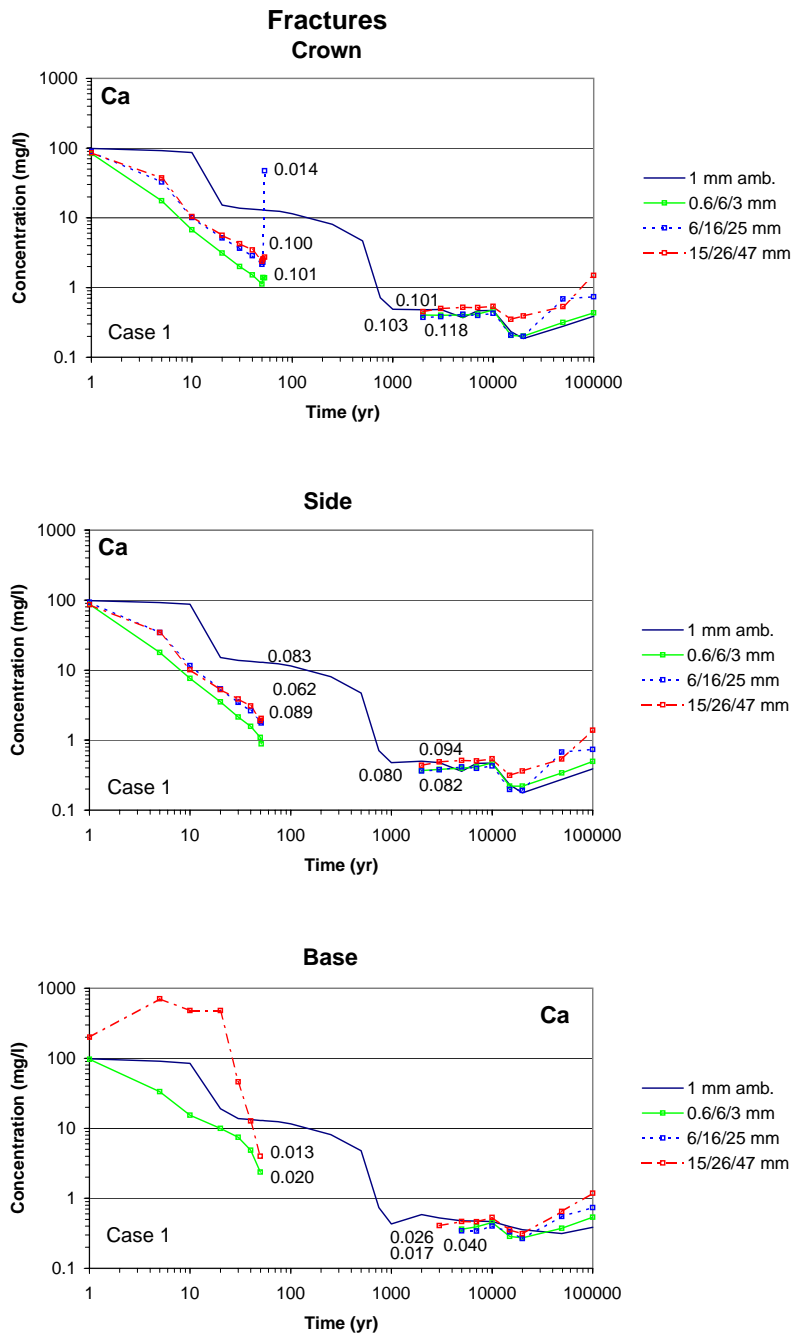
The pH-carbonate-CO₂ data show very different trends whether a Case-1 or Case-2 mineral assemblage is considered. This results from competing effects depending on the relative rates of infiltration, calcite dissolution/precipitation, feldspar dissolution, and calcium-zeolite precipitation. Case-1 simulations are quite sensitive to the effective reaction rates of aluminum silicate minerals and particularly calcium zeolites. The dissolution of feldspars to form zeolites and clays directly affects the pH. For example, the dissolution of albite (Na-feldspar) to form kaolinite (clay) results in an increase in pH, as follows:



It also affects pH indirectly by depleting calcium from solution, which inhibits calcite precipitation as a means of controlling increasing pH and total aqueous carbonate concentrations, as in the following reaction:

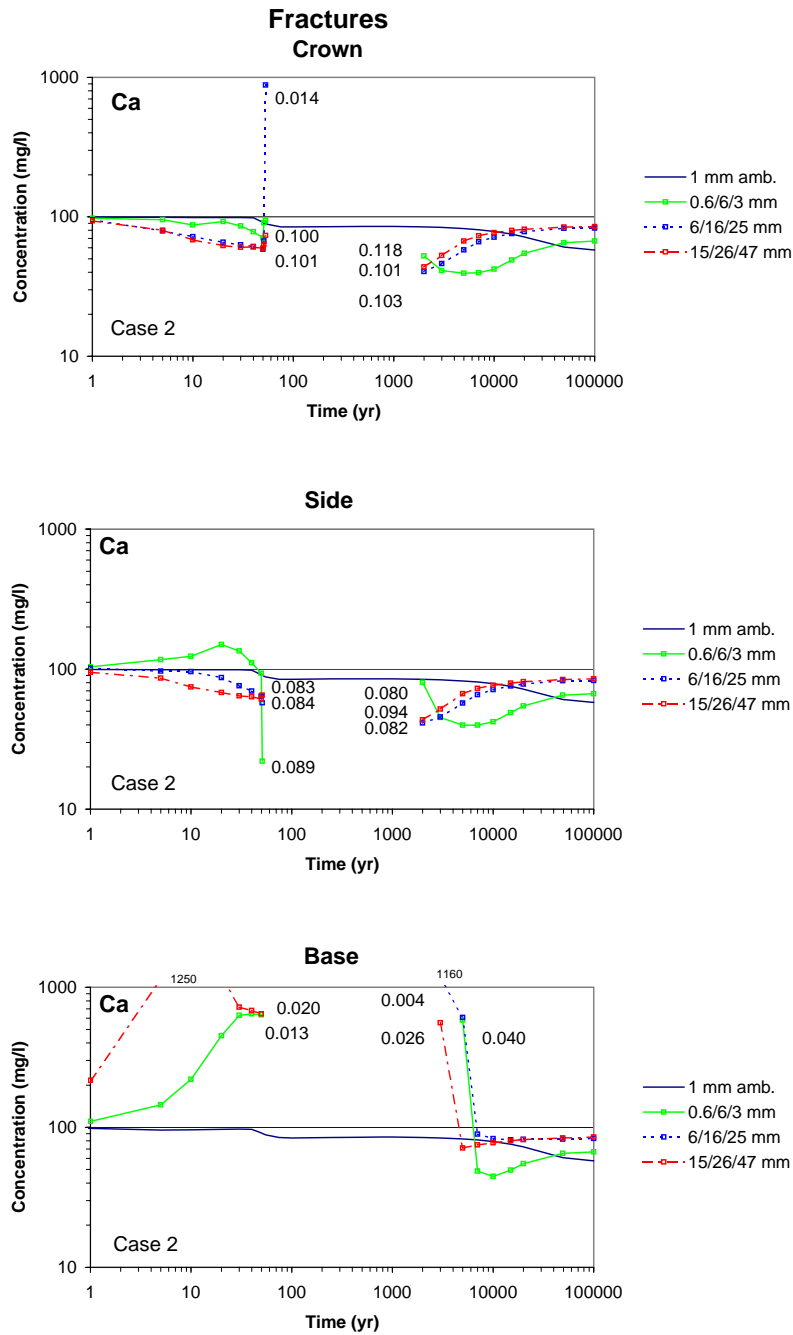


As a result, Case-1 simulations generally yield higher pH and total aqueous carbonate concentrations, and generally lower CO₂ partial pressures than Case-2 simulations. Calcium depletion and increased sodium concentrations are further indicators of feldspar (albite) dissolution and calcium zeolite precipitation in Case 1 (Figure 34 and 36). These trends are not observed in Case 2 (Figures 35 and 37). Evidence that Case-1 simulations overestimate feldspar dissolution and zeolite precipitation rates is further shown by the calcium depletion and increasing sodium concentrations calculated under ambient conditions. In addition, as mentioned earlier, the simulations under ambient conditions (no thermal loading) using the Case-1 mineral assemblage reveal a chemical system that is less “steady” than for Case-2 simulations (e.g., by comparing the ambient curves for pH, bicarbonate, and CO₂ on Figures 28 through 33). This reflects the model uncertainty with respect to reaction rates and the difficulty in reproducing an initially balanced hydrogeochemical system, which depends on infiltration rates and rock properties as well as reaction rates. Given this observation, a reduced set of minerals with better-constrained reaction rates such as for Case 2 is likely to match the pH, bicarbonate, and Ca better than the more complex system. This is shown with simulations of the DST (Section 6.2.7), which indicate that a Case-2 mineral assemblage provides better estimates of pH and CO₂ concentrations than Case 1, compared to waters and gases collected in the first 20 months of heating. However, there is also a possibility that the system may trend to the chemistry of the more complex system over time, particularly when long reaction times are considered (the DST is only an eight-year test, while the drift scale seepage simulations extend to 100,000 years).



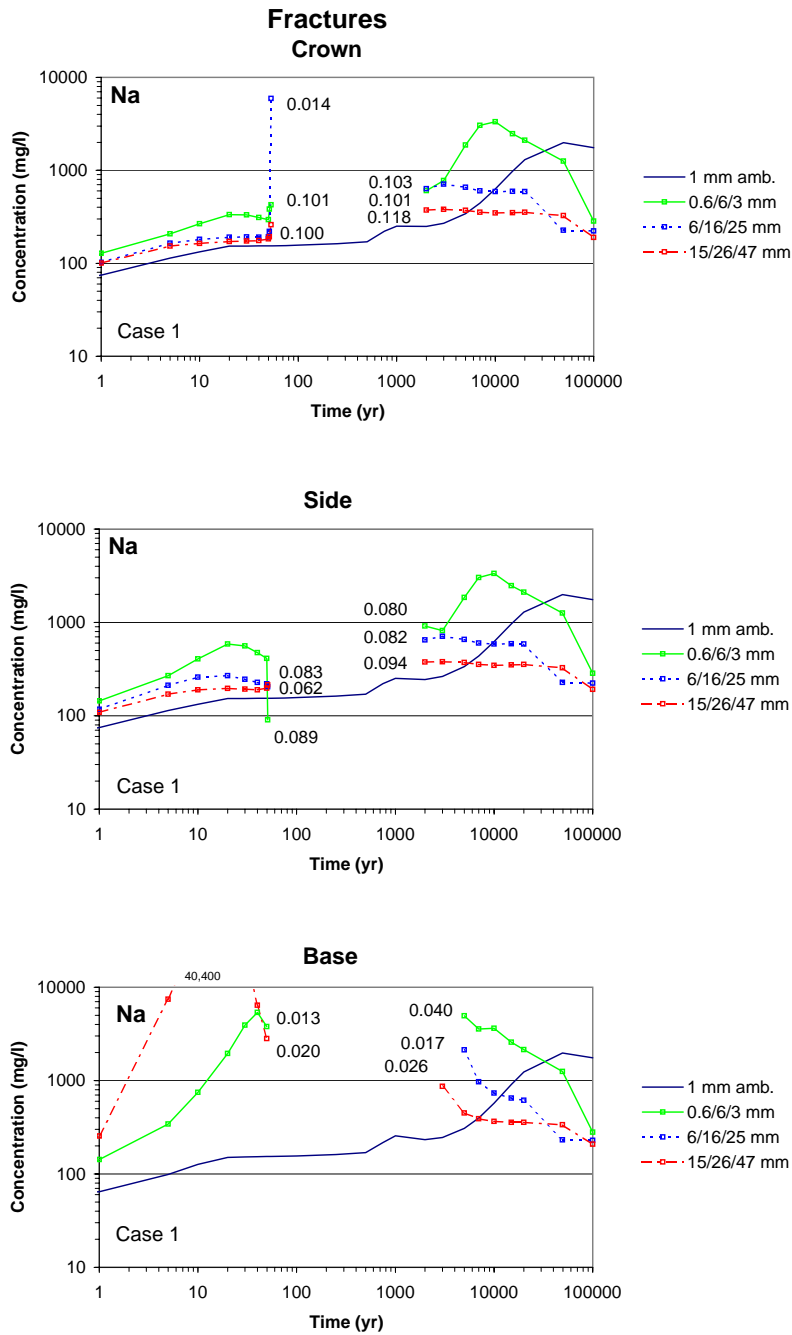
DTN: LB991200DSTTHC.002

Figure 34. Time Profiles of Modeled Total Aqueous Calcium Concentrations in Fracture Water at Three Drift Wall Locations for Different Climate Scenarios (Case 1). The dryout period is left blank. Numbers by each curve indicate the last output liquid saturation before dryout and the first output liquid saturation during rewetting.



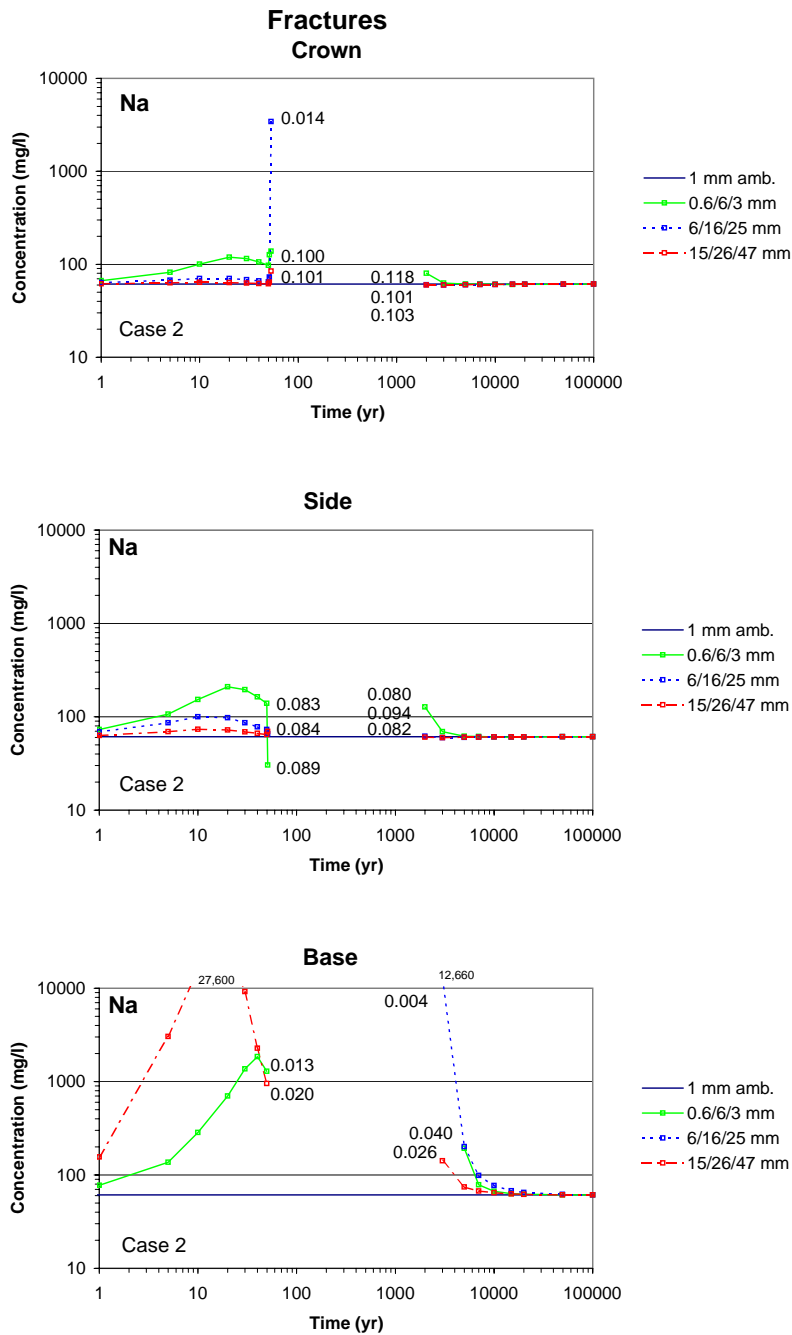
DTN: LB991200DSTTHC.002

Figure 35. Time Profiles of Modeled Total Aqueous Calcium Concentrations in Fracture Water at Three Drift Wall Locations for Different Climate Scenarios (Case 2). The dryout period is left blank. Numbers by each curve indicate the last output liquid saturation before dryout and the first output liquid saturation during rewetting.



DTN: LB991200DSTTHC.002

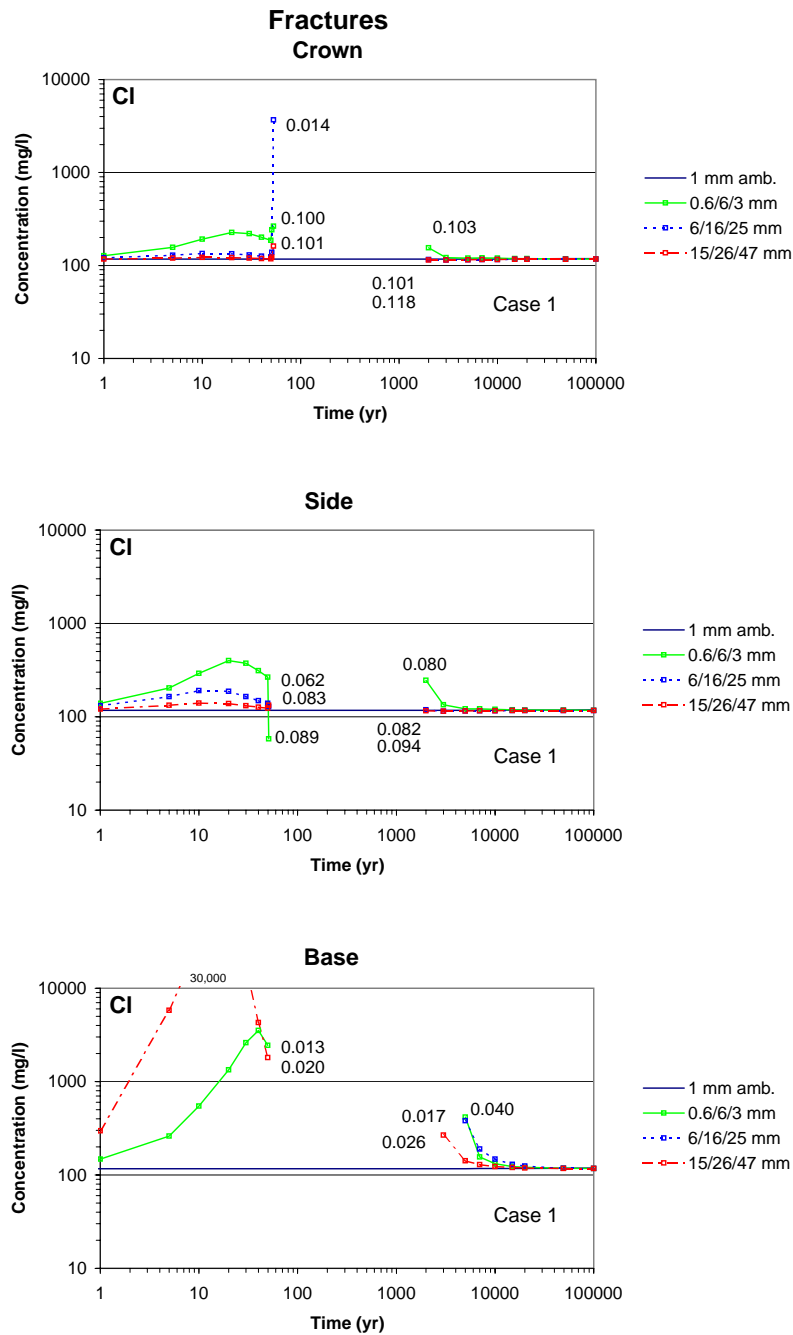
Figure 36. Time Profiles of Modeled Total Aqueous Sodium Concentrations in Fracture Water at Three Drift Wall Locations for Different Climate Scenarios (Case 1). The dryout period is left blank. Numbers by each curve indicate the last output liquid saturation before dryout and the first output liquid saturation during rewetting.



DTN: LB991200DSTTHC.002

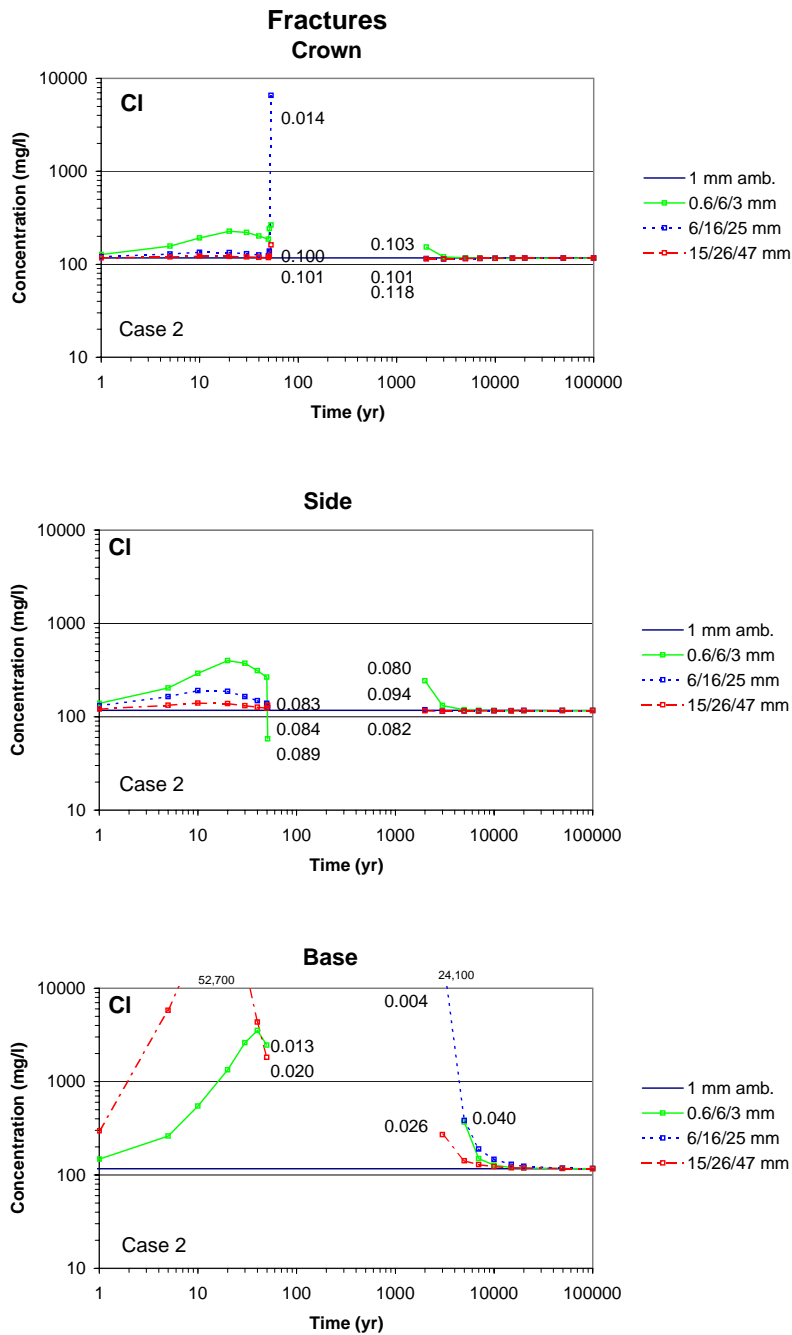
Figure 37. Time Profiles of Modeled Total Aqueous Sodium Concentrations in Fracture Water at Three Drift Wall Locations for Different Climate Scenarios (Case 2). The dryout period is left blank. Numbers by each curve indicate the last output liquid saturation before dryout and the first output liquid saturation during rewetting.

Chloride concentrations computed for Case 1 and Case 2 in fracture water are essentially identical due to the conservative behavior of this aqueous species (i.e. it is not affected by pH or the reaction rates of other minerals in the simulation) (Figures 38 and 39). Differences in the concentration peaks at the drift base between Case 1 and Case 2 result from a slight difference in the times when the geochemical calculation cutoff point was reached. The cutoff point is reached at either a minimum liquid saturation of 0.0001 or a maximum ionic strength of 2, at which point geochemical speciation calculations are suspended in that grid node. Upon rewetting, chloride concentrations drop relatively quickly below 400 mg/l towards ambient values near 110 mg/l.



DTN: LB991200DSTTHC.002

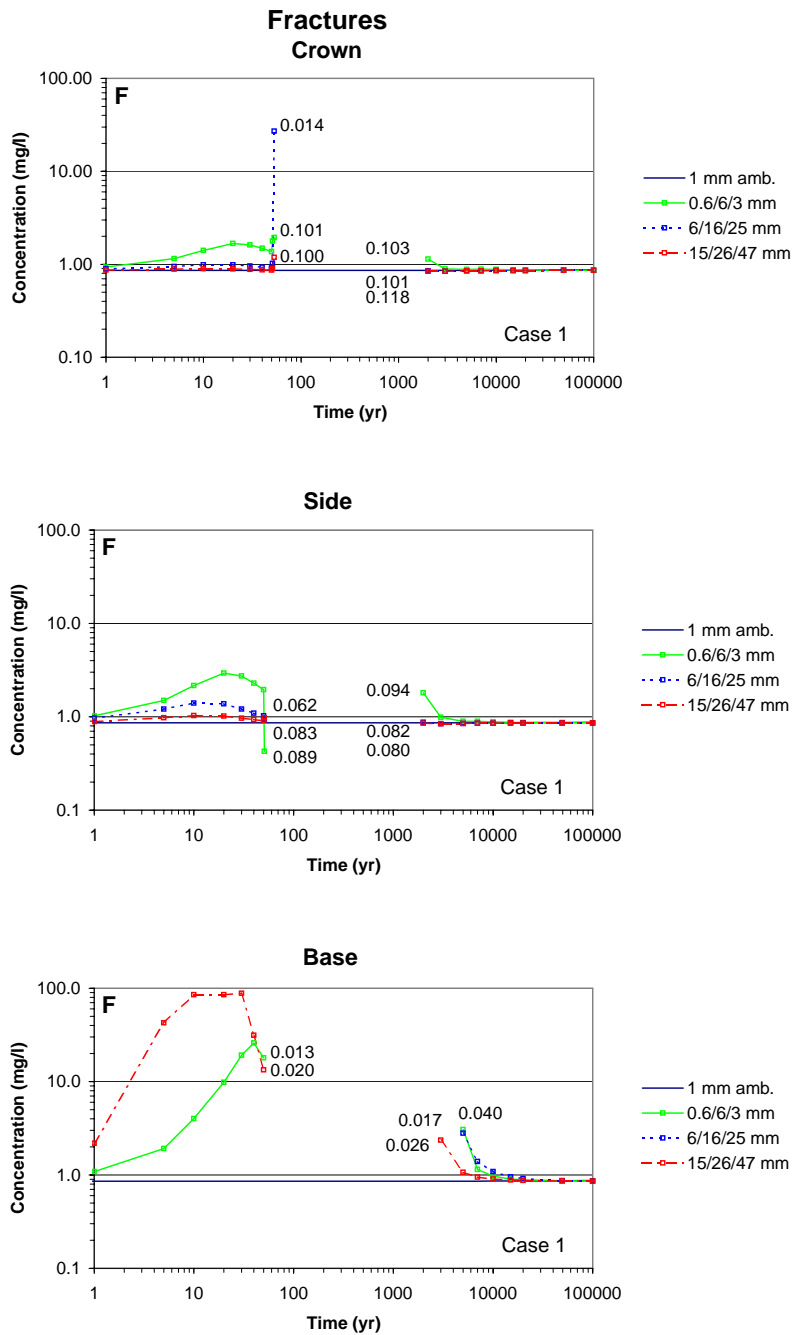
Figure 38. Time Profiles of Modeled Total Aqueous Chloride Concentrations in Fracture Water at Three Drift Wall Locations for Different Climate Scenarios (Case 1). The dryout period is left blank. Numbers by each curve indicate the last output liquid saturation before dryout and the first output liquid saturation during rewetting.



DTN: LB991200DSTTHC.002

Figure 39. Time Profiles of Modeled Total Aqueous Chloride Concentrations in Fracture Water at Three Drift Wall Locations for Different Climate Scenarios (Case 2). The dryout period is left blank. Numbers by each curve indicate the last output liquid saturation before dryout and the first output liquid saturation during rewetting.

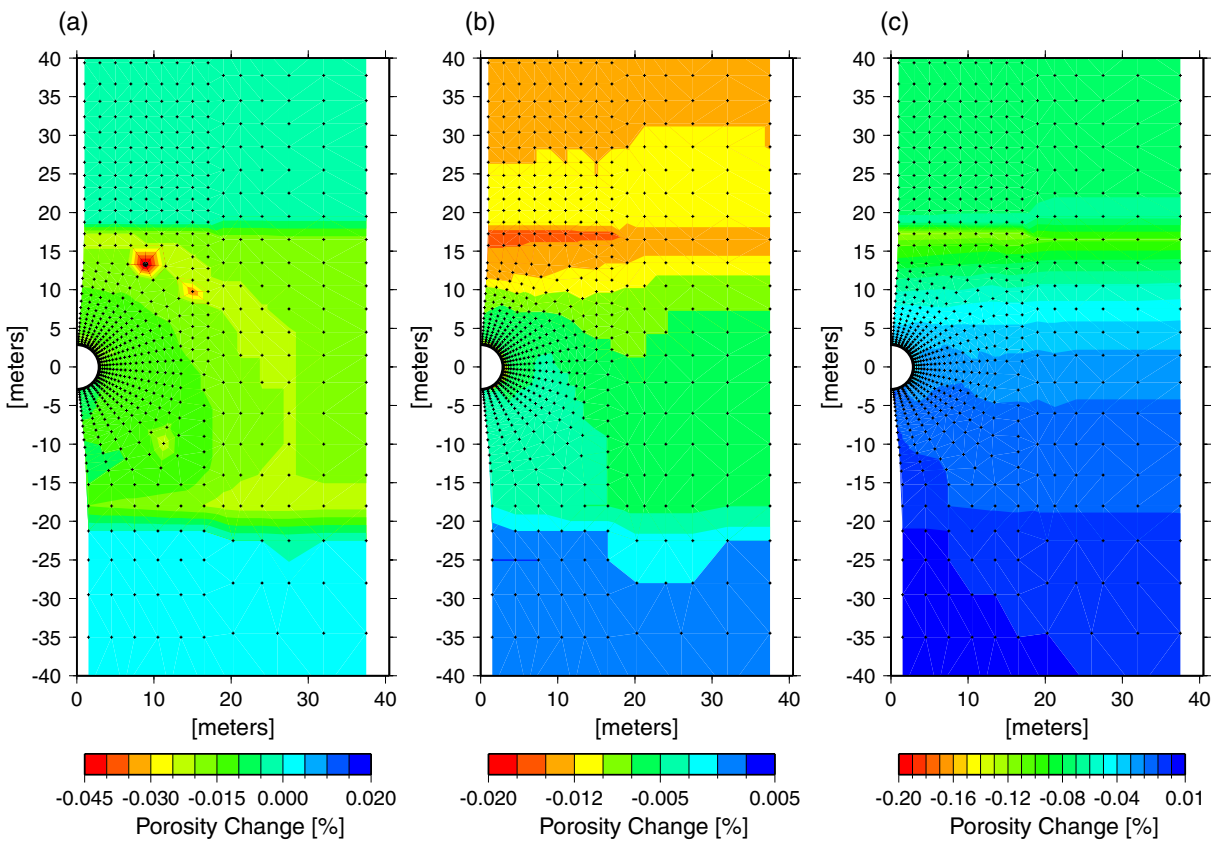
Fluoride was included only in Case 1 simulations. Upon rewetting, fluoride concentrations in fracture water (Figure 40) quickly drop below 2 mg/l towards ambient values of less than 1 mg/l. In the chemical system considered, at intermediate to high pH, fluoride concentrations are not affected significantly by pH and, therefore, the differences between Case 1 and Case 2 simulations should not affect fluoride concentrations, at least at values below the solubility of fluorite (CaF_2). However, at elevated fluoride concentrations, Case 1 simulations may overestimate fluoride concentrations because they may underestimate the amount of calcium in solution, therefore limiting the precipitation of fluorite and removal of fluoride from solution.



DTN: LB991200DSTTHC.002

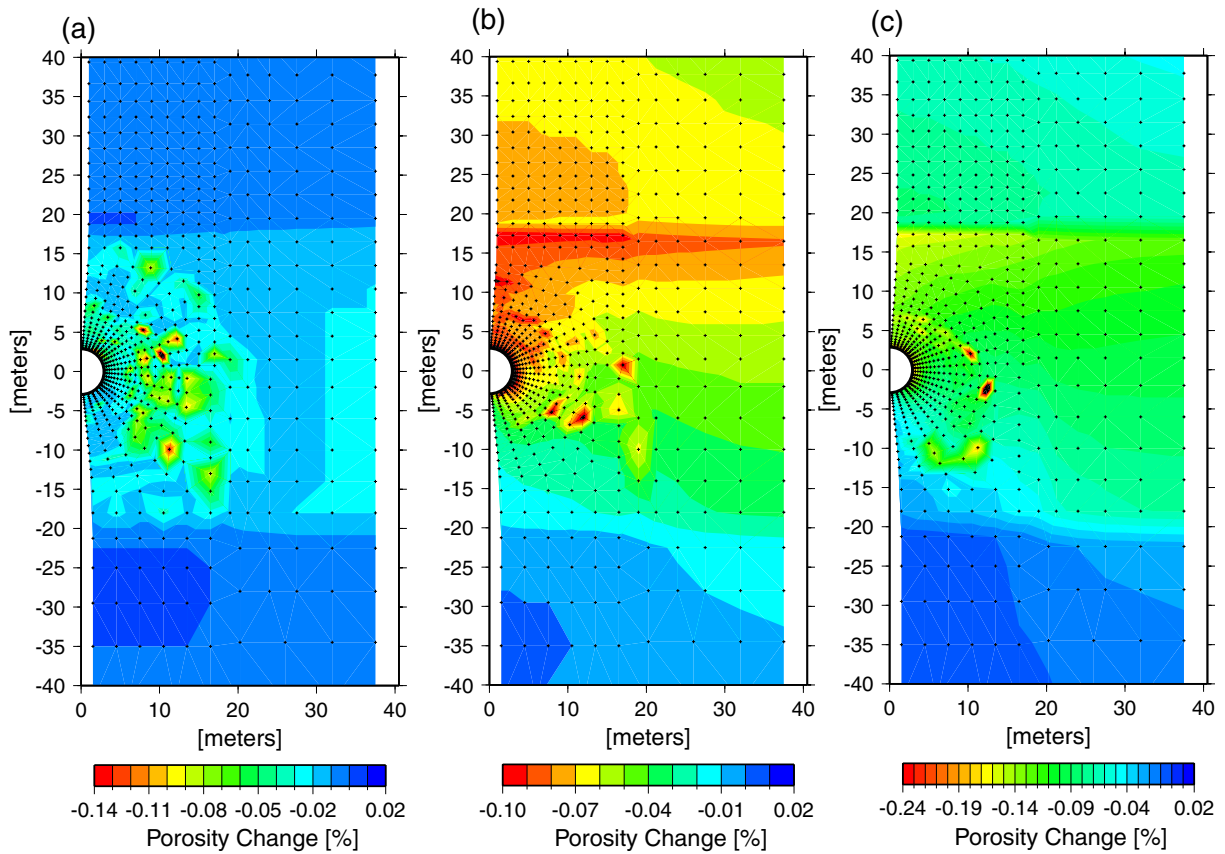
Figure 40. Time Profiles of Modeled Total Aqueous Fluoride Concentrations in Fracture Water at Three Drift Wall Locations for Different Climate Scenarios (Case 1). The dryout period is left blank. Numbers by each curve indicate the last output liquid saturation before dryout and the first output liquid saturation during rewetting.

The calculated change in fracture porosity in the vicinity of the drift was contoured for Case 1 (Figure 41a-c) and Case 2 (Figure 42a-c) for the three infiltration cases considered, at a simulated time of 10,000 years. The maximum porosity reduction (negative in the plots) occurs for the high infiltration case and is predominantly above the drift, adjacent to the tsw33 and tsw34 hydrogeologic unit contact. In all cases, the porosity change is small (less than 0.5 percent of the initial porosity) and mostly negative. The porosity decrease is due primarily to zeolite precipitation in Case 1 and calcite precipitation in Case 2. Because the porosity changes are small, and thus permeability changes are also minor, thermohydrological processes are not significantly affected by mineral precipitation or dissolution. Note that small fluctuations in porosity at individual grid nodes are due to grid orientation effects but do not change the overall pattern.



DTN: LB991200DSTTHC.002

Figure 41. Contour Plot of Modeled Total Fracture Porosity Change at 10,000 years for Three Climate Scenarios: (a) Low, (b) Mean, and (c) High. Red areas indicate maximum decrease in porosity due to mineral precipitation (Case 1).



DTN: LB991200DSTTHC.002

Figure 42. Contour Plot of Calculated Total Fracture Porosity Change at 10,000 years for Three Climate Scenarios: (a) Low, (b) Mean, and (c) High. Red areas indicate maximum decrease in porosity due to mineral precipitation (Case 2).

INTENTIONALLY LEFT BLANK

7. CONCLUSIONS

This AMR describes the conceptual model for the numerical simulation of coupled Thermal-Hydrological-Chemical (THC) processes in the Near-Field Environment (NFE), the Drift Scale Test (DST) THC Model, and the THC Seepage Model. Model results associated with this AMR have been submitted to the Technical Data Management System (TDMS) for use in Performance Assessment and to provide input to the NFE Process Model Report (PMR) and the Unsaturated Zone PMR. The conceptual model provides a comprehensive basis for modeling the pertinent mineral-water-gas reactions in the host rock, under thermal loading conditions, as they influence the NFE water and gas chemistry that may enter potential waste-emplacement drifts over 100,000 years. Data are incorporated from the calibrated thermohydrological property sets, the Three-Dimensional Mineralogical Model (ISM3.0), the UZ Site-Scale Flow and Transport Model, Thermal Test geochemical data (fracture and matrix mineralogy, aqueous geochemistry, and gas chemistry), thermodynamic data (minerals, gases, and aqueous species), data for mineral-water reaction kinetics, and transport data. Simulations of THC processes included coupling between heat, water, and vapor flow, aqueous and gaseous species transport, kinetic and equilibrium mineral-water reactions, and feedback of mineral precipitation/dissolution on porosity, permeability, and capillary pressure (hydrologic properties) for a dual-permeability (fracture-matrix) system. The effect of these coupled THC processes on the time evolution of flow fields in the NFE has been investigated for different climate change scenarios, calibrated property sets, and initial mineralogy. Aqueous species included in the model are H^+ , Ca^{2+} , Na^+ , K^+ , SiO_2 (aq), Mg^{2+} , Al^{3+} , Fe^{3+} , SO_4^{2-} , HCO_3^- , Cl^- , and F^- . Twenty-three minerals are considered including several silica phases, calcite, feldspars, smectites, illite, kaolinite, sepiolite, zeolites, fluorite, hematite, goethite, gypsum, plus volcanic glass. Treatment of CO_2 included exsolution into the gas phase, gas-water equilibration, gaseous diffusion and advection.

Validation of the model was done by comparison of measured gas and water chemistry from the Drift Scale Test (DST) to the results of simulations using the DST THC Model. In particular, simulation results were compared to measured gas-phase CO_2 concentrations and the chemistry of waters collected from hydrology boreholes collected during the test. Comparisons of the model results to the measured changes in CO_2 concentrations over time show that the model captures the initial rise in concentration in all of the borehole intervals where comparisons were made, in areas having very different thermal histories. In those intervals closer to the heaters where an earlier peak in concentration was observed, the model also captured this behavior. However, a second larger peak was observed in those intervals, which was not predicted by the simulations. This discrepancy resulted from the fact that sample cooling during collection removed condensed water vapor from gas samples before analysis, whereas simulation results include water vapor. Because of a sharp reduction in the air mass fraction of the gas phase, it appears that this second peak was a result of the shift in the CO_2 /air ratio in the initial boiling phase, which also undergoes a large spike at the early stages of boiling. Therefore, analysis of dry gas samples are very different from the model data in this time period only.

Comparisons of water chemistry (pH) and CO_2 concentrations in the gas phase from the DST indicate that a simplified set of aqueous species (Case 2) and minerals (calcite, silica phases, gypsum), but including gaseous CO_2 , can describe the general evolution of Drift Scale Test waters

quite closely. Including a wide range of aluminosilicates, such as feldspars, clays and zeolites yields information on additional species (i.e., Al, Fe, F), but their inclusion causes shifts in the water and gas chemistry that are more rapid than is observed. These effects may be more important over longer time periods, but over the time scale of the Drift Scale Test, it is clear that the effective reaction rates and/or thermodynamic properties of these phases will require some refinement.

A THC Seepage Model was developed that incorporated the elements of the EDA II design to represent waste package heating over time, changes in heat load due to ventilation, the effective heat transfer within the drift, the addition of backfill after 50 years, and the THC processes in the NFE. This two-dimensional model incorporated the initial vertical heterogeneity in hydrologic and thermal properties and mineralogy from the surface to the Calico Hills zeolitic unit, along with different initial mineralogy and reactive surface areas in fractures and matrix. A number of cases were evaluated for different calibrated property sets, climate change scenarios, and geochemical systems. Predictions were presented of the water and gas chemistry that may enter the drifts, and data have been submitted that document the temporal frequency of possible seeps based on the times of rewetting around the drifts, along with the net fluxes of water and gas to the drift wall. These predictions are provided for a period of 100,000 years, including a pre-closure period of 50 years with 70% heat removal by ventilation.

The measured water and gas chemistry around the drift, during the early phase of heating and during the dryout period, were similar to those observed in the DST THC simulations. The rewetting period has not yet been observed in the Drift Scale Test, and the THC Seepage simulations indicate that there may be an increase in the CO₂ gas and aqueous carbonate concentrations around the drift during rewetting. The extent of the dryout zone and the time of rewetting were different for each climate history and calibrated property set. As in the Drift Scale Test THC simulations, there were some notable differences in the pH and CO₂ concentrations between the two geochemical systems considered. Based on comparisons of the Drift Scale Test measured water and gas chemistry, it appears that the system with aluminosilicates (Case 1) shifted the pH in fracture condensate waters to values that are from 0.5 to 1 pH unit higher than the observed values. In the THC Seepage Model, the composition of waters reaching the drift wall during rewetting were roughly neutral in pH (7.2 – 8.3) for the system without aluminosilicates (Case 2), and approximately 8.6 – 9.0 for the more complete geochemical system (Case 1). Predicted pH and HCO₃⁻ concentrations in Case 2 simulations are supported by the data from the DST; however, the long term evolution could trend in the direction of the more complex system chemistry (Case 1), if the slow reaction rates of the aluminosilicates limit the changes in water chemistry that can be observed over the short heating time of the DST.

Even with the seemingly higher overall reaction rate for the more complete mineral assemblage, the changes in porosity and permeability in the NFE over 100,000 years were small (less than 1%), and therefore effects on flow and transport were negligible. Comparison of the results of a purely thermohydrologic simulation to that including coupled THC processes showed virtually no differences in the water and gas fluxes, liquid saturations, porosity and permeability around the drift. Mineral precipitation and dissolution did result in early localized heterogeneities in the hydrologic properties around the drift, which increased over time. In both geochemical systems, a zone of enhanced precipitation formed at the contact of the Topopah Spring nonwelded and upper

lithophysal zones, about 15 to 18 meters above the drift center. For both geochemical cases, silica precipitation was subordinate to calcite (Case 2) or zeolites (Case 1), therefore confirming the necessity of considering a comprehensive geochemical system to capture the relevant coupled THC processes in the NFE. Although the geochemical system containing aluminosilicates may overestimate the effect of mineral-water reactions on the geochemistry of waters and gases, it may, however, provide a better upper limit on the extent of changes in hydrological properties than the simplified geochemical system (Case 2).

There are many uncertainties in modeling coupled THC processes because of the large amount of data needed and the complexity of natural systems. These data range from the fundamental thermodynamic properties of minerals, aqueous species, and gases, the kinetic data for mineral-water reactions, to the representation of the unsaturated hydrologic system for the fractured tuffs. In addition, a wealth of site-specific thermohydrologic, geologic, and geochemical data are necessary to describe the initial and boundary conditions. For these reasons, it may not be possible to assign a model uncertainty based on the uncertainties of the data themselves, and therefore model validation gives a true test of whether the system can be described sufficiently well for the intended purposes of the model. Results of simulations of the DST captured the important changes in pH and gas-phase CO₂ concentrations at each location over time well within the range of variation in the measured gas and water concentrations between sampling locations. This provides a sufficient validation of the model's capability for the prediction of spatial and temporal variation in water and gas chemistry.

The impact of TBVs (to-be-verified), associated with input data, on model predictions would not be significant, because the model is validated against measured data. However, TBVs associated with the measured water and gas chemistry from the DST are much more significant, because changes in these data could result in a reevaluation of the model if deviations from the simulation results were much greater. The THC Seepage model did not consider a "no-backfill" case. This case is under investigation and will be reported in future revisions of this document.

INTENTIONALLY LEFT BLANK

8. INPUTS AND REFERENCES

8.1 DOCUMENTS CITED

Apps, J.A. 1970. *The Stability Field of Analcime*. Ph.D. dissertation. Cambridge, Massachusetts: Harvard University. TIC: applied for.

Apps, J.A. and Chang, G.M. 1992. "Correlation of the Na/K Ratio in Geothermal Well Waters with the Thermodynamic Properties of Low Albite and Potash Feldspar." *Proceedings of the 7th International Symposium on Water-Rock Interaction*, 1437–1440. Rotterdam, The Netherlands: A.A. Balkema. TIC: applied for.

Bear, J. 1972. *Dynamics of Fluid in Porous Media*. New York, New York: Dover Publications. TIC: 217568.

Berman, R.G. 1988. "Internally Consistent Thermodynamic Data for Minerals in the System $\text{Na}_2\text{O-K}_2\text{O-CaO-MgO-FeO-Fe}_3\text{O-Al}_2\text{O}_3\text{-SiO}_2\text{-TiO}_2\text{-H}_2\text{O-CO}_2$." *Journal of Petrology*, 29, 445–522. Dallas, Texas: Society of Petroleum Engineers. TIC: 236892.

Bish, D.L.; Carey, J.W.; Levy, S.S.; and Chipera, S.J. 1996. *Mineralogy-Petrology Contribution to the Near-Field Environment Report*. Milestone Report LA-3668. Los Alamos, New Mexico: Los Alamos National Laboratory. ACC: MOL.19961122.0252.

Blum, A.E. and Stillings, L.L. 1995. "Feldspar Dissolution Kinetics." Chapter 7 of *Chemical Weathering Rates of Silicate Minerals*, 31, 291–351. White, A.F. and Brantley, S.L., eds. Washington, D.C.: Mineral Society of America. TIC: 241237.

Carroll, S.; Mroczek, E.; Alai, M.; and Ebert, M. 1998. "Amorphous Silica Precipitation (60 to 120°C): Comparison of Laboratory and Field Rates." *Geochimica et Cosmochimica Acta*, 62, 1379–1396. Amsterdam, The Netherlands: Elsevier Science Publishers. TIC: 243029.

CRWMS M&O (Civilian Radioactive Waste Management System Management & Operating Contractor) 1999a. *Analysis & Modeling Development Plan (DP) for U0110 Drift-Scale Coupled Processes (DST THC Seepage) Models Rev. 00*. TDP-NBS-HS-000007. Las Vegas, Nevada: CRWMS M&O. ACC: MOL.19990830.0378.

CRWMS M&O 1999b. *M&O Site Investigations*. Activity Evaluation, January 23, 1999. Las Vegas, Nevada: CRWMS M&O. ACC: MOL.19990317.0330.

CRWMS M&O 1999c. *M&O Site Investigations*. Activity Evaluation, September 28, 1999. Las Vegas, Nevada: CRWMS M&O. ACC: MOL.19990928.0224.

de Marsily, G. 1986. *Quantitative Hydrogeology: Groundwater Hydrology for Engineers*. Orlando, Florida: Academic Press. TIC: 208450.

Drever J.I. 1997. *Geochemistry of Natural Waters*, 3rd Ed. Upper Saddle River, N.J.: Prentice Hall. TIC: 246732

Dyer, J.R. 1999. "Revised Interim Guidance Pending Issuance of New U.S. Nuclear Regulatory Commission (NRC) Regulations (Revision 01, July 22, 1999), for Yucca Mountain, Nevada." Letter from J.R. Dyer (DOE) to D.R. Wilkins (CRWMS M&O), September 9, 1999, OL&RC: SB-1714, with enclosure, "Interim Guidance Pending Issuance of New U.S. Nuclear Regulatory Commission (NRC) Regulations (Revision 01)." ACC: MOL.19990910.0079.

Ehrlich, R.; Etris, E.L.; Brumfield, D.; Yuan, L.P.; and Crabtree, S.J. 1991. "Petrography and Reservoir Physics III: Physical Models for Permeability and Formation Factor." *AAPG Bulletin*, 75, 1579–1592. Tulsa, Oklahoma: American Association of Petroleum Geologists. TIC: 246294

Fournier, R.O. and Rowe, J.J. 1962. "The Solubility of Cristobalite along the Three-Phase Curve, Gas Plus Liquid Plus Cristobalite." *American Mineralogist*, 47, 897–902. Washington, D.C.: Mineralogical Society of America. TIC: 235380.

Garrels, R.M. and Christ, C.L. 1965. *Solutions, Minerals and Equilibria*. New York: Harper and Row. TIC: 217443.

Inskeep, W.P. and Bloom, P.R. 1985. "An Evaluation of Rate Equations for Calcite Precipitation Kinetics at $p\text{CO}_2$ Less than 0.01 atm and pH Greater than 8." *Geochimica et Cosmochimica Acta*, 49, 2165–2180. Amsterdam, The Netherlands: Elsevier Science Publishers. TIC: 241125.

Johnson, J.W.; Oelkers, E.H.; and Helgeson, H.C. 1992. "SUPCRT92: A Software Package for Calculating the Standard Molal Thermodynamic Properties of Minerals, Gases, Aqueous Species, and Reactions from 1 to 5000 bars and 0 to 1000 degrees C." *Computers and Geosciences*, 18, 899–947. Great Britain: Pergamon Press. TIC: 239019.

Johnson, J.W.; Knauss, K.G.; Glassley, W.E.; DeLoach, L.D.; and Thompson, A.F.B. 1998. "Reactive Transport Modeling of Plug-Flow Reactor Experiments: Quartz and Tuff Dissolution at 240 C." *Journal of Hydrology*, 209 (1–4), 81–111. TIC: 240986.

Klein, C. and Hurlbut, C.S. 1993. *Manual of Mineralogy*, 21st Edition. New York, New York: John Wiley & Sons. TIC: applied for.

Knauss, K.G. and Wolery, T.J. 1989. "Muscovite Dissolution Kinetics as a Function of pH and Time at 70°C." *Geochimica et Cosmochimica Acta*, 53, 1493–1501. Amsterdam, The Netherlands: Elsevier Science Publishers. TIC: 236215.

Knowles-Van Cappellan, V.; Van Cappellan, P.; and Tiller, C. 1997. "Probing the Charge of Reactive Sites at the Mineral-Water Interface: Effect of Ionic Strength on Crystal Growth Kinetics of Fluorite." *Geochimica et Cosmochimica Acta*, 61, 1871–1877. Amsterdam, The Netherlands: Elsevier Science Publishers. TIC: applied for.

Lasaga A.C. 1998. *Kinetic Theory in the Earth Sciences*. Princeton, New Jersey: Princeton University Press. TIC: applied for.

Levy, S.S.; Fabryka-Martin, J.T.; Dixon, P.R.; Liu, B.; Turin, H.J.; and Wolfsberg, A.V. 1997. "Chlorine-36 Investigations of Groundwater Infiltration in the Exploratory Studies Facility at

Yucca Mountain, Nevada. *Scientific Basis for Nuclear Waste Management XX, Material Research Society Symposium Proceedings, Boston, Massachusetts, 465, December 2-6, 1996*, 901–908. Pittsburgh, Pennsylvania: Materials Research Society. TIC: 244801.

Liu, H.H.; Doughty, C.; and Bodvarsson, G.S. 1998. “An Active Fracture Model for Unsaturated Flow and Transport in Fractured Rocks.” *Water Resources Research* 34 (10), 2633–2646. Washington, D.C.: American Geophysical Union. TIC: 243012.

Mazer, J.J.; Bates, J.K.; Bradley, J.P.; Bradley, C.R.; and Stevenson, C.M. 1992. “Alteration of Tectite to Form Weathering Products.” *Nature*, 357, 573-576. London, England: Macmillan Magazines. TIC: 246479.

Nagy, K.L. 1995. “Dissolution and Precipitation Kinetics of Sheet Silicates.” *Chemical Weathering Rates of Silicate Minerals*, 31, 291–351. White, A.F. and Brantley, S.L., eds. Washington, D.C.: Mineral Society of America. TIC: 222496.

Pruess K. 1991. *TOUGH2—A General Purpose Numerical Simulator for Multiphase Fluid and Heat Flow*. Report LBL-29400, UC-251. Berkeley, California: Lawrence Berkeley National Laboratory. ACC: NNA.19940202.0088.

Ragnarsdottir, K.V. 1993. “Dissolution Kinetics of Heulandite at pH 2-12 and 25°C.” *Geochimica et Cosmochimica Acta*, 57, 2439–2449. Amsterdam, The Netherlands: Elsevier Science Publishers. TIC: 222070.

Reed, M.H. 1982. “Calculation of Multicomponent Chemical Equilibria and Reaction Processes in Systems Involving Minerals, Gases, and an Aqueous Phase.” *Geochimica et Cosmochimica Acta*, 46, 513–528. Amsterdam, The Netherlands: Elsevier Science Publishers. TIC: 224159.

Renders, P.J.N.; Gammons, C.H.; and Barnes, H.L. 1995. “Precipitation and Dissolution Rate Constants for Cristobalite from 150 to 300°C.” *Geochimica et Cosmochimica Acta*, 59 (1), 77–85. Amsterdam, The Netherlands: Elsevier Science Publishers. TIC: 226987.

Rimstidt, J.D. 1997. “Quartz Solubility at Low Temperatures.” *Geochimica et Cosmochimica Acta*, 61 (13), 2553–2558. Amsterdam, The Netherlands: Elsevier Science Publishers. TIC: 239020.

Rimstidt, J.D. and Barnes, H.L. 1980. “The Kinetics of Silica-Water Reactions.” *Geochimica et Cosmochimica Acta*, 44, 1683–1699. Amsterdam, The Netherlands: Elsevier Science Publishers. TIC: 219975.

Shock, E.L.; Sassani, D.C.; Willis, M.; and Sverjensky, D.A. 1997. “Inorganic Species in Geologic Fluids: Correlations among Standard Molal Thermodynamic Properties of Aqueous Ions and Hydroxide Complexes.” *Geochimica et Cosmochimica Acta*, 61 (5), 907–950. Amsterdam, The Netherlands: Elsevier Science Publishers. TIC: applied for.

Slider H.C. 1976. *Practical Petroleum Reservoir Engineering Methods*. Tulsa, Oklahoma: The Petroleum Publishing Company. TIC: applied for.

Sonnenthal, E. L. and Bodvarsson, G. S. 1999. "Constraints on the Hydrology of the Unsaturated Zone at Yucca Mountain, NV from Three-Dimensional Models of Chloride and Strontium Geochemistry." *Journal of Contaminant Hydrology*, 38 (1–3), 107–156. Amsterdam, The Netherlands: Elsevier Science Publishers. TIC: 244160.

Sonnenthal, E.L. and Ortoleva, P.J. 1994. "Numerical Simulations of Overpressured Compartments in Sedimentary Basins, in Basin Compartments and Seals." *American Association of Petroleum Geologists Memoir*, 61, 403–416. Ortoleva, P.J. and Al-Shaieb, Z., eds. Tulsa, Oklahoma: American Association of Petroleum Geologists. TIC: 235940

Steeffel, C.I. and Lasaga, A.C. 1994. "A Coupled Model for Transport of Multiple Chemical Species and Kinetic Precipitation/Dissolution Reactions with Application to Reactive Flow in Single Phase Hydrothermal Systems." *American Journal of Science*, 294, 529–592. New Haven, Connecticut: Yale University Press. TIC: 235372.

Stoessell, R.K. 1988. "25°C and 1 atm Dissolution Experiments of Sepiolite and Kerolite." *Geochimica et Cosmochimica Acta*, 52, 365–374. Amsterdam, The Netherlands: Elsevier Science Publishers. TIC: 246452.

Svensson, U. and Dreybrodt, W. 1992. "Dissolution Kinetics of Natural Calcite Minerals in CO₂-Water Systems Approaching Calcite Equilibrium." *Chemical Geology*, 100, 129–145. Amsterdam, The Netherlands: Elsevier Science Publishers. TIC: 246497.

Tester, J.W.; Worley, G.W.; Robinson, B.A.; Grigsby, C.O.; and Feerer, J.L. 1994. "Correlating Quartz Dissolution Kinetics in Pure Water from 25° to 625°C." *Geochimica et Cosmochimica Acta*, 58 (11), 2407–2420. Amsterdam, The Netherlands: Elsevier Science Publishers. TIC: 236776.

Wemheuer, R.F. 1999. "First Issue of FY00 NEPO QAP-2-0 Activity Evaluations." Interoffice correspondence from R.F. Wemheuer (CRWMS M&O) to R.A. Morgan (CRWMS M&O), October 1, 1999, LV.NEPO.RTPS.TAG.10/99-155, with attachments, Activity Evaluation for Work Package #1401213UM1. ACC: MOL.19991028.0162.

Xu, T. and Pruess, K. 1998. *Coupled Modeling of Non-Isothermal Multi-Phase Flow, Solute Transport and Reactive Chemistry in Porous and Fractured Media: 1. Model Development and Validation*. LBNL-42050. Berkeley, California: Lawrence Berkeley National Laboratory. TIC: 243735.

Xu, T.; Pruess, K.; and Brimhall, G. 1999. *An Improved Equilibrium-Kinetics Speciation Algorithm for Redox Reactions in Variable Saturated Subsurface Flow Systems*. LBNL-41789. *Computers and Geosciences*, 25, 655–666. Amsterdam, The Netherlands: Elsevier Science Publishers. TIC: 240019.

Software Cited:

Software Code: AMESH V1.0. STN: 10045-1.0-00.

Software Code: EQ3/6 V7.2b. STN: LLNL: UCRL-MA-110662.

Software Code: SOLVEQ/CHILLER V1.0. STN: 10057-1.0-00.

Software Code: SUPCRT92 V1.0. STN: 10058-1.0-00.

Software Code: TOUGH2 V1.4. STN: 10061-1.4-00.

Software Code: TOUGHREACT V2.2. STN: 10154-2.2-00.

Software Routine: 2kgridv1a.for. ACC: MOL.19991201.0555.

Software Routine: mk_grav2.f. ACC: MOL.19991201.0556.

Software Routine: sav1d-dst2d.f. ACC: MOL.19991201.0557.

Software Routine: mrgdrift.f ACC: see Attachment VIII.

8.2 CODES, STANDARDS, REGULATIONS, AND PROCEDURES

AP-3.10Q, Rev. 1, ICN 1. *Analyses and Models*. Washington, D.C.: U.S. Department of Energy, Office of Civilian Radioactive Waste Management. ACC: MOL.19991019.0467.

AP-SI.1Q, Rev. 2, ICN 0. *Software Management*. Washington, D.C.: U.S. Department of Energy, Office of Civilian Radioactive Waste Management. ACC: MOL.19991014.0233.

DOE 1998. *Quality Assurance Requirements and Description*. DOE/RW-0333P, REV 8. Washington D.C.: DOE OCRWM. ACC: MOL.19980601.0022.

QAP-2-0, Rev. 5. *Conduct of Activities*. Las Vegas, Nevada: CRWMS M&O. ACC: MOL.19980826.0209.

8.3 SOURCE DATA, LISTED BY DATA TRACKING NUMBER

GS950608312272.001. Chemical Data for Pore Water from Tuff Cores of USW NRG-6, NRG7/7A, UZ-14 and UZ-N55, and UE-25 UZ#16. Submittal Date: 05/30/1995

LA9908JC831321.001. Mineralogic Model "MM3.0" Version 3.0. Submittal Date: 08/16/1999.

LA9912SL831151.001. Fracture Mineralogy of Drill Core ESF-HD-TEMP-2. Submittal Date: 01/05/2000

LA9912SL831151.002. Percent Coverage by Fracture-Coating Minerals in Core ESF-HD-TEMP-2. Submittal Date: 01/05/2000.

LASL831151AQ98.001. Mineralogic Characterization of the ESF Single Heater Test Block. Submittal date: 08/31/1998.

LB000121123142.003. Isotope Data for CO₂ Gas Samples Collected from the Hydrology Holes of the ESF Drift Scale Test for the Period August 9, 1999 through November 30, 1999. Submittal Date: 01/21/2000

LB990501233129.004. 3-D UZ Model Calibration Grids for AMR U0000, "Development of Numerical Grids of UZ Flow and Transport Modeling." Submittal date: 09/24/1999.

LB990630123142.003. Fourth, Fifth, and Sixth Quarters TDIF Submission for the Drift Scale Test, September 1998 to May 1999. Submittal date: 06/30/1999.

LB990701233129.002. 3-D Model Calibration Grid for Calculation of Flow Fields using #3 Perched Water Conceptual Model (Non-Perched Water Model). Submittal date: 3/11/2000.

LB990861233129.001. Drift Scale Calibrated 1-D Property Set, FY99. Submittal date: 08/06/1999.

LB990861233129.002. Drift Scale Calibrated 1-D Property Set, FY99. Submittal date: 08/06/1999.

LB990861233129.003. Drift Scale Calibrated 1-D Property Set, FY99. Submittal date: 08/06/1999.

LB991091233129.001. One-Dimensional, Mountain-Scale Calibration for AMR U0035, "Calibrated Properties Model." Submittal date: 10/22/1999.

LB991215123142.001. CO₂ Analyses of Gas Samples Collected from the Drift Scale Test. Submittal date: 3/11/2000.

LB997141233129.001. Calibrated Basecase Infiltration 1-D Parameter Set for the UZ Flow and Transport Model, FY99. Submittal Date: 07/21/1999

LL000114004242.090. TSPA-SR Mean Calculations. Submittal Date: 01/28/2000

LL990702804244.100. Pore Water Data. Submittal Date: 7/13/1999

SN9907T0872799.001. Heat Decay Data and Repository Footprint for Thermal-Hydrologic and Conduction-Only Models for TSPA-SR (Total System Performance Assessment-Site Recommendation). Submittal date: 07/27/1999.

SN9907T0872799.002. Effective Thermal Conductivity for Drift-Scale Models Used in TSPA-SR (Total System Performance Assessment-Site Recommendation). Submittal date: 07/27/1999.

SN9908T0872799.004. Tabulated In-Drift Geometric and Thermal Properties Used in Drift-Scale Models for TSPA-SR (Total System Performance Assessment-Site Recommendation). Submittal date: 08/30/1999.

8.4 OUTPUT DATA, LISTED BY DATA TRACKING NUMBER

LB991200DSTTHC.A01. Kinetic Rate Law Data for Mineral-Water Dissolution and Precipitation: Table 4 of AMR U0110, “Drift-Scale Coupled Processes (DST and THC Seepage) Models.” Submittal date: 3/11/2000.

LB991200DSTTHC.001. Tables showing Geochemical and Drift-Scale Seepage Model Data which are presented in AMR U0110, “Drift-Scale Coupled Processes (DST and THC Seepage) Models.” Submittal date: 3/11/2000.

LB991200DSTTHC.002. Model Input and Output Files, Excel Spreadsheets and Resultant Figures which are presented in AMR U0110, “Drift-Scale Coupled Processes (DST and THC Seepage) Models.” Submittal date: 3/11/2000.

LB991200DSTTHC.003. Mineral Initial Volume Fractions: Attachment II of AMR U0110, “Drift-Scale Coupled Processes (DST and THC Seepage) Models.” Submittal date: 3/11/2000.

LB991200DSTTHC.004. Mineral Reactive Surface Areas: Attachment III of AMR U0110, “Drift-Scale Coupled Processes (DST and THC Seepage) Models.” Submittal date: 3/11/2000.

LB991200DSTTHC.005. Thermodynamic Database: Attachment IV of AMR U0110, “Drift-Scale Coupled Processes (DST and THC Seepage) Models.” Submittal date: 3/11/2000.

LB991200DSTTHC.006. Waste Package Average Heat Transfer: Attachment V of AMR U0110, “Drift-Scale Coupled Processes (DST and THC Seepage) Models.” Submittal date: 3/11/2000.

INTENTIONALLY LEFT BLANK

9. ATTACHMENTS

Attachment I - Document Input Reference Sheet

Attachment II - Mineral Initial Volume Fractions

Attachment III - Mineral Reactive Surface Areas

Attachment IV - Thermodynamic Database

Attachment V - Waste Package Average Heat Transfer

Attachment VI - Effective Thermal Conductivity for In-Drift Open Spaces

Attachment VII - List of Model Input and Output Files

Attachment VIII - Software Routines

.

INTENTIONALLY LEFT BLANK

ATTACHMENT I-DOCUMENT INPUT REFERENCE SHEET

DIRS as of the issue date of this AMR. Refer to the DIRS database for the current status of these inputs.

OFFICE OF CIVILIAN RADIOACTIVE WASTE MANAGEMENT DOCUMENT INPUT REFERENCE SHEET									
1. Document Identifier No./Rev.: MDL-NBS-HS-000001/Rev. 00			Change: <i>JEH 3/31/00</i> N/A	Title: Drift-Scale Coupled Processes (DST, THC Seepage) Models					
Input Document		3. Section	4. Input Status	5. Section Used in	6. Input Description	7. TBV/TBD Priority	8. TBV Due To		
2. Technical Product Input Source Title and Identifier(s) with Version							Unqual.	From Uncontrolled Source	Un-confirmed
2a									
1.	DTN: LA9912SL831151.001. Fracture Mineralogy of Drill Core ESF-HD-TEMP-2. Submittal Date: 1/05/2000.	Entire	N/A- Qualified- Verificatio n Level 2	4.1.2 A-II	DST fracture mineralogy data	N/A	N/A	N/A	N/A
2.	DTN: LA9912SL831151.002. Percent Coverage by Fracture-Coating Minerals in Core ESF-HD-TEMP-2. Submittal Date: 1/05/2000.	Entire	N/A- Qualified- Verificatio n Level 2	4.1.2 A-II	DST fracture mineralogy data	1	N/A	N/A	✓
3.	DTN: GS950608312272.001. Chemical Data for Pore Water from Tuff Cores of USW NRG-6, NRG7/7A, UZ-14 and UZ-N55, and UE-25 UZ#16. Submittal Date: 05/30/1995.	TSw data	N/A- Reference Only	4.1.3	Pore water analyses from the Tptpln unit	1	N/A	N/A	✓
4.	DTN: LA9908JC831321.001. Mineralogic Model "MM3.0" Version 3.0. Submittal Date: 08/16/1999.	Borehole SD-9 XRD data	N/A- Technical Product Output	4.1.2 A-II	Model input and output files for Mineralogic Model (borehole SD-9 XRD data.	N/A	N/A	N/A	N/A
5.	DTN: LASL831151AQ98.001. Mineralogic Characterization of the ESF Single Heater Test Block. Submittal date: 08/31/1998. Initial use.	Entire	N/A- Qualified- Verificatio n Level 2	4.1.2 A-II	Mineral abundances in fractures in SHT	N/A	N/A	N/A	N/A

OFFICE OF CIVILIAN RADIOACTIVE WASTE MANAGEMENT DOCUMENT INPUT REFERENCE SHEET									
1. Document Identifier No./Rev.: MDL-NBS-HS-000001/Rev. 00			Change: <i>N/A</i>		Title: Drift-Scale Coupled Processes (DST, THC Seepage) Models				
Input Document			4. Input Status	5. Section Used in	6. Input Description	7. TBV/TBD Priority	8. TBV Due To		
2. Technical Product Input Source Title and Identifier(s) with Version		3. Section					Unqual.	From Uncontrolled Source	Un-confirmed
2a									
6.	DTN: LB000121123142.003. Isotope Data for CO ₂ Gas Samples Collected From the Hydrology Holes of the ESF Drift Scale Test for the Period August 9, 1999 Through November 30, 1999. Submittal Date: 01/21/2000.		Entire	6.2.7	CO ₂ gas analysis	N/A	N/A	N/A	N/A
7.	DTN: LB990501233129.004. 3-D UZ Model Calibration Grids for AMR U0000, "Development of Numerical Grids of UZ Flow and Transport Modeling." Submittal date: 09/24/1999.		Borehole SD-9 geology (column i64)	6.3.1	Borehole SD-9 geology in 3-D UZ Model Grid (column I 64)	N/A	N/A	N/A	N/A
8.	DTN: LB990630123142.003. Fourth, Fifth, and Sixth Quarters TDIF Submission for the Drift Scale Test, September 1998 to May 1999. Submittal date: 06/30/1999. Initial use.		Entire	6.2.6	Gas CO ₂ Analyses	1	N/A	N/A	✓

OFFICE OF CIVILIAN RADIOACTIVE WASTE MANAGEMENT DOCUMENT INPUT REFERENCE SHEET									
1. Document Identifier No./Rev.: MDL-NBS-HS-000001/Rev. 00			Change: <i>N/A</i>		Title: Drift-Scale Coupled Processes (DST, THC Seepage) Models				
Input Document		3. Section	4. Input Status	5. Section Used in	6. Input Description	7. TBV/TBD Priority	8. TBV Due To		
2. Technical Product Input Source Title and Identifier(s) with Version	2a						Unqual.	From Uncontrolled Source	Un-confirmed
9.	DTN: LB990701233129.002. 3-D Model Calibration Grid for Calculation of Flow Fields using #3 Perched Water Conceptual Model (Non-Perched Water Model). Submittal date: 3/11/00. Initial use.	SAVE file	N/A- Technical Product Output	4	Initial conditions for top and bottom boundaries	N/A	N/A	N/A	N/A
10.	DTN: LB990861233129.001. Drift Scale Calibrated 1-D Property Set, FY99. Submittal date: 08/06/1999. Initial use.	Tables 1 and 2	N/A- Technical Product Output	4.1.1	Calibrated Fracture and Matrix Property sets (for base case infiltration)	1	N/A	N/A	✓
11.	DTN: LB990861233129.002. Drift Scale Calibrated 1-D Property Set, FY99. Submittal date: 08/06/1999.	Tables 1 and 2	N/A- Technical Product Output	4.1.1	Calibrated Fracture and Matrix Property sets (for upper infiltration)	1	N/A	N/A	✓
12.	DTN: LB990861233129.003. Drift Scale Calibrated 1-D Property Set, FY99. Submittal date: 08/06/1999. Initial use.	Tables 1 and 2	N/A- Technical Product Output	4.1.1	Calibrated Fracture and Matrix Property sets (for lower infiltration)	1	N/A	N/A	✓
13.	DTN: LB991091233129.001. One-Dimensional, Mountain-Scale Calibration for AMR U0035, "Calibrated Properties Model." Submittal date: 10/22/1999.	Binfil	N/A- Technical Product Output	6.3.2	Infiltration Rate-Basecase	1	✓	N/A	N/A

OFFICE OF CIVILIAN RADIOACTIVE WASTE MANAGEMENT DOCUMENT INPUT REFERENCE SHEET										
1. Document Identifier No./Rev.: MDL-NBS-HS-000001/Rev. 00			Change: <i>N/A</i>	Title: Drift-Scale Coupled Processes (DST, THC Seepage) Models						
Input Document			4. Input Status	5. Section Used in	6. Input Description	7. TBV/TBD Priority	8. TBV Due To			
2. Technical Product Input Source Title and Identifier(s) with Version		3. Section					Unqual.	From Uncontrolled Source	Un-confirmed	
2a										
14.	DTN: LB991215123142.001. CO2 Analyses of Gas Samples Collected from the Drift Scale Test. Submittal date: 3/11/00.		Entire	TBV-3973	6.2.7	CO ₂ gas analyses (TBV because unqualified)	1	✓	N/A	N/A
15.	DTN: LB997141233129.001. Calibrated Basecase Infiltration 1-D Parameter Set for the UZ Flow and Transport Model, FY99. Submittal Date: 07/21/1999		Table 1	N/A- Technical Product Output	4.1.1	Fracture porosity only	N/A	N/A	N/A	N/A
16.	DTN: SN9907T0872799.001. Heat Decay Data and Repository Footprint for Thermal-Hydrologic and Conduction-Only Models for TSPA-SR (Total System Performance Assessment-Site Recommendation). Submittal date: 07/27/1999. Initial use.		File: Heat TSPA-SR-99184-Ta.xls; Sheet: Drift-Scale (2-D models) column: F	TBV-3599	4.1.7.2	Heat Loading (TBV because unqualified)	1	✓	N/A	N/A

LEA 3/31/00

OFFICE OF CIVILIAN RADIOACTIVE WASTE MANAGEMENT DOCUMENT INPUT REFERENCE SHEET									
1. Document Identifier No./Rev.: MDL-NBS-HS-000001/Rev. 00			Change: N/A	Title: Drift-Scale Coupled Processes (DST, THC Seepage) Models					
Input Document			4. Input Status	5. Section Used in	6. Input Description	7. TBV/TBD Priority	8. TBV Due To		
2. Technical Product Input Source Title and Identifier(s) with Version	3. Section	Unqual.					From Uncontrolled Source	Un-confirmed	
2a									
17.	DTN: SN9907T0872799.002. Effective Thermal Conductivity for Drift-Scale Models Used in TSPA-SR (Total System Performance Assessment-Site Recommendation). Submittal date: 07/27/1999. Initial use.	Files: effkth_info.doc, and toughinpefix.txt	TBV-3975	4.1.7.2	Effective thermal conductivity (TBV because unqualified)	1	✓	N/A	N/A
18.	DTN: SN9908T0872799.004. Tabulated In-Drift Geometric and Thermal Properties Used in Drift-Scale Models for TSPA-SR (Total System Performance Assessment-Site Recommendation). Submittal date: 08/30/1999.	File: Indriftgeom_rev01.doc	TBV-3471	4.1.7.2	Drift design specifications and properties of design elements. (TBV because unqualified)	1	✓	N/A	N/A
19.	Apps, J.A. 1970. <i>The Stability Field of Analcime</i> . Ph.D. dissertation. Cambridge, Massachusetts: Harvard University. TIC: applied for.	Entire	N/A-Reference only	Att. IV-3	Regression of pressure-corrected cristobalite	N/A	N/A	N/A	N/A

OFFICE OF CIVILIAN RADIOACTIVE WASTE MANAGEMENT DOCUMENT INPUT REFERENCE SHEET									
1. Document Identifier No./Rev.: MDL-NBS-HS-000001/Rev. 00			Change: N/A		Title: Drift-Scale Coupled Processes (DST, THC Seepage) Models				
Input Document			4. Input Status	5. Section Used in	6. Input Description	7. TBV/TBD Priority	8. TBV Due To		
2. Technical Product Input Source Title and Identifier(s) with Version		3. Section					Unqual.	From Uncontrolled Source	Un-confirmed
2a									
20.	Apps, J.A. and Chang, G.M. 1992. "Correlation of the Na/K Ratio in Geothermal Well Waters with the Thermodynamic Properties of Low Albite and Potash Feldspar." <i>Proceedings of the 7th International Symposium on Water-Rock Interaction</i> , 1437-1440. Rotterdam, The Netherlands: A.A. Balkema. TIC: 246481.		Entire	Att. IV-3	Log (K) of microcline	N/A	N/A	N/A	N/A
21.	Bear, J. 1972. <i>Dynamics of Fluid in Porous Media</i> . New York, New York: Dover Publications. TIC: 217568.		p. 166	6.1.6.3	Matrix permeability changes	N/A	N/A	N/A	N/A
22.	Berman, R.G. 1988. "Internally Consistent Thermodynamic Data for Minerals in the System Na ₂ O-K ₂ O-CaO-MgO-FeO-Fe ₃ O ₄ -Al ₂ O ₃ -SiO ₂ -TiO ₂ -H ₂ O-CO ₂ ." <i>Journal of Petrology</i> , 29, 445-522. Dallas, Texas: Society of Petroleum Engineers. TIC: 236892.		Entire	Att. IV-3	Log (K) of albite	N/A	N/A	N/A	N/A

OFFICE OF CIVILIAN RADIOACTIVE WASTE MANAGEMENT DOCUMENT INPUT REFERENCE SHEET									
1. Document Identifier No./Rev.: MDL-NBS-HS-000001/Rev. 00			Change: <i>N/A</i>		Title: Drift-Scale Coupled Processes (DST, THC Seepage) Models				
Input Document			4. Input Status	5. Section Used in	6. Input Description	7. TBV/TBD Priority	8. TBV Due To		
2. Technical Product Input Source Title and Identifier(s) with Version		3. Section					Unqual.	From Uncontrolled Source	Un-confirmed
2a									
23.	Bish, D.L.; Carey, J.W.; Levy, S.S.; and Chipera, S.J. 1996. <i>Mineralogy-Petrology Contribution to the Near-Field Environment Report. Milestone Report LA-3668. Los Alamos, New Mexico: Los Alamos National Laboratory. ACC: MOL 19961122.0252.</i>		Entire	Att. IV-3	Zeolitization of tuffs	N/A	N/A	N/A	N/A
24.	Blum, A.E. and Stillings, L.L. 1995. "Feldspar Dissolution Kinetics." Chapter 7 of <i>Chemical Weathering Rates of Silicate Minerals</i> , 31, 291-351. White, A.F. and Brantley, S.L., eds. Washington, D.C.: Mineral Society of America. TIC: 241237.		Entire	Table 4	Kinetic rate law	N/A	N/A	N/A	N/A

OFFICE OF CIVILIAN RADIOACTIVE WASTE MANAGEMENT DOCUMENT INPUT REFERENCE SHEET										
1. Document Identifier No./Rev.: MDL-NBS-HS-000001/Rev. 00			Change: N/A	Title: Drift-Scale Coupled Processes (DST, THC Seepage) Models						
Input Document			4. Input Status	5. Section Used in	6. Input Description	7. TBV/TBD Priority	8. TBV Due To			
2. Technical Product Input Source Title and Identifier(s) with Version		3. Section					Unqual.	From Uncontrolled Source	Un-confirmed	
2a										
25.	Carroll, S.; Mroczek, E.; Alai, M.; and Ebert, M. 1998. "Amorphous Silica Precipitation (60 to 120°C): Comparison of Laboratory and Field Rates." <i>Geochimica et Cosmochimica Acta</i> , 62, 1379-1396. Amsterdam. The Netherlands: Elsevier Science Publishers. TIC: 243029.		p. 1379	N/A - Reference only	Table 4	Kinetic Rate Law	N/A	N/A	N/A	N/A
26.	CRWMS M&O (Civilian Radioactive Waste Management System Management & Operating Contractor) 1999a. <i>Analysis & Modeling Development Plan (DP) for U0110 Drift-Scale Coupled Processes (DST THC Seepage) Models Rev. 00</i> . TDP-NBS-HS-000007. Las Vegas, Nevada: CRWMS M&O. ACC: MOL.19990830.0378.		Entire	N/A - Reference only	Section 1	Plan	N/A	N/A	N/A	N/A
27.	CRWMS M&O 1999b. <i>M&O Site Investigations, January 23, 1999. Activity Evaluation</i> . Las Vegas, Nevada: CRWMS M&O. ACC: MOL.19990317.0330.		Entire	N/A - Reference only	2	Activity Evaluation	N/A	N/A	N/A	N/A

JEH 3/31/00

OFFICE OF CIVILIAN RADIOACTIVE WASTE MANAGEMENT DOCUMENT INPUT REFERENCE SHEET									
1. Document Identifier No./Rev.: MDL-NBS-HS-000001/Rev. 00			Change: N/A		Title: Drift-Scale Coupled Processes (DST, THC Seepage) Models				
Input Document		3. Section	4. Input Status	5. Section Used in	6. Input Description	7. TBV/TBD Priority	8. TBV Due To		
2. Technical Product Input Source Title and Identifier(s) with Version	2a						Unqual.	From Uncontrolled Source	Un-confirmed
28.	CRWMS M&O 1999c. <i>M&O Site Investigations, September 28, 1999. Activity Evaluation.</i> Las Vegas, Nevada: CRWMS M&O. ACC: MOL.19990928.0224.	Entire	N/A - Reference only	2	Activity Evaluation	N/A	N/A	N/A	N/A
29.	CRWMS M&O 1999d. <i>Subsurface Design for Enhanced Design Alternative (EDA) II.</i> Input Request LBL-SSR-99399.R. Las Vegas, Nevada: CRWMS M&O. ACC: MOL.19991203.0130.	Entire	TBV	6.3.1	Drift Spacing	1	N/A	✓	N/A
30.	CRWMS M&O 1999e. <i>Pore Water Data from the Drift Scale Test (DST).</i> Input Request LBL-LNL-99400.R. Las Vegas, Nevada: CRWMS M&O. ACC: MOL.19991203.0129.	HD-PERM-1 and HD-PERM-2 samples	TBV	4.1	Pore water and DST water compositions	1	N/A	N/A	✓
31.	CRWMS M&O 1999f. <i>Local Infiltration Rates.</i> LBL-SNL-99419.T. Las Vegas, Nevada: CRWMS M&O. ACC: to be assigned.	Entire	TBV-3974	6.3.2	Average infiltration rates	1	N/A	N/A	✓

OFFICE OF CIVILIAN RADIOACTIVE WASTE MANAGEMENT DOCUMENT INPUT REFERENCE SHEET									
1. Document Identifier No./Rev.: MDL-NBS-HS-000001/Rev. 00			Change: N/A	Title: Drift-Scale Coupled Processes (DST, THC Seepage) Models					
Input Document			4. Input Status	5. Section Used in	6. Input Description	7. TBV/TBD Priority	8. TBV Due To		
2. Technical Product Input Source Title and Identifier(s) with Version	3. Section	Unqual.					From Uncontrolled Source	Un-confirmed	
2a									
32.	de Marsily, G. 1986. <i>Quantitative Hydrogeology: Groundwater Hydrology for Engineers</i> . Orlando, Florida: Academic Press. TIC: 208450.	p. 233	N/A-Reference only	4.1.6	Tortuosity	N/A	N/A	N/A	N/A
33.	Drever J.I. 1997. <i>Geochemistry of Natural Waters</i> , 3rd Edition. Upper Saddle River, N.J.: Prentice Hall. TIC: 246732.	p. 28	N/A-Reference only	4.1.4, 6.1.3	Debye-Hückel equation	N/A	N/A	N/A	N/A
34.	Dyer, J.R. 1999. "Revised Interim Guidance Pending Issuance of New U.S. Nuclear Regulatory Commission (NRC) Regulations (Revision 01), July 22, 1999), for Yucca Mountain, Nevada." Letter from J.R. Dyer (DOE) to D.R. Wilkins (CRWMS M&O), September 9, 1999, OL&RC:SB-1714, with enclosure, "Interim Guidance Pending Issuance of New U.S. Nuclear Regulatory Commission (NRC) Regulations (Revision 01)." ACC: MOL.19990910.0079.	Entire	N/A Reference only	4	Interim Guidance	N/A	N/A	N/A	N/A

234 3/31/00

OFFICE OF CIVILIAN RADIOACTIVE WASTE MANAGEMENT DOCUMENT INPUT REFERENCE SHEET									
1. Document Identifier No./Rev.: MDL-NBS-HS-000001/Rev. 00			Change: N/A	Title: Drift-Scale Coupled Processes (DST, THC Seepage) Models					
Input Document			4. Input Status	5. Section Used in	6. Input Description	7. TBV/TBD Priority	8. TBV Due To		
2. Technical Product Input Source Title and Identifier(s) with Version	3. Section	Unqual.					From Uncontrolled Source	Un-confirmed	
2a									
35.	Ehrlich, R.; Etris, E.L.; Brumfield, D.; Yuan, L.P.; and Crabtree, S.J. 1991. "Petrography and Reservoir Physics III: Physical Models for Permeability and Formation Factor." <i>AAPG Bulletin</i> , 75, 1579-1592. Tulsa, Oklahoma: American Association of Petroleum Geologists. TIC: applied for.	p. 1582	N/A - Reference only	6.1.5.2	Modified Hagen-Poiseuille relation	N/A	N/A	N/A	N/A
36.	Fournier, R.O. and Rowe, J.J. 1962. "The Solubility of Cristobalite along the Three-Phase Curve, Gas Plus Liquid Plus Cristobalite." <i>American Mineralogist</i> , 47, 897-902. Washington, D.C.: Mineralogical Society of America. TIC: 235380.	Entire	N/A - Reference only	Att. IV-3	Cristobalite solubility	N/A	N/A	N/A	N/A
37.	Garrels, R.M. and Christ, C.L. 1965. <i>Solutions, Minerals and Equilibria</i> . New York: Harper and Rowe. TIC: 217443.	p. 64-66	N/A - Reference only	6.1.3	Activity of water	N/A	N/A	N/A	N/A

OFFICE OF CIVILIAN RADIOACTIVE WASTE MANAGEMENT DOCUMENT INPUT REFERENCE SHEET									
1. Document Identifier No./Rev.: MDL-NBS-HS-000001/Rev. 00		Change: N/A		Title: Drift-Scale Coupled Processes (DST, THC Seepage) Models					
Input Document		3. Section	4. Input Status	5. Section Used in	6. Input Description	7. TBV/TBD Priority	8. TBV Due To		
2. Technical Product Input Source Title and Identifier(s) with Version							Unqual.	From Uncontrolled Source	Un-confirmed
2a									
38.	Inskip, W.P. and Bloom, P.R. 1985. "An Evaluation of Rate Equations for Calcite Precipitation Kinetics at $p\text{CO}_2$ Less than 0.01 atm and pH Greater than 8." <i>Geochimica et Cosmochimica Acta</i> , 49, 2165-2180. Amsterdam, The Netherlands: Elsevier Science Publishers. TIC: 241125.	p. 2178	N/A-Reference only	Table 4	Kinetic rate data for calcite	N/A	N/A	N/A	N/A
39.	Johnson, J.W.; Oelkers, E.H.; and Helgeson, H.C. 1992. "SUPCRT92: A Software Package for Calculating the Standard Molal Thermodynamic Properties of Minerals, Gases, Aqueous Species, and Reactions from 1 to 5000 bars and 0 to 1000 degrees C." <i>Computers and Geosciences</i> , 18, 899-947. Great Britain: Pergamon Press. TIC: 239019.	Entire	N/A-Reference only	Att. IV-3 4.1.4	Thermodynamic properties	N/A	N/A	N/A	N/A
40.	Klein, C. and Hurlbut, C.S. 1993. <i>Manual of Mineralogy</i> , 21st Edition. New York, New York: John Wiley & Sons. TIC: 246258.	p. 665 Entire p. 172	N/A - Reference only	Att. IV-3 4.1.5 4.1.6	General mineralogical discussion	N/A	N/A	N/A	N/A

OFFICE OF CIVILIAN RADIOACTIVE WASTE MANAGEMENT DOCUMENT INPUT REFERENCE SHEET									
1. Document Identifier No./Rev.: MDL-NBS-HS-000001/Rev. 00		Change: N/A		Title: Drift-Scale Coupled Processes (DST, THC Seepage) Models					
Input Document			4. Input Status	5. Section Used in	6. Input Description	7. TBV/TBD Priority	8. TBV Due To		
2. Technical Product Input Source Title and Identifier(s) with Version	3. Section	Unqual.					From Uncontrolled Source	Un-confirmed	
2a									
38.	Inskeep, W.P. and Bloom, P.R. 1985. "An Evaluation of Rate Equations for Calcite Precipitation Kinetics at $p\text{CO}_2$ Less than 0.01 atm and pH Greater than 8." <i>Geochimica et Cosmochimica Acta</i> , 49, 2165-2180. Amsterdam, The Netherlands: Elsevier Science Publishers. TIC: 241125.	p. 2178	N/A-Reference only	Table 4	Kinetic rate data for calcite	N/A	N/A	N/A	N/A
39.	Johnson, J.W.; Oelkers, E.H.; and Helgeson, H.C. 1992. "SUPCRT92: A Software Package for Calculating the Standard Molal Thermodynamic Properties of Minerals, Gases, Aqueous Species, and Reactions from 1 to 5000 bars and 0 to 1000 degrees C." <i>Computers and Geosciences</i> , 18, 899-947. Great Britain: Pergamon Press. TIC: 239019.	Entire	N/A-Reference only	Att. IV-3 4.1.4	Thermodynamic properties	N/A	N/A	N/A	N/A
40.	Klein, C. and Hurlbut, C.S. 1993. <i>Manual of Mineralogy</i> , 21st Edition. New York, New York: John Wiley & Sons. TIC: 246258.	p. 665 Entire p. 172	N/A - Reference only	Att. IV-3 4.1.5 4.1.6	General mineralogical discussion	N/A	N/A	N/A	N/A

OFFICE OF CIVILIAN RADIOACTIVE WASTE MANAGEMENT DOCUMENT INPUT REFERENCE SHEET										
1. Document Identifier No./Rev.: MDL-NBS-HS-000001/Rev. 00			Change: N/A		Title: Drift-Scale Coupled Processes (DST, THC Seepage) Models					
Input Document			4. Input Status	5. Section Used in	6. Input Description	7. TBV/TBD Priority	8. TBV Due To			
2. Technical Product Input Source Title and Identifier(s) with Version		3. Section					Unqual.	From Uncontrolled Source	Un-confirmed	
2a										
41.	Knauss, K.G. and Wolery, T.J. 1989. "Muscovite Dissolution Kinetics as a Function of pH and Time at 70°C." <i>Geochimica et Cosmochimica Acta</i> , 53, 1493-1501. Amsterdam. The Netherlands: Elsevier Science Publishers. TIC: 236215.		Entire	N/A-Reference only	Table 4	Kinetic data	N/A	N/A	N/A	N/A
42.	Knowles-Van Cappellan, V.; Van Cappellan, P.; and Tiller, C. 1997. "Probing the Charge of Reactive Sites at the Mineral-Water Interface: Effect of Ionic Strength on Crystal Growth Kinetics of Fluorite." <i>Geochimica et Cosmochimica Acta</i> , 61 (9), 1871-1877. New York, New York: Pergamon Press. TIC: 246450.		p. 1873	N/A-Reference only	Table 4	Fluorite kinetic data	N/A	N/A	N/A	N/A
43.	Lasaga A.C. 1998. <i>Kinetic Theory in the Earth Sciences</i> . Princeton, New Jersey: Princeton University Press. TIC: applied for.		p. 322 Table 4.1, p. 315 315	N/A-Reference only	4.1.4 and 4.1.6 4.1.6 5	Molecular diameter of CO ₂ Aqueous diffusion coefficient of Cl	N/A	N/A	N/A	N/A

OFFICE OF CIVILIAN RADIOACTIVE WASTE MANAGEMENT
DOCUMENT INPUT REFERENCE SHEET

JEH 3/2/00

Change:
N/A

Title:
Drift-Scale Coupled Processes (DST, THC Seepage) Models

Input Document

2. Technical Product Input Source Title and Identifier(s) with Version

3. Section

4. Input Status

5. Section Used in

6. Input Description

7. TBV/TBD Priority

8. TBV Due To

Unqual.

From Uncontrolled Source

Un-confirmed

2a

41.

Knauss, K.G. and Wolery, T.J. 1989. "Muscovite Dissolution Kinetics as a Function of pH and Time at 70°C." *Geochimica et Cosmochimica Acta*, 53, 1493-1501. Amsterdam. The Netherlands: Elsevier Science Publishers. TIC: 236215.

Entire

N/A-Reference only

Table 4

Kinetic data

N/A

N/A

N/A

N/A

42.

Knowles-Van Cappellan, V.; Van Cappellan, P.; and Tiller, C. 1997. "Probing the Charge of Reactive Sites at the Mineral-Water Interface: Effect of Ionic Strength on Crystal Growth Kinetics of Fluorite." *Geochimica et Cosmochimica Acta*, 61 (9), 1871-1877. New York, New York: Pergamon Press. TIC: 246450.

p. 1873

N/A-Reference only

Table 4

Fluorite kinetic data

N/A

N/A

N/A

N/A

43.

Lasaga A.C. 1998. *Kinetic Theory in the Earth Sciences*. Princeton, New Jersey: Princeton University Press. TIC: applied for.

p. 322

Table 4.1, p. 315
315

N/A-Reference only

4.1.4 and 4.1.6

4.1.6

5

Molecular diameter of CO₂

Aqueous diffusion coefficient of Cl

N/A

N/A

N/A

N/A

OFFICE OF CIVILIAN RADIOACTIVE WASTE MANAGEMENT DOCUMENT INPUT REFERENCE SHEET										
1. Document Identifier No./Rev.: MDL-NBS-HS-000001/Rev. 00			Change: N/A		Title: Drift-Scale Coupled Processes (DST, THC Seepage) Models					
Input Document		3. Section	4. Input Status	5. Section Used in	6. Input Description	7. TBV/TBD Priority	8. TBV Due To			
2. Technical Product Input Source Title and Identifier(s) with Version							Unqual.	From Uncontrolled Source	Un-confirmed	
2a										
44.	Levy, S.S.; Fabryka-Martin, J.T.; Dixon, P.R.; Liu, B.; Turin, H.J.; and Wolfsberg, A.V. 1997. "Chlorine-36 Investigations of Groundwater Infiltration in the Exploratory Studies Facility at Yucca Mountain, Nevada." <i>Scientific Basis for Nuclear Waste Management XX, Material Research Society Symposium Proceedings, Boston, Massachusetts, 465, December 2-6, 1996</i> , 901-908. Pittsburgh, Pennsylvania: Materials Research Society. TIC: 238884.		p. 906, 907-908	N/A-Reference only	6.1.2	Water ages	N/A	N/A	N/A	N/A
45.	Liu, H.H.; Doughty, C.; and Bodvarsson, G.S. 1998. "An Active Fracture Model for Unsaturated Flow and Transport in Fractured Rocks." <i>Water Resources Research</i> 34 (10), 2633-2646. Washington, D.C.: American Geophysical Union. TIC: 243012.		2636-2638	N/A - Reference only	6.1.5.1	Active Fracture Model	N/A	N/A	N/A	N/A

OFFICE OF CIVILIAN RADIOACTIVE WASTE MANAGEMENT DOCUMENT INPUT REFERENCE SHEET										
1. Document Identifier No./Rev.: MDL-NBS-HS-000001/Rev. 00			Change: N/A		Title: Drift-Scale Coupled Processes (DST, THC Seepage) Models					
Input Document			4. Input Status	5. Section Used in	6. Input Description	7. TBV/TBD Priority	8. TBV Due To			
2. Technical Product Input Source Title and Identifier(s) with Version		3. Section					Unqual.	From Uncontrolled Source	Un-confirmed	
2a										
46.	Mazer, J.J.; Bates, J.K.; Bradley, J.P.; Bradley, C.R.; and Stevenson, C.M. 1992. "Alteration of Tectite to Form Weathering Products." <i>Nature</i> , 357, 573-576. London, England: Macmillian Press. TIC: 246479.		p. 573-574 Entire	N/A-Reference only	Table 4 Sect. 5 6.1.4	Glass dissolution rate	N/A	N/A	N/A	N/A
47.	Nagy, K.L. 1995. "Dissolution and Precipitation Kinetics of Sheet Silicates." <i>Chemical Weathering Rates of Silicate Minerals</i> , 31, 291-351. White, A.F. and Brantley, S.L., eds. Washington, D.C.: Mineral Society of America. TIC: 222496.		entire	N/A-Reference only	Table 4	Kaolinite dissolution rate	N/A	N/A	N/A	N/A
48.	Ragnarsdottir, K.V. 1993. "Dissolution Kinetics of Heulandite at pH 2-12 and 25°C." <i>Geochimica et Cosmochimica Acta</i> , 57 (11), 2439-2449. New York, New York: Pergamon Press. TIC: 243920.		p.2439, 2447	N/A-Reference only	p. 23	Zeolite dissolution rate	N/A	N/A	N/A	N/A

OFFICE OF CIVILIAN RADIOACTIVE WASTE MANAGEMENT DOCUMENT INPUT REFERENCE SHEET										
1. Document Identifier No./Rev.: MDL-NBS-HS-000001/Rev. 00			Change: N/A	Title: Drift-Scale Coupled Processes (DST, THC Seepage) Models						
Input Document			4. Input Status	5. Section Used in	6. Input Description	7. TBV/TBD Priority	8. TBV Due To			
2. Technical Product Input Source Title and Identifier(s) with Version		3. Section					Unqual.	From Uncontrolled Source	Un-confirmed	
2a										
49.	Reed, M.H. 1982. "Calculation of Multicomponent Chemical Equilibria and Reaction Processes in Systems Involving Minerals, Gases, and an Aqueous Phase." <i>Geochimica et Cosmochimica Acta</i> , 46, 513-528. Amsterdam, The Netherlands: Elsevier Science Publishers. TIC: 224159.		pp. 514-516	N/A - Reference only	6.1.3	Thermodynamic expressions	N/A	N/A	N/A	N/A
50.	Renders, P.J.N.; Gammons, C.H.; and Barnes, H.L. 1995. "Precipitation and Dissolution Rate Constants for Cristobalite from 150 to 300°C." <i>Geochimica et Cosmochimica Acta</i> , 59 (1), 77-85. New York, New York: Pergamon Press. TIC: 226987.		entire	N/A-Reference only	p. 23	Cristobalite dissolution kinetics	N/A	N/A	N/A	N/A
51.	Rimstidt, J.D. 1997. "Quartz Solubility at Low Temperatures." <i>Geochimica et Cosmochimica Acta</i> , 61 (13), 2553-2558. Amsterdam, The Netherlands: Elsevier Science Publishers. TIC: 239020.		Entire	N/A-Reference only	Table IV-3	Quartz solubility	N/A	N/A	N/A	N/A

OFFICE OF CIVILIAN RADIOACTIVE WASTE MANAGEMENT DOCUMENT INPUT REFERENCE SHEET										
1. Document Identifier No./Rev.: MDL-NBS-HS-000001/Rev. 00			Change: N/A		Title: Drift-Scale Coupled Processes (DST, THC Seepage) Models					
Input Document			4. Input Status	5. Section Used in	6. Input Description	7. TBV/TBD Priority	8. TBV Due To			
2. Technical Product Input Source Title and Identifier(s) with Version		3. Section					Unqual.	From Uncontrolled Source	Un-confirmed	
2a										
52.	Rimstidt, J.D. and Barnes, H.L. 1980. "The Kinetics of Silica-Water Reactions." <i>Geochimica et Cosmochimica Acta</i> , 44, 1683-1699. Amsterdam, The Netherlands: Elsevier Science Publishers. TIC: 219975.		p. 1683	N/A-Reference only	6.1.4	Silica polymorph dissolution kinetics	N/A	N/A	N/A	N/A
53.	Shock, E.L.; Sassani, D.C.; Willis, M.; and Sverjensky, D.A. 1997. "Inorganic Species in Geologic Fluids: Correlations among Standard Molal Thermodynamic Properties of Aqueous Ions and Hydroxide Complexes." <i>Geochimica et Cosmochimica Acta</i> , 61 (5), 907-950. New York, New York: Pergamon Press. TIC: 246451.		entire	N/A-Reference only	Table IV-3	Thermodynamic data	N/A	N/A	N/A	N/A
54.	Slider H.C. 1976. <i>Practical Petroleum Reservoir Engineering Methods</i> . Tulsa, Oklahoma: The Petroleum Publishing Company. TIC: applied for.		p. 280	N/A-Reference only	6.1.6.4	Leverett scaling relation	N/A	N/A	N/A	N/A

OFFICE OF CIVILIAN RADIOACTIVE WASTE MANAGEMENT DOCUMENT INPUT REFERENCE SHEET									
1. Document Identifier No./Rev.: MDL-NBS-HS-000001/Rev. 00		Change: N/A		Title: Drift-Scale Coupled Processes (DST, THC Seepage) Models					
Input Document		3. Section	4. Input Status	5. Section Used in	6. Input Description	7. TBV/TBD Priority	8. TBV Due To		
2. Technical Product Input Source Title and Identifier(s) with Version							Unqual.	From Uncontrolled Source	Un-confirmed
2a									
55.	Sonnenthal, E. L. and Bodvarsson, G. S. 1999. "Constraints on the Hydrology of the Unsaturated Zone at Yucca Mountain, NV from Three-Dimensional Models of Chloride and Strontium Geochemistry." <i>Journal of Contaminant Hydrology</i> 38 (1-3), 107-156. Amsterdam, The Netherlands: Elsevier Science Publishers. TIC: 244160.	pp. 107-108, 140-141	N/A - Reference only	6.1.2	Water chemistry and ages	N/A	N/A	N/A	N/A
56.	Sonnenthal, E.L. and Ortoleva, P.J. 1994. "Numerical Simulations of Overpressured Compartments in Sedimentary Basins, in Basin Compartments and Seals." <i>American Association of Petroleum Geologists Memoir</i> , 61, 403-416. Ortoleva, P.J. and Al-Shaieb, Z., eds. Tulsa, Oklahoma: American Association of Petroleum Geologists. TIC: 235940.	p. 405-406	N/A-Reference only	N/A	Truncated sphere model	N/A	N/A	N/A	N/A

OFFICE OF CIVILIAN RADIOACTIVE WASTE MANAGEMENT DOCUMENT INPUT REFERENCE SHEET										
1. Document Identifier No./Rev.: MDL-NBS-HS-000001/Rev. 00			Change: N/A		Title: Drift-Scale Coupled Processes (DST, THC Seepage) Models					
Input Document			4. Input Status	5. Section Used in	6. Input Description	7. TBV/TBD Priority	8. TBV Due To			
2. Technical Product Input Source Title and Identifier(s) with Version		3. Section					Unqual.	From Uncontrolled Source	Un-confirmed	
2a										
57.	Steefel, C.I. and Lasaga, A.C. 1994. "A Coupled Model for Transport of Multiple Chemical Species and Kinetic Precipitation/Dissolution Reactions with Application to Reactive Flow in Single Phase Hydrothermal Systems." <i>American Journal of Science</i> , 294, 529-592. <i>American Journal of Science</i> , 294, 529-592. New Haven, Connecticut: Yale University Press. TIC: 235372.		pp. 550, 546 540, 541, 568 556	N/A - Reference only	6.1.3 6.1.4 6.1.6.2	Kinetic rate laws, cubic law	N/A	N/A	N/A	N/A
58.	Stoessel, R.K. 1988. "25°C and 1 atm Dissolution Experiments of Sepiolite and Kerolite." <i>Geochimica et Cosmochimica Acta</i> , 52, 365-374. New York, New York: Pergamon Press. TIC: 246452.		Entire	N/A - Reference only	Table IV-3	Thermodynamic data for sepiolite	N/A	N/A	N/A	N/A

OFFICE OF CIVILIAN RADIOACTIVE WASTE MANAGEMENT DOCUMENT INPUT REFERENCE SHEET									
1. Document Identifier No./Rev.: MDL-NBS-HS-000001/Rev. 00		Change: N/A		Title: Drift-Scale Coupled Processes (DST, THC Seepage) Models					
Input Document		4. Input Status	5. Section Used in	6. Input Description	7. TBV/TBD Priority	8. TBV Due To			
2. Technical Product Input Source Title and Identifier(s) with Version	3. Section					Unqual.	From Uncontrolled Source	Un-confirmed	
2a									
59.	Svensson, U. and Dreybrodt, W. 1992. "Dissolution Kinetics of Natural Calcite Minerals in CO ₂ -Water Systems Approaching Calcite Equilibrium." <i>Chemical Geology</i> , 100, 129-145. Amsterdam, The Netherlands: Elsevier Science Publishers. TIC: 246497.	p. 129 Entire	Table 4 4.1.5	Calcite kinetics	N/A	N/A	N/A	N/A	N/A
60.	Tester, J.W.; Worley, G.W.; Robinson, B.A.; Grigsby, C.O.; and Feerer, J.L. 1994. "Correlating Quartz Dissolution Kinetics in Pure Water from 25° to 625°C." <i>Geochimica et Cosmochimica Acta</i> , 58 (11), 2407-2420. Amsterdam, The Netherlands: Elsevier Science Publishers. TIC: 236776.	Entire	Table 4	Quartz dissolution kinetics	N/A	N/A	N/A	N/A	N/A

OFFICE OF CIVILIAN RADIOACTIVE WASTE MANAGEMENT DOCUMENT INPUT REFERENCE SHEET									
1. Document Identifier No./Rev.: MDL-NBS-HS-000001/Rev. 00			Change: N/A		Title: Drift-Scale Coupled Processes (DST, THC Seepage) Models				
Input Document			4. Input Status	5. Section Used in	6. Input Description	7. TBV/TBD Priority	8. TBV Due To		
2. Technical Product Input Source Title and Identifier(s) with Version		3. Section					Unqual.	From Uncontrolled Source	Un-confirmed
2a									
61.	Wemheuer, R.F. 1999. "First Issue of FY00 NEPO QAP-2-0 Activity Evaluations." Interoffice correspondence from R.F. Wemheuer (CRWMS M&O) to R.A. Morgan (CRWMS M&O), October 1, 1999. LV-NEPO.RTPS.TAG.10/99-155, with attachments. Activity Evaluation for Work Package #1401213UM1. ACC: MOL.19991028.0162.		Work Package #1401213UM1	N/A - Reference only	2	N/A	N/A	N/A	N/A
62.	Xu, T. and Pruess, K. 1998. <i>Coupled Modeling of Non-Isothermal Multi-Phase Flow, Solute Transport and Reactive Chemistry in Porous and Fractured Media: 1. Model Development and Validation.</i> LBNL-42050. Berkeley, California: Lawrence Berkeley National Laboratory. TIC: 243735.		Entire	N/A - Reference only	6.1.3	General model description	N/A	N/A	N/A

JSH 3/31/00

OFFICE OF CIVILIAN RADIOACTIVE WASTE MANAGEMENT DOCUMENT INPUT REFERENCE SHEET									
1. Document Identifier No./Rev.: MDL-NBS-HS-000001/Rev. 00		Change: N/A		Title: Drift-Scale Coupled Processes (DST, THC Seepage) Models					
Input Document		3. Section	4. Input Status	5. Section Used in	6. Input Description	7. TBV/TBD Priority	8. TBV Due To		
2. Technical Product Input Source Title and Identifier(s) with Version	2a						Unqual.	From Uncontrolled Source	Un-confirmed
63.	Xu, T.; Pruess, K.; and Brimhall, G. 1999. <i>An Improved Equilibrium-Kinetics Speciation Algorithm for Redox Reactions in Variable Saturated Subsurface Flow Systems</i> . LBNL-41789. <i>Computers and Geosciences</i> . Amsterdam, The Netherlands: Elsevier Science Publishers. TIC: 240019.	Entire	N/A - Reference only	6.1.3	General model description	N/A	N/A	N/A	N/A
64.	Software Code: AMESH V1.0. CSCI: 10045-1.0-00.	Entire	N/A- Qualified/ Verified/ Confirmed	3	General software use	N/A	N/A	N/A	N/A
65.	Software Code: EQ3/6 V7.2b. STN: LLNL: UCRL-MA-110662.	Input code only	N/A- Qualified/ Verified/ Confirmed	3	General software use	N/A	N/A	N/A	N/A
66.	Software Code: SOLVEQ/CHILLER V1.0. STN: 10057-1.0-00.	Entire	N/A- Qualified/ Verified/ Confirmed	3	General software use	N/A	N/A	N/A	N/A
67.	Software Code: SUPCRT92 V1.0. STN: 10058-1.0-00.	Entire	N/A- Qualified/ Verified/ Confirmed	3	General software use	N/A	N/A	N/A	N/A

JSH 3/13/00

OFFICE OF CIVILIAN RADIOACTIVE WASTE MANAGEMENT DOCUMENT INPUT REFERENCE SHEET									
1. Document Identifier No./Rev.: MDL-NBS-HS-000001/Rev. 00			Change: N/A		Title: Drift-Scale Coupled Processes (DST, THC Seepage) Models				
Input Document		3. Section	4. Input Status	5. Section Used in	6. Input Description	7. TBV/TBD Priority	8. TBV Due To		
2. Technical Product Input Source Title and Identifier(s) with Version	2a						Unqual.	From Uncontrolled Source	Un-confirmed
68.	Software Code: TOUGH2 V1.4. STN: 10061-1.4-00.	Entire	N/A- Qualified/ Verified/ Confirmed	3	General software use	N/A	N/A	N/A	N/A
69.	Software Code: TOUGHREACT V2.2. STN: 10154-2.2-00. Initial use.	Entire	TBV-3602	3	General software use	1	✓	N/A	N/A
70.	Software Routine: 2kgridv1a.for. ACC: MOL.19991201.0555.	Entire	N/A- Qualified/ Verified/ Confirmed	3	General software use	N/A	N/A	N/A	N/A
71.	Software Routine: mk_grav2.f. ACC: MOL.19991201.0556.	Entire	N/A- Qualified/ Verified/ Confirmed	3	General software use	N/A	N/A	N/A	N/A
72.	Software Routine: sav1d—dst2d.f. ACC: MOL.19991201.0557.	Entire	N/A- Qualified/ Verified/ Confirmed	3	General software use	N/A	N/A	N/A	N/A
73.	Software Routine: mrgdrift v1.0.	Entire	N/A- Qualified/ Verified/ Confirmed	3	General software use	N/A	N/A	N/A	N/A

OFFICE OF CIVILIAN RADIOACTIVE WASTE MANAGEMENT DOCUMENT INPUT REFERENCE SHEET									
1. Document Identifier No./Rev.: MDL-NBS-HS-000001/Rev. 00			Change: <i>28th 3/21/00</i> N/A		Title: Drift-Scale Coupled Processes (DST, THC Seepage) Models				
Input Document			4. Input Status	5. Section Used in	6. Input Description	7. TBV/TBD Priority	8. TBV Due To		
2. Technical Product Input Source Title and Identifier(s) with Version		3. Section					Unqual.	From Uncontrolled Source	Un-confirmed
2a									
74.	DTN: LL990702804244.100. Pore Water Data. Submittal Date: 7/13/99	Entire	N/A- Qualified-Verification Level 2	Table 2 Table 3 6.2.7.3.1	Mineral composition from water samples collected from boreholes.	N/A	N/A	N/A	N/A
75.	DTN: LL000114004242.090. TSPA-SR Mean Calculations. Submittal Date: 01/28/00	Table 5-3	N/A- Qualified-Verification Level 2	Table 2	Average Infiltrations for 2-D drift-scale models.	N/A	N/A	N/A	N/A

AP-3.15Q.1

Rev. 06/30/1999

ATTACHMENT II-MINERAL INITIAL VOLUME FRACTIONS

Submitted with this AMR under DTN: LB991200DSTTHC.003.

Table II-1. Volume Fractions of Primary Minerals

Unit	Rock Name	Zone	K-feldspar	Albite	Anorthite	Ca-Smectite	Na-Smectite	Mg-Smectite	K-Smectite	Illite	Tridymite
Tcw3	tcwm3	1	0.0946	0.0699	0.0024	0.0407	0.0175	0.0407	0.0175	0.0129	0.0000
	tcwf3	2	0.0946	0.0699	0.0024	0.0407	0.0175	0.0407	0.0175	0.0129	0.0000
Ptn1	ptnm1	3	0.0377	0.0279	0.0009	0.0643	0.0276	0.0643	0.0276	0.0204	0.0000
	ptnf1	4	0.0377	0.0279	0.0009	0.0643	0.0276	0.0643	0.0276	0.0204	0.0000
Ptn2	ptnm2	5	0.0449	0.0332	0.0011	0.0568	0.0244	0.0568	0.0244	0.0180	0.0000
	ptnf2	6	0.0449	0.0332	0.0011	0.0568	0.0244	0.0568	0.0244	0.0180	0.0000
Ptn3	ptnm3	7	0.0156	0.0116	0.0004	0.0095	0.0041	0.0095	0.0041	0.0030	0.0000
	ptnf3	8	0.0156	0.0116	0.0004	0.0095	0.0041	0.0095	0.0041	0.0030	0.0000
Ptn4	ptnm4	9	0.0806	0.0595	0.0020	0.0209	0.0090	0.0209	0.0090	0.0066	0.0000
	ptnf4	10	0.0806	0.0595	0.0020	0.0209	0.0090	0.0209	0.0090	0.0066	0.0000
Ptn5	ptnm5	11	0.0965	0.0712	0.0024	0.0090	0.0039	0.0090	0.0039	0.0029	0.0000
	ptnf5	12	0.0965	0.0712	0.0024	0.0090	0.0039	0.0090	0.0039	0.0029	0.0000
Ptn6	ptnm6	13	0.0855	0.0631	0.0021	0.0329	0.0141	0.0329	0.0141	0.0104	0.0000
	ptnf6	14	0.0855	0.0631	0.0021	0.0329	0.0141	0.0329	0.0141	0.0104	0.0000
Tsw31	tswm1	15	0.2358	0.1741	0.0059	0.0001	0.0001	0.0001	0.0001	0.0000	0.0000
	tswf1	16	0.2358	0.1741	0.0059	0.0001	0.0001	0.0001	0.0001	0.0000	0.0000
Tsw32	tswm2	17	0.4025	0.2973	0.0100	0.0027	0.0012	0.0027	0.0012	0.0009	0.0919
	tswf2	18	0.2435	0.1798	0.0061	0.0174	0.0074	0.0174	0.0074	0.0055	0.0556
Tsw33	tswm3	19	0.3051	0.2253	0.0076	0.0131	0.0056	0.0131	0.0056	0.0042	0.1071
	tswf3	20	0.1846	0.1363	0.0046	0.0237	0.0102	0.0237	0.0102	0.0075	0.0648
Tsw34	tswm4	21	0.3096	0.2286	0.0077	0.0081	0.0035	0.0081	0.0035	0.0026	0.0489
	tswf4	22	0.1873	0.1383	0.0047	0.0207	0.0089	0.0207	0.0089	0.0066	0.0296
Tsw35	tswm5	23	0.3051	0.2253	0.0076	0.0082	0.0035	0.0082	0.0035	0.0026	0.0597
	tswf5	24	0.1846	0.1363	0.0046	0.0207	0.0089	0.0207	0.0089	0.0066	0.0361
Tsw36	tswm6	25	0.3094	0.2285	0.0077	0.0074	0.0032	0.0074	0.0032	0.0024	0.0137
	tswf6	26	0.1872	0.1382	0.0047	0.0202	0.0087	0.0202	0.0087	0.0064	0.0083
Tsw37	tswm7	27	0.3057	0.2257	0.0076	0.0079	0.0034	0.0079	0.0034	0.0025	0.0077
	tswf7	28	0.1849	0.1366	0.0046	0.0205	0.0088	0.0205	0.0088	0.0065	0.0047
Tsw38	tswm8	29	0.0878	0.0648	0.0022	0.0180	0.0077	0.0180	0.0077	0.0057	0.0054
	tswf8	30	0.0878	0.0648	0.0022	0.0180	0.0077	0.0180	0.0077	0.0057	0.0054
Ch2	ch2mz	31	0.0370	0.0273	0.0009	0.0060	0.0026	0.0060	0.0026	0.0019	0.0000
	ch2fz	32	0.0370	0.0273	0.0009	0.0060	0.0026	0.0060	0.0026	0.0019	0.0000

Table II-1. Volume Fractions of Primary Minerals (cont.)

Unit	Rock Name	Zone	Cristobalite	Quartz	Glass	Hematite	Calcite	Stellerite	Heulandite	Mordenite	Clinoptilolite
Tcw3	tcwm3	1	0.1323	0.0037	0.4580	0.0000	0.0000	0.0000	0.0329	0.0110	0.0659
	tcwf3	2	0.1323	0.0037	0.4580	0.0000	0.0000	0.0000	0.0329	0.0110	0.0659
Ptn1	ptnm1	3	0.0000	0.0009	0.7283	0.0000	0.0000	0.0000	0.0000	0.0000	0.0000
	ptnf1	4	0.0000	0.0009	0.7283	0.0000	0.0000	0.0000	0.0000	0.0000	0.0000
Ptn2	ptnm2	5	0.0350	0.0157	0.6895	0.0002	0.0000	0.0000	0.0000	0.0000	0.0000
	ptnf2	6	0.0350	0.0157	0.6895	0.0002	0.0000	0.0000	0.0000	0.0000	0.0000
Ptn3	ptnm3	7	0.0763	0.0009	0.8652	0.0000	0.0000	0.0000	0.0000	0.0000	0.0000
	ptnf3	8	0.0763	0.0009	0.8652	0.0000	0.0000	0.0000	0.0000	0.0000	0.0000
Ptn4	ptnm4	9	0.0524	0.0139	0.7254	0.0000	0.0000	0.0000	0.0000	0.0000	0.0000
	ptnf4	10	0.0524	0.0139	0.7254	0.0000	0.0000	0.0000	0.0000	0.0000	0.0000
Ptn5	ptnm5	11	0.0214	0.0094	0.7679	0.0024	0.0000	0.0000	0.0000	0.0000	0.0000
	ptnf5	12	0.0214	0.0094	0.7679	0.0024	0.0000	0.0000	0.0000	0.0000	0.0000
Ptn6	ptnm6	13	0.0083	0.0142	0.7129	0.0024	0.0070	0.0000	0.0000	0.0000	0.0000
	ptnf6	14	0.0083	0.0142	0.7129	0.0024	0.0070	0.0000	0.0000	0.0000	0.0000
Tsw31	tswm1	15	0.0915	0.0047	0.4550	0.0050	0.0276	0.0000	0.0000	0.0000	0.0000
	tswf1	16	0.0915	0.0047	0.4550	0.0050	0.0276	0.0000	0.0000	0.0000	0.0000
Tsw32	tswm2	17	0.1516	0.0079	0.0152	0.0044	0.0095	0.0011	0.0000	0.0001	0.0000
	tswf2	18	0.0917	0.0048	0.0092	0.0027	0.0257	0.3257	0.0000	0.0001	0.0000
Tsw33	tswm3	19	0.2336	0.0760	0.0000	0.0036	0.0000	0.0000	0.0000	0.0000	0.0000
	tswf3	20	0.1413	0.0460	0.0000	0.0022	0.0200	0.3250	0.0000	0.0000	0.0000
Tsw34	tswm4	21	0.2588	0.1202	0.0000	0.0004	0.0000	0.0000	0.0000	0.0000	0.0000
	tswf4	22	0.1566	0.0727	0.0000	0.0002	0.0200	0.3250	0.0000	0.0000	0.0000
Tsw35	tswm5	23	0.1660	0.2037	0.0000	0.0017	0.0050	0.0000	0.0000	0.0000	0.0000
	tswf5	24	0.1004	0.1232	0.0000	0.0010	0.0230	0.3250	0.0000	0.0000	0.0000
Tsw36	tswm6	25	0.1509	0.2643	0.0000	0.0020	0.0000	0.0000	0.0000	0.0000	0.0000
	tswf6	26	0.0913	0.1599	0.0000	0.0012	0.0200	0.3250	0.0000	0.0000	0.0000
Tsw37	tswm7	27	0.2273	0.2004	0.0000	0.0005	0.0000	0.0000	0.0000	0.0000	0.0000
	tswf7	28	0.1375	0.1212	0.0000	0.0003	0.0200	0.3250	0.0000	0.0000	0.0000
Tsw38	tswm8	29	0.1557	0.0244	0.5629	0.0000	0.0000	0.0000	0.0119	0.0040	0.0238
	tswf8	30	0.1557	0.0244	0.5629	0.0000	0.0000	0.0000	0.0119	0.0040	0.0238
Ch2	ch2mz	31	0.1609	0.0326	0.0000	0.0000	0.0000	0.0000	0.2166	0.0722	0.4333
	ch2fz	32	0.1609	0.0326	0.0000	0.0000	0.0000	0.0000	0.2166	0.0722	0.4333

ATTACHMENT III-MINERAL REACTIVE SURFACE AREAS

Submitted with this AMR under DTN: LB991200DSTTHC.004.

Table III-1. Reactive Surface Areas for Primary Minerals (matrix minerals in cm²/g mineral, fracture minerals in m²/m³ medium).

Unit	Rock Name	Zone	K-feldspar	Albite	Anorthite	Ca-Smectite	Na-Smectite	Mg-Smectite	K-Smectite	Illite	Tridymite
Tcw3	tcwm3	1	98.0	98.0	98.0	1516.3	1516.3	1516.3	1516.3	1516.3	98.0
	tcwf3	2	394.8	394.8	394.8	394.8	394.8	394.8	394.8	394.8	394.8
Ptn1	ptnm1	3	7.6	7.6	7.6	2253.3	2253.3	2253.3	2253.3	2253.3	7.6
	ptnf1	4	142.8	142.8	142.8	142.8	142.8	142.8	142.8	142.8	142.8
Ptn2	ptnm2	5	8.6	8.6	8.6	2484.8	2484.8	2484.8	2484.8	2484.8	8.6
	ptnf2	6	184.6	184.6	184.6	184.6	184.6	184.6	184.6	184.6	184.6
Ptn3	ptnm3	7	7.1	7.1	7.1	1721.5	1721.5	1721.5	1721.5	1721.5	7.1
	ptnf3	8	1099.6	1099.6	1099.6	1099.6	1099.6	1099.6	1099.6	1099.6	1099.6
Ptn4	ptnm4	9	9.3	9.3	9.3	2356.2	2356.2	2356.2	2356.2	2356.2	9.3
	ptnf4	10	44.5	44.5	44.5	44.5	44.5	44.5	44.5	44.5	44.5
Ptn5	ptnm5	11	11.0	11.0	11.0	2666.7	2666.7	2666.7	2666.7	2666.7	11.0
	ptnf5	12	276.2	276.2	276.2	276.2	276.2	276.2	276.2	276.2	276.2
Ptn6	ptnm6	13	10.0	10.0	10.0	2666.7	2666.7	2666.7	2666.7	2666.7	10.0
	ptnf6	14	1553.3	1553.3	1553.3	1553.3	1553.3	1553.3	1553.3	1553.3	1553.3
Tsw31	tswm1	15	57.0	57.0	57.0	694.3	694.3	694.3	694.3	694.3	57.0
	tswf1	16	1102.4	1102.4	1102.4	1102.4	1102.4	1102.4	1102.4	1102.4	1102.4
Tsw32	tswm2	17	109.2	109.2	109.2	1317.4	1317.4	1317.4	1317.4	1317.4	109.2
	tswf2	18	530.8	530.8	530.8	530.8	530.8	530.8	530.8	530.8	530.8
Tsw33	tswm3	19	105.6	105.6	105.6	1303.3	1303.3	1303.3	1303.3	1303.3	105.6
	tswf3	20	1056.7	1056.7	1056.7	1056.7	1056.7	1056.7	1056.7	1056.7	1056.7
Tsw34	tswm4	21	89.8	89.8	89.8	1086.6	1086.6	1086.6	1086.6	1086.6	89.8
	tswf4	22	2126.9	2126.9	2126.9	2126.9	2126.9	2126.9	2126.9	2126.9	2126.9
Tsw35	tswm5	23	98.2	98.2	98.2	1195.3	1195.3	1195.3	1195.3	1195.3	98.2
	tswf5	24	1382.3	1382.3	1382.3	1382.3	1382.3	1382.3	1382.3	1382.3	1382.3
Tsw36	tswm6	25	90.8	90.8	90.8	1098.1	1098.1	1098.1	1098.1	1098.1	90.8
	tswf6	26	1289.1	1289.1	1289.1	1289.1	1289.1	1289.1	1289.1	1289.1	1289.1
Tsw37	tswm7	27	82.4	82.4	82.4	996.5	996.5	996.5	996.5	996.5	82.4
	tswf7	28	1746.2	1746.2	1746.2	1746.2	1746.2	1746.2	1746.2	1746.2	1746.2
Tsw38	tswm8	29	40.4	40.4	40.4	526.7	526.7	526.7	526.7	526.7	40.4
	tswf8	30	1746.2	1746.2	1746.2	1746.2	1746.2	1746.2	1746.2	1746.2	1746.2
Ch2	ch2mz	31	44.5	44.5	44.5	2024.7	2024.7	2024.7	2024.7	2024.7	44.5
	ch2fz	32	1570.8	1570.8	1570.8	1570.8	1570.8	1570.8	1570.8	1570.8	1570.8

DTN: LB991200DSTTHC.004

Table III-1. Reactive Surface Areas for Primary Minerals (matrix minerals in cm²/g

Unit	Rock		Cristobalite	Quartz	Glass	Hematite	Calcite	Stellerite	Heulandite	Mordenite	Clinoptilolite
	Name	Zone									
Tcw3	tcwm3	1	98.0	98.0	98.0	128.7	128.7	128.7	128.7	128.7	128.7
	tcwf3	2	394.8	394.8	394.8	394.8	394.8	394.8	394.8	394.8	394.8
Ptn1	ptnm1	3	7.6	7.6	7.6	9.6	9.6	9.6	9.6	9.6	9.6
	ptnf1	4	142.8	142.8	142.8	142.8	142.8	142.8	142.8	142.8	142.8
Ptn2	ptnm2	5	8.6	8.6	8.6	10.5	10.5	10.5	10.5	10.5	10.5
	ptnf2	6	184.6	184.6	184.6	184.6	184.6	184.6	184.6	184.6	184.6
Ptn3	ptnm3	7	7.1	7.1	7.1	7.3	7.3	7.3	7.3	7.3	7.3
	ptnf3	8	1099.6	1099.6	1099.6	1099.6	1099.6	1099.6	1099.6	7.3	7.3
Ptn4	ptnm4	9	9.3	9.3	9.3	10.0	10.0	10.0	10.0	10.0	10.0
	ptnf4	10	44.5	44.5	44.5	44.5	44.5	44.5	44.5	44.5	44.5
Ptn5	ptnm5	11	11.0	11.0	11.0	11.3	11.3	11.3	11.3	11.3	11.3
	ptnf5	12	276.2	276.2	276.2	276.2	276.2	276.2	276.2	276.2	276.2
Ptn6	ptnm6	13	10.0	10.0	10.0	11.3	11.3	11.3	11.3	11.3	11.3
	ptnf6	14	1553.3	1553.3	1553.3	1553.3	1553.3	1553.3	1553.3	1553.3	1553.3
Tsw31	tswm1	15	57.0	57.0	57.0	59.0	59.0	59.0	59.0	59.0	59.0
	tswf1	16	1102.4	1102.4	1102.4	1102.4	1102.4	1102.4	1102.4	1102.4	1102.4
Tsw32	tswm2	17	109.2	109.2	109.2	111.9	111.9	111.9	111.9	111.9	111.9
	tswf2	18	530.8	530.8	530.8	530.8	530.8	530.8	530.8	530.8	530.8
Tsw33	tswm3	19	105.6	105.6	105.6	110.7	110.7	110.7	110.7	110.7	110.7
	tswf3	20	1056.7	1056.7	1056.7	1056.7	1056.7	1056.7	1056.7	1056.7	1056.7
Tsw34	tswm4	21	89.8	89.8	89.8	92.3	92.3	92.3	92.3	92.3	92.3
	tswf4	22	2126.9	2126.9	2126.9	2126.9	2126.9	2126.9	2126.9	2126.9	2126.9
Tsw35	tswm5	23	98.2	98.2	98.2	101.5	101.5	101.5	101.5	101.5	101.5
	tswf5	24	1382.3	1382.3	1382.3	1382.3	1382.3	1382.3	1382.3	1382.3	1382.3
Tsw36	tswm6	25	90.8	90.8	90.8	93.2	93.2	93.2	93.2	93.2	93.2
	tswf6	26	1289.1	1289.1	1289.1	1289.1	1289.1	1289.1	1289.1	1289.1	1289.1
Tsw37	tswm7	27	82.4	82.4	82.4	84.6	84.6	84.6	84.6	84.6	84.6
	tswf7	28	1746.2	1746.2	1746.2	1746.2	1746.2	1746.2	84.6	84.6	84.6
Tsw38	tswm8	29	40.4	40.4	40.4	44.7	44.7	44.7	44.7	44.7	44.7
	tswf8	30	1746.2	1746.2	1746.2	1746.2	1746.2	1746.2	1746.2	1746.2	1746.2
Ch2	ch2mz	31	44.5	44.5	44.5	171.9	171.9	171.9	171.9	171.9	171.9
	ch2fz	32	1570.8	1570.8	1570.8	1570.8	1570.8	1570.8	1570.8	1570.8	1570.8

DTN: LB991200DSTTHC.004

ATTACHMENT IV – THERMODYNAMIC DATABASE

Submitted as Accepted Data under DTN: LB991200DSTTHC.005.

Table IV-1. Minerals.

Mineral	Molecular Weight (g/mol)	Molecular Volume (cm ³ /mol)	Reaction Stoichiometry ¹	log (K)						ref
				0 (°C)	25 (°C)	60 (°C)	100 (°C)	150 (°C)	200 (°C)	
albite-low	262.223	100.07	(1)alio2-, (1)na+, (3)sio2(aq)	-21.694	-20.177	-18.362	-16.684	-15.094	-13.986	4
anorthite	278.207	100.79	(2)alio2-, (1)ca+2, (2)sio2(aq)	-20.398	-19.188	-18.333	-17.852	-17.629	-17.703	1
calcite	100.087	36.934	(1)ca+2, (-1)h+, (1)hco3-	2.226	1.849	1.333	0.774	0.1	-0.584	1
SiO2(amor.)	60.084	29	(1)sio2(aq)	-2.871	-2.663	-2.423	-2.205	-1.99	-1.82	7
crystalite-a	60.084	25.74	(1)sio2(aq)	-3.63	-3.332	-2.99	-2.678	-2.371	-2.129	6
fluorite	78.075	24.542	(1)ca+2, (2)f-	-10.31	-10.037	-9.907	-9.967	-10.265	-10.784	1
goethite	88.854	20.82	(1)hfeo2	-12.78	-11.483	-10.202	-9.208	-8.407	-7.92	1
glass1	56.588	23.978	(-0.0362)h2o, (0.15)alio2-, (0.0021)ca+2, (0.0654)h+, (0.0042)k+, (0.0003)mg+2, (0.0756)na+, (0.7608)sio2(aq), (0.007)hfeo2	-4.7	-4.54	-4.35	-4.16	-3.98	-3.86	13
glass	60.084	29	(1)sio2(aq)	-2.871	-2.663	-2.423	-2.205	-1.99	-1.82	12
gypsum	172.172	74.69	(2)h2o, (1)ca+2, (1)so4-2	-4.533	-4.482	-4.609	-4.903	-5.41	-6.127	1
hematite	159.692	30.274	(-1)h2o, (2)hfeo2	-26.439	-23.927	-21.485	-19.661	-18.293	-17.573	1
illite	378.963	135.08	(0.44)h2o, (2.06)alio2-, (1.12)h+, (0.5)k+, (0.22)mg+2, (3.72)sio2(aq)	-45.354	-41.926	-38.294	-34.994	-31.867	-29.606	4
microcline	278.332	108.741	(1)alio2-, (1)k+, (3)sio2(aq)	-24.861	-22.91	-20.619	-18.526	-16.549	-15.154	4
kaolinite	258.16	99.52	(1)h2o, (2)alio2-, (2)h+, (2)sio2(aq)	-43.073	-39.895	-36.336	-33.181	-30.212	-28.082	4
quartz	60.084	22.688	(1)sio2(aq)	-4.079	-3.739	-3.349	-2.992	-2.642	-2.365	5
sepiolite	323.913	142.83	(5.5)h2o, (-4)h+, (2)mg+2, (3)sio2(aq)	17.28	15.76	13.83	12.08	10.45	9.23	8
tridymite	60.084	26.586	(1)sio2(aq)	-3.872	-3.567	-3.193	-2.821	-2.394	-1.984	10
smectite-ca	365.394	132.51	(0.52)h2o, (1.77)alio2-, (0.145)ca+2, (0.96)h+, (0.52)h2o, (1.77)alio2-, (0.96)h+, (0.26)mg+2, (0.29)na+, (3.97)sio2(aq)	-42.523	-39.519	-36.156	-33.159	-30.303	-28.219	9
smectite-na	366.25	132.51	(0.52)h2o, (1.77)alio2-, (0.96)h+, (0.26)mg+2, (0.29)na+, (3.97)sio2(aq)	-42.628	-39.528	-36.049	-32.937	-29.956	-27.761	9
smectite-mg	363.107	132.51	(0.52)h2o, (1.77)alio2-, (0.96)h+, (0.405)mg+2, (3.97)sio2(aq)	-42.583	-39.613	-36.289	-33.325	-30.498	-28.435	9
smectite-k	370.921	132.51	(0.52)h2o, (1.77)alio2-, (0.96)h+, (0.29)k+, (0.26)mg+2, (3.97)sio2(aq)	-43.004	-39.829	-36.275	-33.11	-30.093	-27.885	4
steller/10	281.733	133.1	(2.8)h2o, (0.79)alio2-, (0.39)ca+2, (0.01)na+, (2.81)sio2(aq)	-20.918	-19.404	-17.676	-16.103	-14.564	-13.428	11
heuland/10	279.347	126.64	(2.6)h2o, (0.8)alio2-, (0.33)ca+2, (0.04)k+, (0.1)na+, (2.8)sio2(aq)	-20.872	-19.32	-17.55	-15.94	-14.365	-13.202	11
mordeni/10	269.631	127.35	(2.2)h2o, (0.6)alio2-, (0.15)ca+2, (0.09)k+, (0.21)na+, (3)sio2(aq)	-19	-17.51	-15.802	-14.238	-12.694	-11.523	11
clinopt/10	277.66	126.41	(2.6)h2o, (0.68)alio2-, (0.28)ca+2, (0.08)k+, (0.04)na+, (2.92)sio2(aq)	-19.999	-18.463	-16.704	-15.095	-13.52	-12.309	11
Gas:	Molecular Weight (g/mol)	Molecular Diameter (m)								
CO2(g)	44.01	2.50E-10	(-1)h2o, (1)h+, (1)hco3-	-7.677	-7.818	-8.053	-8.36	-8.77	-9.217	1

NOTES: ¹ Negative number in parenthesis indicate the molecule is on the left side of equation
Minerals names or abbreviations above are those used in the database and may not exactly match names used in the text of the report. Names ending by /10 indicate the stoichiometry, molecular weight, molar volume, and log(K) values for those minerals were divided by 10 compared to original data. Glass phases glass1 and glass were used in Case 1 and Case 2 simulations, respectively.

Table IV-2. Aqueous Species.

Aqueous Species	a _o	Charge	Reaction Stoichiometry	log(K)						ref.
				0 (°C)	25 (°C)	60 (°C)	100 (°C)	150 (°C)	200 (°C)	
CO2(aq)	3	0	(-1)h2o, (1)h+, (1)hco3-	-6.58	-6.345	-6.268	-6.388	-6.724	-7.197	1
CO3-2	5	-2	(-1)h+, (1)hco3-	10.624	10.329	10.13	10.084	10.2	10.465	1
OH-	3	-1	(1)h2o, (-1)h+	14.94	13.995	13.027	12.255	11.631	11.284	1
Al(OH)2+	4	1	(1)alo2-, (2)h+	-13.656	-12.289	-10.831	-9.6	-8.53	-7.823	1
HAlO2	3	0	(1)alo2-, (1)h+	-7.08	-6.45	-5.846	-5.409	-5.121	-5.035	1
Al+3	9	3	(-2)h2o, (1)alo2-, (4)h+	-25.795	-22.883	-19.571	-16.582	-13.676	-11.409	1
AlOH+2	4.5	2	(-1)h2o, (1)alo2-, (3)h+	-20.069	-17.926	-15.568	-13.519	-11.624	-10.242	1
CaCl+	4	1	(1)ca+2, (1)cl-	0.673	0.696	0.589	0.357	-0.04	-0.533	1
CaCl2(aq)	0	0	(1)ca+2, (2)cl-	0.452	0.644	0.629	0.381	-0.159	-0.911	1
CaCO3(aq)	0	0	(1)ca+2, (-1)h+, (1)hco3-	7.502	7.002	6.452	5.964	5.468	5.018	1
CaHCO3+	4	1	(1)ca+2, (1)hco3-	-1.095	-1.047	-1.159	-1.418	-1.859	-2.4	1
CaSO4(aq)	0	0	(1)ca+2, (1)so4-2	-2.071	-2.111	-2.265	-2.511	-2.91	-3.433	1
CaF+	4	1	(1)ca+2, (1)f-	-0.655	-0.682	-0.862	-1.17	-1.649	-2.215	1
HSiO3-	4	-1	(1)h2o, (-1)h+, (1)sio2(aq)	10.323	9.953	9.468	9.084	8.85	8.839	1
HCl(aq)	3	0	(1)cl-, (1)h+	0.661	0.67	0.689	0.62	0.41	0.092	1
KCl(aq)	0	0	(1)cl-, (1)k+	1.71	1.495	1.216	0.924	0.575	0.215	1
KHSO4(aq)	0	0	(1)h+, (1)k+, (1)so4-2	-0.435	-0.814	-1.479	-2.294	-3.341	-4.431	1
KSO4-	4	-1	(1)k+, (1)so4-2	-0.885	-0.88	-0.99	-1.194	-1.52	-1.919	1
HF(aq)	3	0	(1)h+, (1)f-	-2.985	-3.168	-3.474	-3.848	-4.338	-4.859	1
MgCl+	4	1	(1)cl-, (1)mg+2	0.049	0.135	0.055	-0.182	-0.607	-1.139	1
MgCO3(aq)	0	0	(-1)h+, (1)hco3-, (1)mg+2	7.74	7.35	6.926	6.563	6.204	5.872	1
MgHCO3+	4	1	(1)hco3-, (1)mg+2	-1.08	-1.036	-1.164	-1.436	-1.88	-2.415	1
MgSO4(aq)	3	0	(1)mg+2, (1)so4-2	-2.139	-2.412	-2.837	-3.347	-4.073	-4.955	1
MgF+	4	1	(1)mg+2, (1)f-	-1.387	-1.352	-1.478	-1.739	-2.168	-2.688	1
NaCl(aq)	3	0	(1)cl-, (1)na+	0.829	0.777	0.651	0.473	0.214	-0.093	1
NaOH(aq)	3	0	(1)h2o, (-1)h+, (1)na+	15.645	14.795	13.8	12.885	11.971	11.221	1
NaCO3-	4	-1	(-1)h+, (1)hco3-, (1)na+	9.815	9.814	10.075	10.649	11.568	12.632	2
NaHCO3(aq)	3	0	(1)hco3-, (1)na+	-0.373	-0.154	0.11	0.411	0.793	1.213	1
NaHSiO3	0	0	(1)h2o, (-1)h+, (1)na+, (1)sio2(aq)	8.414	8.304	8.053	7.829	7.684	7.658	1
NaF(aq)	0	0	(1)na+, (1)f-	1.082	0.998	0.833	0.624	0.338	0.011	1
FeO2-	4	-1	(-1)h+, (1)hfeo2	10.231	9.602	8.839	8.111	7.38	6.821	3
FeO+	4	1	(-1)h2o, (1)h+, (1)hfeo2	-7.324	-6.368	-5.372	-4.561	-3.865	-3.393	3
Primary Aqueous Species:			Mol. Wt. (g/mol)							
H2O	3	0	18.015							1
AlO2-	4	-1	58.98							1
Ca+2	6	2	40.078							1
Cl-	3	-1	35.453							1
H+	9	1	1.008							1
HCO3-	4	-1	61.017							1
K+	3	1	39.098							1
Mg+2	8	2	24.305							1
Na+	4	1	22.99							1
SiO2(aq)	3	0	60.084							1
SO4-2	4	-2	96.064							1
F-	4	-1	18.998							1
HFeO2	3	0	88.854							3

Table IV-3. References

ref. no	Reference
1	EQ3/6 V7.2b database data0.com.R2 Aug.2.1995 (STN: LLNL:UCRL-MA-110662). Mostly calculated with SUPCRT92 and associated databases (Johnson et al. 1992).
2	EQ3/6 database data0.com.R6 Dec.3.1996 (STN: LLNL:UCRL-MA-110662)
3	Log(K) calculated using SUPCRT92 (Johnson et al. 1992) with Fe+3 and Fe(III)-OH data from Shock et al. 1997 added to SPRONS.DAT version dated 3/14/96 (the latter is the database of SUPCRT92). See Scientific Notebook YMP-LBNL-YWT-NS-1.1 p. 104-110.
4	Log(K) calculated using SUPCRT92 (Johnson et al. 1992) with thermodynamic properties from various sources (Berman 1988 for albite; Kulik and Aja 1995 for illite and k-smectite; Robie and Hemingway 1995 for kaolinite; Apps and Chang 1992 for microcline) added to SPRONS.DAT version dated 3/14/96 (the latter is the database of SUPCRT92), then corrected to reflect the quartz solubility data of Rimstidt (1997). See Scientific Notebook YMP-LBNL-YWT-JA-1A p. 39-41.
5	Rimstidt (1997)
6	Regression by Apps (1970) of pressure-corrected cristobalite solubility data derived from measurements by Fournier and Rowe (1962). See Scientific Notebook YMP-LBNL-YWT-JA-1A p. 39-41.
7	Regression by Apps (1970) from a number of literature sources. See Scientific Notebook YMP-LBNL-YWT-JA-1A p. 39-41.
8	Stoessell (1988)
9	Recalculated from log(K) data for montmor-k, montmor-ca, montmor-mg, and montmor-k in EQ3/6 V7.2b database (see ref. 1), as described in Scientific Notebook YMP-LBNL-YWT-JA-1A p. 39-41.
10	From log(K) data for quartz and trydimite in ref.1 above, then corrected with the quartz solubility data of Rimstidt (1997). See Scientific Notebook YMP-LBNL-YWT-NS-1.1 p. 113-114. Molar volume from molecular weight in ref.1 and density in Klein and Hurlbut (1993, p. 665).
11	Log(K) calculated using SUPCRT92 (Johnson et al. 1992) with zeolite formulas and thermodynamic data from Scientific Notebook YMP-LBNL-YWT-JA-1A, pp. 57-60 added to SPRONS.DAT version dated 3/14/96 (the latter is the database of SUPCRT92), then corrected to reflect the quartz solubility data of Rimstidt (1997). See Scientific Notebooks YMP-LBNL-YWT-JA-1A p. 48-50 and YMP-LBNL-YWT-NS-1.1 p. 111-113.
12	Same composition and log(K) as amorphous silica
13	Formula from composition by Bish et al. (1996). Log(K) at 25°C was calculated by equilibrating the glass with the initial water composition (Section 4.1.3) using SOLVEQ V1.0 and adjusting the log(K) value to yield approximately 100 ppm SiO ₂ (aq.) in solution at 25°C. Log(K) values at higher temperatures were then adjusted to maintain the same degree of amorphous silica undersaturated with the equilibrated glass at all temperatures. See Scientific Notebook YMP-LBNL-YWT-NS-1.1 p. 114-116.

ATTACHMENT V–WASTE PACKAGE AVERAGE HEAT TRANSFER

Submitted with this AMR under DTN: LB991200DSTTHC.006.

Table V-1.

Time (years)	Total Heat (no ventilation) (W/meter)	Model Heat Load (W/meter)
0.01	1540.413	462.124
0.02	1538.978	461.693
0.03	1538.078	461.424
0.04	1537.190	461.157
0.05	1536.297	460.889
0.06	1535.411	460.623
0.07	1534.536	460.361
0.08	1533.632	460.090
0.09	1532.778	459.833
0.10	1531.892	459.568
0.15	1527.633	458.290
0.20	1523.418	457.025
0.25	1519.360	455.808
0.30	1515.371	454.611
0.35	1511.471	453.441
0.40	1507.662	452.299
0.45	1503.928	451.178
0.50	1500.288	450.087
0.55	1496.715	449.014
0.60	1493.234	447.970
0.65	1489.795	446.938
0.70	1486.453	445.936
0.75	1483.142	444.943
0.80	1479.935	443.981
0.85	1476.770	443.031
0.90	1473.664	442.099
0.95	1470.592	441.178
1.0	1467.611	440.283
1.5	1439.923	431.977
2.0	1415.942	424.783

DTN: SN9907T0872799.001 (Total Heat)

NOTE: Point at 50.001 years was interpolated between original data points at 50 and 55 years. From 0 to 50 years: Model Heat Load = Total Heat x 0.3 (70% heat removal).

Table V-1. (Cont.)

Time (years)	Total Heat (no ventilation) (W/meter)	Model Heat Load (W/meter)
2.5	1394.705	418.412
3.0	1375.415	412.624
3.5	1358.036	407.411
4.0	1341.878	402.563
4.5	1326.553	397.966
5.0	1312.104	393.631
5.5	1296.809	389.043
6.0	1282.270	384.681
6.5	1268.766	380.630
7.0	1255.846	376.754
7.5	1242.619	372.786
8.0	1229.944	368.983
8.5	1217.624	365.287
9.0	1205.763	361.729
9.5	1193.723	358.117
10	1182.073	354.622
15	1074.598	322.379
20	983.485	295.045
25	901.588	270.476
30	829.938	248.981
35	767.015	230.104
40	710.239	213.072
45	659.213	197.764
50	614.555	184.367
50.001	614.547	614.547
55	574.043	574.043
60	537.708	537.708
65	504.775	504.775
70	476.139	476.139
75	449.277	449.277
80	425.849	425.849
85	404.184	404.184
90	385.201	385.201
95	367.303	367.303

DTN: SN9907T0872799.001 (Total Heat)

NOTE: Point at 50.001 years was interpolated between original data points at 50 and 55 years. From 0 to 50 years: Model Heat Load = Total Heat x 0.3 (70% heat removal).

Table V-1. (Cont.)

Time (years)	Total Heat (no ventilation) (W/meter)	Model Heat Load (W/meter)
100	351.814	351.814
150	253.283	253.283
200	208.867	208.867
250	182.764	182.764
300	164.855	164.855
350	150.949	150.949
400	139.546	139.546
450	129.712	129.712
500	121.251	121.251
550	113.640	113.640
600	107.056	107.056
650	101.089	101.089
700	95.546	95.546
750	90.641	90.641
800	85.985	85.985
850	81.688	81.688
900	77.753	77.753
950	74.214	74.214
1000	71.169	71.169
1500	49.114	49.114
2000	38.723	38.723
2500	33.617	33.617
3000	30.482	30.482
3500	28.676	28.676
4000	27.425	27.425
4500	26.223	26.223
5000	25.254	25.254
5500	24.204	24.204
6000	23.596	23.596
6500	22.687	22.687
7000	21.910	21.910
7500	21.344	21.344
8000	20.553	20.553
8500	19.948	19.948

DTN: SN9907T0872799.001 (Total Heat)

NOTE: Point at 50.001 years was interpolated between original data points at 50 and 55 years. From 0 to 50 years: Model Heat Load = Total Heat x 0.3 (70% heat removal).

Table V-1. (Cont.)

Time (years)	Total Heat (no ventilation) (W/meter)	Model Heat Load (W/meter)
9000	19.308	19.308
9500	18.729	18.729
10000	18.144	18.144
15000	13.570	13.570
20000	10.633	10.633
25000	8.594	8.594
30000	7.027	7.027
35000	5.908	5.908
40000	5.071	5.071
45000	4.407	4.407
50000	3.868	3.868
55000	3.378	3.378
60000	3.041	3.041
65000	2.671	2.671
70000	2.425	2.425
75000	2.192	2.192
80000	1.985	1.985
85000	1.817	1.817
90000	1.692	1.692
95000	1.562	1.562
100000	1.457	1.457

DTN: SN9907T0872799.001 (Total Heat)

NOTE: Point at 50.001 years was interpolated between original data points at 50 and 55 years. From 0 to 50 years: Model Heat Load = Total Heat x 0.3 (70% heat removal).

ATTACHMENT VI-EFFECTIVE THERMAL CONDUCTIVITY FOR IN-DRIFT OPEN SPACES

Table VI-1. Pre-closure

Time		Factor
(sec)	(year)	
0.00000E+00	0.0	0.400
3.15360E+07	1.0	0.775
4.73040E+07	1.5	0.825
6.30720E+07	2	0.858
9.46080E+07	3	0.899
1.26144E+08	4	0.923
1.57680E+08	5	0.941
1.89216E+08	6	0.956
2.20752E+08	7	0.966
2.52288E+08	8	0.975
2.83824E+08	9	0.982
3.15360E+08	10	0.988
3.46896E+08	11	0.993
3.78432E+08	12	0.997
4.73040E+08	15	1.000
6.30720E+08	20	0.994
7.88400E+08	25	0.979
8.19936E+08	26	0.976
8.51472E+08	27	0.972
9.46080E+08	30	0.961
1.10376E+09	35	0.941
1.26144E+09	40	0.921
1.57680E+09	50	0.887

DTN: SN9907T0872799.002

NOTE: $K_{thermal}$ is calculated as Max. $K_{thermal}$ x Factor
 Maximum $K_{thermal}$ (W/m-K) = 10.443

Table VI-2. Postclosure

Time		Factor	
(sec)	(year)	Inner	Outer
1.57680E+09	50	0.887	0.887
1.60834E+09	51	0.872	0.800
1.63987E+09	52	0.915	0.849
1.73448E+09	55	0.984	0.935
1.89216E+09	60	1.000	0.983
2.04984E+09	65	0.990	1.000
2.20752E+09	70	0.968	0.999
2.36520E+09	75	0.941	0.990
2.39674E+09	76	0.936	0.987
2.42827E+09	77	0.931	0.986
2.52288E+09	80	0.916	0.980
2.83824E+09	90	0.874	0.963
3.15360E+09	100	0.833	0.940
3.18514E+09	101	0.829	0.937
3.31128E+09	105	0.813	0.924
3.46896E+09	110	0.796	0.910
3.78432E+09	120	0.767	0.890
4.09968E+09	130	0.746	0.879
4.41504E+09	140	0.729	0.873
5.04576E+09	160	0.703	0.864
5.67648E+09	180	0.679	0.847
6.30720E+09	200	0.659	0.836
6.93792E+09	220	0.638	0.816
7.88400E+09	250	0.617	0.800
9.46080E+09	300	0.587	0.775
1.10376E+10	350	0.563	0.754
1.26144E+10	400	0.540	0.731
1.41912E+10	450	0.519	0.709
1.57680E+10	500	0.506	0.698
1.73448E+10	550	0.497	0.692
1.89216E+10	600	0.491	0.688
2.20752E+10	700	0.476	0.677
2.52288E+10	800	0.462	0.664
2.83824E+10	900	0.450	0.652

DTN: SN9907T0872799.002

NOTE: $K_{thermal}$ is calculated as Max. $K_{thermal}$ x Factor
 Maximum $K_{thermal}$ (W/m-K) Inner=3.426,
 Outer=9.068

Table VI-2. Postclosure (Cont.)

Time		Factor	
(sec)	(year)	Inner	Outer
3.15360E+10	1000	0.439	0.642
3.46896E+10	1100	0.431	0.633
3.78432E+10	1200	0.423	0.624
4.09968E+10	1300	0.414	0.615
4.41504E+10	1400	0.406	0.606
4.73040E+10	1500	0.398	0.597
5.04576E+10	1600	0.392	0.590
5.67648E+10	1800	0.382	0.577
6.30720E+10	2000	0.370	0.563
6.93792E+10	2200	0.363	0.552
7.88400E+10	2500	0.353	0.540
9.46080E+10	3000	0.342	0.524
1.10376E+11	3500	0.334	0.512
1.26144E+11	4000	0.327	0.501
1.41912E+11	4500	0.321	0.493
1.57680E+11	5000	0.317	0.486
1.89216E+11	6000	0.308	0.474
2.20752E+11	7000	0.302	0.464
2.52288E+11	8000	0.296	0.455
3.15360E+11	10000	0.286	0.441
4.73040E+11	15000	0.267	0.413
6.30720E+11	20000	0.255	0.395
9.46080E+11	30000	0.237	0.371
1.26144E+12	40000	0.228	0.358
1.57680E+12	50000	0.222	0.350
1.89216E+12	60000	0.218	0.344
2.52288E+12	80000	0.212	0.337
3.15360E+12	100000	0.209	0.333

DTN: SN9907T0872799.002

NOTE: $K_{thermal}$ is calculated as Max. $K_{thermal}$ x Factor
 Maximum $K_{thermal}$ (W/m-K) Inner=3.426,
 Outer=9.068

ATTACHMENT VII–LIST OF INPUT AND OUTPUT FILES

The following types files were submitted to the TDMS under DTN:LB991200DSTTHC.002:

1. Input and output files of simulations with the reactive transport model TOUGHREACT V2.2. For each simulation, these files were concatenated into one file using the Unix *tar* utility then compressed using the Unix *gzip* utility. Resulting concatenated/compressed files have the extension *.tar.gz*.
2. Summary Excel spreadsheets of model output data at three locations around the drift (crown, side, and base).

DST simulations input and output files (concatenated/compressed files)

dst99amr_8.tar.gz DST simulations with reduced set of minerals (Case 2)
 dst99amr_9.tar.gz DST simulations with full set of minerals (Case 1)

THC Seepage Model simulations input and output files (concatenated/compressed files)

thc1mm_amb1.tar.gz THC simulation, 1 mm/year basecase infiltration , reduced mineral set - 0 to 50 years
 thc1mm_amb1a.tar.gz THC simulation, 1 mm/year basecase infiltration, reduced mineral set - 50 to 100,000 years
 thc1mm_amb2.tar.gz THC simulation, 1 mm/year basecase infiltration, full mineral set - 0 to 50 years
 thc1mm_amb2a.tar.gz THC simulation, 1 mm/year basecase infiltration, full mineral set - 50 to 20,000 years
 thc1mm_amb2b.tar.gz THC simulation, 1 mm/year basecase infiltration, full mineral set - 20,000 to 100,000 years

Other file names have similar designations as shown in the examples below. The file name shows the infiltration rates used in each simulation (e.g., *6_16_25* means 6mm/year from 0 to 600 years, 16mm/year from 600 to 2000 years, and 25mm/year from 2000 to 100,000 years). For THC simulations, the last digit in the file name is *3* for simulations with the reduced mineral set, and *4* for the full mineral set (e.g., *thc6_16_25_3* means 6/16/25mm/year with reduced mineral set). The last letters *a*, *b*, *c*, or *d* are used for time designations

th6_16_25_3.tar.gz Simulation without reactive transport (TH only) - 0 to 50 ears
 th6_16_25_3a.tar.gz Simulation without reactive transport (TH only) - 50 to 600 years
 th6_16_25_3b.tar.gz Simulation without reactive transport (TH only) - 600 to 2000 years
 th6_16_25_3c.tar.gz Simulation without reactive transport (TH only) - 2000 to 100,000 years
 thc0.6_6_3_4.tar.gz THC simulation, full mineral set - 0 to 50 years
 thc0.6_6_3_4a.tar.gz THC simulation, full mineral set - 50 to 600 years
 thc0.6_6_3_4b.tar.gz THC simulation, full mineral set - 600 to 2000 years

thc0.6_6_3_4c.tar.gz THC simulation, full mineral set - 2000 to 20,000 years
 thc0.6_6_3_4d.tar.gz THC simulation, full mineral set - 20,000 to 100,000 years
 .
 .
 .
 etc...

Contents of .tar.gz files

FLOW.INP	Rock thermal and hydrological properties, run flags and other specifications (input)
FLOW.OUT	Thermal and hydrological results (gas/liquid saturation, T, P, air mass fraction, etc.) (output)
GENER	Infiltration rates, heat load, and effective thermal conductivity (input)
INCON	Initial thermal and hydrological conditions (T, P, liquid saturation, etc.) (input)
MESH	Input numerical mesh (input)
SAVE	Thermal and hydrological conditions (T, P, liquid saturation, etc.) to use for restarting a run (output, same format as INCON file)
TABLE	Miscellaneous output data
VERS	Miscellaneous output data
LINEQ	Miscellaneous output data
CHEMICAL.INP	Water chemistry, mineralogy, and CO ₂ partial pressure data (input)
SOLUTE.INP	Run flags and other data relating to reactive transport (input)
thermokapps2.05.dat	Thermodynamic database (input)
TEC_CONC.DAT	Calculated concentrations of aqueous species (moles/liter) at each grid node (two records for each node - first record for fractures and second record for matrix) (output)
TEC_MIN.DAT	Calculated volume fraction change for minerals at each grid node (two records for each node - first record for fractures and second record for matrix) (output)
TEC_GAS.DAT	Calculated CO ₂ volume fraction at each grid node (two records for each node - first record for fractures and second record for matrix) (output)
TIME.DAT	Chemistry data at selected grid nodes (output) (not used in this this AMR)
chdump.dat	Chemical speciation of initial water (output)
INCHEM	Chemistry data at all grid nodes to use for restarting a run (input)
SAVECHEM	Chemistry data at all grid nodes to use for restarting a run (output, same format as INCHEM file)
ITER.DAT	Iteration information (output)
run_log.dat	Miscellaneous run-time information. Note: Mass balances are not printed out correctly in this file for runs that have been restarted (i.e., starting at times different than zero).

Summary spreadsheets of output data (also used for plotting time profiles)

The data in these files were extracted from output files FLOW.OUT, TEC_CONC.DAT, TEC_MIN.DAT, and TEC_GAS.DAT for each simulation.

case1_0.6.xls	THC, full mineral set, 0.6/6/3 mm/year infiltration
case1_6.xls	THC, full mineral set, 6/16/25 mm/year infiltration
case1_15.xls	THC, full mineral set, 15/25/47mm/year infiltration
case2_0.6.xls	THC, reduced mineral set, 0.6/6/3 mm/year infiltration
case2_6.xls	THC, reduced mineral set, 6/16/25 mm/year infiltration
case2_15.xls	THC, reduced mineral set, 15/25/47mm/year infiltration
case1_1amb.xls	THC, no heat load, full mineral set, 1 mm/year infiltration
case2_1amb.xls	THC, no heat load, reduced mineral set, 1 mm/year infiltration
th_only_6.xls	TH (heat but no reaction), 6/16/25 mm/year infiltration

ATTACHMENT VIII
SOFTWARE ROUTINES

**YMP-LBNL
 REVIEW RECORD**

1. QA: L
 2. Page 1 of 1

3. Originator: Nick Spycher
 4. Document Title: Documentation for Routine **mk grav2.f v.1.0** (Option 1 per AP-SI.1Q/Rev. 2/ICN4, Sec. 5.1)
 5. Document Number: N/A 6. Revision/Mod.: N/A 7. Draft: N/A
 8. Governing Procedure Number: AP-SI.1Q 9. Revision/Mod: 2/4

REVIEW CRITERIA YMP-LBNL-QIP-6.1, Atch. 5, p. 18 Routine Review Criteria

10. Standard Review Criteria (One time use Option 1)
 (Taken from Attachment 5)

11. Specific Review Criteria:
 Source: AP-SI.1Q/Rev. 2/ICN4, Sec. 5.1.1 (One time use routine)
 Attached: _____
 Scientific notebook/data associated with this review as noted on Attachment 3

12. Comment Documentation:
 Comment Sheets
 Review Copy Mark-up

13. YMP-LBNL Project Manager (PM): Gudmundur S. Bodvarsson

14. Reviewer	Org./Discipline	Review Criteria	Reviewer	Org./Discipline	Review Criteria
<u>E. Sonnenthal</u>	<u>LBNL</u>	<u>Technical</u>	_____	_____	_____
_____	_____	_____	_____	_____	_____
_____	_____	_____	_____	_____	_____

VIII-2 JSA 3/3/00

COMMENTS DUE: 15. Due Date: <u>2/18/00</u> 16. Originator/Review Coordinator: <u>Nick Spycher</u> Print Name	REVIEW BY: 17. <u>Eric Sonnenthal</u> Print Name 18. <u>Eric Sonnenthal</u> <u>3/2/00</u> Signature Date 19. Mandatory Comments: <input type="checkbox"/> Yes <input checked="" type="checkbox"/> No	CONCURRENCE: 21. Document Draft No: <u>NA</u> Date: _____ 22. Reviewer: <u>Eric Sonnenthal</u> <u>3/2/00</u> Signature Date 23. PM: <u>[Signature]</u> <u>3/3/00</u> Signature Date
	ORIGINATOR/REVIEW COORDINATOR (After response completed): 20. <u>N. Spycher</u> <u>3/2/00</u> Print Name/Signature Date	DISPUTE RESOLUTION: (if applicable) 24. PM: _____ Signature Date

YMP-LBNL
 COMMENT SHEET

QA: L

1. Document Title: Routine Documentation for mk_grav2.f v1.0		2. Page <u>1</u> of <u>1</u>		
3. Document No. N/A	4. Revision/ Change/Mod: N/A	5. Draft N/A	6. <input checked="" type="checkbox"/> Q <input type="checkbox"/> NQ	
7. Reviewer: Eric Sonnenthal				
8. NO. CODE	9. SECT./PARA./P#	10. COMMENT	11. RESPONSE	12. ACCEPT
		<p>--NO COMMENTS--</p> <p>The documentation for this routine was reviewed and it was found to meet the requirements of AP-SI.1Q/Rev. 2/ICN4. The test case was checked by both hand calculation and by running the code as needed to fully check the test case. The test case fully checks the routine for the input specified and proves that the routine produces acceptable results.</p>		

VII-3 JEH 3/3/00

STANDARD REVIEW CRITERIA

Routine/Macro Review Criteria, Option 1

NOTE: Where a checklist item does not apply to the software product, check "N/A".

	Yes	No	N/A	
R/M-1	X			The information given below is to be documented in the technical product, in which the routine/macro is used to support. Does the routine/macro include: Name of routine/macro with version/Operating System/hardware environment
R/M-2	X			Name of commercial software used to write the routine/macros with version/Operating System/hardware used to develop it
R/M-3	X			Test Plan <ul style="list-style-type: none"> • Explanation whether this is a routine or macro and a description of what it does • The source code (this section shall include equations or algorithms form software setup (Labview, Excel, etc.) • Description of test(s) to be performed (be specific) • Specified range of input values to be used and why the range is valid
R/M-4	X			Test Results <ul style="list-style-type: none"> • Output from test (explain difference between input range used and possible input) • Description of how the testing shows that the results are correct for the specified input • List of limitations or assumptions to this test case (s) and code in general • Electronic files identified by name and location (included if necessary to perform the tests)
R/M-5	X			Supporting Information. Include background information, such as revision to a previous routine or macro or explanation of the steps performed to run the software. Include listing of all electronic files and codes used. Attach Scientific Notebook pages with appropriate information annotated.

Modified per AP-SI.1Q, R2, ICN 4

V111-5 JEH 3/31/00

YMP-LBNL Software Routine/Macro Documentation—Option 1
AP-SI.1Q, Rev. 2, ICN 1, Software Management

Document once in the technical product, data submittal, or scientific notebook where used and cross-reference thereafter each time it is used in another document.

The star (*) denotes mandatory items. Other items may want to be considered for documentation as applicable, but if not used, mark N/A.

1. SOFTWARE ROUTINE IDENTIFICATION

* Routine/macro name and version number:

mk-grav2.f v1.0

* Name and version identification of the industry standard software under which the routine/macro was developed (e.g., Excel 97, Sun OS 5.1 FORTRAN 90, etc.):

FORTRAN 77 / 90 Platforms: { PC DOS (under MS Windows), Digital VAX Fortran / MS Visual Fortran 5.0-A, Sun Ultra Sparc Solaris SUNOS 5.5, Sun S77 4.0 compiler } (same code works on both)

2. DESCRIPTION AND TESTING

Brief description of purpose or function of routine/macro including the execution environment (can be 1 sentence):

Reads AMESH output files and creates TOUGH2 mesh input files (PC and unix platforms)

* Page(s) containing a listing of the source code of the routine/macro:

Binder A-1 attached to notebook YMP-LBNL-DSM-NS-1, folder "mk-grav2"

* Page(s) listing the executable or any data files, including test data input and output files:

YMP-LBNL-DSM-NS-1, p. 56

* Documentation that the routine/macro provides correct results for a specified range of input parameters. Include the range of input parameter values for which results were verified:

YMP-LB^{NL}GA^{NL}-DSM-NS-1 p. 53 - 56

NS. 2/7/00

NS. 2/7/00

NS. 2/7/00

Description of test cases and test results. Refer to notebook pages or other documentation.

(Showing a short example [1-2 lines] of input and output helps demonstrate correct operation.):

YMP-LBNL-DSM-NS1 p. 53-56

Identification of any limitations on the routine/macro applications or validity:

Current assignment of "rock" types for in-drift components are design-specific for the TTC Seepage Model runs (1999)

3. SUPPORTING INFORMATION

* Technical reviewer (according to YMP-LBNL-QIP 6.1) who reviewed work and date:

Eric Sonnenthal 2/7/00

VIII-6 JETH 3/31/00

1/14/00

QA mk grav2 utility program v1.0

Objective: test/verify mk grav2 (for program parts used in the THC Seepage Model: gravity vector calculation, drift node labeling, mesh file creation)

(mk-grav)

The original version of this code was created by J Birkblazer at LBNL (note book YMP-LBNL-JRA-2, p.11) ~~single user name~~ by ~~NS 1/4/99~~ ~~mk-grav~~ at LBNL. Here, I will be QA'ing only the parts of the code that generate data used in the THC seepage model.

Description of computer program

This program reads output files from AMESH v1.0 (STN 10045-1.0-00) (files eleme and conne) and creates TOUGH2 (STN 10007-1.4-02) mesh input files (the ELEM and CONNE blocks of TOUGH2 input data file). The only calculated data in the TOUGH2 input file that are not already in the AMESH output files are the gravity vector data. Program mk grav2 also labels grid blocks according to their position within the drift. It also adds ^{one} top and ^{one} bottom boundary grid blocks in the mesh, and adds other grid blocks relating to the drift-scale test simulations - the latter are not used in the THC seepage simulations and I removed them from the output files.

ns. 1/14/00
mk grav2 creates
ELEM.new
CONNE.new
files

check/verify results

- gravity vector calculations ns. 1/14/00
- Test problem: pick ^{four} three pairs of adjacent points in the THC Seepage model mesh and calculate the gravity vector data by hand for these points and compare with the output of mk grav2. Results should match the hand-calculated data within the precision of input ^{output} data.

SIGNATURE
READ AND UNDERSTOOD

VIII-7 JSA 3/31/00

DATE 1/14/00
DATE 19

to ut files

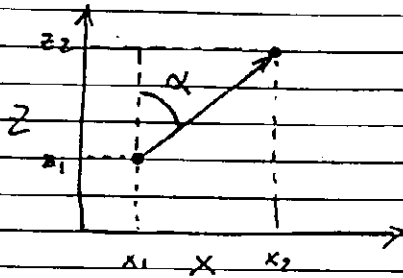
= 1)

sheet
ns.
1/14/00

of
des.
w/ed

60

2



$$\cos(\alpha) = \frac{\text{adjacent side}}{\text{hypot}} = \frac{dz}{\sqrt{(x_2-x_1)^2 + (z_2-z_1)^2}}$$

$\cos(\alpha)$ is the value calculated by `mk_grav2` for input into `TOUGH2`, with convention (see `TOUGH2` user manual) that $g \cdot \cos(\alpha) < 0$ if $z_2 > z_1$ and $g \cdot \cos(\alpha) > 0$ if $z_2 < z_1$ (we use $g = -9.81 \text{ m/s}^2$) so $\cos(\alpha)$ above is positive).

Verifying calculations are shown below:

(from `CONN`.new file)

connection (node to node)	X and Z data from AMESH (elem file) X1 and Z1 for first node; X2 and Z2 for second node as listed				dx=X2-X1 (m)	dz=Z2-Z1 (m)	calculated from above formula cos(alpha)	calculated with mk_grav2 cos(alpha)
	X1 (m)	Z1 (m)	X2 (m)	Z2 (m)				
10 to 325	4.304283E+00	-3.774755E+00	3.631902E+00	-4.425485E+00	-6.723810E-01	-6.507300E-01	-6.95443E-01	-6.954E-01
1069 to 1070	2.025000E+01	-2.800000E+01	2.400000E+01	-2.800000E+01	3.750000E+00	0.000000E+00	0.00000E+00	0.000E+00
739 to 1037	2.400000E+01	1.500000E+00	2.400000E+01	-2.000000E+00	0.000000E+00	-3.500000E+00	-1.00000E+00	-1.000E+00
700 to 820	1.700000E+01	4.280000E+01	2.025000E+01	4.600000E+01	3.250000E+00	3.200000E+00	7.01604E-01	7.016E-01

The last two columns show agreement between computed and hand calculated $\cos(\alpha)$ values.

• output formats and content

By comparing input files `elem` and `conn` with output files `ELEM`.new and `CONN`.new files, I checked that the data read in the input files was correctly output in the output files. The fact that `TOUGH2` reads the data in the `CONN`.new and `ELEM`.new files correctly (i.e. without errors) indicates there are no formatting problems. The top and bottom boundary node data and connections were checked by hand (i.e. check location, large volume for boundary, connection distances and areas by comparing with input data in `conn` file - note: boundary connections are identified in the `conn` file by boundary element names starting with a "*" character).

• check top and bottom boundary grid blocks data and connections

SIGNATURE _____ DATE 1/4 20
 READ AND UNDERSTOOD _____ DATE 1/4 18 00
 VIII-8 9.5# 3/5/100 DATE 19

con't 1/5/99
pr. 1/5/00

The data below, from mk_grav2 output, shows that data for top and bottom boundaries grid nodes and connections are correctly output by mk_grav2. Connection distances and areas are not calculated (distance 1 is set equal to the distance calculated by amesh between each grid block and connected side boundary (in conne file), and distance 2 arbitrarily set to 1×10^{-7}) but I rechecked the data to see if they are consistent with the total model width (40.5 m) and input top & bottom elevations (220.7 & -335.3 m, respectively).

Boundary elements from mk_grav2.f output (from ELEME.new file)

grid node	type	volume (m3)	X (m)	Z (m)
tt001	topbo	1.00E+50	0.00	220.70
bb001	botbo	1.00E+50	0.00	-335.30

checks okay

Boundary connections from mk_grav2.f output (from CONNE.new file)

connection	flag (ISOT)	distance1 (m)	distance2 (m)	area (m2)	cos(alpha)
top	667tt001	3.25E+00	1.0000E-07	4.000E+00	1.00E+00
top	668tt001	3.25E+00	1.0000E-07	4.000E+00	1.00E+00
top	669tt001	3.25E+00	1.0000E-07	3.500E+00	1.00E+00
top	670tt001	3.25E+00	1.0000E-07	2.500E+00	1.00E+00
top	735tt001	3.25E+00	1.0000E-07	4.125E+00	1.00E+00
top	946tt001	3.25E+00	1.0000E-07	5.000E+00	1.00E+00
top	947tt001	3.25E+00	1.0000E-07	5.875E+00	1.00E+00
top	948tt001	3.25E+00	1.0000E-07	5.750E+00	1.00E+00
top	949tt001	3.25E+00	1.0000E-07	5.750E+00	1.00E+00
bottom	1013bb001	2.42E+01	1.0000E-07	1.200E+01	-1.00E+00
bottom	1033bb001	2.42E+01	1.0000E-07	1.080E+01	-1.00E+00
bottom	1107bb001	2.42E+01	1.0000E-07	1.762E+01	-1.00E+00

Input grid block data (from AMESH output file eleme)

grid node	type	volume (m3)	X (m)	Z (m)
667	rock1	2.41E+01	1.20E+01	2.17E+02
668	rock1	2.41E+01	8.00E+00	2.17E+02
669	rock1	2.11E+01	4.00E+00	2.17E+02
670	rock1	1.51E+01	1.00E+00	2.17E+02
735	rock1	2.49E+01	1.60E+01	2.17E+02
946	rock1	2.98E+01	2.03E+01	2.17E+02
947	rock1	3.43E+01	2.60E+01	2.17E+02
948	rock1	3.44E+01	3.20E+01	2.17E+02
949	rock1	3.46E+01	3.75E+01	2.17E+02
1013	rock1	5.40E+02	7.50E+00	-3.11E+02
1033	rock1	4.89E+02	1.65E+01	-3.11E+02
1107	rock1	7.93E+02	2.93E+01	-3.11E+02

Check top and bottom boundary elevation = $Z + (\text{distance1}) \cdot \text{sign}(\cos(\alpha))$

220.7
220.7
220.7
220.7
220.7
220.7
220.7
220.7
220.7
220.7
-335.3
-335.3
-335.3

sum top area >> 4.050E+01
sum bot area >> 4.050E+01

model uniform thickness = 1 m
model top width = (sum top area)/(model thickness) = 40.5 (m)
model bottom width = (sum bot area)/(model thickness) = 40.5 (m)

checks ok

SIGNATURE
READ AND UNDERSTOOD

DATE 1/5/99
19 06

n.s. 45197

- check labeling of "rock" types. This is done visually by comparing the mesh figure on p. 18 with the drift plans on p. 11. On p. 10, grid block centers are plotted with colors and shapes according to their designation assigned by mk-grav2 (note, these ^{assignments} are problem-specific, hard-wired in the code, and may be changed in the future for other designs).

Location of files

• verification files

on hydra/users/raid/nspycher/react/seep-99/grid3/

leme	} input to mk-grav2 (AMESH v1.0 output)
conn	
ELEMF.new	} mk-grav2 output
CONN - new	

- Code (Fortran 77)

on hydra/users/raid/nspycher/react/seep-99/grid-utility
mk-grav2.f

Source listing

Attached in Binder A-1, folder mk-grav2 f

SIGNATURE
READ AND UNDERSTOOD

[Signature]
VIII-10 2011

DATE 1/5/2018 00
DATE 19

```

      program mk_grav
c Version: v1.0
c ns99/6 dont'cutout drift, identify elements in drift
c ns99/7 change model-dependent lengths
c ns99/8 flag in-drift features

c reads eleme and conne after amesh - construction
c converts coordinate system into vertical
c recalculates the gravity cosine
c adds concrete invert
c
c also adds a OPEN DRIFT element, connected to wall or invert
c elements, to allow for gas and liquid flow to leave, not
c for heat
c
      implicit double precision(a-h,o-z)
      parameter (me = 16000)
      parameter (mc = 36000)
      parameter (nh = 1000)
      character*5 id(me)
      character*5 tfeld(me)
      dimension x(3,me),a(mc),voll(me)
      dimension ec(me)
      dimension e(2,mc)
      dimension cc(2,mc)
      dimension hsh(nh)
      dimension ind(me)
      call rmesh
      &(rdrift,ne,id,tfeld,x,ec,e,a,cc,hsh,ind,me,mc,nh,ixyz,voll)
      stop
      end

c
      subroutine rmesh
      &(rdrift,ne,id,tfeld,x,ec,e,a,cc,hsh,ind,me,mc,nh,ixyz,voll)
      implicit double precision(a-h,o-z)
      character*5 id(me)
      character*1 text
      character*5 texte
      character*5 tfeld(me)
      dimension x(3,me),vboun(2,1000)
      dimension a(mc)
      dimension ec(me)
      dimension e(2,mc)
      dimension cc(2,mc)
      dimension hsh(nh)
      dimension ind(me),iboun(1000)
      dimension voll(me)
      dimension zgeol(4)
      character*5 wrd, wrd2
      data zgeol/-156.76,-26.68,14.0,99.39/
      pi=3.141592654

c
c ns99/7/21 change these parameters (xmax and xmin apparently not used)
      xmax=40.5
      xmin=0.0
      ymax=220.7
      ymin=-335.3

c
      open(unit=1,file='eleme',status='old')
      rewind(1)
      read(1,'(a)',end=40) wrd
      if(wrd .ne. 'eleme' .and. wrd .ne. 'ELEM') then
         stop 'no eleme in MESH'
      endif
      open(unit=2,file='ELEM.new',status='unknown')
      rewind(2)
      write(2,'(a)') 'ELEM'

c
      ne = 0
      locat = 1
      index=0
10  read(1,'(a,10x,a,2e10.4,10x,3e13.6)',end=40)
      & id(ne + 1),texte,vol,vl,x1,y1,z1

```

VH-11 JEH 3/31/00

```

x(1,ne+1) = x1
x(2,ne+1) = y1
x(3,ne+1) = z1
if(id(ne+1) .ne. ' ') then
  dl = dsqrt(x1*x1+y1*y1)
c cut-out heater drift
cns99/6      if(dl.lt.2.74) goto 10
c define heater element
  texte='rock '
c ns99/6      if(dl.lt.3.2) texte='wall '
              if(dl.lt.2.95.and(dl.gt.2.75) texte='wall '
              if(dl.lt.2.75.and(dl.ge.2.60) texte='wallx'
c
c ns99/8 flag drift geometries
c   outer zone
  if(dl.lt.2.60) texte='outr '
c   backfill
  ybf=2.250-(2.25-1.)/2.564*x1
  if(y1.le.ybf.and(dl.lt.2.75) then
    texte='dbak '
    if(dl.ge.2.60) texte='wallb'
  endif
c   between waste package and dripshield (inner)
  dl2 = dsqrt(x1*x1 + (y1+0.805)*(y1+0.805))
  if(dl2.le.(1.251)) texte='innr '
  if(x1.lt.1.251.and.y1.gt.(-2.144)
  & .and.y1.lt.-0.805) texte='innr '
c   concrete invert
  angle=atan((y1+0.805)/x1)*180./3.14159
  if(y1.le.(-2.144).and.angle.le.-38..and(dl.lt.2.75) then
    texte='cinv '
    if(dl.ge.2.60) texte='wallc'
  endif
c   waste package
  if(dl2.le.(1.67/2)) texte='wpck '
ccc end ns 99/8
c
c
c   ne=ne+1
c
c   tfeld(ne)=texte
  voll(ne)=vol
c
c   ind(ne) = ne
  if(x1 .ne. 0.0 .or. y1 .ne. 0.0 .or. z1 .ne. 0.0) locat = 0
  goto 10
endif
call hash(id,ind,hsh,ne,nh,ec)
if(locat .ne. 0) then
  do i = 1, ne
    x(1,i) = -999.d0
    x(2,i) = -999.d0
  enddo
  open(unit=2,file='locat',status='old')
  read(2,'(a)',end=50) wrd
  if(wrd .ne. 'locat' .and. wrd .ne. 'LOCAT') then
    stop 'no locat in locat'
  endif
  20 read(2,'(a5,5x,2f20.0)',end=50) wrd, x1, y1
  if(wrd .ne. ' ') then
    nul = ihash(wrd, id,ind,hsh,ne,nh)
    if(nul .eq. 0) then
      goto 20
    endif
    x(1,nul) = x1
    x(2,nul) = y1
    goto 20
  endif
  close(unit=2)
endif
endif
if(ne .ge. me) then
  stop 'Exceeded maximum number of elements'
endif

```

2 VIII-12 JEH 3/31/80

```

nel = 0
ne2 = ne
do while(nel .lt. ne2)
  x1 = x(1,nel+1)
  y1 = x(2,nel+1)
  z1 = x(3,nel+1)
  if(x1 .ne. -999.d0 .or. y1 .ne. -999.d0) then
    if(nel .eq. 0) then
      xhi = x1
      xlo = x1
      yhi = y1
      ylo = y1
      zhi = z1
      zlo = z1
    else
      xhi = max(xhi,x1)
      xlo = min(xlo,x1)
      yhi = max(yhi,y1)
      ylo = min(ylo,y1)
      zhi = max(zhi,z1)
      zlo = min(zlo,z1)
    endif
    nel = nel + 1
  else if(x(1,ne2) .eq. -999.d0 .and. x(2,ne2) .eq. -999.d0) then
    ne2 = ne2 - 1
  else
    wrd = id(nel+1)
    x(1,nel+1) = x(1,ne2)
    x(2,nel+1) = x(2,ne2)
    x(3,nel+1) = x(3,ne2)
    id(nel+1) = id(ne2)
    x(1,ne2) = x1
    x(2,ne2) = y1
    x(3,ne2) = z1
    id(ne2) = wrd
  endif
enddo
if(ixyz .eq. 0) then
  xhi = xhi - xlo
  yhi = yhi - ylo
  zhi = zhi - zlo
  if(zhi .le. min(xhi,yhi)) then
    ixyz = 3
  else if (yhi .le. min(xhi,zhi)) then
    ixyz = 2
  else
    ixyz = 1
  endif
endif
if(ixyz .eq. 2) then
  do i = 1, nel
    x(2,i) = x(3,i)
  enddo
elseif(ixyz .eq. 1) then
  do i = 1, nel
    x(1,i) = x(2,i)
    x(2,i) = x(3,i)
  enddo
endif
call hash(id,ind,hsh,ne,nh,ec)
close(1)
open(unit=1,file='conne',status='unknown')
rewind(1)
read(1,'(a)',end=40) wrd
if(wrd .ne. 'conne' .and. wrd .ne. 'CONNE') then
  stop 'no conne in MESH'
endif
open(unit=3,file='CONNE.new',status='unknown')
rewind(3)
write(3,*)
write(3,'(a)') 'CONNE'
nc = 0
do i = 1, ne

```

VIII-13 JEH 3/31/00

```

        ec(i) = 0
    enddo
    neadd=0
    nboun=0
30  read(1, '(2a,19x,a,4e10.4)', end=40)
    & wrd, wrd2, text, v1, v2, a(nc+1), v3
    if(wrd .ne. ' ' .and. wrd .ne. '+++ ') then
        nc = nc + 1
        nu1 = ihash(wrd, id, ind, hsh, ne, nh)
        nu2 = ihash(wrd2, id, ind, hsh, ne, nh)
        if(nu1 .eq. 0) then
            write(6,60) wrd, nc+1
            if(nu2 .ne. 0) then
                nboun=nboun+1
                iboun(nboun)=nu2
                vboun(1, nboun)=v2
                vboun(2, nboun)=a(nc)
            endif
            goto 30
        else if(nu2 .eq. 0) then
            write(6,60) wrd2, nc+1
            if(nu1 .ne. 0) then
                nboun=nboun+1
                iboun(nboun)=nu1
                vboun(1, nboun)=v1
                vboun(2, nboun)=a(nc)
            endif
            goto 30
        endif
    endif

c
c check for gravity vector change
c
        x1 = x(1, nu1)
        x2 = x(1, nu2)
        y1 = x(3, nu1)
        y2 = x(3, nu2)
        z1 = x(2, nu1)
        z2 = x(2, nu2)
c unity vector for connection
        dx = x2-x1
        dy = y2-y1
        dz = z2-z1
        dl = dsqrt(dx*dx+dy*dy+dz*dz)
c unity vector for gravity
c dc > 0: nu2 above nu1
c dc < 0: nu2 below nu1
        dc = dz/dl

c
        write(3, '(2a,19x,a,4e10.4)')
    & wrd, wrd2, text, v1, v2, a(nc), dc
c
        e(1, nc) = nu1
        e(2, nc) = nu2
        if(nu1 .gt. nel .or. nu2 .gt. nel) goto 30
        cc(1, nc) = ec(nu1)
        cc(2, nc) = ec(nu2)
        ec(nu1) = nc
        ec(nu2) = nc
        goto 30
    endif
c define boundaries
c only one element for top, bottom, alcove, respectively
        ibouna=ne+1
c top boundary
        texte(1:1)='t'
        texte(2:2)='t'
        write(texte(3:3), '(i1)')0
        write(texte(4:4), '(i1)')0
        write(texte(5:5), '(i1)')1
        nu2=ne+1
        id(nu2)=texte
        tfeld(nu2)='topbo'
c
        voll(nu2)= 0.1

```

VIII-14 J2H 3/31/00

```

    voll(nu2) = 1.d50
    x(1,nu2) = 0.0d0
    x(2,nu2) = ymax
    x(3,nu2) = 0.0
c bottom boundary
    texte(1:1)='b'
    texte(2:2)='b'
    write(texte(3:3),'(i1)')0
    write(texte(4:4),'(i1)')0
    write(texte(5:5),'(i1)')1
    nu2=ne+2
    id(nu2)=texte
    tfeld(nu2)='botbo'
    voll(nu2)=1.e50
    x(1,nu2) = 0.0d0
    x(2,nu2) = ymin
    x(3,nu2) = 0.0
c
c open drift boundary
    texte(1:1)='d'
    texte(2:2)='r'
    write(texte(3:3),'(i1)')0
    write(texte(4:4),'(i1)')0
    write(texte(5:5),'(i1)')1
    nu2=ne+3
    id(nu2)=texte
    tfeld(nu2)='drift'
    voll(nu2)= 0.5*2.75*2.75*3.141593
    x(1,nu2) = 0.0
    x(2,nu2) = 0.0
    x(3,nu2) = 0.0
c
    ne=ne+3

c boundary connections
    text='1'
    nel=0
    do i=1,nboun
        nul=iboun(i)
        x1 = x(1,nul)
        y1 = x(2,nul)
        z1 = x(3,nul)
        v1 = vboun(1,i)
        v2 = vboun(2,i)
c
c calculate v3 (gravity vector from geometry)
c
        x2 = 0.0
        y2 = 0.0
c unity vector for connection
        dx = x2-x1
        dy = y2-y1
        dl = dsqrt(dx*dx+dy*dy)
c unity vector for gravity
        dc = dy/dl
        v3=dc
c boundary top
        if(dabs(y1+v1-ymax).lt.0.1)then
c write connection
            write(3,'(2a,19x,a,4e10.4)')
            & id(nul),id(ibouna),text,v1,1.e-7,vboun(2,i),1.0
c boundary bottom
        elseif(dabs(y1-v1-ymin).lt.0.1)then
c write connection
            write(3,'(2a,19x,a,4e10.4)')
            & id(nul),id(ibouna+1),text,v1,1.e-7,vboun(2,i),-1.0
        endif
c
        texte=tfeld(nul)
c wall connection to drift
        x1 = x(1,nul)
        x2 = 0.0
        z1 = x(2,nul)

```

VIII-15 JSH 3/31/00

```

      z2 = 0.0
c unity vector for connection
      dx = x2-x1
      dz = z2-z1
      dl = dsqrt(dx*dx+dz*dz)
c unity vector for gravity
      dc = dz/dl
c write connection drift to first wall element
c (no gravity)
c ns99/6      if(texte.eq.'wall '.and.vboun(2,i).gt.0.55d0)
              if(texte.eq.'wall ')
                & write(3,'(2a,19x,a,4e10.4)')
                & id(nul),id(ibouna+2),text,0.01,0.01,vboun(2,i),dc
c
              x1=x(1,nul)
              y1=x(3,nul)
              z1=x(2,nul)
c
              enddo
444 continue
c
c write initial condition, particularly at top and bottom layer
c
      do i=1,ne+nel
        write(2,'(a,10x,a,2e10.4,10x,3e10.4)')
        & id(i),tfeld(i),voll(i),0.0,x(1,i),0.0,x(2,i)
      enddo
      close(1)
      close(unit=2)
      close(unit=3)
      return
40 stop 'Premature EOF on MESH'
50 stop 'Premature EOF on locat'
60 format(' Unknown element "',a,'" at connection',i5)
end
c
subroutine hash(id,ind,hsh,ne,nh,h)
implicit double precision(a-h,o-z)
character*5 id(ne)
dimension ind(ne)
dimension h(ne)
dimension hsh(nh)
character*5 w1
do j = 1, ne
  w1 = id(j)
  if(w1(4:4) .eq. '0') w1(4:4) = ' '
  n = 0
  do i = 1, 5
    n = n + i * ichar(w1(i:i))
  enddo
  h(j) = mod(n,nh) + 1
enddo
il = 1
do i = 1, nh
  i2 = il
  do j = i2, ne
    k = ind(j)
    if(h(k) .eq. i) then
      h(k) = 0
      ind(j) = ind(il)
      ind(il) = k
      il = il + 1
    endif
  enddo
  hsh(i) = il
enddo
return
end
c
integer function ihash(wrd,id,ind,hsh,ne,nh)
implicit double precision(a-h,o-z)
character*5 id(ne)
dimension ind(ne)

```

VIII-16 JEA 3/31/60

```
dimension hsh(nh)
character*5 wrd, w1, w2
w1 = wrd
if(w1(4:4) .eq. '0') w1(4:4) = ' '
n = 0
do i = 1, 5
  n = n + i * ichar(w1(i:i))
enddo
n = mod(n,nh) + 1
i1 = 1
if(n .gt. 1) i1 = hsh(n - 1)
i2 = hsh(n) - 1
do i = i1, i2
  ihash = ind(i)
  w2 = id(ihash)
  if(w2(4:4) .eq. '0') w2(4:4) = ' '
  if(w1 .eq. w2) then
    if(ihash .gt. ne) ihash = 0
    return
  endif
enddo
ihash = 0
return
end
```

A VIII-17 JE# 3/14/00

**YMP-LBNL
REVIEW RECORD**

1. QA: L
2. Page 1 of 1

3. Originator: N. Spycher
 4. Document Title: 2kgridv1a.for Software Routine/Macro Documentation - Option 1
 5. Document Number: _____ 6. Revision/Mod.: V1.0 7. Draft: NA
 8. Governing Procedure Number: YMP-LBNL-QAP-6.1 9. Revision/Mod: 5/0

REVIEW CRITERIA

10. Standard Review Criteria YMP-LBNL-QIP-6.1, R5, M 0
Technical Review Criteria
(Taken from Attachment 5)
 11. Specific Review Criteria: p-2 (attached)
 Source: AP-51.1 Q, Rev 2, ICN3, sec 5.1.1
 Attached: p 2 and 3 (attached)
 Scientific notebook/data associated with this review as noted on Attachment 3

12. Comment Documentation:
 Comment Sheets
 Review Copy Mark-up

13. YMP-LBNL Project Manager (PM): Gudmundur S. Bodvarsson

14. Reviewer	Org./Discipline	Review Criteria	Reviewer	Org./Discipline	Review Criteria
<u>E. Sonnenthal</u>	<u>LBNL</u>	<u>Technical</u>	_____	_____	_____
_____	_____	_____	_____	_____	_____
_____	_____	_____	_____	_____	_____

VIII-18 JET 3/3/00

COMMENTS DUE: 15. Due Date: <u>2/18/2000</u> 16. Originator/Review Coordinator: <u>N. Spycher</u> Print Name	REVIEW BY: 17. <u>Eric Sonnenthal</u> Print Name 18. <u>Eric Sonnenthal</u> <u>2/10/00</u> Signature Date 19. Mandatory Comments: <input type="checkbox"/> Yes <input checked="" type="checkbox"/> No	CONCURRENCE: 21. Document Draft No: _____ Date: _____ 22. Reviewer: <u>Eric Sonnenthal</u> <u>3/3/00</u> Signature Date 23. PM: <u>[Signature]</u> <u>3/3/00</u> Signature Date
	ORIGINATOR/REVIEW COORDINATOR (After response completed): 20. _____ Print Name/Signature Date	DISPUTE RESOLUTION: (if applicable) 24. PM: _____ Signature Date

YMP-LBNL Software Routine/Macro Documentation—Option 1
AP-SI.1Q, Rev. 2, ICN 2, Software Management

Document once in the technical product, data submittal, or scientific notebook where used and cross-reference thereafter each time it is used in another document.

The star () denotes mandatory items. Other items may want to be considered for documentation as applicable, but if not used, mark N/A.*

1. SOFTWARE ROUTINE IDENTIFICATION

* Routine/macro name and version number:

* Name and version identification of the industry standard software under which the routine/macro was developed (e.g., Excel 97, Sun OS 5.1 FORTRAN 90, etc.):

2. DESCRIPTION AND TESTING

Brief description of purpose or function of routine/macro including the execution environment (can be 1 sentence):

* Page(s) containing a listing of the source code of the routine/macro:

* Page(s) listing the executable or any data files, including test data input and output files:

* Documentation that the routine/macro provides correct results for a specified range of input parameters. Include the range of input parameter values for which results were verified:

Description of test cases and test results. Refer to notebook pages or other documentation. (Showing a short example [1-2 lines] of input and output helps demonstrate correct operation.):

Identification of any limitations on the routine/macro applications or validity:

3. SUPPORTING INFORMATION

* Technical reviewer (according to YMP-LBNL-QIP 6.1) who reviewed work and date:

V111-19 JEH 3/31/00

**YMP-LBNL
 COMMENT SHEET**

QA: L

1. Document Title: 2kgridv1a.for Software Routine/Macro Documentation Qualification		2. Page _____ of _____		
3. Document No.	4. Revision/ Change/Mod: NA	5. Draft NA	6. <input type="checkbox"/> Q <input type="checkbox"/> NQ	
7. Reviewer: <i>Eric Sonnenthal</i>				
8. NO. CODE	9. SECT./PARA/P#	10. COMMENT	11. RESPONSE	12. ACCEPT
		<i>no comments</i>		

V111-21 J24 3/31/00

YMP-LBNL Software Routine/Macro Documentation—Option 1
AP-SI.1Q, Rev. 2, ICN 2, Software Management

Document once in the technical product, data submittal, or scientific notebook where used and cross-reference thereafter each time it is used in another document.

The star (*) denotes mandatory items. Other items may want to be considered for documentation as applicable, but if not used, mark N/A.

1. SOFTWARE ROUTINE IDENTIFICATION

* Routine/macro name and version number:

2kgrid v1a. for v1.0

* Name and version identification of the industry standard software under which the routine/macro was developed (e.g., Excel 97, Sun OS 5.1 FORTRAN 90, etc.):

FORTRAN 90 for PC's MS DOS (under MS Windows)

2. DESCRIPTION AND TESTING

Brief description of purpose or function of routine/macro including the execution environment

(can be 1 sentence): Generates dual-k grid. This is the same software as DKMgenerator v1.0 (STN MOL.1999090.0315) with minor modifications

* Page(s) containing a listing of the source code of the routine/macro:

YMP-LBNL-DSM-NS-1 p.67 (points to source listing)

* Page(s) listing the executable or any data files, including test data input and output files:

YMP-LBNL-DSM-NS-1 p.67

* Documentation that the routine/macro provides correct results for a specified range of input parameters. Include the range of input parameter values for which results were verified:

YMP-LBNL-DSM-NS-1 p.65-67

Also see QA documents for DKMgenerator v1.0 (STN: MOL.1999090.0315)

Description of test cases and test results. Refer to notebook pages or other documentation.

(Showing a short example [1-2 lines] of input and output helps demonstrate correct operation.):

YMP-LBNL-DSM-NS-1 p.65-66

Identification of any limitations on the routine/macro applications or validity:

This software was tested against "Q" code DKMgenerator v1.0 only for the THC Seepage Model grid used for AMR U0110

3. SUPPORTING INFORMATION

* Technical reviewer (according to YMP-LBNL-QIP 6.1) who reviewed work and date:

Eric Sonnenthal 2/10/00

VIII-22 JEH 3/31/00

2/7/00

QA of 2kgridv1a.for

NS 2/7/00

Objective: test/verify this code against DKMgenerator V1.0 (STN: MOL. 199909.0315). The latter is a Q version of 2kgridv1a.for. As mentioned at the bottom of p. 8, 2kgridv1a.for is the same code as the original 2kgridv1a.for provided to me by Yu Shu Wu at LBNL, except of one c'out line. Yu Shu Wu has qualified this code under the name DKMgenerator V1.0 (with some modifications from the original version). The objective here is to ensure that the version I used (2kgridv1a.for) produces the same output as the Q version DKMgenerator V1.0, with the exception of a one character difference in the grid block names.

Description of software

This is a dual-permeability grid generator for the TOUGH2 family of codes. See QA documentation for DKMgenerator V1.0 (MOL. 199909.0315). The version tested here works on a PC (DOS under MS Windows).

Check/verify results

The program is run as described on p. 8 and 9. I ran the same input files as those described on p. 8 and 9 (2kgrid.dat, connec.dat, Framtr.dat for grid3a mesh) with DKMgenerator V1.0 and compared the results with my original output from 2kgridv1a. Except for the grid block names, which differed by one character due to the change made in 2kgridv1a.for, results were identical (see next page)

SIGNATURE _____

READ AND UNDERSTOOD _____

DATE _____

DATE _____

19

19

VIII-23

JEH
5/21/00

output from DKM generator V1.0 (2kgridv1. for

ELEME					
Fa 1	tswF40.5579E-020.1000E+01	2.492	0.000	-1.7470	
Ma 1	tswM40.5523E+000.0000E+00	1.992	0.000	-1.7470	
Fa 2	tswF40.8737E-030.1000E+01	2.643	0.000	-1.8790	
Ma 2	tswM40.8650E-010.0000E+00	2.143	0.000	-1.8790	
Fa 3	tswF40.1054E-020.1000E+01	2.804	0.000	-2.0210	
Ma 3	tswM40.1043E+000.0000E+00	2.304	0.000	-2.0210	
Fa 4	tswF40.1312E-020.1000E+01	2.992	0.000	-2.1860	
Ma 4	tswM40.1299E+000.0000E+00	2.492	0.000	-2.1860	
Fa 5	tswF40.1624E-020.1000E+01	3.207	0.000	-2.3740	
Ma 5	tswM40.1608E+000.0000E+00	2.707	0.000	-2.3740	
Fa 6	tswF40.2033E-020.1000E+01	3.451	0.000	-2.5880	
Ma 6	tswM40.2013E+000.0000E+00	2.951	0.000	-2.5880	

Identical*

output from 2kgridv1a. for

ELEME				
F 1	tswF40.5579E-020.1000E+01	2.492	0.000	-1.7470
M 1	tswM40.5523E+000.0000E+00	1.992	0.000	-1.7470
F 2	tswF40.8737E-030.1000E+01	2.643	0.000	-1.8790
M 2	tswM40.8650E-010.0000E+00	2.143	0.000	-1.8790
F 3	tswF40.1054E-020.1000E+01	2.804	0.000	-2.0210
M 3	tswM40.1043E+000.0000E+00	2.304	0.000	-2.0210
F 4	tswF40.1312E-020.1000E+01	2.992	0.000	-2.1860
M 4	tswM40.1299E+000.0000E+00	2.492	0.000	-2.1860
F 5	tswF40.1624E-020.1000E+01	3.207	0.000	-2.3740
M 5	tswM40.1608E+000.0000E+00	2.707	0.000	-2.3740
F 6	tswF40.2033E-020.1000E+01	3.451	0.000	-2.5880
M 6	tswM40.2013E+000.0000E+00	2.951	0.000	-2.5880

output from DKM generator V1.0 (2kgridv1. for

CONNE				
Fa 1Fa 16	10.1733E+000.1733E+000.2756E+010.7934E+00			1
Ma 1Ma 16	10.1733E+000.1733E+000.2756E+010.7934E+00			
Fa 1Fa316	10.2166E+000.2166E+000.2759E+01-.6954E+00			1
Ma 1Ma316	10.2166E+000.2166E+000.2759E+01-.6954E+00			
Fa 1Fa 2	10.1000E+000.1000E+000.4057E+00-.6593E+00			1
Ma 1Ma 2	10.1000E+000.1000E+000.4057E+00-.6593E+00			
Fa 2Fa 17	10.1864E+000.1864E+000.2079E+000.7934E+00			1
Ma 2Ma 17	10.1864E+000.1864E+000.2079E+000.7934E+00			
Fa 2Fa317	10.2329E+000.2329E+000.2082E+00-.6954E+00			1
Ma 2Ma317	10.2329E+000.2329E+000.2082E+00-.6954E+00			
Fa 2Fa 3	10.1075E+000.1075E+000.4363E+00-.6593E+00			1
Ma 2Ma 3	10.1075E+000.1075E+000.4363E+00-.6593E+00			

Identical*

output from 2kgridv1a. for

CONNE				
F 1F 16	10.1733E+000.1733E+000.2756E+010.7934E+00			1
M 1M 16	10.1733E+000.1733E+000.2756E+010.7934E+00			
F 1F 316	10.2166E+000.2166E+000.2759E+01-.6954E+00			1
M 1M 316	10.2166E+000.2166E+000.2759E+01-.6954E+00			
F 1F 2	10.1000E+000.1000E+000.4057E+00-.6593E+00			1
M 1M 2	10.1000E+000.1000E+000.4057E+00-.6593E+00			
F 2F 17	10.1864E+000.1864E+000.2079E+000.7934E+00			1
M 2M 17	10.1864E+000.1864E+000.2079E+000.7934E+00			
F 2F 317	10.2329E+000.2329E+000.2082E+00-.6954E+00			1
M 2M 317	10.2329E+000.2329E+000.2082E+00-.6954E+00			
F 2F 3	10.1075E+000.1075E+000.4363E+00-.6593E+00			1
M 2M 3	10.1075E+000.1075E+000.4363E+00-.6593E+00			

* The only difference between both codes is

SIGNATURE

READ AND UNDERSTOOD

DATE

19

DATE

19

VIII-24 Jett 3/5/80

1.0 (2kgridv1a) the "a" 's are removed from the grid block names and replaced with a blank.

0.000 -1.7470
0.000 -1.7470
0.000 -1.8790
0.000 -1.8790
0.000 -2.0210
0.000 -2.0210
0.000 -2.1850
0.000 -2.1860
0.000 -2.3740
0.000 -2.3740
0.000 -2.5880
0.000 -2.5880

location of files

Source code and I/O files are on Hydra:

usersraid/nspycher/sect/sep 99/grid3/mk_grid3a/
/dualk_pc_calcs3a/

2KGRIDV1a.for source code (for PC!)
2KGRIDV1a.exe PC executable

0.000 -1.7470
0.000 -1.7470
0.000 -1.8790
0.000 -1.8790
0.000 -2.0210
0.000 -2.0210
0.000 -2.1860
0.000 -2.1860
0.000 -2.3740
0.000 -2.3740
0.000 -2.5880
0.000 -2.5880

2kgrid.dat }
connec.dat } input files (see p. 8 and 9)
Flasmtc.dat }

2kgrid.out summary output info
{ connec.dat output mesh connections
{ eleme.dat output elemgrid blocks

These are in TOUGH2 input format and represent the dual-k mesh.

1.0 (2kgridv1a) DKM generator v1.0 source code and I/O files for the same problem are on my PC (DOE# 6362008)

10.7934E+00 1
10.7934E+00 1
1-.6954E+00 1
1-.6954E+00 1
1-.6593E+00 1
1-.6593E+00 1
10.7934E+00 1
10.7934E+00 1
1-.6954E+00 1
1-.6954E+00 1
1-.6593E+00 1
1-.6593E+00 1

D:\seepage_99\geol_grid\qa_test_dkmgener

2kgridv1a.for } source and executable
2kgridv1a.exe } (for PC).

↑
(same as above)

↓

10.7934E+00 1
10.7934E+00 1
1-.6954E+00 1
1-.6954E+00 1
1-.6593E+00 1
1-.6593E+00 1
10.7934E+00 1
10.7934E+00 1
1-.6954E+00 1
1-.6954E+00 1
1-.6593E+00 1
1-.6593E+00 1

Source listing

Attached in binder A-1, folder 2kgridv1a.for

19
19

SIGNATURE
READ AND UNDERSTOOD

[Signature]
4/14-25 83/1100

DATE 2/7 1999
DATE 19

This utility simply assigns a geologic name to all elements according to their location in the z direction (i.e. looks up contact elevations in the contact3a.dat file and assign the right geologic name. in our case (SW33, SW34 etc.)

9 • Run eos9 v.1.4 (dummy run)

input: ELEMEN.new
 CONNE.new
 FLOW.INP (dummy input file)

output: MESH

This step is only to generate a MESH file in TOUGH2 format we will use the bottom portion of the file (the list of connected element indexes) for the dual-k generator

10 • create input file 2kgrid.dat for dualk generator 2kgrid v1 for ^{n.s. 11/22/99} input into

- 1st record: nel, nconne $\phi = \text{zero}$
- insert element data from elemen-new.dat without ELEMEN header
- insert connection data from MESH file (only down to "+++" record, excluded and without CONNE header)
- edit file to replace "tt" in top boundary element names by "tb"

11 • create connec.dat for input into the dual k generator 2kgrid v1. for

- insert in this file the bottom part of the MESH file that is below the "+++" record

n.s. 11/22/99
 From to show W/D LABEL

run 2kgrid v1a. for a dual-k grid generator
 This is the same PC-only version of 2kgrid v1 for with one line that the code skips inserting letter in

n.s. 11/22/99
 from on my PC (will not work)

SIGNATURE _____
 READ AND UNDERSTOOD _____

DATE ... 2 1999
 DATE ... 19

VIII-26 2/27/100

The second character of the output element identification string.

input: 2kgrid.dat (see above)
 connec.dat (see above)
 Fractmtr.dat

This file contains the fracture/matrix connection data as follows (in columns):

N.S. 11/22/99

elem ID	fract aperture	fract frequency	fract/matr connec.
elem ID	(not used)	1/m	area (m ² /m ³)
ID porosity	↓	↓	↓
(col 1)	(col 2)	(col 3)	(col 4)

This file was provided by Yu Shw WU (LBNL) with fracture porosity, frequency, and connection areas from the calibrated property set DTN: LB 990601233129.001

output: eleme.dat
 conne.dat

13 • create file mesh.dual by appending eleme.dat and conne.dat together. This is the dual-k mesh in TOUGH2 format

14 • edit mesh.dual to put a flag for downstream weighting at the ptn/tsw contact:
 For eos3 or eos9 the flag is ISOT = -2
 For toughreact2.2 the flag is ISOT = -15

!!! Remember to change this flag when switching between eos 3 / eos 9 v1.4 and toughreact2.2 runs !!!

15 • The 2^D mesh is complete (without the drift). This is the mesh used for running steady state conditions. The drift is added later as described on p. 11-18 for simulations of thermal loading or ambient with drift. Total of 2216 grid nodes (without drift)

SIGNATURE _____ DATE 11/22 1999
 READ AND UNDERSTOOD _____ DATE 19

```

c
c to generate dual-permeability grid from ECM or single-porosity grid
c ysw 2/10/97
c to generate 2k grid using new meshes from Pan, ysw 6/4/98
c to generate 2d-2k grid using new meshes from Pan, ysw 11/19/98
c
c 2kgridv1.for: DKMgenerator v1.0
c ns99/7/21 c'out line that puts a character in the element ID
c use lower case for fract/matrix letter and boundaries
c
c
c
c IMPLICIT REAL*8 (A-H,O-Z)
c
c parameter (maxuni=200)
c parameter (maxuni=200, maxcol=9000)
c parameter (nmax=99900)
c parameter (ncmax=999000)
c dimension bapert(maxuni),dspac(maxuni),volf(maxuni)
c dimension bapert(maxuni),dspac(maxuni),volf(maxuni),azcol(maxcol)
c dimension afm_v(maxuni)
c dimension d(10), vol(nmax)
c dimension ifmcol(nmax)
c character*3 elecol(maxcol)
COMMON/elem/eleme(nmax),rock(nmax)
COMMON/CORD2/delz(nmax),nzunit(10)
COMMON/CORD3/del1(ncmax),del2(ncmax),area(ncmax),beta(ncmax)
COMMON/CORD4/next1(ncmax),next2(ncmax),iunit(nmax),ifmnc(nmax)
COMMON/CORD5/iso(ncmax)
c character*5 eleme
c character*5 rock, rockf, rockm
c character*5 rock, rocks, rockf, rockm
c character*5 ell,el2
CHARACTER FRACT*1,MATRX*1,EL3*3
CHARACTER FRACT*1,MATRX*1,EL3*3, EL0*2
c 1 EM0*2, EM3*3
CHARACTER*5 ELEM(nmax)
CHARACTER*5 ELEMo(nmax),urock(maxuni)
CHARACTER*5 ELEMf(nmax),ELEMm(nmax)
CHARACTER*3 col(nmax), col_o
CHARACTER*2 s2,e2,s21,e21
c CHARACTER*2 s2,e2,s21,e21, sk
CHARACTER*1 m1, m21
CHARACTER*5 fm1,fm2
c
c character laya*1
c character lay*2,laya*1, layc*1
c dimension laya(82)
c dimension laya(62)
c dimension lay(28),laya(52),layc(28)
c
c data lay /'11','12','13'
c & , '21','22','23','24','25'
c & , '31','32','33','34'
c & , '41','42','43'
c & , '51','52','53'
c & , '61','62','63','64','65'
c & , '71','72','73','74','75'/
c
c data laya/ 'a','b','c','d','e','f','g','h','i',
c & 'j','k','l','m','n','o','p','q','r',
c & 's','t','u','v','w','x','y','z','A','B',
c & 'C','D','E','F','G','H','I','J','K','L',
c & 'M','N','O','P','Q','R','S','T','U','V',
c & 'W','X','Y','Z',
c & '!', '@', '#', '$', '%', '^', '&', '*', '(', ')',
c & '-', '_', '=', '+', '[', '{', '}', '\', '|',
c & ':', ';', ':', '<', '>', '/', '?', '-'/
cc data layc/ 'a','b','c',
cc & 'd','e','f','g','h','i',
cc & 'j','k','l','m','n','o','p','q','r',
cc & 's','t','u','v','w','x','y','z','A','Z'/

```

y VIII-28 Jeth 3/3/10

```

c
c
c
c
c
OPEN(UNIT=14,FILE='2kgrid.dat',FORM='FORMATTED',STATUS='OLD')
OPEN(UNIT=24,FILE='connec.dat',FORM='FORMATTED',STATUS='OLD')
OPEN(UNIT=16,FILE='2kgrid.out',FORM='FORMATTED',STATUS='UNKNOWN')
OPEN(UNIT=17,FILE='eleme.dat',FORM='FORMATTED',STATUS='UNKNOWN')
OPEN(UNIT=27,FILE='conne.dat',FORM='FORMATTED',STATUS='UNKNOWN')
open(unit=44,file='framtr.dat',form='formatted',status='unknown')

c
DATA FRACT  //F//
DATA MATRX  //M//

c
READ(14,*) nmesh, nconn,if2phi
c
READ(14,*) nmesh, nconn, ifref, if2phi
read(44,*) ifdim, nunit, fact_fv, fact_fau, fact_zv, fact_vv
1
, fact_tv

c
c
c
i2phi=0 no double-porosity grid for fault nodes
c
i2phi=1 use double-porosity grid for fault nodes
c
do i=1, nunit
  read(44,144) urock(i),volf(i),bapert(i),dspac(i),afm_v(i)
c6
  read(44,144) urock(i),volf(i),bapert(i),dspac(i)
  dspac(i)=1./dspac(i)
  enddo
144 format(a5,5x,4(E10.3))
cc
do i=1, ntcoll
cc
  READ(44,420) EL0,EL3,EM0,EM3,ISOT,D1,D2,AREAX,BETAX
cc
  azcol(i)=areax
cc
  elecol(i)=EL3
cc
  enddo
READ(24,421) (next1(i),next2(i), i=1, nconn)
421 format(8(2i5))

c
c
c
  ifdim = 1, for 1d, vertical, uniform, parallel fracture networks.
c
  nunit= total # of hydrogeologic units, currently = 4, TCn, PTn, TSw, and CHn
c
  ntcoll= total # of vertical rock columns
c
  volf(i) = fracture volume fraction or porosity for unit i
c
  bapert(i) = fracture aperture for unit i
c
  dspac(i) = fracture spacing for unit i
c
  afm_v(i) = fracture/matrix interface area per unit volume of rock (m**2/m**3)
c
  afactor = f-m interface area reduction factor for unit i
c
  azcol(j) = horizontal cross area for column j
c
  elecol(j) = last three characters of column element j
c
               which has area of azcol(j).
c
  nmesh = total # of gridblocks
c
  nconn = total # of connections
c
c
420 FORMAT(2(A2,A3),15X,I5,4E10.4)
c
c
c
c
c
c
c
  READ(14,*) nmesh,nconn
  write(16,*) ' total number of meshes = ', nmesh
  write(16,*) ' total number of connections = ', nconn
19 FORMAT(A2,a1,A2, i5,5x, A5,E10.4,E10.4,10X,4f10.4)
c
c
  ka=0
  col_o='jjj'

c
  WRITE(17,210)
210 FORMAT('ELEME')
212 FORMAT(' ')
213 FORMAT('CONNE')

c
c
do n=1,nmesh

```

7 VIII-29 JEA 3/3/00

```

READ(14,19) s2,m1,e2, nm, rock(n),VOLX,AHTX,X,Y,Z
sk=s2
ELEM(n)=s2//m1//e2
ELEM0(n)=elem(n)
ELEMf(n)=elem(n)
ELEMm(n)=elem(n)
c rocks=rock(n)
if(elem(n)(1:2).eq.'tb') then
  ELEM(n)(1:2)='tp'
  ELEM0(n)(1:2)='tp'
  ELEMf(n)(1:2)='tp'
  ELEMm(n)(1:2)='tp'
  rock(n)='topbd'
  ifminc(n)=0
elseif(elem(n)(1:2).eq.'bb') then
  ELEM(n)(1:2)='bt'
  ELEM0(n)(1:2)='bt'
  ELEMf(n)(1:2)='bt'
  ELEMm(n)(1:2)='bt'
  rock(n)='botbd'
  ifminc(n)=0
elseif(elem(n)(1:2).eq.'??') then
  ELEM(n)(1:2)='RP'
  ELEM0(n)(1:2)='RP'
  ELEMf(n)(1:2)='RP'
  ELEMm(n)(1:2)='RP'
c rock(n)='repos'
  ifminc(n)=0
else
  ifminc(n)=1
endif

c
c ifminc=0 no minc for top and bottom elements
c ifminc=1 minc 2-k for TCw, PTn, TSw, CHc and CHz, and all non top or bot nodes
c ifminc=2 minc 2-phi fault nodes
c
c
c COL(n)=m1//e2
c vol(n)=volx
c iunit(n)=0
c
c
c
c if(ifminc(n).eq.0) goto 404
  ifmcol(n)=0
c ifmcol(n)=0 using F/M starting eleme names
c ifmcol(n)=1 using f/m starting eleme names
c ifmcol(n)=2 using A/B starting eleme names
c ifmcol(n)=3 using C/D starting eleme names
  if(col_o.ne.elem0(n)(3:5)) ka=0
  col_o=elem0(n)(3:5)
  ka=ka+1
  if(ka.le.82) then
    s2(2:2)=laya(ka)
  elseif(ka.gt.82.and.ka.le.164) then
    ifmcol(n)=1
    s2(2:2)=laya(ka-82)
  elseif(ka.gt.164.and.ka.le.246) then
    ifmcol(n)=2
    s2(2:2)=laya(ka-164)
  elseif(ka.gt.246.and.ka.le.328) then
    ifmcol(n)=3
    s2(2:2)=laya(ka-246)
  endif
ccns99/7/21      ELEM(n)(2:2)=s2(2:2)
c
c goto 303
c enddo
c
c ELEM(n)=s2//m1//e2
c
c ifault=0

```

7 VIII-30 1st 3/31/00

```

rockf=rock(n)
rockm=rock(n)
if(rock(n)(4:5).eq.'bo')
1   or.rock(n)(4:5).eq.'fl'
1   or.rock(n)(4:5).eq.'ol'
1   or.rock(n)(4:5).eq.'dr'
1   or.rock(n)(4:5).eq.'du'
1   or.rock(n)(4:5).eq.'gh'
1   or.rock(n)(4:5).eq.'Gh'
1   or.rock(n)(4:5).eq.'im'
1   or.rock(n)(4:5).eq.'pa'
1   or.rock(n)(4:5).eq.'se'
1   or.rock(n)(4:5).eq.'so'
1   or.rock(n)(4:5).eq.'sp'
1   or.rock(n)(4:5).eq.'su'
1   or.rock(n)(4:5).eq.'to') then
c
c fault blocks
c if use bouuble-porosity grid for faults
c
    if(if2phi.eq.0) then
        ifminc(n)=1
    elseif(if2phi.eq.1) then
        ifminc(n)=2
    endif
c
    if(rock(n)(1:3).eq.'tcw') then
        goto 202
    elseif(rock(n)(1:3).eq.'ptn') then
        goto 202
    elseif(rock(n)(1:3).eq.'tsw') then
        goto 202
    else
c change fault rock names in CHn to unified name
        rock(n)(1:3)='chn'
    endif
    rockf=rock(n)
    rockm=rock(n)
c
202    continue
c
c setup dual-permeability rock names
c
    if(rock(n)(4:5).eq.'bo') then
        rockf(4:4)=FRACT
        rockf(5:5)='b'
        rockm(4:4)=MATRX
        rockm(5:5)='b'
        ifault=1
    elseif(rock(n)(4:5).eq.'fl') then
        rockf(4:4)=FRACT
        rockf(5:5)='f'
        rockm(4:4)=MATRX
        rockm(5:5)='f'
        ifault=1
    elseif(rock(n)(4:5).eq.'ol') then
        rockf(4:4)=FRACT
        rockf(5:5)='f'
        rockm(4:4)=MATRX
        rockm(5:5)='f'
        ifault=1
    elseif(rock(n)(4:5).eq.'dr') then
        rockf(4:4)=FRACT
        rockf(5:5)='d'
        rockm(4:4)=MATRX
        rockm(5:5)='d'
        ifault=1
    elseif(rock(n)(4:5).eq.'du') then
        rockf(4:4)=FRACT
        rockf(5:5)='u'
        rockm(4:4)=MATRX
        rockm(5:5)='u'
        ifault=1

```

AVIII-31 JSH 3/31/00

```

elseif(rock(n)(4:5).eq.'gh') then
  rockf(4:4)=FRACT
  rockf(5:5)='g'
  rockm(4:4)=MATRX
  rockm(5:5)='g'
  ifault=1
elseif(rock(n)(4:5).eq.'im') then
  rockf(4:4)=FRACT
  rockf(5:5)='i'
  rockm(4:4)=MATRX
  rockm(5:5)='i'
  ifault=1
elseif(rock(n)(4:5).eq.'pa') then
  rockf(4:4)=FRACT
  rockf(5:5)='p'
  rockm(4:4)=MATRX
  rockm(5:5)='p'
  ifault=1
elseif(rock(n)(4:5).eq.'se') then
  rockf(4:4)=FRACT
  rockf(5:5)='e'
  rockm(4:4)=MATRX
  rockm(5:5)='e'
  ifault=1
elseif(rock(n)(4:5).eq.'so') then
  rockf(4:4)=FRACT
  rockf(5:5)='s'
  rockm(4:4)=MATRX
  rockm(5:5)='s'
  ifault=1
elseif(rock(n)(4:5).eq.'sp') then
  rockf(4:4)=FRACT
  rockf(5:5)='l'
  rockm(4:4)=MATRX
  rockm(5:5)='l'
  ifault=1
elseif(rock(n)(4:5).eq.'su') then
  rockf(4:4)=FRACT
  rockf(5:5)='n'
  rockm(4:4)=MATRX
  rockm(5:5)='n'
  ifault=1
elseif(rock(n)(4:5).eq.'to') then
  rockf(4:4)=FRACT
  rockf(5:5)='o'
  rockm(4:4)=MATRX
  rockm(5:5)='o'
  ifault=1
endif

c
c uniform properties for all faults
c
  rockf(4:4)=FRACT
  rockf(5:5)='f'
  rockm(4:4)=MATRX
  rockm(5:5)='f'
  ifault=1

  else
c non-fault blocks
c
  if(rock(n)(4:5).eq.'vi') then
c vi for vitric unit
    rockf(4:4)=FRACT
    rockf(5:5)='v'
    rockm(4:4)=MATRX
    rockm(5:5)='v'
  elseif(rock(n)(4:5).eq.'Ze') then
c
c ze for zeolitic
    rockf(4:4)=FRACT
    rockf(5:5)='z'
    rockm(4:4)=MATRX

```

p. VIII-32 p. 44 3/31/00

```

      rockm(5:5)='z'
      elseif(rock(n)(4:5).eq.'tr') then
c   tr for transitional zone between v and z
      rockf(4:4)=FRACT
      rockf(5:5)='t'
      rockm(4:4)=MATRX
      rockm(5:5)='t'
      elseif(rock(n)(1:3).eq.'ch6') then
      rockf(4:4)=FRACT
      rockf(5:5)='z'
      rockm(4:4)=MATRX
      rockm(5:5)='z'
      elseif(rock(n)(1:3).eq.'pp1') then
      rockf(4:4)=FRACT
      rockf(5:5)='z'
      rockm(4:4)=MATRX
      rockm(5:5)='z'
      elseif(rock(n)(1:3).eq.'pp2'.or.rock(n)(1:3).eq.'pp3') then
      rockf(4:4)=FRACT
      rockf(5:5)='d'
      rockm(4:4)=MATRX
      rockm(5:5)='d'
      elseif(rock(n)(1:3).eq.'pp4') then
      rockf(4:4)=FRACT
      rockf(5:5)='z'
      rockm(4:4)=MATRX
      rockm(5:5)='z'
      elseif(rock(n)(1:3).eq.'bf2') then
      rockf(4:4)=FRACT
      rockf(5:5)='z'
      rockm(4:4)=MATRX
      rockm(5:5)='z'
      elseif(rock(n)(1:3).eq.'bf3') then
      rockf(4:4)=FRACT
      rockf(5:5)='d'
      rockm(4:4)=MATRX
      rockm(5:5)='d'
c   elseif(rock(n)(1:3).eq.'tr3'.or.rock(n)(1:3).eq.'tr2') then
      elseif(rock(n)(1:3).eq.'tr2') then
      rockf(4:4)=FRACT
      rockf(5:5)='z'
c   rockf(5:5)='v'
      rockm(4:4)=MATRX
      rockm(5:5)='z'
c   rockm(5:5)='v'
      elseif(rock(n)(1:3).eq.'tr3') then
      rockf(4:4)=FRACT
      rockf(5:5)='d'
c   rockf(5:5)='v'
      rockm(4:4)=MATRX
      rockm(5:5)='d'
c   rockm(5:5)='v'
      else
c   for non CHn rocks
      rockf(4:4)=FRACT
      rockm(4:4)=MATRX
      endif
      endif
c
c
      if(ifminc(n).gt.0) then
      do i=1, nunit
      if(rock(n).eq.urock(i)) then
      iunit(n)=i
      goto 304
      endif
      enddo
      write(16,321) rock(n), n
      stop
      endif
304   continue
321   format (//,'no rock card is defined for ',A5, ' n =', i5//)
c

```

f VIII-33 JSH 3/31/00

```

c
c
c for unit fracture volume fractions
c here increase Vf by a factorv for steady-state run only
c
c
404 continue
if(ifminc(n).eq.0) then
  WRITE(17,7) elem(n), rock(n), vol(n), AHTX,X,Y,Z
else
  iun=iunit(n)
  vfact=fact_fv
  Vf=VOLf(iun)*VOLX
  Vm=(1.-VOLf(iun))*VOLX
  s2(1:1)=FRACT
cc  rockf=rock(n)
cc  rockm=rock(n)
c   elemf(n)=s2//m1//e2
c   elemf(n)=elem(n)
  if(ifmcol(n).eq.0) then
    elemf(n)(1:1)=FRACT
  elseif(ifmcol(n).eq.1) then
    elemf(n)(1:1)='f'
  elseif(ifmcol(n).eq.2) then
    elemf(n)(1:1)='A'
  elseif(ifmcol(n).eq.3) then
    elemf(n)(1:1)='C'
  endif
  ahtx=1.0d0
  xfd=0.5d0
  WRITE(17,7) elemf(n), rockf,Vf*vfact,AHTX,X+xfd,Y,Z
c  WRITE(17,7) s2,m1,e2, rockf,Vf*vfact,AHTX,X+xfd,Y,Z
c  WRITE(17,7) s2,m1,e2, rockf,Vf*vfact,AHTX,X,Y,Z
c  delz(n)=x
c  s2(1:1)=MATRX
c  elemm(n)=s2//m1//e2
c  elemm(n)=elem(n)
  if(ifmcol(n).eq.0) then
    elemm(n)(1:1)=MATRX
  elseif(ifmcol(n).eq.1) then
    elemm(n)(1:1)='m'
  elseif(ifmcol(n).eq.2) then
    elemm(n)(1:1)='B'
  elseif(ifmcol(n).eq.3) then
    elemm(n)(1:1)='D'
  endif
  ahtx=0.0d0
c
c for zeolites v=v*fact_zv
c for vitric units v=v*fact_vv
c
  zfact=1.0d0
  if(rockm(5:5).eq.'z') then
    zfact=fact_zv
  elseif(rockm(5:5).eq.'v') then
    zfact=fact_vv
  elseif(rockm(5:5).eq.'t') then
    zfact=fact_tv
  elseif(ifault.eq.1) then
    zfact=fact_fau
  endif
  WRITE(17,7) elemm(n), rockm,Vm*zfact,AHTX,X,Y,Z
c  WRITE(17,7) s2,m1,e2, rockm,Vm*zfact,AHTX,X,Y,Z
endif
c
  WRITE(16,77) elemf(n), elemm(n), ifminc(n), elemo(n)
7  FORMAT(A5, 10X,a5,2E10.4,10X,f10.3,f10.3,f10.4)
c 7  FORMAT(A2,a1,A2,10X,a5,2E10.4,10X,f10.3,f10.3,f10.4)
77  FORMAT(A5,10X,a5,10X,'ifminc=', i4, 5x, a5)
  enddo
c
  WRITE(17,212)
  WRITE(27,213)

```

7 VIII-34 JEH 3/31/00

```

C
C
C*****READ CONNECTION DATA.*****
C
      icon_ff=1
      icon_fm=2
      icon_nm=0
      do n =1 , nconn
        READ(14,20) s2,m1,e2,s21,m21,e21,ISOT,D1,D2,AREAX,BETAX
        area(n)=areax
        iso(n)=isot
20      FORMAT(2(a2,a1,a2),15X,I5,4E10.4)
C
C-----GENERATE GLOBAL FRACTURE CONNECTION DATA.
c      f-f & m-m connections for all both minc blocks
c      fracture (MINC)- non minc blocks (fault, PTN, top and bottom bc's)
c      between non minc blocks, kept the same (fault, PTN, top and bottom bc's)
c
      n1=next1(n)
      n2=next2(n)
      if(ifminc(n1).gt.0.and.ifminc(n2).gt.0) then
        if(ifminc(n1).eq.1.and.ifminc(n2).eq.1) then
c for 2-k
          WRITE(27,115) elemf(n1),elemf(n2),ISOT,D1,D2,AREAX,BETAX
            1      , icon_ff
          WRITE(27,115) elemm(n1),elemm(n2),ISOT,D1,D2,AREAX,BETAX
          elseif(ifminc(n1).eq.1.and.ifminc(n2).eq.2) then1
c for 2k-2phi
          WRITE(27,115) elemf(n1),elemf(n2),ISOT,D1,D2,AREAX,BETAX
            1      , icon_ff
          elseif(ifminc(n1).eq.2.and.ifminc(n2).eq.1) then
c for 2k-2phi
          WRITE(27,115) elemf(n1),elemf(n2),ISOT,D1,D2,AREAX,BETAX
            1      , icon_ff
          elseif(ifminc(n1).eq.2.and.ifminc(n2).eq.2) then
c for 2phi-2phi
          WRITE(27,115) elemf(n1),elemf(n2),ISOT,D1,D2,AREAX,BETAX
            1      , icon_ff
          endif
c
          elseif(ifminc(n1).gt.0.and.ifminc(n2).eq.0) then
            if(ifminc(n1).eq.1) then
c for 2k-ecm
              WRITE(27,115) elemf(n1),elem(n2),ISOT,D1,D2,AREAX,BETAX
              WRITE(27,115) elemm(n1),elem(n2),ISOT,D1,D2,AREAX,BETAX
              elseif(ifminc(n1).eq.2) then
c for 2phi-ecm
                WRITE(27,115) elemf(n1),elem(n2),ISOT,D1,D2,AREAX,BETAX
                endif
                elseif(ifminc(n1).eq.0.and.ifminc(n2).gt.0) then
                  if(ifminc(n2).eq.1) then
c for 2k-ecm
                    WRITE(27,115) elem(n1), elemf(n2),ISOT,D1,D2,AREAX,BETAX
                    WRITE(27,115) elem(n1), elemm(n2),ISOT,D1,D2,AREAX,BETAX
                    elseif(ifminc(n2).eq.2) then
c for 2phi-ecm
                      WRITE(27,115) elem(n1), elemf(n2),ISOT,D1,D2,AREAX,BETAX
                      endif
                      else
                        WRITE(27,115) elem(n1),elem(n2) , ISOT,D1,D2,AREAX,BETAX
                      endif
                    115 FORMAT(2(a5),15X,I5,4E10.4,i5)
c 105 FORMAT(a5, a2,a1,a2,15X,I5,4E10.4)
c 125 FORMAT(a2,a1,a2,a5,15X,I5,4E10.4)
c 135 FORMAT(2(a2,a1,a2),15X,I5,4E10.4)
                    enddo
C
C-----COME HERE FOR MATRIX-FRACTURE FLOW CONNECTIONS.
c
c      iun=1
c      do n=1,nmesh

```

VIII-35 JCH 3/31/00

```

      if(ifminc(n).eq.0) goto 3391
      iun=iunit(n)
      volx=vol(n)
      apertur=bapert(iun)
      spacing=dspac(iun)
      EL3=COL(n)
      az_max=0.0d0
cc      if(ifref.eq.0) then
c for non-local refinements at repository
cc      do k=1,ntcol
cc          if(elecol(k).eq.EL3) then
cc              thickb=volx/azcol(k)
cc              areaz=azcol(k)
cc              goto 3351
cc          endif
cc      enddo
cc      elseif(ifref.eq.1) then
c for local refinements at repository
cc      do k=1,nconn
cc          n1=next1(k)
cc          n2=next2(k)
cc          isox=iso(k)
cc          if(isox.eq.3) then
cc              if(n.eq.n1.or.n.eq.n2) then
c select largest vertical connection areas
cc                  if(area(k).gt.az_max) az_max=area(k)
cc              endif
cc          endif
cc      enddo
cc      areaz=az_max
cc      thickb=volx/areaz
c
cc      endif
c3351 continue
      d(1)=0.0
cc      alsq=sqrt(areaz)
      if(ifdim.eq.1) then
cc          d(2)=spacing/6.0
cc          xigma=alsq/spacing
cc          aunit=2.*alsq*thickb
      elseif(ifdim.eq.2) then
cc          d(2)=spacing/8.0
cc          xigma=areaz/(spacing*spacing)
cc          aunit=4.*(spacing-apertur)*thickb
      elseif(ifdim.eq.3) then
cc          d(2)=spacing/10.0
cc          xigma=volx/spacing**3.0
cc          aunit=6.0*(spacing-apertur)**2.0
      endif
c
c
c
      factora=1.0d0
      AREAX=volx*afm_v(iun)
cc      AREAX=xigma*aunit*factora
      fm1=elemf(n)
      fm2=elemm(n)
      WRITE(27,103) fm1, fm2, D(1), D(2), AREAX, icon_fm
      3391 continue
      enddo
c 102 FORMAT(2(A5),18X,'-9',3E10.4,10x,i5)
c 103 FORMAT(2(A5),18X,'-9',3E10.4,10x,i5)
      103 FORMAT(2(A5),17X,'-10',3E10.4,10x,i5)
c
      WRITE(27,212)
c
c      write(16,*) 'new x = x + d2'
c      write(16,1115) (delz(n),n=1,nmesh)
c1115 FORMAT(f10.3)
c
      STOP
      END

```

✓ V111-36 104 3/21/00

```

      if(ifminc(n).eq.0) goto 3391
      iun=iunit(n)
      volx=vol(n)
      apertur=bapert(iun)
      spacing=dspac(iun)
      EL3=COL(n)
      az_max=0.0d0
cc     if(ifref.eq.0) then
c for non-local refinements at repository
cc     do k=1,ntcol
cc       if(elecol(k).eq.EL3) then
cc         thickb=volx/azcol(k)
cc         areaz=azcol(k)
cc         goto 3351
cc       endif
cc     enddo
cc     elseif(ifref.eq.1) then
c for local refinements at repository
cc     do k=1,nconn
cc       n1=next1(k)
cc       n2=next2(k)
cc       isox=iso(k)
cc       if(isox.eq.3) then
cc         if(n.eq.n1.or.n.eq.n2) then
c select largest vertical connection areas
cc           if(area(k).gt.az_max) az_max=area(k)
cc         endif
cc       endif
cc     enddo
cc     areaz=az_max
cc     thickb=volx/areaz
c
cc     endif
c3351 continue
      d(1)=0.0
cc     alsq=sqrt(areaz)
      if(ifdim.eq.1) then
cc       d(2)=spacing/6.0
cc       xigma=alsq/spacing
cc       aunit=2.*alsq*thickb
      elseif(ifdim.eq.2) then
cc       d(2)=spacing/8.0
cc       xigma=areaz/(spacing*spacing)
cc       aunit=4.*(spacing-apertur)*thickb
      elseif(ifdim.eq.3) then
cc       d(2)=spacing/10.0
cc       xigma=volx/spacing**3.0
cc       aunit=6.0*(spacing-apertur)**2.0
      endif
c
c
c
      factora=1.0d0
      AREAX=volx*afm_v(iun)
cc     AREAX=xigma*aunit*factora
      fm1=elemf(n)
      fm2=elemm(n)
      WRITE(27,103) fm1, fm2, D(1), D(2), AREAX, icon_fm
      3391 continue
    enddo
c 102 FORMAT(2(A5),18X,'-9',3E10.4,10x,i5)
c 103 FORMAT(2(A5),18X,'-9',3E10.4,10x,i5)
      103 FORMAT(2(A5),17X,'-10',3E10.4,10x,i5)
c
      WRITE(27,212)
c
c write(16,*) 'new x = x + d2'
c write(16,1115) (delz(n),n=1,nmesh)
c1115 FORMAT(f10.3)
c
      STOP
      END

```

✓ Vlll-36 104 3/31/00

YMP-LBNL REVIEW RECORD

1. QA: L
2. Page 1 of 1

3. Originator: N. Spycher

4. Document Title: sav1d_dst2d v1.0 Software Routine/Macro Documentation - Option 1

5. Document Number: _____ 6. Revision/Mod.: V1.0 7. Draft: NA

8. Governing Procedure Number: YMP-LBNL-QAP-6.1 9. Revision/Mod: 5/0

REVIEW CRITERIA

10. Standard Review Criteria YMP-LBNL-QIP-6.1, R5, M 0
Technical Review Criteria
 (Taken from Attachment 5)

11. Specific Review Criteria: AP-SI. 1 Q, Rev. 2, I, CN 3
 Source: _____
 Attached: p 2 & 3
 Scientific notebook/data associated with this review as noted on Attachment 3

12. Comment Documentation:
 Comment Sheets
 Review Copy Mark-up

13. YMP-LBNL Project Manager (PM): Gudmundur S. Bodvarsson

14. Reviewer	Org./Discipline	Review Criteria	Reviewer	Org./Discipline	Review Criteria
<u>E. Sonnenthal</u>	<u>LBNL</u>	<u>Technical</u>	_____	_____	_____
_____	_____	_____	_____	_____	_____
_____	_____	_____	_____	_____	_____

VIII-37 JEH 3/31/00

<p>COMMENTS DUE:</p> <p>15. Due Date: <u>2/18/2000</u></p> <p>16. Originator/Review Coordinator: <u>N. Spycher</u> Print Name</p>	<p>REVIEW BY:</p> <p>17. <u>Eric Sonnenthal</u> Print Name</p> <p>18. <u>Eric Sonnenthal</u> <u>2/10/00</u> Signature Date</p> <p>19. Mandatory Comments: <input type="checkbox"/> Yes <input checked="" type="checkbox"/> No</p> <p>ORIGINATOR/REVIEW COORDINATOR (After response completed):</p> <p>20. _____ Print Name/Signature Date</p>	<p>CONCURRENCE:</p> <p>21. Document Draft No: _____ Date: _____</p> <p>22. Reviewer: <u>Eric Sonnenthal</u> <u>3/3/00</u> Signature Date</p> <p>23. PM: <u>[Signature]</u> <u>3/5/00</u> Signature Date</p> <p>DISPUTE RESOLUTION: (if applicable)</p> <p>24. PM: _____ Signature Date</p>
---	---	--

YMP-LBNL Software Routine/Macro Documentation—Option 1
AP-SI.1Q, Rev. 2, ICN 2, Software Management

Document once in the technical product, data submittal, or scientific notebook where used and cross-reference thereafter each time it is used in another document.

The star () denotes mandatory items. Other items may want to be considered for documentation as applicable, but if not used, mark N/A.*

1. SOFTWARE ROUTINE IDENTIFICATION

* Routine/macro name and version number:

~~S~~

* Name and version identification of the industry standard software under which the routine/macro was developed (e.g., Excel 97, Sun OS 5.1 FORTRAN 90, etc.):

2. DESCRIPTION AND TESTING

Brief description of purpose or function of routine/macro including the execution environment (can be 1 sentence):

* Page(s) containing a listing of the source code of the routine/macro:

* Page(s) listing the executable or any data files, including test data input and output files:

* Documentation that the routine/macro provides correct results for a specified range of input parameters. Include the range of input parameter values for which results were verified:

Description of test cases and test results. Refer to notebook pages or other documentation. (Showing a short example [1-2 lines] of input and output helps demonstrate correct operation.):

Identification of any limitations on the routine/macro applications or validity:

3. SUPPORTING INFORMATION

* Technical reviewer (according to YMP-LBNL-QIP 6.1) who reviewed work and date:

VIII-38 JEH 3/31/00

**YMP-LBNL
 COMMENT SHEET**

QA: L

1. Document Title: sav1d_dst2d v1.0 Software Routine/Macro Documentation Qualification		2. Page _____ of _____		
3. Document No.	4. Revision/ Change/Mod: NA	5. Draft NA	6. <input type="checkbox"/> Q <input type="checkbox"/> NQ	
7. Reviewer: Eric Sonnenthal				
8. NO. CODE	9. SECT./PARA./P#	10. COMMENT	11. RESPONSE	12. ACCEPT
		No comment		

VIII-40 per 3/31/00

YMP-LBNL Software Routine/Macro Documentation—Option 1
AP-SI.1Q, Rev. 2, ICN 2, Software Management

Document once in the technical product, data submittal, or scientific notebook where used and cross-reference thereafter each time it is used in another document.

The star (*) denotes mandatory items. Other items may want to be considered for documentation as applicable, but if not used, mark N/A.

1. SOFTWARE ROUTINE IDENTIFICATION

* Routine/macro name and version number:

save1d_dst2d v1.0

* Name and version identification of the industry standard software under which the routine/macro was developed (e.g., Excel 97, Sun OS 5.1 FORTRAN 90, etc.):

Fortran 77 (under Unix Sun OS Solaris)

2. DESCRIPTION AND TESTING

Brief description of purpose or function of routine/macro including the execution environment (can be 1 sentence):

creates an INCON file (for TOUGH2 input) for a 2-D mesh from existing INCON and MESH data for a 1-D column

* Page(s) containing a listing of the source code of the routine/macro:

YMP-LBNL-DSM-NS-1 p. 70-71

* Page(s) listing the executable or any data files, including test data input and output files:

YMP-LBNL-DSM-NS-1 p. 70

* Documentation that the routine/macro provides correct results for a specified range of input parameters. Include the range of input parameter values for which results were verified:

YMP-LBNL-DSM-NS-1 p. 69, 68

Description of test cases and test results. Refer to notebook pages or other documentation.

(Showing a short example [1-2 lines] of input and output helps demonstrate correct operation.):

YMP-LBNL-DSM-NS-1 p. 68-69

Identification of any limitations on the routine/macro applications or validity:

Input data must be for a 1-D vertical column, output data for a 2-D vertical section. The 2-D incon data is assigned based on nearest point in 1-D column

3. SUPPORTING INFORMATION

* Technical reviewer (according to YMP-LBNL-QIP 6.1) who reviewed work and date:

Eric Sonnenthal 2/10/00

VIII-41 JEH 3/31/00

2/8/00

QA of utility saved_dst2d.f v1.0

Objective: test/verify this utility program.
It was used by E. Sonnenhual in AMR Uallo to prepare INCON files for DST simulations.

Description of software

This routine reads the MESH and SAVE files output from TOUGH2 simulation for a one-dimensional (vertical 1-D column) mesh, and create an INCON file for a vertical 2-D section using "initial condition" properties from the 1-D column located at the nearest elevation from the ^{N.S. 2/8/00} location points in the 2-D section. It also converts the point elevations of the 1-D column from true elevations to It assumes z coordinates in the 1-D vertical column are true elevations above msl, while z coordinates in the 2-D vertical section are with respect to an origin located at 1047.71 m above msl (center of the heater drift of the Draft Scale Test).

check/verify results

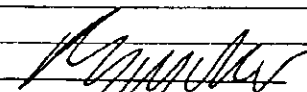
This was done by running the routine and verifying by hand that initial conditions properties for the 2-D section are assigned the values of the points nearest in elevations in the 1-D column, as described ble below.

Input files: MESH 1-D mesh
SAVE incon properties for 1-D mesh
MESH 2D.dual 2-D mesh

output file INCON_2D.dual

^{N.S. 2/8/00}
Verify Verifying procedure as follows:

SIGNATURE _____
READ AND UNDERSTOOD _____


VIII-42 JET 3/31/00

DATE 2/8 187000
DATE 19 _____

- Use Excel to sort original 1-D column 2 data in MESH in ascending order
arbitrarily p. 5 2/18/00 to hand check
- Pick up n points n in 2-D mesh (see below)
- Pick up n ^{corresponding} points at nearest elevation in the 1-D mesh and verify that the incos data for these points was correctly assigned to the points of the 2-D mesh (see below)

Spreadsheet summarizing "hand check" of utility code sav1d_dst2.d
N. Spycher 2/7/00

Points arbitrarily selected in 2-D mesh file							
ELEME	type	vol	other	x	y	z	
fb001	fbou	1.00E+50	0.00E+00	0.00	0.00	-156.80	
mb001	mbou	1.00E+50	0.00E+00	0.00	0.00	-156.80	
f 970	tsw35	2.04E+00	0.00E+00	-54.00	0.00	-75.00	
m 970	msw35	1.84E+02	0.00E+00	-54.00	0.00	-75.00	
f 895	tsw34	1.56E-01	0.00E+00	-18.00	0.00	-20.00	
m 895	msw34	1.55E+01	0.00E+00	-18.00	0.00	-20.00	
f1971	tsw34	3.85E-02	0.00E+00	-14.91	0.00	7.07	
m1971	msw34	3.81E+00	0.00E+00	-14.91	0.00	7.07	
f 619	tsw33	2.98E+00	0.00E+00	81.50	0.00	84.19	
m 619	msw33	4.49E+02	0.00E+00	81.50	0.00	84.19	
ft001	fbou	1.00E+50	0.00E+00	0.00	0.00	99.39	
mt001	mbou	1.00E+50	0.00E+00	0.00	0.00	99.39	

Corresponding points in input 1-D mesh (at nearest z)							
ELEME	other	vol	dumm	x	y	z	z-1047.71
F5211	tswF6	4.37E-02	1.00E+00	0.50	0.00	889.50	-158.21
M5211	tswM6	2.87E+00	0.00E+00	0.00	0.00	889.50	-158.21
F4203	tswF5	3.48E-02	1.00E+00	0.50	0.00	973.60	-74.11
M4203	tswM5	3.13E+00	0.00E+00	0.00	0.00	973.60	-74.11
F3403	tswF4	3.05E-02	1.00E+00	0.50	0.00	1027.00	-20.71
M3403	tswM4	3.02E+00	0.00E+00	0.00	0.00	1027.00	-20.71
F3412	tswF4	3.05E-02	1.00E+00	0.50	0.00	1054.00	6.29
M3412	tswM4	3.02E+00	0.00E+00	0.00	0.00	1054.00	6.29
F3324	tswF3	2.01E-02	1.00E+00	0.50	0.00	1133.00	85.29
M3324	tswM3	3.03E+00	0.00E+00	0.00	0.00	1133.00	85.29
F3328	tswF3	2.01E-02	1.00E+00	0.50	0.00	1146.00	98.29
M3328	tswM3	3.03E+00	0.00E+00	0.00	0.00	1146.00	98.29

INCON data for above points (from output file INCON_2D.dual)	
These match the 1-D data from SAVE (2nd record of data blocks)	
fb001	0.90371918257980E+050.10979533373430E+020.28903689991140E+02
mb001	0.90371938581910E+050.10118078764840E+020.28903689983000E+02
f 970	0.89528138439380E+050.10980440833820E+020.27239548427760E+02
m 970	0.89528138429300E+050.10142255127450E+020.27239548433900E+02
f 895	0.88996380616760E+050.10972377179820E+020.26219665160550E+02
m 895	0.88996380298840E+050.10068032492330E+020.26219665162750E+02
f1971	0.88721742379880E+050.10972277996340E+020.25771170222800E+02
m1971	0.88721742358320E+050.10053264929490E+020.25771170225020E+02
f 619	0.87929238652200E+050.10976070096890E+020.23859207147790E+02
m 619	0.87929238408970E+050.10207505857720E+020.23859207235030E+02
ft001	0.87807381000770E+050.10976032948200E+020.23556987198180E+02
mt001	0.87807726208190E+050.10207050840800E+020.23556987407360E+02

INCON data for above points (input from input file SAVE)	
F5211	0.99000000E+00 0.99080000E-12 0.99080000E-12 0.99080000E-12
M5211	0.9037191825798E+05 0.1097953337343E+02 0.2890368999114E+02
F4203	0.99000000E+00 0.12880000E-11 0.12880000E-11 0.12880000E-11
M4203	0.8952813843938E+05 0.1098044083382E+02 0.2723954842776E+02
F3403	0.99000000E+00 0.27570000E-12 0.27570000E-12 0.27570000E-12
M3403	0.8899638061676E+05 0.1097237717982E+02 0.2621966516055E+02
F3412	0.99000000E+00 0.27570000E-12 0.27570000E-12 0.27570000E-12
M3412	0.8872174237988E+05 0.1097227799634E+02 0.2577117022280E+02
F3324	0.99000000E+00 0.54950000E-12 0.54950000E-12 0.54950000E-12
M3324	0.8792923865220E+05 0.1097607009689E+02 0.2385920714779E+02
F3328	0.99000000E+00 0.54950000E-12 0.54950000E-12 0.54950000E-12
M3328	0.8780738100077E+05 0.1097603294820E+02 0.2355698719818E+02

Perfect match, thus verified

SIGNATURE _____
READ AND UNDERSTOOD _____

DATE _____ 19 ____
DATE _____ 19 ____

VIII-43 2/24 3/21/00

Location of files

On Hydra:

usersraid/nspycher/grid-progs/sav1d_dst2d/

sav1d_dst2d.f	source code
sav1d_dst2d	executable (Sun Sparc Solaris)

MESH input

SAVE input

MESH_2D.dual input

INCON_2D.dual output

verify.xls spreadsheet for verification (see p.6)

Source code listing

```

c      program sav1d_dst2d
c      program reads 1D.dual INCON and MESH files and generates a 2D INCON file

      character*5  text1,text2
      character*80 text
      real*8       vol,aht,x1,x2,zcol(400),press(400),
&sat(400),temp(400),x3,dmin,dmin1,lsat,gsat

      open(unit=1,file="MESH",
&status="unknown")
      open(unit=2,file="SAVE",
&status="unknown")
      open(unit=3,file="MESH_2D.dual",
&status="unknown")
      open(unit=4,file="INCON_2D.dual",
&status="unknown")
      i=1
      read(1,'(a)')

1     read(1,'(a,10x,a,2e10.4,10x,3e10.4)')
&text1,text2,vol,aht,x1,x2,zcol(i)
      zcol(i)=zcol(i)-1047.71d0
      if(text1.eq.'BT001') go to 2
      i=i+1
      go to 1
2     close(unit=1)
      itot = i
      read(2,'(a)') text
      write(*,*) itot
      do j =1,itot
c         read(2,'(a)') text1
c         write(*,'(a)') text1
c         read(2,'(3(1x,e19.13))')
&press(j),sat(j),temp(j)
c         write(*,'(5(1x,e19.13))')
c         &press(j),sat(j),temp(j),lsat,lsat
      enddo

```

SIGNATURE

READ AND UNDERSTOOD

DATE

19

DATE

19

VIII-44 JET 3/31/00

```

write(4,'(a)') 'INCON'
read(3,'(a)')
3 read(3,'(a,10x,a,2e10.4,10x,3e10.4)')
&text1,text2,vol,aht,x1,x2,x3
if(text1.eq.' ') go to 8
write(4,'(a)') text1

dmin = 1.d30
do k = 1,itot
  dmin1 = dabs(x3-zcol(k))
  if(dmin1.lt.dmin) then
    kmin = k
    dmin = dmin1
c   write(*,*) dmin,kmin
  endif
enddo
c   write(*,*) kmin,zcol(kmin),text1
c   if(text1(2:2).eq.'i'.or.text1(2:2).eq.'I') go to 7
   if(text1(1:2).eq.'dr'.or.text1(1:2).eq.'od'.or.
&text1(1:2).eq.'al') go to 6
   if(text2(1:1).eq.'f') then
     write(4,'(3e20.14)') press(kmin),sat(kmin),temp(kmin)
   else
     write(4,'(3e20.14)') press(kmin+1),sat(kmin+1),
&temp(kmin+1)
   endif
   go to 3
6   write(4,'(3e20.14)') press(kmin),0.97761d0,temp(kmin)
   go to 3
c 7   write(4,'(3e20.14)') press(kmin),sat(kmin),temp(kmin)
c   go to 3
8   stop
end

```

SIGNATURE _____
 READ AND UNDERSTOOD _____

DATE 2/9 192000
 DATE _____ 19 _____

VIII-45 184 3/31/00

**YMP-LBNL
 REVIEW RECORD**

1. QA: L ^{DM 2/7/00}
 2. Page 1 of 3

3. Originator: N. Spycher
 4. Document Title: mrgdrift v1.0 Software Routine/Macro Documentation - Option 1
 5. Document Number: _____ 6. Revision/Mod.: V1.0 7. Draft: NA
 8. Governing Procedure Number: YMP-LBNL-QAP-6.1 9. Revision/Mod: 5/0

REVIEW CRITERIA

10. Standard Review Criteria YMP-LBNL-QIP-6.1, R5, M 0
Technical Review Criteria
 (Taken from Attachment 5)
 11. Specific Review Criteria:
 Source: _____
 Attached: YMP-LBNL Software Routine/Macro Documentation - Option 1
 Scientific notebook/data associated with this review as noted on Attachment 3
 12. Comment Documentation:
 Comment Sheets
 Review Copy Mark-up
 13. YMP-LBNL Project Manager (PM): Gudmundur S. Bodvarsson
 14. Reviewer Org./Discipline Review Criteria Reviewer Org./Discipline Review Criteria
E. Sannenthal LBNL Technical _____ _____ _____
 _____ _____ _____
 _____ _____ _____

VIII-46 GET 3/3/00

COMMENTS DUE: 15. Due Date: <u>2/18/2000</u> 16. Originator/Review Coordinator: <u>N. Spycher</u> Print Name	REVIEW BY: 17. <u>Eric Sannenthal</u> Print Name 18. <u>Eric Sannenthal</u> <u>2/7/00</u> Signature Date 19. Mandatory Comments: <input checked="" type="checkbox"/> Yes <input type="checkbox"/> No	CONCURRENCE: ^{DM 2/7/00} 21. Document Draft No: <u>NA</u> Date: <u>2/7/00</u> 22. Reviewer: <u>E. Sannenthal</u> <u>2/7/00</u> Signature Date 23. PM: <u>[Signature]</u> <u>3/3/00</u> Signature Date
	ORIGINATOR/REVIEW COORDINATOR (After response completed): 20. <u>[Signature]</u> <u>2/7/00</u> Print Name/Signature Date	DISPUTE RESOLUTION: (if applicable) 24. PM: _____ Signature Date

**YMP-LBNL
 COMMENT SHEET**

QA: L

1. Document Title: mrgdrift v1.0 Software Routine/Macro Documentation Qualification		2. Page <u>1</u> of <u>1</u>		
3. Document No. YMP-LBNL-DSM-NS-1	4. Revision/ Change/Mod: NA	5. Draft NA	6. <input checked="" type="checkbox"/> Q <input type="checkbox"/> NQ	
7. Reviewer: <i>Eric Sonnenthal</i> <i>Eric Sonnenthal</i>				
8. NO. CODE	9. SECT./PARA./P#	10. COMMENT	11. RESPONSE	12. ACCEPT
1. M	1.	designate platform, e.g. Solaris, MS windows, etc	done that	<i>ES.</i> 2/7/00

VIII-47 gen 3/21/00

YMP-LBNL Software Routine/Macro Documentation—Option 1
AP-SI.1Q, Rev. 2, ICN 1, Software Management

Document once in the technical product, data submittal, or scientific notebook where used and cross-reference thereafter each time it is used in another document.

The star (*) denotes mandatory items. Other items may want to be considered for documentation as applicable, but if not used, mark N/A.

1. SOFTWARE ROUTINE IDENTIFICATION

* Routine/macro name and version number:

mrqdrift.f v1.0

* Name and version identification of the industry standard software under which the routine/macro was developed (e.g., Excel 97, Sun OS 5.1 FORTRAN 90, etc.):

FORTRAN 77/90

*platforms: { PC DOS (under MS Windows)
Digital Fortran Compiler / MS Visual Fortran 5.5
(same code works on both) { Sun Ultra Sparc Solaris SUNOS 5.5
Sun f77 4.0 compiler*

2. DESCRIPTION AND TESTING

Brief description of purpose or function of routine/macro including the execution environment (can be 1 sentence):

Merges the geologic mesh with the drift mesh for Yucca Mountain TOUGH2 and TOUGHREACT simulations

* Page(s) containing a listing of the source code of the routine/macro:

Binder A-1, folder "mrqdrift.f", attached to notebook YMP-LBNL-DSM-NS-1

* Page(s) listing the executable or any data files, including test data input and output files:

YMP-LBNL-DSM-NS-1 p. 60

* Documentation that the routine/macro provides correct results for a specified range of input parameters. Include the range of input parameter values for which results were verified:

YMP-LBNL-DSM-NS-1 p. 57-60

Description of test cases and test results. Refer to notebook pages or other documentation. (Showing a short example [1-2 lines] of input and output helps demonstrate correct operation.):

YMP-LBNL-DSM-NS-1 p. 57-60

YMP-LBNL-DSM-NS-1 p. 16-17

Identification of any limitations on the routine/macro applications or validity:

The meshes to merge must have a specific format described at the top of the source code listing.

3. SUPPORTING INFORMATION

* Technical reviewer (according to YMP-LBNL-QIP 6.1) who reviewed work and date:

Eric Sonnenthal 2/7/00

VIII-49 JEH 3/31/00

NS-45600

1/5/2000 QA of mrgdrift.f utility programs v1.0

Objective: test/verify mrgdrift.f v1.0

Description of software

This is a Fortran 77 utility used to merge the geologic mesh and drift mesh for the TIC seepage model simulations (p 16-17)

check/verify results

This routine does not calculate any data per say but "weeds" out rock nodes at the drift location in the geologic mesh and replaces them with drift nodes, thus merging drift and rock around it. The things to check to make sure this utility works properly include:

- correct identification/selection of nodes at the drift wall ^{and at other locations} in both meshes (geologic & drift)
- correct connections between drift and rock
- make sure ^{original} mesh data are unchanged except at the drift wall
- make sure the original rock nodes at the drift location are weeded out of the final (merged) mesh; same for original waste nodes

• Identification and selection of nodes at the drift wall and around the waste package. This was verified by the following procedure:

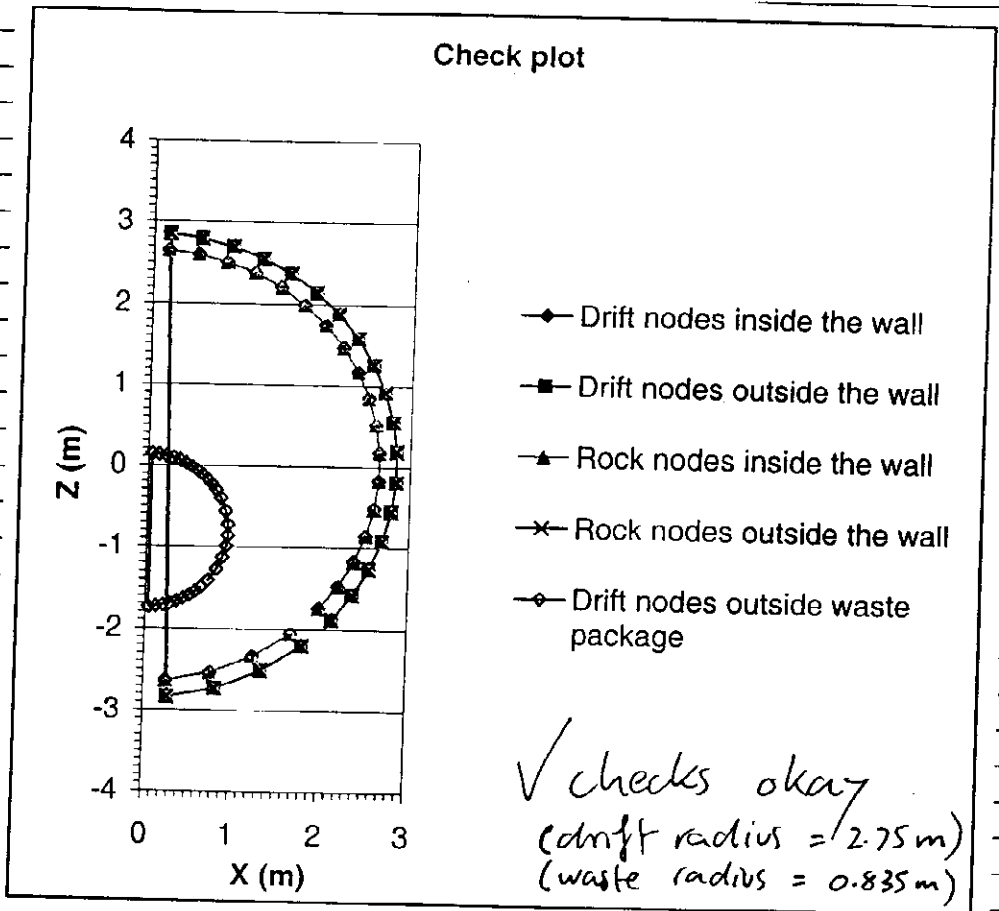
- 1) take a list of nodes identified in the mrgdrift.out file (e.g. nodes ^{selected as these} in the geologic mesh outside/at the drift wall location)
- 2) use this list of nodes to "grep" ^{data from} for those nodes (x, y, z etc) ^{from NS-45600} out of the original mesh files (mesh.dual for the geologic mesh and mesh.dr2.dat for the drift mesh)
- 3) use the "grep" d data (x and z in this case) to plot the location of each point using excel, and visually verify that the selected points fall where they are supposed to be (e.g. directly outside the drift wall)
- 4) repeat 1,2,3 above for other lists of selected nodes

SIGNATURE
READ AND UNDERSTOOD

DATE 1/5 2000
DATE 19

VIII-30 12/31/00

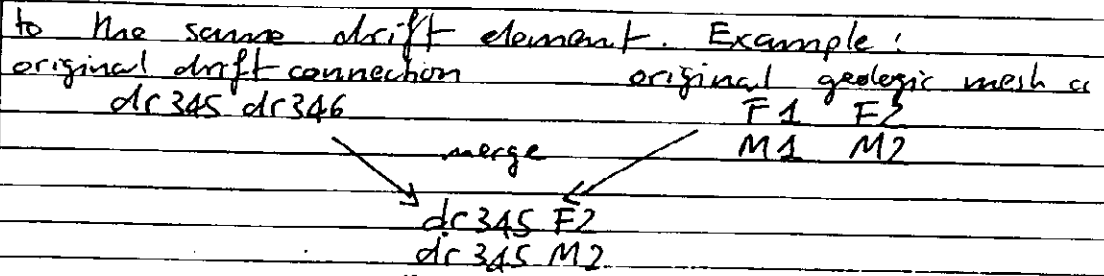
(e.g. nodes at wall inside drift around the waste package), and show all points on one graph for visual check, as shown below



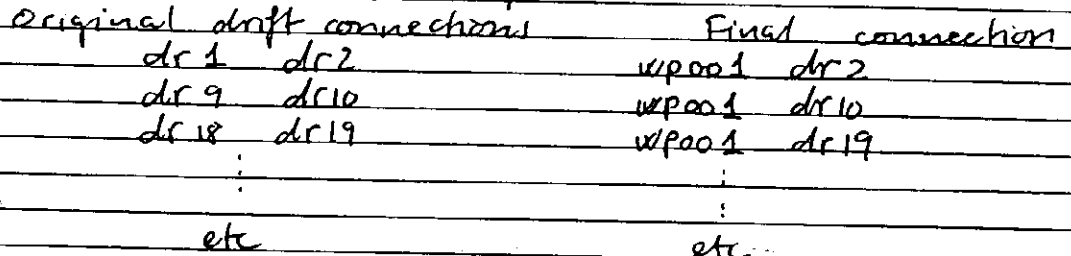
• check correct connections between rocks and drift
 This was done by ^{hand} comparing the lists of connections
 output in the mergedrift.out file (geologic connection
 at wall) and drift connection at wall) with
 the rock-drift connections and waste-inner
 connections output in the mesh file for the
 merged rock & drift data (mesh.out). Note: the
 connection distances, areas, and gravity vector
 are not changed from the original data for
 drift wall connections; simply, the name of the
 geologic mesh element inside the drift is switched
 with the name of the drift mesh element at
 that location, and the connection is repeated
 for fractures and matrix at the same location (i.e.
 both fractures and matrix outside the drift connect

as
 15100
 and
 drift
 waste-
 inner
 connection

SIGNATURE _____ DATE 1/5 19 2000
 READ AND UNDERSTOOD _____ DATE 3/31/05 19



(visually) (weeded out dr 346 and F1 and M1)
 This was checked to be done correctly. For the waste package, original "pie" elements in the waste package are replaced with one waste element. Example:



This was visually checked to be done correctly ("weeded out dr 1, dr 9, dr 18... etc")

- check waste package element volume
 r waste package = 0.235 m (p. 11)
 model thickness $b = 1$ m
 Volume = half package because we use $\frac{1}{2}$ drift
 $V = 0.5 \pi r^2 b = 1.095 \text{ m}^3$
 This value matches the one output in mesh.out

1/6/00
 bit
 ion

- Ensure original mesh data are unchanged except at drift wall and waste package element. This was done ^{N.S. 1/6/00} by ^{N.S. 1/6/00} comparing the original mesh files (mesh.dual and mesh.dat) with the output mesh file (mesh.out) using the compare file command of my text editor (Nexpad - the compare file command works like the "diff" unix command (To do this I had to remove some extra zeros and blanks in the files to be compared in order to outline only differences that may be indicative of a problem).

- Ensure ^{original} drift mesh nodes outside the drift and geologic mesh nodes inside the drift, and drift mesh nodes inside waste package are weeded out of the final mesh. This was checked by running

SIGNATURE _____ DATE 1/6 19 2000
 READ AND UNDERSTOOD _____ DATE 3/31/00 19

VIII-52 #2# 3/31/00

"diffs" as for previous comparisons (previous items on p. _____)

- overall check: the fact that simulation plots (see AMR 00110) show node centers at correct locations further ensures mrgdrift.f works correctly

N0120/00110 ps. 2/10/00

Location of files

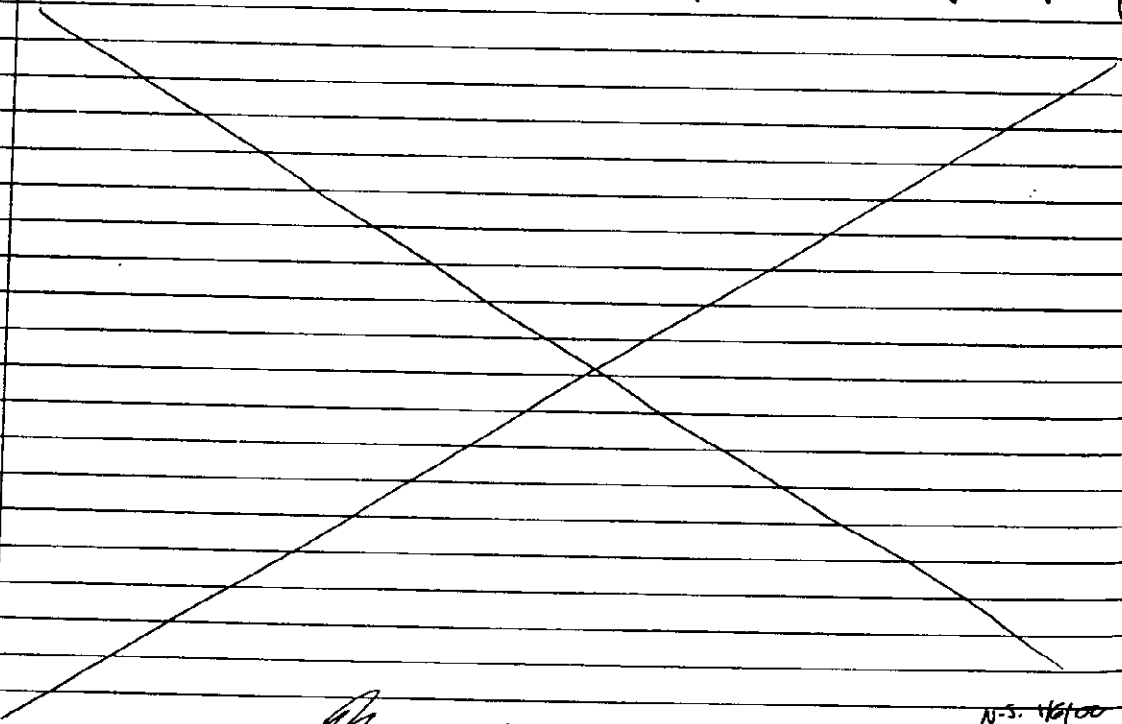
Excel spreadsheets that helped in the checking are in `by area/users/and/react/seep_99/check-mrgdrift/check_node_connection/check_node_selection`

Input and output files are also in this folder:

input	{ mesh.dual	original geologic mesh on
	{ mesh.dr2.dat	" drift mesh only
output	{ mesh.out	final "merged" mesh
	{ mrgdrift.out	list of nodes and connections for info only.

Source Listing

Attached in binder A-1, folder mrgdrift.f



SIGNATURE [Signature] DATE 1/6/00
 READ AND UNDERSTOOD [Signature] DATE 18/00

VIII-53 3/31/00 19

N-5. 16/00

on p. 13. This was only done for a few points, a few fell on (or very close to) the boundaries lines separating the zones.

9. Plotted the mesh with tecplot to verify the gridling and assignment of nodes. This was done in two steps:
- run sec2tec.f to convert segmt file to tecplot-format file
 - run zone.el.f to create tecplot-format file with grid block center coordinates and designat (i.e. dbak, innr... etc.) read from the ELEM new file.

M. J. Under

cont 11/24

Merging the geologic mesh and drift mesh

Both meshes were merged using a utility called mrgdrift.f. This utility reads both meshes and replaces the "pie-shaped" elements in the geologic mesh (at the location of the drift) with the drift mesh. The following are comments from the source code:

```

c Both meshes MUST have drift wall contact areas that exactly overlap for
c each grid block at wall contact locations, so that connections do not
c need to be modified (no recalulation of area and gravity angle).
c What the program does:
c - reads the geologic dual-k mesh, which must include "pie"-shaped
c elements at the location of the drift
c - reads the inner-drift single-K mesh, which must include elements
c at the drift wall which align exactly with the "pie"-shaped elements
c of the geologic mesh. Must also include at least one row of elements
c outside the drift too.
c - replace the pie elements with the inner-drift elements at the drift wall
c - take out the pie elements at the waste package location and replace
c the waste package by one circular element
c - adjust all connections accordingly, with very small connection from
c the inside of waste package to its surface
  
```

Input:

- mesh_geo.dat (default name)
This is the geologic mesh file (p. 6-10) in TOUGH2 format (e.g. mesh.dual on p. 6)
- mesh_dr.dat
This is the drift mesh file (p. 11-15) in TOUGH2 format (e.g. mesh_dr2.dat on p. 15)

SIGNATURE _____

READ AND UNDERSTOOD _____

DATE 11/24 19 99

DATE _____ 19 _____

VIII-54 JEH 3/31/00

other run-specific input data relating to the meshes to be merged:

2.75	!drad	drift radius
0.2	!sizout1	width of 1st row of gridblocks outside, in geol mesh
0.05	!sizin1	width of 1st row of gridblocks inside, in geol mesh
0.2	!sizout2	width of 1st row of gridblocks outside, in drift mesh
0.20	!sizin2	width of 1st row of gridblocks inside, in drift mesh
0.15	!sizinn2	width of 2nd row of gridblocks inside, in drift mesh
0.835	!wprad	waste package radius
0.2	!sizwp	width of 1st row of gridblocks against waste package
-0.805	!zoffs	Z offset between drift center and waste package center

The program uses these data to sort through the nodes of both input meshes, to weed out unwanted grid blocks, and to create drift-geologic mesh connections.

Output:

- mesh.out (default name)
This is the ^{N.S. 11/23/99} merged meshes that will be used for the ITC seepage model. See figure next page.

- mrgdrift.out
This is a file summarizing the names of grid nodes at the drift wall and new connections for checking purposes.

The final mesh (next page) was checked by plotting and examining the rock-drift connections to make sure both meshes were merged correctly. Note: a segment file of the merged meshes was done by merging the segment files of the individual meshes after weeding out overlapping points (using excel and sorting the data).

Note: The grid nodes coordinates in the mesh files are not used by TOUGH2 and TOUGHREACT. The coordinates are there for plotting purposes. The dual-k grid generator (e.g. step 12 on p.8) offsets the x coordinates of all the fracture nodes by ± 0.5 m in the mesh files, which created problems when plotting drift and fracture nodes.

SIGNATURE

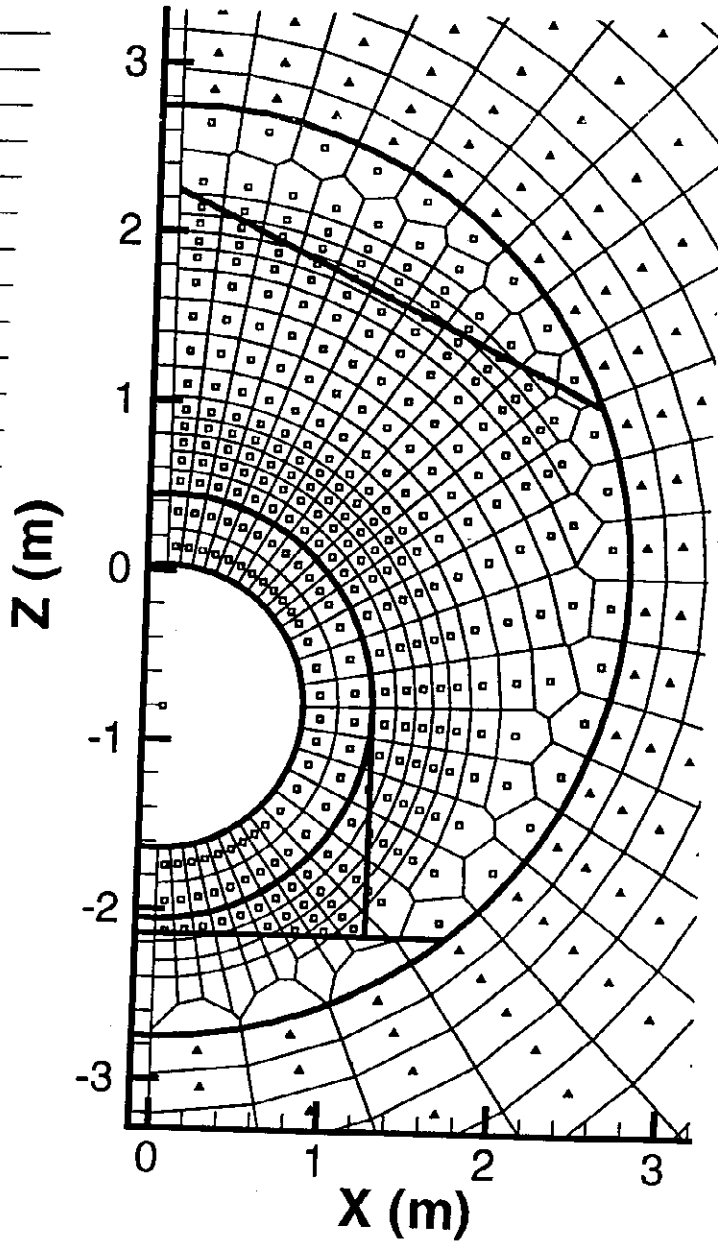
READ AND UNDERSTOOD

DATE 11/24 19 99

DATE 19

VIII-55 JEH 3/31/00

Final mesh for THC seepage model, in the vicinity of the drift.



△ TSW34

□ light blue
outer zone

□ blue-purple
backfill

□ green
inner zone

□ yellow
invert

center (1 node)
is waste pack

NS-424/99

data (i.e. they were offset by 0.5 m). So, I reset the x coordinates of fractures from the mesh out file to a value identical to the x coordinates of matrix nodes, for the final MESH file used for the THC Seepage Model (I did this with excel).

SIGNATURE _____

READ AND UNDERSTOOD _____

DATE 4/24 19 99

DATE _____ 19 _____

VIII-56 JEH 3/31/00

```

program mrgdrift
c   Version V1.0
c*** Program to merge single-k inner-drift mesh with dual-k surrounding grid
c   N.Spycher August 1999
c
c   Both meshes MUST have drift wall contact areas that exactly overlap for
c   each grid block at wall contact locations, so that connections do not
c   need to be modified (no recalculatation of area and gravity angle).
c   What the program does:
c   - reads the geologic dual-k mesh, which must include "pie"-shaped
c     elements at the location of the drift
c   - reads the inner-drift single-K mesh, which must include elements
c     at the drift wall which align exactly with the "pie"-shaped elements
c     of the geologic mesh. Must also include at least one row of elements
c     outside the drift too.
c   - replace the pie elements with the inner-drift elements at the drift wall
c   - take out the pie elements at the waste package location and replace
c     the waste package by one circular element
c   - adjust all connections accordingly, with very small connection from
c     the inside of waste package to its surface
c
c   Pointers to mesh elements and connections:
c
c     idin1(i)  i=1,nin1    indexes of elements in geologic mesh abutting wall inside
c     idout1(i) i=1,nout1   indexes of elements in geologic mesh abutting wall outside
c
c     idin2(i)  i=1,nin2    indexes of elements in drift mesh abutting wall inside
c     idout2(i) i=1,nout2   indexes of elements in drift mesh abutting wall outside
c     idinn2(i) i=1,ninn2   indexes of elements in drift mesh 2nd row inside
c     iwp(i)    i=1,nwp     indexes of elements in waste package
c     iwpo(i)   i=1,nwpo    indexes of elements abutting waste package
c
c     idcon1(i) i=1,nncon1  indexes of connections across wall in geologic mesh
c     idcon2(i) i=1,nncon2  indexes of connections across wall in drift mesh
c     idcon2a(i) i=1,nncon2a indexes of connections from wall to 2nd row inward in drift mesh
c     idcon2b(i) i=1,nncon2b indexes of connections from waste pack to around it
c
c     iloc1(i) i=1,nncon1  =1 if first element in connection (geol mesh) is overlapping
c     iloc2(i) i=1,nncon1  =1 if first element in connection (drift mesh) is overlapping
c     iloc2a(i) i=1,nncon1 =1 if first element in connection (drift mesh) is overlapping
c
c     icnel1(i,n) i=1,nel1 n=1,ncnel1(i)  connections for each element (geol mesh)
c     icnel2(i,n) i=1,nel2 n=1,ncnel2(i)  connections for each element (drift mesh)
c     iconnel(i,2) i=1,ncon1              indexes of elements in connection
c     iconne2(i,2) i=1,ncon2              indexes of elements in connection
c
c   Flags and other
c
c     ikeep1(i) i=1,nel1  flag=1 to keep element
c     ikeep2(i) i=1,nel2  flag=1 to keep element
c     ickeep1(i) i=1,ncon1 flag=1 to keep connection
c     ickeep2(i) i=1,ncon2 flag=1 to keep connection
c
c     ncon1      number of original connections in geologic mesh
c     ncon2      number of original connections in drift mesh
c     nel1       number of original elements in geologic mesh
c     nel2       number of original elements in drift mesh
c
c   implicit real*8 (a-h,o-z)
c
c   parameter (maxel1=5000, maxel2=500, inp1=10, inp2=11, iout1=12)
c   parameter (maxcon1=10000, maxcon2=1000, maxel3=500, maxel4=100)
c   character*5 elem1(maxel1), elem2(maxel2)
c   character*5 rknaml(maxel1), rknam2(maxel2), dummy
c   character*5 dummy1(maxcon1)
c   character*10 connel(maxcon1), conne2(maxcon2), dum
c   character*80 default
c   character*1 ans
c
c   real*8 voll(maxel1), dum1(maxel1),
c   &      x1(maxel1), y1(maxel1), z1(maxel1)
c   real*8 isot1(maxcon1), d11(maxcon1), d21(maxcon1),

```

✓ VIII-57 J&H 3/31/00

```

&   areal(maxcon1),grav1(maxcon1)
real*8 vol2(maxel2),dum2(maxel2),
&   x2(maxel2),y2(maxel2),z2(maxel2)
real*8 x2orig(maxel2), z2orig(maxel2)
real*8 isot2(maxcon2),d12(maxcon2),d22(maxcon2),
&   area2(maxcon2),grav2(maxcon2)

real*8 az_con1(maxel3),az_con2(maxel3),az_con2a(maxel3)

integer ikeep1(maxel1),ikeep2(maxel2),idin1(maxel3),idin2(maxel3),
&   idout1(maxel3),idout2(maxel3),idinn2(maxel3),iwp(maxel4),
&   iwpo(maxel4)
integer idcon1(maxcon1),idcon2(maxel3),idcon2a(maxel3),
&   idcon2b(maxel3)
integer iloc1(maxel3),iloc2(maxel3),iloc2a(maxel3)
integer ickeep1(maxcon1),ickeep2(maxcon2)

integer icnel1(maxel1,15),ncnel1(maxel1),iconnel(maxcon1,2)
integer icnel2(maxel1,15),ncnel2(maxel1),iconne2(maxcon2,2)

logical exists

do i=1,maxel1
  ncnel1(i)=0
  ikeep1(i)=1
enddo
do i=1,maxel2
  ncnel2(i)=0
  ikeep2(i)=1
enddo
do i=1,maxcon1
  ickeep1(i)=1
enddo
do i=1,maxcon2
  ickeep2(i)=1
enddo

c
c --- Opens i/o files
c
c   dump file for cheking puposes
open (unit=20,file='mrgdrift.out', status = 'unknown')
c
c   default input parameter values
c   optional read from file
inquire (file='mrgdrift.par', exist = exists)
if(exists) then
  open (unit=22,file='mrgdrift.par', status = 'old')
  read(22,*) drad
  read(22,*) sizout1
  read(22,*) sizin1
  read(22,*) sizout2
  read(22,*) sizin2
  read(22,*) sizinn2
  read(22,*) wprad
  read(22,*) sizwp
  read(22,*) zoffs
  close(22)
else
  drad=2.75
  sizout1=.2
  sizin1=.05
  sizout2=.2
  sizin2=.15
  sizinn2=.15
  wprad=1.67/2.
  sizwp=.2
  zoffs=-.805
endif

write(*,"{//5x,'Enter name of geologic mesh (default='
& 'mesh_geo.dat)',/5x,':> '$)"}
  default='mesh_geo.dat'
call open_old(inpl,default)

```

1 VIII-5B JEH 3/31/00

```

write(*,"(/5x,'Is this a dual-K mesh? (y/n default=y):> ',5)")
read(*,"(a1)") ans
if(ans.eq.' ' .or.(ans.ne.'n'.and.ans.ne.'N')) ans='y'
ifm=2
if(ans.ne.'y') ifm=1

write(*,"(/5x,'Enter name of inner-drift mesh (single-K)'
& ' (default=mesh_dr.dat)',/5x,':> ',5)")
  default='mesh_dr.dat'
  call open_old(inp2,default)

write(*,"(/5x,'Enter the name of new mesh to create'
& ' (default=mesh.out)',/5x,':> ',5)")
  default='mesh.out'
  call open_new(iout1,default)

c
write(*,"(/5x,'Enter drift radius (drift must be centered at'
& ' <0;0>)',/5x,'(default=',f10.5,':> ',5)") drad
read(*,"(a10)") dum
if(dum.ne.' ') read(dum,*) drad

c
write(*,"(/5x,'Enter the size of 1st blocks outside the drift '
& /5x,'in the geologic mesh (default=',f10.5,':> ',5)") sizout1
read(*,"(a10)") dum
if(dum.ne.' ') read(dum,*) sizout1

c
write(*,"(/5x,'Enter the size of 1st blocks inside the drift '
& /5x,'in the geologic mesh (default=',f10.5,':> ',5)") sizin1
read(*,"(a10)") dum
if(dum.ne.' ') read(dum,*) sizin1

c
write(*,"(/5x,'Enter the size of 1st blocks inside the drift '
& /5x,'in the drift mesh (default=',f10.5,':> ',5)") sizin2
read(*,"(a10)") dum
if(dum.ne.' ') read(dum,*) sizin2

c
sizinn2=0.
write(*,"(/5x,'Move connection distances for these blocks '
& ',against the wall ?'/5x,'(y/n default=no) :> ',5)")
read(*,"(a1)") ans
if(ans.eq.' ' .or.(ans.ne.'y'.and.ans.ne.'Y')) ans='n'
if(ans.ne.'n') then
  write(*,"(/5x,'Moving connection distances requires two rows'
& ' of grid blocks',/5x,'radially aligned against the drift wall'
& ' inside the drift mesh!')")

c
write(*,"(5x,'Enter the size of 2nd blocks inside the drift '
& /5x,'in the drift mesh (default=',f10.5,':> ',5)") sizinn2
read(*,"(a10)") dum
if(dum.ne.' ') read(dum,*) sizinn2
endif

c
write(*,"(/5x,'Enter the size of 1st blocks outside the drift '
& /5x,'in the drift mesh (default=',f10.5,':> ',5)") sizout2
read(*,"(a10)") dum
if(dum.ne.' ') read(dum,*) sizout2

c
write(*,"(/5x,'Enter waste package radius'
& /5x,'(default=',f10.5,' :> ',5)") wprad
read(*,"(a10)") dum
if(dum.ne.' ') read(dum,*) wprad

c
write(*,"(/5x,'Enter the size blocks against the waste package'
& /5x,'in the drift mesh (default=',f10.5,':> ',5)") sizwp
read(*,"(a10)") dum
if(dum.ne.' ') read(dum,*) sizwp

c
write(*,"(/5x,'Enter waste package center z offset'
& /5x,'(default=',f10.5,' :> ',5)") zoffs
read(*,"(a10)") dum
if(dum.ne.' ') read(dum,*) zoffs

c

```

y VIII-59 JEH 3/31/00

```

c --- Read Input files
c
c --- Geologic mesh file
dummy='
do while(dummy.ne.'ELEME'.and.dummy.ne.'eleme')
  read(inp1,"(a5)",end=50) dummy !skip header
enddo
50 if(dummy.ne.'ELEME'.and.dummy.ne.'eleme') then
  write(*,*) '...no ELEME header in geologic mesh file'
  stop
endif
do i=1,maxell
  read(inp1,405,end=60)elem1(i),rknam1(i),voll1(i),dum1(i),
  & x1(i),y1(i),z1(i)
  if(elem1(i).eq.' ') goto 60
enddo
60 nell = i-1
if(nell.ge.maxell) goto 504
write(*,"(5x,'...read ',i5,' elements in geologic mesh')")nell
c
dummy='
do while(dummy.ne.'CONNE'.and.dummy.ne.'conne')
  read(inp1,"(a5)",end=70) dummy !skip header
enddo
70 if(dummy.ne.'CONNE'.and.dummy.ne.'conne') then
  write(*,*) '...no CONNE header in geologic mesh file'
  stop
endif
do i=1,maxcon1
  read(inp1,406,end=80)conne1(i),isot1(i),d11(i),d21(i),
  & areal(i),grav1(i),dummy1(i)
  if(conne1(i).eq.' ')goto 80
enddo
80 ncon1 = i-1
if(ncon1.ge.maxcon1) goto 504
write(*,"(5x,'...read ',i5,' connections in geologic mesh')")ncon1
close(inp1)

c --- Drift mesh file
dummy='
do while(dummy.ne.'ELEME'.and.dummy.ne.'eleme')
  read(inp2,"(a5)",end=90) dummy !skip header
enddo
90 if(dummy.ne.'ELEME'.and.dummy.ne.'eleme') then
  write(*,*) '...no ELEME header in drift mesh file'
  stop
endif
do i=1,maxel2
  read(inp2,405,end=60)elem2(i),rknam2(i),vol2(i),dum2(i),
  & x2(i),y2(i),z2(i)
  x2orig(i)=x2(i)
  z2orig(i)=z2(i)
  if(elem2(i).eq.' ') goto 100
  elem2(i)(1:2)='dr'
enddo
100 nel2 = i-1
if(nel2.ge.maxel2) goto 506
write(*,"(5x,'...read ',i5,' elements in drift mesh')")nel2
c
dummy='
do while(dummy.ne.'CONNE'.and.dummy.ne.'conne')
  read(inp2,"(a5)",end=110) dummy !skip header
enddo
110 if(dummy.ne.'CONNE'.and.dummy.ne.'conne') then
  write(*,*) '...no CONNE header in drift mesh file'
  stop
endif
do i=1,maxcon2
  read(inp2,406,end=120)conne2(i),isot2(i),d12(i),d22(i),
  & area2(i),grav2(i)
  if(conne2(i).eq.' ')goto 120
  conne2(i)(1:2)='dr'
  conne2(i)(6:7)='dr'

```

VIII-60 JSH 2/31/00

```

        enddo
120   ncon2 = i-1
        if(ncon2.ge.maxcon2) goto 506
        write(*,"(5x,'...read',i5,' connections in drift mesh')")ncon2
        close(inp2)

        write(*,"(/5x,'...working.....'/)")
c
c ---Point to connections for each element
c
c   Geologic mesh
        do i=1,ncon1
            do j=1,nel1
                imatch=0
                if(connel(i)(1:5).eq.elem1(j).or.
&         connel(i)(6:10).eq.elem1(j)) then
                    ncnell(j)=ncnell(j)+1
                    if(ncnell(j).gt.15) then
&             write(*,"(/5x,'number of connections exceed 15 at
&             ,a5,' These will be skipped!')") elem1(j)
                    goto 125
                endif
                icnell(j,ncnell(j))=i
                imatch=imatch+1
                if(connel(i)(1:5).eq.elem1(j)) iconnel(i,1)=j
                if(connel(i)(6:10).eq.elem1(j)) iconnel(i,2)=j
                if(imatch.eq.2) goto 125
            endif
        enddo
125   continue
        enddo
c   Drift mesh
        do i=1,ncon2
            do j=1,nel2
                imatch=0
                if(conne2(i)(1:5).eq.elem2(j).or.
&         conne2(i)(6:10).eq.elem2(j)) then
                    ncnel2(j)=ncnel2(j)+1
                    if(ncnel2(j).gt.15) then
&             write(*,"(/5x,'number of connections exceed 15 at
&             ,a5,' These will be skipped!')") elem2(j)
                    goto 130
                endif
                icnel2(j,ncnel2(j))=i
                imatch=imatch+1
                if(conne2(i)(1:5).eq.elem2(j)) iconne2(i,1)=j
                if(conne2(i)(6:10).eq.elem2(j)) iconne2(i,2)=j
                if(imatch.eq.2) goto 130
            endif
        enddo
130   continue
        enddo
c
c ---Point to drift elements at wall (blocks abutting the drift)
c   and pie-shaped drift elements in geologic mesh
        k=0
        j=0
        do i=1,nel1
            rad=dsqrt(x1(i)*x1(i)+z1(i)*z1(i))
            if(elem1(i)(1:1).eq.'F')          !fracture X offset by 0.5
&         rad=dsqrt((x1(i)-0.5)*(x1(i)-0.5)+z1(i)*z1(i))
            if(rad.ge.drad.and.rad.lt.(drad+sizout1)) then
                j=j+1
                if(j.gt.maxel3) goto 500
                idout1(j)=i
            elseif(rad.lt.drad) then
                k=k+1
                if(k.gt.maxel3) goto 500
                idin1(k)=i
                ikeep1(i)=0
            endif
        enddo
        nout1=j

```

VIII-61 JEH 3/31/00

```

nin1=k
write(*,“(//5x, 'number of outside wall elements in geol. mesh ',
& i5)”) nout1
write(*,“(5x, 'number of inside wall elements in geol. mesh ',
& i5)”) nin1
if(nout1.ne.nin1) then
write(*,“(//5x, 'number of inside and outside elements should'
& ' be the same'”)
stop
endif

c
c ---Point to drift elements at wall (inside/outside drift)
c and pie-shaped elements at waste package in drift mesh
k=0
j=0
m=0
n=0
do i=1,nel2
rad=dsqrt(x2(i)*x2(i)+z2(i)*z2(i))
radw=dsqrt(x2(i)*x2(i)+(z2(i)-zoffs)*(z2(i)-zoffs))
if(rad.ge.drad.and.rad.lt.(drad+sizout2)) then
j=j+1
if(j.gt.maxel3) goto 500
idout2(j)=i
ikeep2(i)=0
elseif(rad.lt.drad.and.rad.gt.(drad-sizin2)) then
k=k+1
if(k.gt.maxel3) goto 500
idin2(k)=i
elseif(sizin2.ne.0..and.rad.lt.(drad-sizin2).and
& rad.ge.(drad-sizin2-sizin2))then
m=m+1
if(m.gt.maxel3) goto 500
idinn2(m)=i
elseif(radw.le.wprad) then
n=n+1
if(n.gt.maxel4) goto 502
iwp(n)=i
ikeep2(i)=0
elseif(radw.gt.wprad.and.radw.le.(wprad+sizwp)) then
nn=nn+1
if(nn.gt.maxel4) goto 502
iwpo(nn)=i
endif
enddo
nout2=j
nin2=k
ninn2=m
nwp=n
nwpo=nn
write(*,“(//5x, 'number of outside wall elements in drift mesh ',
& i5)”) nout2
write(*,“(5x, 'number of inside wall elements in drift mesh ',
& i5)”) nin2
write(*,“(5x, 'number of 2nd row elements inside drift mesh ',
& i5)”) ninn2
write(*,“(5x, 'number of waste package elements in drift mesh ',
& i5)”) nwp
write(*,“(5x, 'number of elements against waste package ',
& i5)”) nwpo
if(nout2.ne.nin2) then
write(*,“(//5x, 'number of inside and outside elements should'
& ' be identical in drift mesh'”)
stop
endif
if(ninn2.ne.0.and.nin2.ne.ninn2) then
write(*,“(//5x, 'number of inside 1st and 2nd row elements should'
& ' be the same in the drift mesh'”)
stop
endif
if(ifm*nout2.ne.nout1) then
write(*,“(//5x, 'number of outside elements in geol. mesh should'

```

VIII -62 JEA 3/21/00

```

& ' equal',/5x,i5,'x number of outside elements in drift mesh'
& ')") ifm
  stop
endif
if(nwp.ne.nwpo) then
  write(*,"(/5x,'number of waste package elements should'
& ' be same as number of elem. abutting waste'")
  stop
endif

write(*,"(/5x,'....working.....'/)")

c
c --Point to connections between drift and rock
c
c ---geologic mesh
  nncon1=0      :number of connections
c  loop through elem at wall inside (overlapping one)
  do i=1,nin1
    m=idin1(i)  !inner elem index (geol grid)
c  loop through its connections
    jtot=ncnell(m)
    do j=1,jtot
      ic=icnell(m,j)
c  loop through elem against wall outside
      do k=1,nout1
        n=idout1(k)  !outer elem index (geol grid)
        if(connel(ic)(1:5).eq.elem1(n).or.
&  connel(ic)(6:10).eq.elem1(n)) then
          nncon1=nncon1+1
          if(nncon1.gt.maxel3) goto 500
          idcon1(nncon1)=ic
          ickeep1(ic)=0  !note:we will keep, but print at the end
          iloc1(nncon1)=1  !flag=1 if inner elem is first in connection
          if(connel(ic)(1:5).eq.elem1(n)) iloc1(nncon1)=2
c          azimuth of inner element in connection
          az_con1(nncon1)=datan(z1(m)/x1(m))*180/3.14159
          if(elem1(m)(1:1).eq.'F')
&          az_con1(nncon1)=datan(z1(m)/(x1(m)-0.5))*180/3.14159
        endif
      enddo
    enddo
  enddo

  write(*,"(/5x,'number of connections at wall in geol. mesh ',
& i5)") nncon1

c
c ---drift mesh
  nncon2=0
  nncon2a=0
c  loop through elem at wall inside (overlapping one)
  do i=1,nin2
    m=idin2(i)  !inner elem index
c  loop through its connections
    jtot=ncnel2(m) !total connection at this element
    do j=1,jtot
      ic=icnel2(m,j)
c  loop through elem against wall outside
      do k=1,nout2
        n=idout2(k)  !outer elem index
        if(conne2(ic)(1:5).eq.elem2(n).or.
&  conne2(ic)(6:10).eq.elem2(n)) then
          nncon2=nncon2+1
          if(nncon2.gt.maxel3) goto 500
          idcon2(nncon2)=ic
          ickeep2(ic)=0  !will not keep these
          iloc2(nncon2)=1  !flag=1 if inner elem is first in connection
          if(conne2(ic)(1:5).eq.elem2(n)) iloc2(nncon2)=2
c          azimuth of inner element in connection
          az_con2(nncon2)=datan(z2(m)/x2(m))*180./3.14159
        endif
      enddo
    enddo
  enddo
c  loop through elem inside (2nd row)

```

1 VIII-63 JSH 3/31/00

```

do k=1,ninn2
  n=idinn2(k)      !outer elem index
  if(conne2(ic)(1:5).eq.elem2(n).or.
  &   conne2(ic)(6:10).eq.elem2(n)) then
    nncon2a=nncon2a+1
    if(nncon2a.gt.maxel3) goto 500
    idcon2a(nncon2a)=ic
    ickeep2(ic)=0  !note:we will keep, but print at the end
    iloc2a(nncon2a)=1 !flag=1 if inner elem is first in connection
    if(conne2(ic)(1:5).eq.elem2(n)) iloc2a(nncon2a)=2
    azimuth of inner element in connection
    az_con2a(nncon2a)=datan(z2(m)/x2(m))*180./3.14159
  endif
enddo
enddo
enddo
do not keep any connections involving outside elements
do k=1,nout2
  n=idout2(k)      !outer elem index
  jtot=ncnel2(n)  !total connections at this element
  do j=1,jtot
    ic=icnel2(n,j)
    ickeep2(ic)=0
  enddo
enddo

write(*,"(5x,'number of connections at wall in drift mesh ',
& i5)") nncon2
write(*,"(5x,'number of connections wall-2nd row in drift mesh ',
& i5)") nncon2a
if(ninn2.ne.0.and.nncon2a.ne.nncon2) then
  write(*,"(//5x,'number of connections at wall and 2nd row should'
& ' be the same in both meshes')")
  stop
endif
c
c --- dump some info in mrgdrift.out file
c
write(20,*) ' gelologic mesh elements at wall - outside'
do j=1,nout1
  i=idout1(j)
  write(20,405)elem1(i),rknam1(i)
enddo
write(20,*) ' gelologic mesh elements at wall - inside'
do j=1,nin1
  i=idin1(j)
  write(20,405)elem1(i),rknam1(i)
enddo
write(20,*) ' drift mesh elements at wall - outside'
do j=1,nout2
  i=idout2(j)
  write(20,405)elem2(i),rknam2(i)
enddo
write(20,*) ' drift mesh elements at wall - inside, 1st row'
do j=1,nin2
  i=idin2(j)
  write(20,405)elem2(i),rknam2(i)
enddo
write(20,*) ' drift mesh elements at wall - inside, 2nd row'
do j=1,ninn2
  i=idinn2(j)
  write(20,405)elem2(i),rknam2(i)
enddo
write(20,*) ' drift mesh elements in waste package '
do j=1,nwp
  i=iwp(j)
  write(20,405)elem2(i),rknam2(i)
enddo
write(20,*) ' drift mesh elements abutting waste package '
do j=1,nwpo
  i=iwpo(j)
  write(20,405)elem2(i),rknam2(i)
enddo

```

VIII-64 JEA 3/31/60

```

write(20,*) ' geologic connections at wall'
do j=1,nncon1
  i=idcon1(j)
  write(20,"(a10,i10,5f10.4)")conne1(i),isot1(i),d11(i),d21(i),
&   area1(i),grav1(i),az_con1(j)
enddo
write(20,*) ' drift connections at wall'
do j=1,nncon2
  i=idcon2(j)
  write(20,"(a10,i10,5f10.4)")conne2(i),isot2(i),d12(i),d22(i),
&   area2(i),grav2(i),az_con2(j)
enddo
write(20,*) ' drift connections at wall - 2nd row'
do j=1,nncon2a
  i=idcon2a(j)
  write(20,"(a10,i10,5f10.4)")conne2(i),isot2(i),d12(i),d22(i),
&   area2(i),grav2(i),az_con2a(j)
enddo
write(20,*) ' drift connections waste-inner'
c
c ---Now replace connections of waste pack elements
c
c   loop through elements abutting waste package

nncon2b=0
do i=1,nwpo
  m=iwpo(i)      !inner elem index
  loop through its connections
  jtot=ncnel2(m) !total connection at this element
  do j=1,jtot
    ic=icnel2(m,j)
    loop through waste package elements
    do k=1,nwp
      n=iwp(k)      !outer elem index
      if(conne2(ic)(1:5).eq.elem2(n)) then
        azim=datan(z2(m)/x2(m))*180./3.14159
        write(20,"(a10,i10,5f10.4)")conne2(ic),isot2(ic),
&          d12(ic),d22(ic),area2(ic),grav2(ic),azim
        conne2(ic)(1:5) = 'wp001'
        d12(ic)=1.d-6
        nncon2b=nncon2b+1
        idcon2b(nncon2b)=ic
        ickeep2(ic)=0      !note:we will keep, but print at the end
      elseif(conne2(ic)(6:10).eq.elem2(n)) then
        azim=datan(z2(m)/x2(m))*180./3.14159
        write(20,"(a10,i10,5f10.4)")conne2(ic),isot2(ic),
&          d12(ic),d22(ic),area2(ic),grav2(ic),azim
        conne2(ic)(6:10) = 'wp001'
        d22(ic)=1.d-6
        nncon2b=nncon2b+1
        idcon2b(nncon2b)=ic
        ickeep2(ic)=0      !note:we will keep, but print at the end
      endif
    enddo
  enddo
enddo

close (20)

c
c Now we replace the inner/outer connection in the geologic mesh
c with the one from the drift mesh - i.e. replace the
c connecting distance to the drift wall with the inner-drift
c element and its connecting distance (no need to change connecting
c areas or grav angle because both meshes exactly overlap)
c
  if(nncon2a.eq.0) nncon2a=1
  do i=1,nncon1
    do j=1,nncon2
      do k=1,nncon2a
        match connections in both meshes by their azimuth
        (within 0.5 degrees)

```

J VIII-65 JEM 2/21/00

```

toler1=dabs(az_con1(i)-az_con2(j))
toler2=dabs(az_con1(i)-az_con2a(k))
if(ninn2.eq.0) toler2=0.
if(toler1.le.0.5d0.and.toler2.le.0.5d0) then
  a1=area1(idcon1(i))
  a2=area2(idcon2(j))
  g1=grav1(idcon1(i))
  g2=grav2(idcon2(j))
  checks that grids overlapp (just in case)
  if(dabs(a1-a2)/a1.gt.0.001)
    & write(*,"(5x,'warning, areas differ by more than .1%'
    & ' between connections ',a10,' and ',a10)")
    & conne1(idcon1(i)),conne2(idcon2(j))
  if(dabs(g1-g2)/g1.gt.0.001)
    & write(*,"(5x,'warning, grav differ by more than .1%'
    & ' between connections ',a10,' and ',a10)")
    & conne1(idcon1(i)),conne2(idcon2(j))
  if(ilocl1(i).eq.1) then
    if(iloc2(j).eq.1) then
      conne1(idcon1(i))(1:5)=conne2(idcon2(j))(1:5)
      d11(idcon1(i))=d12(idcon2(j))

  c move point against drift/wall boundary
    if(ninn2.ne.0) then
      d11(idcon1(i))=1.d-6
      compute new coordinate of point
      iel=iconne2(idcon2(j),1)
      dr=dsqrt(x2(iel)*x2(iel)+z2(iel)*z2(iel))
      x2(iel)=x2orig(iel)+(d12(idcon2(j))-1.d-6)/dr*x2(iel)
      z2(iel)=z2orig(iel)+(d12(idcon2(j))-1.d-6)/dr*z2(iel)
      adjust connection to 2nd row accordingly
      if(iloc2a(k).eq.1) then
        d12(idcon2a(k))=d12(idcon2a(k))+d12(idcon2(j))-1.d-6
        iloc2a(k)=0 !flag so change is made only once
      elseif(iloc2a(k).eq.2) then
        d22(idcon2a(k))=d22(idcon2a(k))+d12(idcon2(j))-1.d-6
        iloc2a(k)=0 !flag so change is made only once
      endif
    endif
    elseif(iloc2(j).eq.2) then
      conne1(idcon1(i))(1:5)=conne2(idcon2(j))(6:10)
      d11(idcon1(i))=d22(idcon2(j))

  c move point against drift/wall boundary
    if(ninn2.ne.0) then
      d11(idcon1(i))=1.d-6
      compute new coordinate of point
      iel=iconne2(idcon2(j),2)
      dr=dsqrt(x2(iel)*x2(iel)+z2(iel)*z2(iel))
      x2(iel)=x2orig(iel)+(d22(idcon2(j))-1.d-6)/dr*x2(iel)
      z2(iel)=z2orig(iel)+(d22(idcon2(j))-1.d-6)/dr*z2(iel)
      adjust connection to 2nd row accordingly
      if(iloc2a(k).eq.1) then
        d12(idcon2a(k))=d12(idcon2a(k))+d22(idcon2(j))-1.d-6
        iloc2a(k)=0 !flag so change is made only once
      elseif(iloc2a(k).eq.2) then
        d22(idcon2a(k))=d22(idcon2a(k))+d22(idcon2(j))-1.d-6
        iloc2a(k)=0 !flag so change is made only once
      endif
    endif
  endif
  elseif(ilocl1(i).eq.2) then
    if(iloc2(j).eq.1) then
      conne1(idcon1(i))(6:10)=conne2(idcon2(j))(1:5)
      d21(idcon1(i))=d12(idcon2(j))

  c .. move point against drift/wall boundary
    if(ninn2.ne.0) then
      d21(idcon1(i))=1.d-6
      compute new coordinate of point
      iel=iconne2(idcon2(j),1)

```

18 VIII-66 JEST 3/31/60

```

dr=dsqrt(x2(iel)*x2(iel)+z2(iel)*z2(iel))
x2(iel)=x2orig(iel)+(d12(idcon2(j))-1.d-6)/dr*x2(iel)
z2(iel)=z2orig(iel)+(d12(idcon2(j))-1.d-6)/dr*z2(iel)
c      adjust connection to 2nd row accordingly
          if(iloc2a(k).eq.1) then
              d12(idcon2a(k))=d12(idcon2a(k))+d12(idcon2(j))-1.d-6
          elseif(iloc2a(k).eq.2) then
              d22(idcon2a(k))=d22(idcon2a(k))+d12(idcon2(j))-1.d-6
          endif

          endif
elseif(iloc2(j).eq.2) then
conne1(idcon1(i))(6:10)=conne2(idcon2(j))(6:10)
d21(idcon1(i))=d22(idcon2(j))

c      move point against drift/wall boundary
if(ninn2.ne.0) then
d21(idcon1(i))=1.d-6
c      compute new coordinate of point
iel=iconne2(idcon2(j),2)
dr=dsqrt(x2(iel)*x2(iel)+z2(iel)*z2(iel))
x2(iel)=x2orig(iel)+(d22(idcon2(j))-1.d-6)/dr*x2(iel)
z2(iel)=z2orig(iel)+(d22(idcon2(j))-1.d-6)/dr*z2(iel)
c      adjust connection to 2nd row accordingly
          if(iloc2a(k).eq.1) then
              d12(idcon2a(k))=d12(idcon2a(k))+d22(idcon2(j))-1.d-6
              iloc2a(k)=0      !flag so change is made only once
          elseif(iloc2a(k).eq.2) then
              d22(idcon2a(k))=d22(idcon2a(k))+d22(idcon2(j))-1.d-6
              iloc2a(k)=0      !flag so change is made only once
          endif
          endif
          endif
          goto 240
      endif
  enddo
240  continue
    enddo
  enddo

c
c ---now get rid of older connections
c
c      remove connections among inner elem in geol mesh
do i=1,nin1
  m=idin1(i)      !inner elem index (geol grid)
c      loop through its connections
  jtot=ncnell(m)
  do j=1,jtot
    ic=icnell(m,j)
c      loop through inner elem
    do k=1,nin1
      n=idin1(k)      !outer elem index (geol grid)
      if(conne1(ic)(1:5).eq.elem1(n).or.
&      conne1(ic)(6:10).eq.elem1(n)) ickeep1(ic)=0
    enddo
  enddo
enddo

c      remove connections among old waste package elem
do i=1,nwp
  m=iwp(i)      !waste package indexes
c      loop through its connections
  jtot=ncnel2(m)
  do j=1,jtot
    ic=icnel2(m,j)
c      loop through waste pack elements
    do k=1,nwp
      n=iwp(k)      !outer elem index (geol grid)
      if(conne2(ic)(1:5).eq.elem2(n).or.
&      conne2(ic)(6:10).eq.elem2(n)) ickeep2(ic)=0
    enddo
  enddo
enddo

```

✓ VIII-67 JEA 3/31/00

```

        enddo
      enddo
    enddo

c
c ---write new mesh elements
c
      write(iout1, "('ELEM')")
      do i=1,nel1          !geologic mesh elements
        if(ikkeep1(i).eq.1)
          & write(iout1,405)elem1(i),rknam1(i),voll1(i),dum1(i),
          & x1(i),y1(i),z1(i)
        enddo
      do i=1,nel2          !drift mesh elements
        if(ikkeep2(i).eq.1)
          & write(iout1,405)elem2(i),rknam2(i),vol2(i),dum2(i),
          & x2(i),y2(i),z2(i)
        enddo
c
c make only one waste package element (half package for half grid)
      vol=1.d0*3.14159*wprad*wprad*0.5      !assumes 1m thickness 2-D section
      i=iwp(1)
      write(iout1,405) 'wp001',rknam2(i),vol,dum2(i),
      & 0.d0,0.d0,(0.d0+zoffs)

c
c ---write new connections
c
c
c      geologic mesh connections except drift-wall ones
      write(iout1, "('CONNE')")
      do i=1,ncon1
        if(ikkeep1(i).eq.1)
          & write(iout1,406)conne1(i),isot1(i),d11(i),d21(i),
          & areal(i),grav1(i),dummy1(i)
        enddo
c
c      drift-wall connections
c
c      note:write here for convenience, ikkeep was set to 0 for these
      do j=1,ncon1
        i=idcon1(j)
        write(iout1,406)conne1(i),isot1(i),d11(i),d21(i),
        & areal(i),grav1(i),dummy1(i)
      enddo
c
c      drift-at-wall to 2nd drift row connections
c
c      note:write here for convenience, ikkeep was set to 0 for these
      if(ninn2.ne.0) then
        do j=1,ncon2a
          i=idcon2a(j)
          write(iout1,406)conne2(i),isot2(i),d12(i),d22(i),
          & area2(i),grav2(i)
        enddo
      endif
c
c      inner-drift connections
      do i=1,ncon2
        if(ikkeep2(i).eq.1)
          & write(iout1,406)conne2(i),isot2(i),d12(i),d22(i),
          & area2(i),grav2(i)
        enddo
      do j=1,ncon2b
        i=idcon2b(j)
        write(iout1,406)conne2(i),isot2(i),d12(i),d22(i),
        & area2(i),grav2(i)
      enddo
      write(iout1,*)      !ending blank line

      write(*, "(//5x, '.....done!//)")
      close(iout1)
      stop

500 write(*, "(//5x, 'Maximum array dimension exceeded (maxel3)')")
      stop
502 write(*, "(//5x, 'Maximum array dimension exceeded (maxel4)')")

```

Y VIII-68 JSH 9/21/00

```

stop
504 write(*, "(/5x, 'maxell or maxcon1 may be exceeded' )")
stop
506 write(*, "(/5x, 'maxel2 or maxcon2 may be exceeded ' )")
stop

```

```

c
405 format (a5,10x,a5,d10.4,e10.4,10x,3f10.4)
406 format (a10,15x,i5,4e10.4,a5)
c
end

```

```

subroutine open_old (iunit,default)
c*****
c Opens an old file (By N.S. 5/98)
c
c implicit integer (i-n)
c implicit real*8 (a-h,o-z)
logical exists
character*80 filenam,default

ifirst=1
10 if(ifirst.eq.0) write(*, "(/5x, 'Enter another file name:> '$) ")
ifirst=0
read(*, "(a40)") filenam
if(filenam.eq.' ') filenam = default
inquire (file = filenam, exist = exists)
if(exists) then
open (unit=iunit, file=filenam, status='old', err=100)
return
endif

c
write(*, "(5x, 'Warning! File does not exists!/')")
goto 10

c
100 write(*, "(/'Error while opening the file - stop'/)")
stop
end

```

```

subroutine open_new (iunit,default)
c*****
c Opens a new file (By N.S. 5/98)
c
c implicit integer (i-n)
c implicit real*8 (a-h,o-z)
logical exists
character*80 filenam,default
character*1 ans
ifirst=1

10 if(ifirst.eq.0) write(*, "(/5x, 'Enter another file name:> '$) ")
ifirst=0
read(*, "(a40)") filenam
if(filenam.eq.' ') filenam = default
inquire (file = filenam, exist = exists)
if(exists) then
write(*, "(5x, 'File already exists. Replace ? (y/n) :>'$) ")
read(*, "(a1)") ans
if(ans.ne.'Y'.and.ans.ne.'y') goto 10
end if
open (unit = iunit, file = filenam, status = 'unknown', err=100)
c
return

100 write(*, "(/'Error while opening the file - stop'/)")
stop
end

```

X VIII-69 JSH 3/31/00